CHARACTERIZATION OF SWIFT HEAVY ION INDUCED MODIFICATION IN POLYMERIC MATERIALS

ABSTRACT

OF THE

THESIS

SUBMITTED FOR THE AWARD OF THE DEGREE OF

Doctor of Philosophy

IN

APPLIED PHYSICS

BY

SYYED ASAD ALI

Under the Guidance of

Prof. S. A. H. Naqvi
(Supervisor)

Prof. Rajendra Prasad
(Co-supervisor)

DEPARTMENT OF APPLIED PHYSICS
FACULTY OF ENGINEERING & TECHNOLOGY
ALIGARH MUSLIM UNIVERSITY
ALIGARH (INDIA)

2008

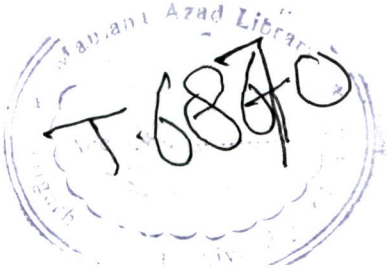
T.6870

ABSTRACT

Polymers have existed in natural form since the beginning of life and have played crucial roles in the processes of life. Early man exploited naturally occurring polymers as materials of basic requirements such as clothing, Shelter, food, tools, weapons, decoration, playing and writing etc. However, the origin of modern polymer industry, commonly, is accepted as being in the nineteenth century with the discoveries in the field of modification of certain natural polymes. Polymers have now become indispensable materials and it is very difficult to think of daily life without them. Virtually modern synthetic polymers have replaced the use of metals in many cases. Polymers are in fact engineering materials and are replacing metals in every application. The demand of modern day life for high performing and special polymers, has thrown a challenge to polymer chemists, physists and technologists to come up with new polymers and also to modify existing polymers.

Swift Heavy Ion (SHI) irradiation provides a unique way of material modification by including such a high degree of localized electronic excitation which otherwise is not possible by any other means. Its effect on the materials depends mainly on the electronic energy loss of the ion in material and ion fluence. The ions lose their energy as they pass through the material. The energy lost is either spent in displacing atoms (of the sample) by elastic collisions or it is spent in exciting or ionizing the atoms via inelastic collisions. The former is the dominant process at low energies. The inelastic collisions are dominant at higher energies (MeV).

Irradiation of polymers leads towards processes like cross-linking of the polymer chains, chain-scission, oxidative degradation and changes in unsaturations, evolution of gaseous products etc. The extent of these depends upon the nature of the polymer, ion parameters and its energy and irradiation conditions. Investigation on the effects of ion irradiation on polymers has become, in recent years, a subject of interest to both scientists engaged in basic research and engineers with practical applications. For scientists, heavy ion irradiation offers an extremely powerful tool to modify polymers under strictly

controllable conditions and to characterize the effect of such modifications on the resultant physical, chemical, structural and the other properties.

A lot of work in the field of ion beam treatment has been carried out to investigate the interaction of charged particles with matter. The application of ion beams now a days range from the use of low energy ions in the field of surface technology to the application of relativistic heavy ions in radiation therapy.

Positron Annihilation Lifetime Spectroscopy (PALS) has been developed into a powerful characterization tool for the study of free volume size and free volume fraction in polymeric materials and technologically relevant materials. By measuring the lifetimes of the positron, it may be possible to get fairly accurate estimates of the free volume holes of angstrom (2-10 Å) range. The atomic scale free volume holes are detected on the basis that positronium (Ps) atoms are formed and localized in the free volume holes.

During the past two decades, positronium (Ps), the bound state of a positron (e^+) with an electron (e^-) has been used as a probe of molecular solids, especially of polymers. Thus many applications of the positron annihilation techniques have been developed as Ps presents a rather unique probe for the quantitative study (viz size, concentration) of the free spaces present in these solids: intrinsic or extrinsic defects, as well as free volumes. In recent years Positron Annihilation Spectroscopy has provided a unique probe to study the size and number distribution of the sub nanometer cavities.

UV-Vis spectroscopy is the powerful analytical tool which gives an idea about the value of optical band-gap energy (E_g) and thus provides an important tool for investigation.

Infrared spectroscopy is one of the most powerful analytical techniques which offers the possibility of chemical identification. Fourier Transform Infra-Red spectroscopy technique can be employed to investigate the ion beam induced changes of polymers to shed light on bond breaking. The nature of chemical bonds of polymers can

be studied through the characterization of the vibration modes determined by FTIR spectroscopy.

X-ray diffraction(XRD) provides a fast and reliable tool for qualitative identification of crystalline phases. The condition for diffraction of a beam of X-rays from a crystals is governed by the Bragg equation. Any modifications of the polymers structure upon irradiation, is reflected in its diffraction pattern.

The dielectric response of material provides information about the orientational translational adjustment of mobile charges present in the dielectric medium in response to an applied electric field and also about the potential charge carriers which may be formed by splitting of covalent, atomic or molecular bonds under the influence of the energetic ions.

Swift heavy ion (SHI) irradiation of the polymeric samples was carried out at 15 UD Pelletron Accelerator at Inter University Accelerator Centre (IUAC), New Delhi, India and Variable Energy Cyclotron Centre (VECC), Kolkata, India. The details of irradiating ions and polymers are given below:

I. Irradiation carried out at 15 UD Pelletron at IUAC, New Delhi.

By 100 MeV Si^{8+} ions

(a) 40μm thick Makrofol- KG and 30μm thick Makrofol-N to the fluences 10^{10}, $3x10^{10}$, 10^{11}, $3x10^{11}$, $6x10^{11}$ and 10^{12} ions/cm^2

(b) 250μm thick Polyethersulphone (PES) to the fluences 10^{10}, 10^{11}, 0^{12} and $5x10^{12}$ ions/cm^2.

(c) 50μm thick Polyethylene Trephthalate (PET) to the fluences 10^{10}, $3x10^{10}$, 10^{11}, $3x10^{11}$, $3x10^{13}$ ions/cm^2

(d) 50μm thick Polypropylene (PP) to the fluences 10^{10},$3x10^{10}$,10^{11}, $3x10^{11}$, $6x10^{11}$ and 10^{12} ions/cm^2

(e) 125μm thick PMMA to the fluences 10^{10}, 10^{11}, 10^{12} and $5x10^{12}$ ions/cm^2.

By 95 MeV O^{6+} ions

(f) 170μm thick PEO-salt (17% & 19%) to the fluences 10^{10}, 10^{11}, 10^{12} and 10^{13} ions/cm^2.

(g) 225μm thick LEXAN (PC) to the fluences 10^{10}, 10^{11}, 10^{12},10^{13} and $2x10^{13}$ ions/cm^2.

(h) 80μm thick PVDF to the fluences 10^{10}, 10^{11}, 10^{12} and 10^{13} ions/cm^2.

(i) 50μm thick LDPE to the fluences 10^{10}, 10^{11}, 10^{12} and 10^{13} ions/cm^2.

By 50 MeV Li^{3+} ions

(j) 50μm thick LDPE to the fluences $5x10^{10}$, 10^{11}, 10^{12} and 10^{13} ions/cm^2.

(k) 125μm thick PMMA to the fluences 10^{10}, 10^{11}, 10^{12}, $5x10^{12}$ and 10^{13} ions/cm^2.

(l) 250μm thick PES to the fluences $5x10^{12}$ and 10^{13} ions/cm^2

(m) 250μm thick PN-6,6 to the fluences $5x10^{10}$, 10^{11}, 10^{12}, $5x10^{12}$, 10^{13} and $2x10^{13}$ ions/cm^2

By 70 MeV C^{5+} ions

(n) 250μm thick Polyamide Nylon-6 polymer to the fluences of $9.3x10^{11}$,$3.7x10^{12}$, 1.8×10^{13}, $3.7 x10^{13}$ ions/cm^2

II. Irradiation carried out at Variable Energy Cyclotron (VECC), Kolkata, India.

By 145 MeV Ne^{6+} ions

(a) 40μm thick Makrofol-KG to the fluences 10^{10}, 10^{11}, 10^{12} and 10^{13} ions/cm^2.

(b) 250μm thick PES to the fluences 10^{12} and 10^{13} ions/cm^2

(c) 100μm thick PTFE to the fluences 10^{10}, 10^{11}, 10^{12} and 10^{13} ions/cm^2

(d) 50μm thick PP to the fluences 10^{8}, 10^{10}, 10^{11}, 10^{12} and 10^{13} ions/cm^2

(e) 80 μm thick PVDF to the fluences of 10^{10}, 10^{11}, 10^{12} and 10^{13} ions/cm^2

(f) 125 μm thick PMMA to the fluences of 10^{10}, 10^{11}, 10^{12} and 10^{13} ions/cm^2.

Chapter – I describes the introduction to the topic of the thesis and the significance in the field of material science, classification of polymers and the utility of polymers, Heavy ion energy deposit in solids, Energy loss processes i.e Inelastic collision of incident ions with the target(Electronic Stopping '**Se**') and Elastic collision with screened target nuclei(Nuclear stopping '**Sn**') as well as significance of modification in the properties of polymeric materials induced by heavy ion irradiation have been discussed. Mechanism of formation of ion tracks in polymers by Swift Heavy Ions (SHI) is described. Damages in polymers by SHI irradiation i.e. Cross-linking, Scissoring of the main polymer chain, Gas Liberation, Side chain decomposition., Scission at branch points, Changes in chemical structure and Changes in crystallinity in partially crystalline polymers have been discussed..

Chapter – II gives an account and description of the experimental techniques with their relevant details used in the measurements carried out in the present study. This chapter covers the details of (i) The materials: Polymers studied and their chemical structure (ii) Brief description of 15 MV Pelletron Accelerator at Inter University, Accelerator Centre (IUAC), New Delhi India .(iii) General purpose scattering chamber used for irradiation (iv) Variable Energy Cyclotron Centre (VECC), Kolkata. (v) Positron Annihilation Lifetime (PAL) measurements techniques as well as DBS. (vi) Ultraviolet–visible (UV-Vis) spectroscopy. (vii) Fourier Transform infrared (FTIR) spectroscopy (viii) X-Ray Diffraction (ix) Dielectric constant measurements

Chapter–III This chapter deals with the characterization of free volume measurements carried out using Positron Annihilation Lifetime Spectroscopy (PALS) and Doppler Broadening Spectroscopy (DBS). Swift Heavy Ion induced modification in free volume properties of Makrofol-KG, Polyethersulphone (PES) and Polystyrene (PS) irradiated by 100 MeV Si^{8+} ions; Makrofol-KG, PVDF and PES irradiated by 145 MeV Ne^{6+} ions; PEO-salt and Lexan Polycarbonate irradiated by 95 MeV O^{6+} ions; PN-6,6 and PS irradiated by 50 MeV Li^{3+} ions and Polyamide nylon-6 irradiated by 70 MeV C^{5+} ions to different fluences has been characterized by PALS and DBS.

Chapter IV In this chapter, the results of characterization of modification optical and chemical properties of various polymeric materials induced by swift heavy ions through Ultraviolet–Visible (UV-Vis) spectroscopy and Fourier Transform Infrared (FT-IR) spectroscopic analyses are presented. Significant changes of different amounts have been observed in optical and chemical response of the polymers after irradiation with Si^{8+}, Ne^{6+}, O^{6+} and Li^{3+} ions of energies 100 MeV, 145 MeV, 95 MeV and 50 MeV respectively.

Chapter V This chapter describes the results of characterization of modification in structural and electrical properties induced by ions through X ray diffraction, a.c. conductivity and dielectric constant measurements. The polymers were irradiated with different ions obtained from Pelletron accelerator and Variable Energy Cyclotron. Significant changes have been observed in dielectric response of the polymers as a function of ion beam parameters such as fluence etc.

CHARACTERIZATION OF SWIFT HEAVY ION INDUCED MODIFICATION IN POLYMERIC MATERIALS

THESIS

SUBMITTED FOR THE AWARD OF THE DEGREE OF

Doctor of Philosophy

IN

APPLIED PHYSICS

BY

SYYED ASAD ALI

Under the Guidance of

Prof. S. A. H. Naqvi
(Supervisor)

Prof. Rajendra Prasad
(Co-supervisor)

DEPARTMENT OF APPLIED PHYSICS
FACULTY OF ENGINEERING & TECHNOLOGY
ALIGARH MUSLIM UNIVERSITY
ALIGARH (INDIA)

2008

Dedicated

to

My Parents

DEPARTMENT OF APPLID PHYSICS
ALIGARH MUSLIM UNIVERSITY
ALIGARH-202 002, (U.P.) INDIA

Phone: Off. (0571) 2703167
to 2703176*
Ext. : 3035 (Office)
3036 (Chairman)
Fax : 91 (0571) 700042

CERTIFICATE

This is to certify that work presented in the thesis entitled **"Characterization of Swift Heavy Ion Induced Modification in Polymeric Materials"** which is being submitted by Mr. Syyed Asad Ali for the award of the degree of Doctor of Philosophy in Applied Physics, to the Department of Applied Physics, Faculty of Engineering & Technology, Aligarh Muslim University, Aligarh has been carried out under our supervision and guidance.

We, further certify that Mr. Syyed Asad Ali has fulfilled the requirements of Aligarh Muslim University, Aligarh for the submission of Ph.D. thesis.

PROF. S. ALIM H. NAQVI
(SUPERVISOR)

PROF. RAJENDRA PRASAD
(CO-SUPERVISOR)

Acknowledgements

It is a matter of great pleasure for me to avail this opportunity to carry out this work under Dr. Rajendra Prasad, Professor Emeritus and former Chairman, Department of Applied Physics, Z. H. College of Engineering & Technology, Aligarh Muslim University, Aligarh, India. So first of all, I wish to express my deep sense of gratitude to Prof. Rajendra Prasad for his valuable guidance. I am indebted to him for numerous stimulating discussions, critical comments and encouragement during the entire course of this work.

I have great pleasure to express my sincere gratitude to my supervisor, Dr. S. Alim H. Naqvi, Professor and former Chairman, Department of Applied Physics, Z. H. College of Engineering and Technology, Aligarh Muslim University, Aligarh, India for his valuable guidance, encouragement, moral support and helpful suggestions during this work.

I would like to extend my thankfulness to Prof. Alimuddin, Chairman, Department of Applied Physics for providing me all the facilities available in the department and encouragement.

I take this opportunity to thank Prof. Javed Husain, Prof. Afzal Ahmad, Dr. Ameer Azam, Dr. M.A. Suhail and Dr. Shakeel Khan and all other faculty members of the department of Applied Physics who have been very helpful to me.

My special thanks go to Dr. Rajesh Kumar, Young Scientist, D.S.T., Govt. of India in the Department of Applied Physics, A.M.U. Aligarh and presently Lecturer in Indraprasth University, Delhi for his cooperation, help, encouragement, sympathetic behavior and moral support for many insights into the aim of my work.

Thanks are due to Dr. A.K. Sinha, Director UGC-DAE Consortium for Scientific Research (CSR), Kolkata Centre for providing the experimental facilities. I also express my sincere thanks to Dr. D. Das, Scientist, UGC-DAE-CSR, Kolkata Centre. Dr. U De, Variable Energy Cyclotron Centre(VECC), Kolkata, Dr. D.K. Avasthi, Dr. R. G. Sonkawade, Mr. S. A. Khan, Mr. Fouran Singh and Mr. P. Kulariya, Inter University Accelerator Centre (IUAC), New Delhi.

I wish to express my sincere thanks to Prof. P.M.G. Nambissan, Saha Institute of Nuclear Physics, Kolkata for providing the experimental facilities and for many useful suggestions.

I am also extremely indebted to my colleagues, Dr. Sikandar Ali, Dr. Mohd. Chaman, Mr. Ajay Kumar Mahur. Mr. K. M. Batoo, Mr. Faheem Ahmad, Mr. Mohd. Zubair and all research Scholar in the department and my friends Dr. Naseem Ahmad Khan, and M. Asad Khan, for all the helps provided to me during the course of this study.

Thanks are due to Ms. Shagufta Parveen, Dept. of Chemistry, A.M.U., Aligarh for her constant help in the formation of polymer composites and many useful discussions.

I am greatly indebted to my parents, Mr. Syyed Ahsan Ali and Mrs. Syyeda Afzaal Fatima, my aunty Mrs. Ansari Begum and my sisters who never deprived me of the freedom for exploration and their affection encouraged me at every stage of my study.

My most affectionate thanks go to my brothers Mr. Syyed Hasnain Ali, Mr. Shakeel Ahmad Farooqui, Mr. S. Wazahat Ali and my uncle Mr. Mushfiq Husain who have been a source of strength for me.

I am thankful to Mr. Mohd. Rafique (STA), Mr. Shahabuddin (LDC), Mr. Shamsul Hasan (T.A.), Mr. Kamal Garg (TA) and all the member of the non-teaching staff in the department for their help.

Financial assistance in the form of Junior Research Fellowship (JRF) from Inter University Accelerator Centre (IUAC), New Delhi is gratefully acknowledged.

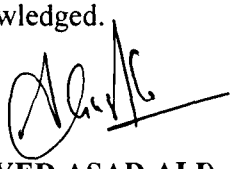

(SYED ASAD ALI)

CONTENTS

Chapter-I Introduction

Chapter-II Experimental Techniques

Chapter-I

Chapter I

INTRODUCTION

1.1 Polymers

Polymers are macromolecules built up by linking together a large number of much smaller molecules. The small molecules, which combine with each other to form polymer molecules, are termed as monomers and the process by which they combine with each other is known as Polymerization. There may be hundreds, thousands, tens of thousands or more monomer molecules linked together in a polymer molecule and are called as polymers. Thus polymers have long chain and are high molecular weight compounds in which many small molecules combine together. If a monomer combines with itself, it forms a homopolymer, if two, then copolymer and if three then terpolymer is formed and so on.

Polymers have existed in natural form since the beginning of life and have played crucial roles in the processes of life. Early man exploited naturally occurring polymers as materials of basic requirements such as clothing, Shelter, food, tools, weapons, decoration, playing and writing etc. However, the origin of modern polymer industry, commonly, is accepted as being in the nineteenth century with the discoveries in the field of modification of certain natural polymers [1].

1.1.1 Organization of Polymers

Molecular structure and the arrangements of the polymer chains are important factors in determining their properties. Polymers are organized at several distinct levels [2].

- The primary is the monomer chemical structure, characterized by the presence of given functional groups and related electronic structure.
- The secondary structure is the chain characterized by the spatial arrangement of some 10^2 to 10^5 repetitive units in the polymer chains. In general, the macromolecules exhibit a broad molecular distribution.

- ❖ The tertiary structure is global form of the macromolecules as determined by weak van der Waals forces, hydrogen bonds and the sum of conformational constraints. In general, the molecular chains are not linearly extended but wrapped up or folded (typical fold length 10-100nm) with some free volume in between. They can be thread-like, branched or cross-linked through covalent bond, either as individual separate units or entangled with others.

- ❖ This leads to amorphous or crystalline arrangements (typical 1-10μm) as the quaternary structures. Most polymeric single crystals consist of many platelets (lamellae) kept one over the other in decreasing order of size. The folding of the macromolecules chain takes place during polymerization. Here, the long chains are accommodated into narrow lamellae, their thickness being typically around 10 nm and the molecular chain length being around 100 to 1000 nm.

- ❖ The unit cell or lamellae eventually may arrange globally in still larger units, the so-called spherulites (typical size around 100μm).

- ❖ The polymer's side groups and their geometrical arrangement influence the polymer properties strongly. There exists a practically infinite number of so called conformations of a given polymer chain due to its large size and rotational degrees of freedom of most covalent bonds that gives rise to a random, strongly entangled arrangement of the polymer chains in concentrated solutions and in the melt.

Polymers have now become indispensable materials and it is very difficult to think of daily life without them. Virtually modern synthetic polymers have replaced the use of metals in many cases. Polymers are in fact engineering materials and are replacing metals in every application [3]. Some of the advantages of using polymers in place of metals are:

(i) They are lightweight, resistant to corrosion effects and are chemically inert.

(ii) They have good thermal/electrical insulation capacity, good strength, dimensional stability and toughness.

(iii) They have easy workability and good dye ability and their fabrication costs are low.

(iv) They are transparent in appearance, can absorb mechanical shock and show resistance to abrasion effects.

The demand of modern day life for high performing and special polymers, has thrown a challenge to polymer chemists, physists and technologists to come up with new polymers and also to modify existing polymers.

1.1.2 Classification of Polymers

A large number of chemical compounds undergo polymerization process in different reaction conditions and the resulting polymers exhibit wide range of physical, chemical, mechanical, thermal and electrical properties. Thus the polymers are classified on the basis of their origin and can broadly be classified as natural and synthetic polymers. Depending on their structure the polymers can be classified as linear, branched and cross-linked polymers. High-density polyethylene is linear polymer, while low density polyethylene is branched polymer.

Polymers are also classified as organic, elemento-organic and inorganic polymers. Organic polymers have chains consisting of C-C linkages, and apart from carbon atoms have hydrogen, oxygen, nitrogen, sulphur and halogen atoms in the side chains. Element organic polymers include (i) macromolecules whose chains are composed of carbon as well as heteroatom (except N, S, O and halogen atoms) and (ii) inorganic chains in which side groups contain carbon atoms directly linked to the chain.

Polymers can be classified as fibers, plastics, resins, and rubbers based on the nature and extent of secondary valence forces and mobility among the constitutional repeat units. Polymers may be charged or uncharged. Charged polymers have some free functional groups e.g. polyacrylic acid (anionic polymer) or polyethylimine (cationic polymer).

Polymers may also be classified as amorphous or crystalline depending upon their morphological behavior. Most linear polymers take on new shapes by application of heat and pressure. They are thus called thermoplastics whereas the cross-linked polymers cannot be made to flow or melt irreversibly and are said to be thermosetts. This feature depends on the spatial arrangement of the monomeric units with respect to each other. If the monomer molecules have been linked together in one continuous length to form the polymer molecules, the polymers are termed as linear polymers. Branched

polymers are those in which there are side branches of linked monomer molecules protruding from various central branch points along the main polymer chain. Figure-1.1 shows different type of polymers. It can be seen that there may be several different kinds of branched polymers. The presence of branching in a polymer usually effects many important polymer properties. The most significant property change brought about by branching is the decrease in crystallinity.

The polymers in which the polymer molecules are linked to each other at points other than ends, are said to be cross-linked Figure1.1. Cross-linking can be made to occur during the polymerization process by the use of appropriate monomers. It can also be modified by the irradiation of heavy ions.

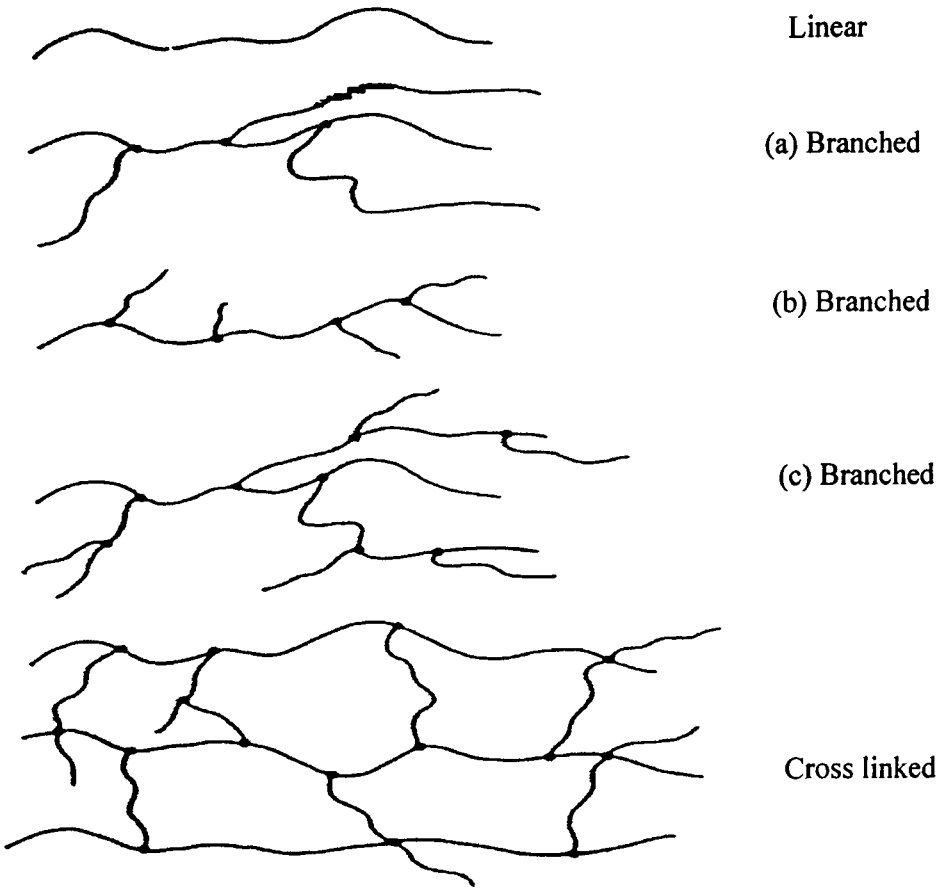

Figure 1.1: Structure of linear, branched and cross-linked polymers.

1.1.3 Properties and uses of Polymers

Due to their chemical structure, spatial arrangement of monomeric units, molecular weight and its distribution and crystallinity, polymers show a wide range of physical, mechanical, thermal and electric characteristics [4-6]. Polymers have vast technological and scientific applications. Polymers exist only as solid or liquid but never in gaseous form, as they decompose before reaching their boiling point [7]. Polymers have applications in almost all fields, such as industry, science and technology due to their low cost, easy processibility, low weight, high corrosion resistance, high electric resistance and durability etc. Polymers are fast replacing metals and alloys in many applications in the field of industry, science and technology.

As ionizing radiations can modify the physico-chemical properties of the polymers in a controlled way, the field of ion induced modification in polymers and their characterization has emerged as a very challenging field owing to its vast technological implications. If the effect is undesirable, the term "degradation" is commonly used which may cause addition, cross-linking, substitution, hydrolysis, chain scission etc. leading to different type of polymers.

1.1.4 Effect of Temperature on Polymers

The temperature of the sample during irradiation plays a significant role in the type of free radical that will be generated. For example, irradiation of polyethylene at liquid nitrogen temperatures prevents the formation of allyl double bonds during the irradiation. The free radicals formed during the irradiation are frozen into the solid and react when the sample is heated to higher temperature. Moreover, Chapiro [8] has shown that irradiation of polyethylene in the molten state causes the formation of more cross-links than at room temperature [9].

1.2 Heavy Ions

Atoms consist of nuclei and electrons. If some of negatively charged electrons orbiting the tiny positively charged nucleus are removed from the atom, an ion is left. If heavy atoms undergo this process, they are called heavy ions. In the last two decades heavy ions have emerged as a major tool in atomic and nuclear physics. Light and heavy

atoms ionized to a high degree resemble those found in hot stars and hence the actual situation in stars could be simulated and clarified through the laboratory on the earth. The information about a nuclear structure can be obtained by the production of deformed heavy system by the ions of different energies. Various areas of research in nuclear physics are: nuclear reactions, fusion reactions and study of high spin states etc. The relativistic heavy ion collision gives the challenging and wide-open frontier of modern nuclear science. Discovery of new elements and search for the super heavy elements is another field where the heavy ion research is aimed at. Development of techniques for accelerating particle led to a construction of new accelerators and modification in accelerators which provide the heavy ion beam energy from few MeV to several GeV per nucleon.

1.2.1 Range of Ion

The distance over which an ion dissipates its energy completely via elastic and inelastic collision is called the ion range. The nuclear energy loss occurs in discrete amounts ranging from eV to several keV during each collision. On the contrary, the electronic loss occurs continuously and acts as a drag force on the moving ion. Due to the *probabilistic nature of energy transfer process, the amount of energy loss varies from one* collision to the other and is reflected as a statistical variation in the ranges of the individual ions. This leads to a straggling in the ion range.

1.2.2 Heavy Ion Energy Deposition in Solids

When an energetic ion penetrates into a medium, it loses by two processes: inelastic interactions with target electrons and elastic interactions with screened target nuclei. The former process is called "electronic stopping", and the later "nuclear stopping". The energy ΔE, an ion loses when moving a given path ΔX, is stochastic quantity i.e. the different ions of the same beam will lose different amount of energy. The mean value of the energy loss $\Delta E/\Delta X$, $(\Delta x \rightarrow 0)$ for a large number of ions is termed as stopping power S, which is the sum of the two above said energy losses and is given by

$$S = -\frac{dE}{dx} = S_e + S_n \tag{1.1}$$

where S_e and S_n, are the electronic and nuclear stopping power respectively.

At high energies of the order of MeV, the ion interacts with electrons of the target atoms. The material is ionized and/or electrons are transferred to higher states. Since the mass of the electron is small, the initial direction of the ion in the solid remains almost unchanged. At low energies (0.1-10 keV), the nuclear energy loss predominates: the ion collides with the target nucleus and transfers energy and, momentum to recoil atom. As a result of which, atoms are displaced and the direction of the ion changes. Typical curves for both types of stopping powers are given in Figure 1.2.

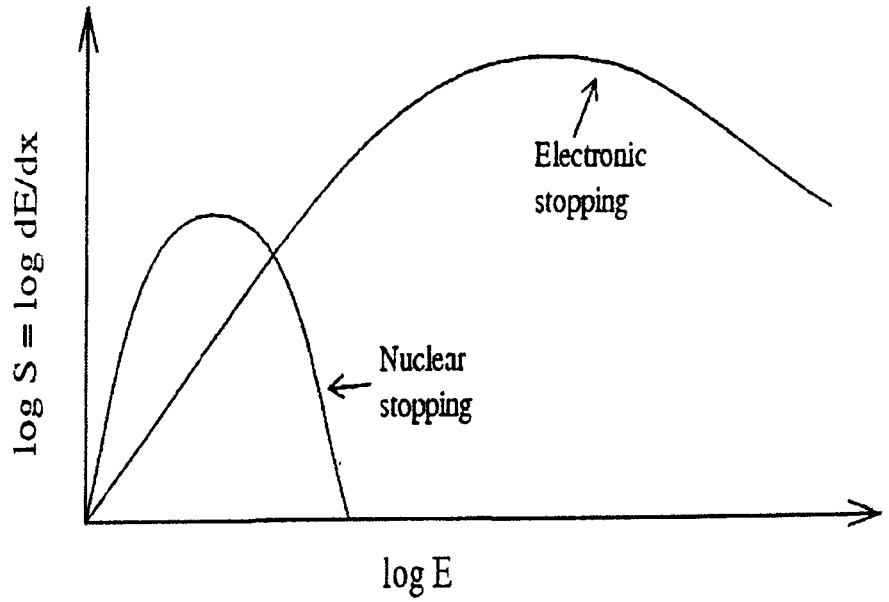

Figure 1.2: Qualitative curve of the energy loss of an ion in the material as function of the ion energy, shown on a log-log scale [10]

1.2.3 Formation of ion tracks in polymers by Swift Heavy Ions (SHI)

Due to the passage of charged particles through insulating solids like polymers, narrow paths of intense damage are created on atomic scale which is generally called the latent tracks. Track formation depends upon the process by which heavy ions loose energy as they pass through, slow down and stop in a solid. When a fast moving particle

moves through solid due to interaction of orbital electrons of the atom and those around the atoms that make up the solid, it looses all or some of its orbital electrons. In an ionization process the charged nuclear particle transfers some of its kinetic energy to the atomic electrons with which it encounters. The electrons are thereby either raised to an excited energy state or completely removed from the atom, thus causing it to become ionized. Thus heavy charged particles loose their energy mostly by ionizing the atoms of the absorbing material in which they pass through. Particle tracks are formed in many insulating materials and some semiconductors, but not in metals [11]. Track formation in solids mainly depends upon

(i) Total energy loss rate (J = dE/dx)

(ii) Angle of incidence of the ion with respect to the detector surface.

The rate at which the ion loses energy (J = dE/dx) or causes certain alteration in solid is related to the production of track in that material. The value of this energy loss J must be higher than a particular value called critical value J_c for track formation. The value of J_c for one solid is same for all the particles and is different for different solids. The incidence angle of the ion with respect to the surface of the detector also determines the track formation in the detector. There exists a certain angle θ_c (angle between the direction of incident ion and the surface of the detector) such that the incident charged particles entering the detector surface at an angle less than a certain minimum value θ_c, its track can not be revealed by chemical etching. When a charged ion of atomic number Z traverses the solid, its orbital electrons interact with the electrons of the atom of which the solid is made of. As a result a fast moving atom of atomic number Z would rapidly become an ion by being stripped of all or some of its orbital electrons. Therefore, the ion acquires a net positive charge Z* which can be empirically expressed as [12].

$$Z^* = Z\left[1 - \exp\left(-130\ \frac{\beta}{Z^{2/3}}\right)\right] \qquad (1.2)$$

Where β is the speed of ion relative to the velocity of light. At higher velocities $Z^* \approx Z$ and the dominant interaction is due to the electrical force between the ion and atomic electrons in the solid. As a result of this interaction, atomic electrons in the solids can be excited to high energy levels or can be stripped out of the atom. In polymers, excitation

can lead to the breakage of molecular chains and formation of free radicals. The ejected out electrons in atoms called delta rays, can cause further ionization and excitation if they have enough energy. In inorganic solids primary ionization is the major source of the track damage and the secondary effects of delta rays are unimportant. However, in polymers primary ionization as well as delta rays Contributes to the formation of track. The track may be a more or less cylindrical region of ion as shown in Figure1.3.

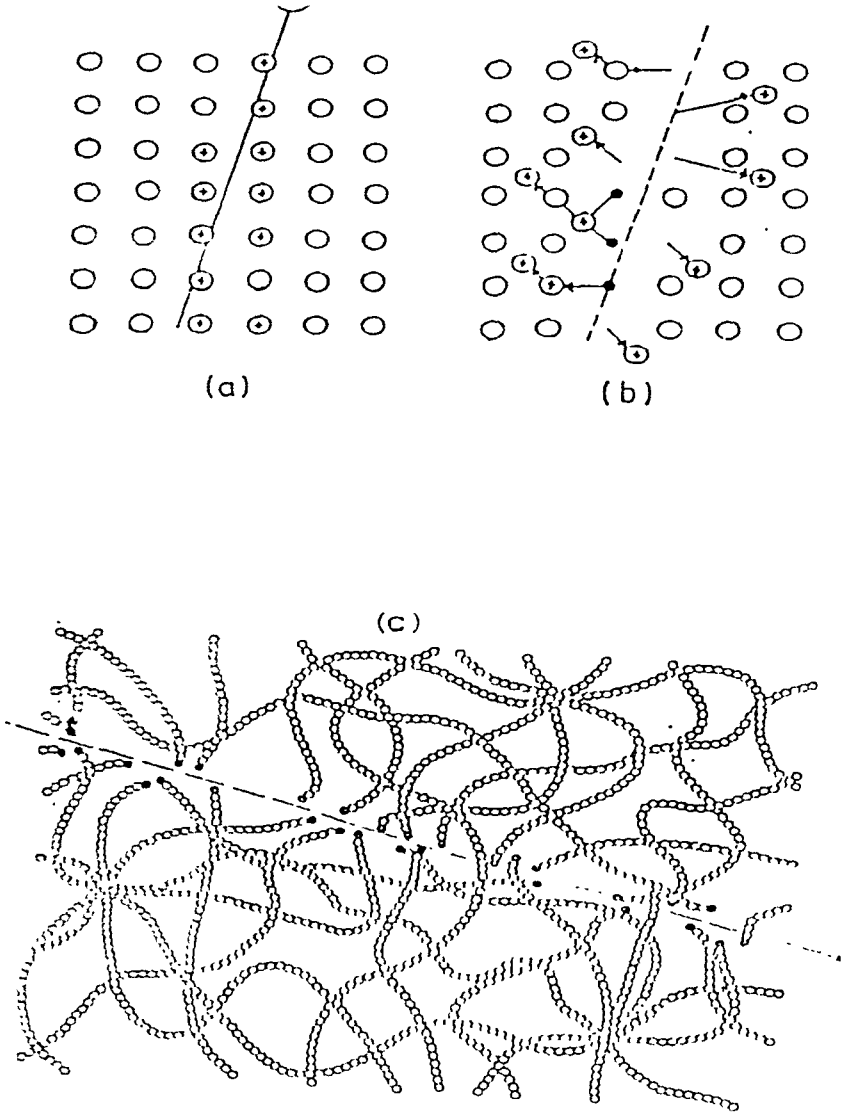

Figure 1.3: Track formation in crystalline solids and polymers.

1.3 Energy loss processes

The following processes are involved in energy loss of the particle:

(i) Electronic Stopping **'Se'**: Inelastic collision of incident ion with target atomic Electrons resulting in excitation and ionization of the target atoms.

(ii) Nuclear stopping **'Sn'**: elastic collision with screened target nuclei, resulting in the displacement of target nuclei.

1.3.1 Electronic Stopping Power (Se)

The atoms in the material are just spectators to the passage of energetic ions and they are not displaced from their sites in this process. These spectator atoms get either excited or ionized due to interaction of atomic electrons with energetic ion. The theory of electronic energy loss of highly energetic ions in solids was first given by Bohr [13]. He derived the expression for S_e on the basis of a model which considered the target as a collection of harmonic oscillators whose frequency was determined by optical absorption data. The work was extended to relativistic ions by Bethe[14] and Bloch[15]. They solved the energetic ion loss problem quantum mechanically in first Born approximation. The expression that describes the electronic energy loss of a highly energetic ion in a solid is known as Bohr-Bethe formula and is written as

$$S_e = -\left(\frac{d_E}{dx}\right) = \frac{4\pi e^4 Z_p^2 Z_t N_t}{m_e v^2}\left[\ln\left(\frac{2m_e v^2}{I}\right) - \ln\left(1-\frac{v^2}{c^2}\right) - \frac{v^2}{c^2}\right] \tag{1.3}$$

where v and Z_p are the velocity and charge of the projectile ion, Z_t and N_t are the atomic number density of the target atoms, m_e is the electronic charge.The parameter I represents the average excitation and ionization potential of the target material, and is unusually an experimentally determined parameter of each element. For non-relativistic projectile ions, only the first term in square brackets of equation (1.3) is generally valid for different types of ions provided their velocity remains large compared to the velocities of the orbital electrons in the target atoms. It can be seen from this equation that for a given non-relativistic ion S_e varies as $1/v^2$, or inversely with ion energy. This is due the fact that if

the velocity of the ion is low, it spends a greater time in the vicinity of the electron, and thus it transfers grater impulse and hence larger energy to the electron.

1.3.2 Nuclear Stopping Power (S_n)

Nuclear energy loss arises from elastic collisions between the energetic ion and target nuclei, which cause atomic displacements and phonons. Displacement occurs when the colliding particle imparts energy greater than certain displacement threshold energy to a target atom. The threshold energy depends upon the target and it is the amount of energy a recoil atom (from target) requires to overcome the binding forces and to move more than one atomic spacing away from its original site. Otherwise, knock-on atoms cannot escape their sites and their energy dissipates as atomic vibrations i.e. phonons. Since the nuclear collisions occur between two atoms with electrons around their nuclei, the interaction of an ion with a target nucleus is treated as the scattering of two screened particles. Nuclear stopping is derived with consideration of the momentum transfer from ion to target atom and the inter-atomic potential between them. Thus nuclear stopping varies with ion velocity as well as the charges of two colliding atoms. Nuclear stopping becomes important when an ion slows down to approximately the Bohr velocity (orbital electron velocity). For this reason, the maximum nuclear energy loss occurs near the end of the ion track, for high energy ions. When an ion shows down in passing through a solid, it eventually requires orbital electrons one by one as its velocity becomes comparable with the orbital velocities of less and less tightly bound electrons [16-18].

1. 3. 3 Delta Rays (δ-rays)

While moving in a solid, an energetic ion undergoes two types of collisions with the target electrons. One of these is called glancing collision and it involves inelastic scattering, where small momentum is transferred to the target electrons via distant resonant collisions. The other is called knock-on collision and it refers to elastic scattering, where large momentum transfer takes place via close collisions.Glancing collisions are quite frequent but each collision involves a small energy loss (<100 eV). On the other hand, knock-on collisions are very infrequent but each collisions imparts a large

energy to a target electron (>100 eV). Theoretical and experimental evidence suggested that approximately one halfof the electronic energy loss is due to glancing collisions and the other half to knock-on collisions [19, 20].

Both glancing and knock-on collisions transfer energy in two ways: electronic excitation and ionization. Electronic excitation is the process in which an orbital electron is raised to a higher energy level. All excited electrons eventually lose energy as they thermalize. In addition, an orbital electron is ejected from the atom. The ejected electron is often called delta ray (δ-ray) or secondary electron. The primary (due to ion) ionization and excitation occur close to the path of the ion, while secondary ionization and excitation are spread over large distance from the core of the track. The complete energy loss process can be viewed in the Figure 1.4.

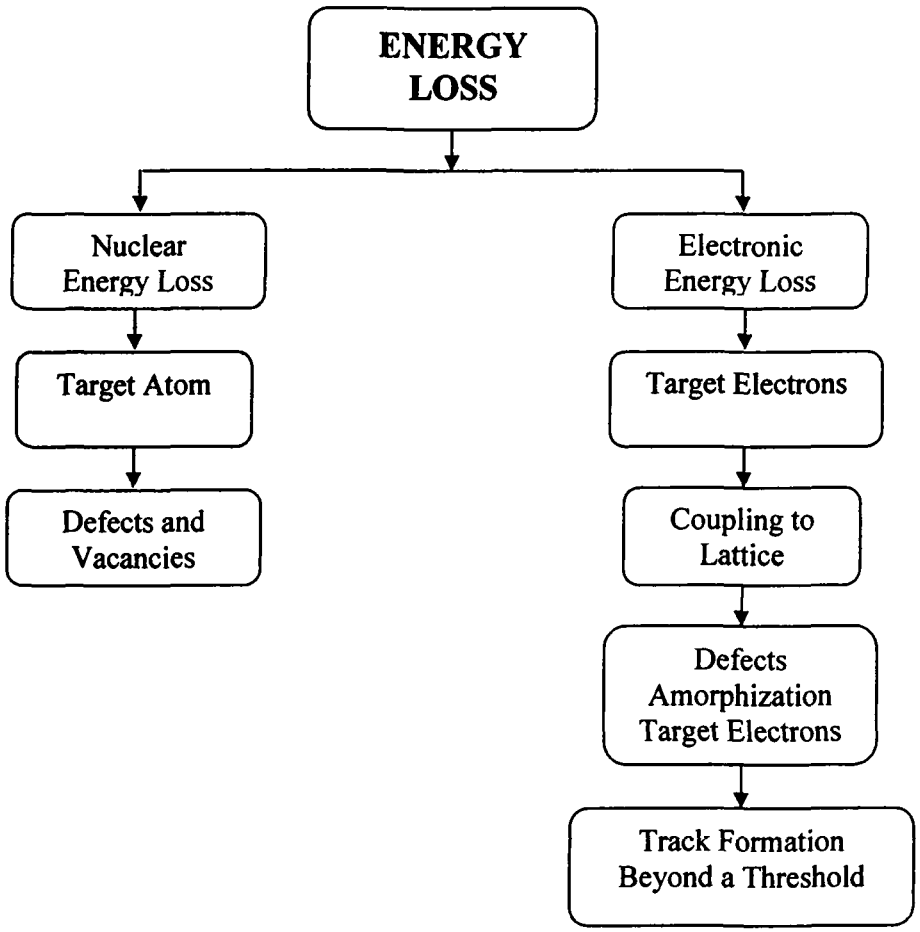

Figure 1.4: Energy Loss Process

1.4 General effects on polymer by SHI irradiation

In a wide range of polymers, the following major modifications are observed as a result of irradiation to heavy ions:

(a) Cross-linking, i.e. the formation of lateral chemical bonds between different polymer chains.

(b) Degradation, i.e. the scissoring of the main polymer chain.

(c) Gas Liberation, usually H_2 but sometimes include CH_4, CO and CO_2 and other products of side chain decomposition.

(d) Scission at branch points, the severed sections often remaining trapped within the polymer matrix.

(e) Changes in chemical structure, e.g. the production or elimination of unsaturation.

(f) End Linking and cyclization. The molecular ends newly produced by scission being active, may combine with other molecules at the side bonds leading to end linking. Monomers belonging to one and the same molecules may be linked together leading to cyclization.

(g) Changes in crystallinity in partially crystalline polymers.

1.4.1 Cross-linking and Degradation

Most of the changes in the physical properties of polymers are due to either cross linking or degradation. Cross-linking is the formation of a lateral chemical bond between two polymer molecules resulting in an increase of molecular weight of the polymer. It is generally found to occur at random, proportional to the radiation dose, so that eventually it will convert the polymer into a three dimensional network. Degradation refers to the scission of the main chain bonds resulting in a reduction of molecular weight of the

polymer. It is generally found to occur at random proportional to the dose, eventually converting the polymer into a low molecular weight material. The reduction in molecular weight can be readily followed by reduced viscosity, increased osmotic pressure and increased extent of light scattering.

Both cross-linking and degradation occur simultaneously when polymers are irradiated, but one of them predominating over the other, depending on the chemical structure of polymers. It is generally observed [21] that polymers with structure $-CH_2-CR_1R_2-$ where either R_1 or R_2 or both hydrogen atoms, predominantly crosslink; whereas others with both R_1 and R_2 as bulky side groups, predominantly degrade. The classification of polymers into cross-linking and degrading type according to this scheme is shown in the Table (1.1).

Recently, Tsuda and Oikawa [22] theoretically examined the criterion for cross - linking and degradation and found that the effect of radiation on polymers can be interpreted as chemical reactions in the excited states. Degradation occurs when little or no activation energy is required in the main chain cleavages reaction while cross - linking occurs when moderate or large activation energy is required in the main chain cleavage reaction but little or no activation energy is needed in the C – H bond cleavage reaction.

Table - 1.1

Cross-linking and degrading polymers

Cross-linking Polymers	Degrading Polymers
Polyethylene	Polyisobutylene
Polypropylene	Poly-α-methyl styrene
Polystyrene	Polymethacrylates
Polyacrylates	Polymethacrylamide
Polyacrylamide	Polyvinyl dine chloride
Polyvinyl chloride	Cellulose
Polyamides	Cellulose acetate
Polyesters	Polytetrafluoroethylene
Polyvinylpyrolidone	Polytrifluorochloroethylene
Natural rubber	Polymethacrylic acid
Synthetic rubbers (except	Poly-α-methacrylonitrile
Polyisobutylene)	Polyethylene terephthalate
Polysiloxanes	Polyoxymethylene
Polyvinyl alcohols	
Polyacrolein	
Polyacrylic acid	
Polyvinyl alkyl ethers	
Polyvinyl methyl ketone	
Polyethylene	
Chlorinated polyethylene	
Chlorosulphonated polyethylene	
Polyacrylonitrile	
Sulphonated polystyrene	
Polyethylene oxide	

1.5 Application of Polymer Irradiation

Polymers and polymerization are backbone of many industrial applications. Irradiation of polymers has been widely studied over the last few decades because it can be used to change, in a controlled way, the physical and chemical properties of polymers [23]. So, radiation processing has emerged as a powerful tool in enhancing industrial and medical applications of polymers in terms of technological improvements of properties and in providing an environmental-friendly process option [24]. Polymers with specific properties that can be achieved by using (i) traditional ionizing radiation: gamma rays, energetic electrons and protons, or (ii) non-traditional ionizing radiation: swift heavy ion beams of keV or MeV [25]. Some of their applications are

- Gamma-irradiation is used in many industrial purposes, including polymer processing and treatment of medical equipment [26-28]. Another growing application is the sterilization of food [29]. Low doses from 0.1 to 10 kGy are sufficient to preserve food products from sprouting or contamination by bacteria and mould [30].
- In biomedical applications, the surface of the polymer is modified to achieve biocompatibility; monomers are transformed into hydrogels; bioactive materials are immobilized within a polymer matrix, etc.
- Electron beam induced cross-linking of polymers is an established industrial technology, especially in the following areas[31]
  1. cross-linking of cable insulation, tubes, pipes and moulding
  2. vulcanization of elastomers
  3. processing of foam plastics
  4. heat shrink materials
- Electron induced grafting is also tacking up a prominent role in industrial applications. Properties that can be improved by grafting of polymers surfaces include: adhesion, wet ability, printability, biocompatibility, thermal stability, flammability and resistance to certain chemicals [31].

- Curing is defined as the use of electron beam or ultraviolet radiation as an energy source to induce a rapid conversion of especially formulated 100% reactive liquids to solids. Irradiation by electrons leads to free- radical or cationic polymerization and cross-linking. In industry, radiation curing is often in competition with thermal drying. The radiation process offers significant advantages over thermal process: no solvent release, reduction of the energy consumption, high production rates, smaller space requirement and only moderate temperature during curing [31]. Electron beam curing of solvents coatings, inks, paints and adhesive have gained acceptance as productive and environment technology.

- Some fluorinated polymers, such as the polytetrafluoro ethylene, show a macroscopic erosion effect, as a molecular emission of CF_3 and CF_2, induced by the incident ions. The created micro channels can be used to produce micro filters or perforated micro pipes [32].

- Hydrogenated polymers, such as polyethylene, loose hydrogen during the ion irradiation and hence become rich in carbon at high ion dose; the residual polymer presents a high chemical stability and high electrical conductivity. Processed polymers can be used to realize homocomptible surfaces or conductive channels in insulators [33].

- Polymers are often used as components in nuclear reactors, particle accelerators, radiation sources, space vehicles etc. Theses polymers may be exposed to a low level, prolonged irradiation with deleterious effect after a long period of service time. A loss of mechanical and electrical properties may have serious (negative) consequence on the functions these materials perform. In these cases, monitoring, detection and stabilization of radiation effects is of great concern [10, 34].

1.6 Radiation Induced Modification Processes in Polymers

Irradiation of polymers leads towards processes like cross-linking of the polymer chains, chain-scission, oxidative degradation and changes in unsaturations, evolution of gaseous products etc. [35-38]. The extent of these depends upon the nature of the polymer, irradiation conditions and post irradiation conditions. The irradiation conditions

include the parameters of the bombarding particle, atmosphere and temperature. Under irradiation, the energy is transferred to the medium in ionizations and excitations. Having absorbed energy, polymers suffer bond cleavages, giving rise to non-saturated fragments called "free radicals" and these are responsible for most of the chemical transformations observed in polymers [39]. Figure 1.5 illustrates various functional chemical entities created by irradiation [40].

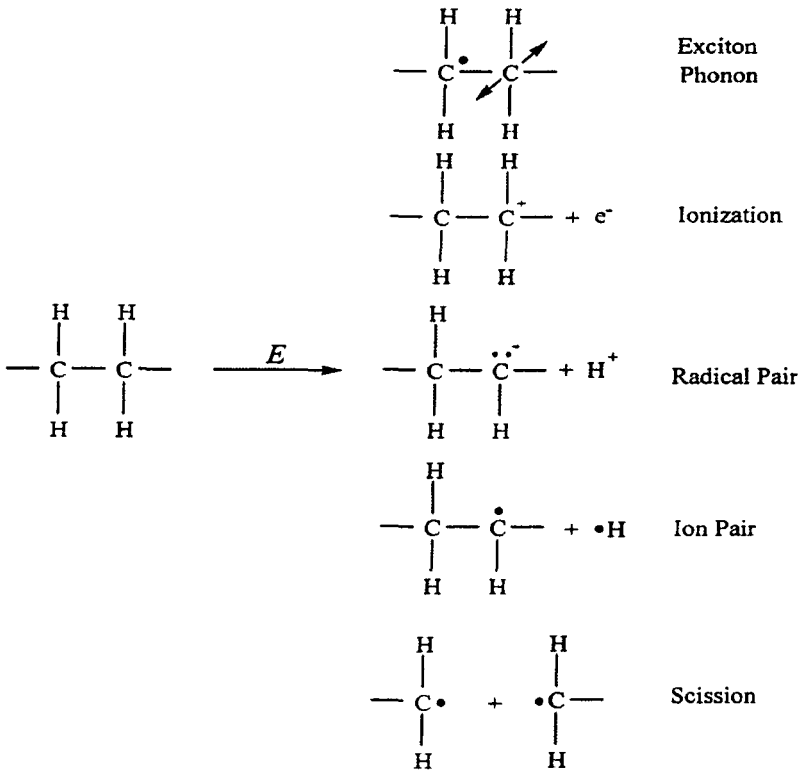

Figure 1.5: Typical effects of irradiation, which include electronic excitation, phonons, ionization, ion pair formation, radical formation, and chain scission [41]

1.7 Significance of Radiations in the field of material Science

Investigation on the effects of ion irradiation on polymers has become, in recent years, a subject of interest to both scientists engaged in basic research and engineers with practical applications. For scientists, heavy ion irradiation offers an extremely powerful tool to modify polymers under strictly controllable conditions and to study the effect of such modifications on the resultant physical, chemical, structural and the other properties. Industrial, radiation induced polymerization; radiation grafting and radiation curing of polymers constitute a few among the several other areas where radiation processing

appears to be either economically competitive or technologically advantageous, as compared to the conventional methods. In space technology, the effects of radiation on space vehicle components now represent an important aspect of engineering specification and design. Finally, the increasing importance of nuclear power has also added to the demand for materials with special performance characteristics in nuclear environments.

Irradiation of polymers results in a number of physical and chemical changes, both temporary and permanent. These modified properties are not due to any change in nuclear structure, but arise from new electronic configurations and hence new chemical reactions. Many of these reactions can be initiated by chemical means, but high-energy ion radiation has a number of distinct advantages. It can penetrate and induce reactions in solid state, over a wide range of temperatures and environments. This subject has been exhaustively reviewed in the literature [42, 43].

Many field such as micro-electronics, biology and medicine, surface and membrane technology, magneto-optics and low temperature physics require a high degree of geometric control on a microscopic scale. Ion irradiation offers a possibility to modify the properties of the materials in a controlled way on microscopic scale. Ionizing radiation have a definite range of penetration, a high local confinement of deposited energy and can be stored in definitely in many insulators and can be used to initiate a phase transformation process that modifies the material along the latent track. One ion suffices to induce- physically and chemically a submicroscopic change in the target material and thereby can render it susceptible to the development process [10]. A lot of work in the field of ion beam treatment has been carried out to investigate the interaction of charged particles with matter. The application of ion beams now a days range from the use of low energy ions in the field of surface technology to the application of relativistic heavy ions in radiation therapy.

1.8 Motivation

The motivation behind the present work is to characterize swift heavy ion induced modifications in the optical, chemical, structural, electrical, surface, thermal and free volume properties of the polymers using UV-Vis spectroscopy, Fourier Transform Infra-Red (FTIR) Spectroscopy, X-Ray Diffraction, Die electric Constant study and Positron Annihilation Lifetime Spectroscopy (PALS) and Doppler Broadening Spectroscopy (DBS) etc.

References

[1] R. J. Young and P.A. Lovell, in "Introduction to polymer" 1, Chapman and Hall, India (1991).

[2] D. Fink, Fundamentals of Ion –Irradiated Polymer, Springer (2004).

[3] P. Bahadur, N.V. Sastry, Principles of Polymer Science, Narosa Publishing House (2007).

[4] Fred W. Billmeyer, Jr, John Wiley and Sons, 1994.

[5] Gowariker V.R., Vishwanathan N.V. and Sreedhar J. in Polymer Science, 1986, New Age International (P) Ltd, Publishers.

[6] G.S. Misra, Introductory Polymer Chemistry, 1993, Johan Wiley and Sons.

[7] Rodriguez F. Principles of Polymer Systems, (1974) 26-49.

[8] F. Khoylou and A. A. Katbab, Radia. Phys. and Chem.,42 (1-3)(1993)219.

[9] Radiation –induced changes affecting polyester based polyurethane binder, By Sujita Basi pierpoint, Ph.D. Thesis, University of Maryland at college Park.(2002).

[10] R. Sophr, Ion Track: Principles and applications, Eds. K. P. Bethge Viewag, Frankful (1990).

[11] Fleischer R. L., Price P.B. and Walker R.M., J. Appl. Physics, 36 (1965) 3645.

[12] Heckman H.H., Perkins B.L., Simon W.G., Smith F.M. and Barkas W. (1960), Phys. Rev., 117,544.

[13] N. Bohr, Philosophical Magazine 25 (1913)10.

[14] H. A. Bethe, Ann. Physik (1930)5325

[15] F. Bloch, Ann. Physik16 (1933)287.

[16] J. Lindhard, M. Scharff, Physical Review 124(1961)128.

[17] J. Lindhard, Danske Mat. Fys. Medd.34(1965)1.

[18] J. lindhard , M. Scharff, H. E. Schiott, (Notes on atomic collision, II) Mat.-fys. Medd 33, 14 (1963)1.

[19] J. F. Ziegler, J.P. Biersack, U. Littmark, The stopping power of ions in solids, Pergamon Press, Oxford, (1980).

[20] G. Szenes, F. Pàszti, Á Pèter and A. I. Popov, Nucl. Instr. and Meth. B166/167(2004)949.

[21] Miller A. A., Lawton E. J. and Balwit J. S., J. Polym. Sci., 14, 503 (1954).

[22] Tsuda M. and Oikawa S., J. Polym. Sci. Polym. Chem. Ed., 17, 3759 (1979).

[23] P. Mazzoldi, G. W. Arnold (Eds.), Ion Beam Modifications of Insulators,

Vol. 2, Elsevier, Amsterdam (1987).

[24] R. M. Iyer and V Markovic, Nucl. Instr. and Meth.B105 (1995)238.

[25] G. Marletta, S. Pignataro, A. Toh, I. Bertoti, T. Szekey, B. Kessler, Macro. 24 (1991) 99.

[26] A. Singh J. Silverman, Radiation Processing of Polymers, Hanser Verlag, New York, 1992.

[27] M.S. Jahan, K.S. McKinney, Nucl. Instr. and Meth.B151 (1999)207.

[28] D. J. Carlson, S. Falicki, J.M. Cooke, D.J. Grosciniak, Prog. Pacific Polym. Sci. 3(1994)171.

[29] C.H. McMurray, M.F. Petterson, E.M. Stewart, Chem. Ind.(1998)433.

[30] J. Mallègol, D.J. Carlsson and L. Deschénes, Nucl. Instr. and Meth.B185 (1-4)(2001)283.

[31] R. Mehnert, Nucl. Instr. and Meth.B105 (1995)348.

[32] B. A. Banks, in: Ion bombardment modifications of surfaces, Eds. O. Auciello and R. Kelly (Elsevier, Amsterdam, 1984)399.

[33] T. Venkatesan, L. Calcagno, B. S. Elman, G. Foti, in: Ion bombardment modification insulators, Eds. P Mazzoldi and C.W. Arnold (Elsevier, Amsterdam, 1987)p-301.

[34] S. A. Barenberg, MRS Bulletin 16 (9) (1961) 26.

[35] G. Marletta, F. Iacona, Nucl. Instr. and Meth.B46 (1990)295.

[36] V. Kulshrestha, K. Awasthi, N. K. Acharya, M. Singh P.V. Bhagwat, Y. K. Vijay, Polymer Bulletin 56(2006)427.

[37] L. Calcagno, G. Compagini and G. Foti, Nucl. Instr. and Meth.B65 (1-4) (1992) 413.

[38] E. Balanzat, S. Bouffard, A. Bouquerel, J. Devy and Chr. Gaté, Instr. and Meth. B116 (1-4) (1996)159.

[39] C. Trautmann, K. Schwartz and T. Stecknreiter, Nucl. Instr. and Meth.B156 (1999)162.

[40] A. Chapiro, Nucl. Instr. and Meth.B32 (1988)111.

[41] E. H. Lee, Nucl. Instr. and Meth.B151 (1999)29.

[42] Wolform Schnabel, in Jellinek H. H.G. (Ed.) 'Aspects of degradation and stabilization of polymers', Elsevier (1978).

[43] S. W. Shalbay, J. Polym. Sci., Macromolecular Reviews, 14 (1979) 419.

Chapter-II

Chapter II

Experimental Techniques

2.1 Introduction

This Chapter deals with brief description of the equipments with their relevant details and specifications used in the experiments carried out and various characterization techniques for the measurements employed in this thesis. The present work involves the following stages:

[1] The materials: Polymers studied and their chemical structure.

[2] Brief description of 15 MV Pelletron Accelerator at Inter University, Accelerator Centre (IUAC), New Delhi and heavy ion beams from it.

[3] Material science chamber for irradiation

[4] Positron Source.

[5] Positron Annihilation Lifetime Measurements.

[6] Ultra Violet (UV-Vis.) Spectroscopy

[7] Fourier Transform Infra-Red (FTIR) Spectroscopy.

[8] X-Ray Diffraction (XRD) study

[9] Dielectric constant measurements

2.2 The materials

The polymeric materials investigated in the present study are:

(i) Makrofol-KG Polycarbonate

(ii) Makrofol-N Polycarbonate

(iii) Lexan Polycarbontae

(iv) Polyethersulphone (PES)

(v) Polyamide Nylon-6

(vi) Polyamide Nylon-6, 6

(vii) Polytetrafluoroethylene (PTFE)

(viii) Polyethylene terephthalate (PET)

(x) Polypropylene (PP)

(xi) Polymethyl methacrylate (PMMA)

(xii) Polystyrene (PS)

(xiii) Polyvinylidene fluoride (PVDF)

(xiv) Low Density Polyethylene (LDPE)

(xv) Polyethylene Oxide –salt (PEO-salt)

(xvi) Polyanilinegraphite (PANI-GRP) pellets

2.2.1 Makrofol-KG, Makrofol-N and Lexan Polycarbonates

Makrofol polycarbonates manufactured by a casting process in the form of thin sheets were obtained from Bayer AG, Lever Kussen, West Germany. (C_{16} H_{14} O_3) as Lexan polycarbonate was manufactured by General Electric Co. of U. S. A. Polycarbonate (PC) or specially polycarbonate of bisphenol- A, is an amorphous polymer with attractive engineering properties including high impact strength, low moisture absorption, good dimensional stability and high light transmission. Polycarbonate gets its name from the carbonate groups in its backbone chain. However, these polycarbonates have different type of behavior. Different types of Makrofol polycarbonates such as Makrofol-KG, KL, E, and N etc. are produced by different manufacturing processes and are expected to behave in differently [1]. Out of these Makrofol-KG contains a light amount of a colour dye while Makrofol-N is a trade name of yellow polycarbonate.

Makrofol polycarbonate plastics (much useful as heavy ions as well as fission track detectors) were originally used as insulators in electrical devices. Makrofol-KG, KL

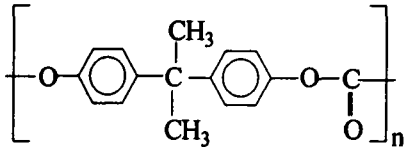

and N are not sensitive to particles having Z > 2 and Z > 8 respectively [2]. Makrofol-KG, KL and N are not sensitive to α-particles and other lighter charged particles. The shape of tracks produced by heavy ions and fission fragments are needle like with a slight spread towards its tail. The chemical structure of Polycarbonate (PC) is

2.2.2 Polyethersulphone (PES)

Aromatic polymers such as Polyethersulphone (PES) are finding extensive use in electronics, in particular in sensor applications. The physical properties of these films may be tailored as has been shown that ion irradiation improves the sensor properties of PES films[3-5]. PES flat films were procured from Good Fellow, Cambridge Ltd., England (U.K.) and have the structure:

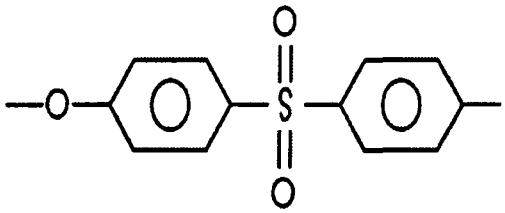

2.2.3 Polyamide Nylon– 6 (PN-6) and Polyamide Nylon-6,6 (PN-6,6) Polymers

These polymers were obtained from Good fellow, Cambridge Limited, England. The polyamides are a family of thermoplastics e.g. Polyamide Nylon–6, Nylon-6,6 and Nylon-610 which are among the toughest engineering plastics with high vibration–damping capacity, abrasion resistance, inherent lubricity and high load capacity for high speed bearings. They have a low coefficient of friction and good flexibility. Pigment – stabilized types are not affected by ultraviolet radiation and have good chemical resistance. Polyamides are used extensively as high performance plastics materials

because of their unique combination of superior mechanical, electrical, chemical and thermal properties. Applications include bearings, electrical insulators, gears, wheels, screw fasteners, cams, latches, fuel lines and rotary seals. The molecular structure of Polyamide Nylon-6, polymer used for present study is

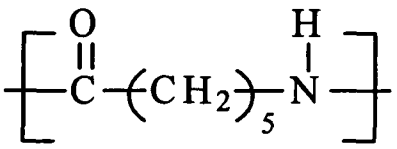

2.2.4 Polytetrafluoroethylene (PTFE)

Polytetrafluoroethylene (PTFE) has been classified for many years as a polymer that undergoes main chain scission by irradiation [6]. In some recent papers [7-10] it is described that PTFE is cross linked by ionizing radiation in an oxygen-free atmosphere at a temperature above its melting point. Therefore, the effect of irradiation on high crystalline PTFE (at room temperature) has to be smaller than an amorphous PTFE (in the melt). Additionally further qualitative changes will be expected by irradiation of molten PTFE. Lappan et al [11] have also studied the behavior of PTFE on such special irradiation conditions. PTFE Polymer was procured from Good fellow, Cambridge Ltd. England (UK). The chemical structure of PTFE is:

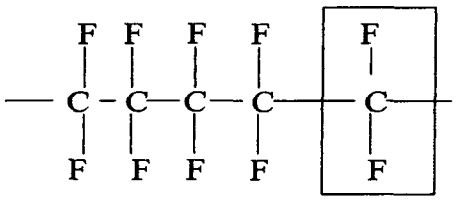

2.2.5 Polyethylene terephthalate (PET)

Polyethylene terephthalate (PET) is a polyester having a high melting point due to the presence of aromatic ring and a very good mechanical strength. It is semi crystalline in nature and is resistant to heat and moisture and virtually unattacked by many chemicals. It has extensive use in textile fibers. The changes brought about in physico-chemical properties of PET as a result of exposure to light as well as heavy ions have been a subject of investigation for many years. Mishra et al [12] studied the changes in its

thermal and chemical properties by exposing it to swift light ions, protons. Steckenreiter et al [13] did an in depth study of chemical modification of PET exposed to Swift Heavy Ions of molybdenum and krypton. Recently Liu et al [14] and Zhu et al [15] have extended its study by exposing it to heavy ions of argon, krypton, xenon and uranium having energy in the range of 1.4-2.7 GeV. Singh et al [16] too have also recently reported a study on the electrical and structural properties of PET films modified by 50 MeV lithium ions PET Polymer was procured from Good fellow, Cambridge Ltd. England (UK). The chemical structure of PET is.

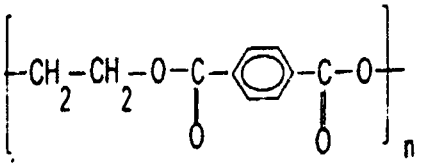

2.2.6 Polypropylene (PP)

Polypropylene is a vinyl polymer and is similar to polyethylene only that on every other carbon atom in the backbone chain has a methyl group attached to it. Polypropylene can be made from the polymerization of monomer propylene. Polypropylene is the lightest known industrial polymer, and it has high strength-to- weight ratio. Being highly crystalline, it exhibits high stiffness, hardness and tensile strength and has excellent mechanical and dielectric properties. PP in the form of flat films was procured from Good Fellow, Cambridge Ltd. England (U.K.). The chemical structure of PP is.

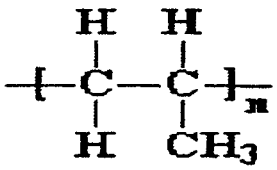

2.2.7 Polymethyle methacrylate (PMMA)

Molecular weight of a polymer is of major importance in its synthesis and application. Interesting and valuable mechanical properties that are uniquely associated with polymeric materials are a consequence of their high molecular weights [17]. Polymethyl methacrylate (PMMA), is completely amorphous but it has high strength and excellent dimensional stability due to its rigid polymer chains. PMMA has exponential

optical clarity, very good weather ability, and impact resistance. It is an excellent material which is easy to structure and has the desired optical properties [18]. PMMA, known as a positive photo-resist for its degradation upon irradiation, has been the subject of investigations in radiolysis than many other polymers. This was partly due to a growing interest in the application of PMMA in ion beam lithography, in the semiconductor industry [19]. Besides wide range utilization of PMMA polymer such as its extensive use in expanding optical networks in the field of telecommunication, PMMA polymers have many application such as diffusers, indoor and outdoor lighting, lenses, and contact lenses. PMMA Polymer was procured from Good fellow, Cambridge Ltd. England (UK). The chemical structure of PMMA is.

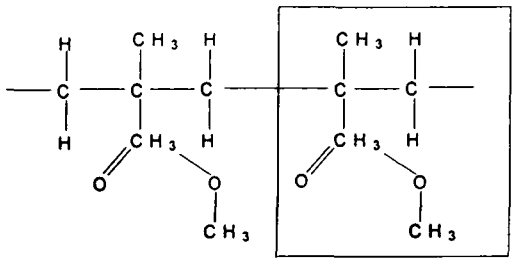

2.2. 8 Polystyrene (PS)

Polystyrene is polymer of having wide industrial applications. Its radiation chemistry has been extensively studied. It is the most radiation resistant of the polymers and hence occupies a unique position in the study of radiation effects. Polystyrene sheets were obtained from Good fellow, Cambridge Limited, England. The molecular structure of polystyrene is:

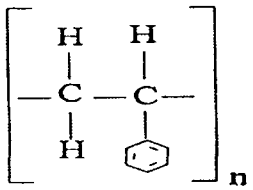

2.2.9 Polyvinylidene fluoride (PVDF)

PVDF is a specialty plastic material in the fluoropolymer family. it is used generally in applications requiring the highest purity, strength, and resistance to solvents, acids, bases and heat and low smoke generation during a fire event. Compared to other fluoropolymers, it has an easier melt process because of its relatively low melting point. It

has a relatively low density and low cost compared to the other fluoropolymers. It is available as piping products, sheet, tubing, films, plate and an insulator for premium wire. It can be injected, molded or welded and is commonly used in the chemical, semiconductor, medical and defense industries, as well as in lithium ion batteries. PVDF paints have extremely good gloss and color retention, and they are in use on many prominent buildings around the world, e.g. the Petronas Towers in Malaysia and Taipei 101 in Taiwan, as well as on commercial and residential metal roofing. PVDF membranes are used for western blots for immobilization of proteins, due to its non-specific affinity for amino acids The (PVDF) in the form of flat films was procured from Good Fellow, Cambridge Ltd. England (U.K.). The chemical structure of PVDF is

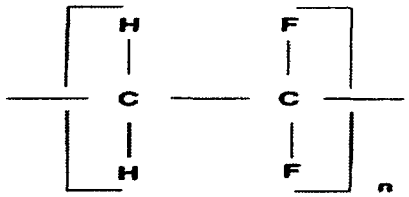

2.2.10 Low Density Polyethylene (LDPE)

Polyethylene is a vinyl polymer, made from the monomer ethylene. Vinyl polymers are the polymers made from vinyl monomers i.e. small molecules containing carbon-carbon double bonds.

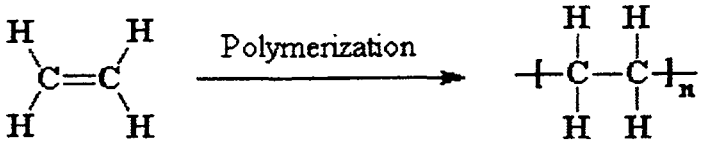

Ehtylene Polyehtylene

So, a molecule of polyethylene is nothing more than a long chain of carbon atoms, with two hydrogen atoms attached to each carbon, like,

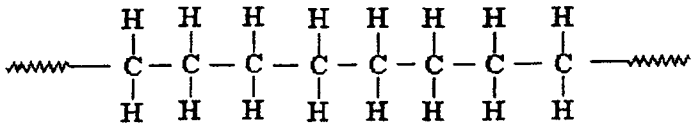

Sometimes some of the carbon atoms, instead of having hydrogen attached to them will have long chains of polyethylene attached to them. Polyethylene is of two types (i) Branched polyethylene, known as low density polyethylene or (LDPE).(ii)

Linear polyethylene, known as high density polyethylene or (HDPE); as shown in Figure 2.1.

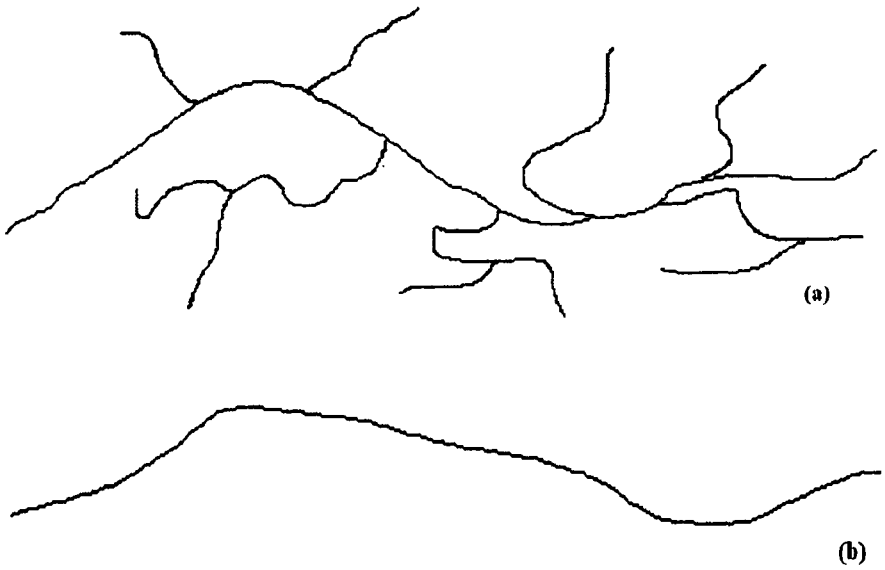

Figure 2.1: (a) Branched polyethylene or (LDPE) (b) Linear polyethylene or HDPE

Polyethylene is one of the common polymers utilized in various fields; engineering, medical, and agricultural and even our daily life. LDPE Polymer was procured from Good fellow, Cambridge Ltd. England (UK).

2.2.11 Polyethylene Oxide –salt (PEO-salt)

Solution-cast films each of total mass 3g of PEO (BDH, England) and of average molecular weight 600 Kg/mol complexes with NH_4ClO_4 (Fluka AG, 99.5% purity) were prepared in salt concentration of 17% and 19%. Pure PEO is non conducting while its complex $PEO_{(1-x)}$ $(NH_4ClO_4)_x$ with weight fraction x = 17%, 19% is an ion conducting polymer.

2.2.12 Polyaniline-graphite (PANI-GRP) pellet

Synthesis and investigation of electro physical properties of polymer composites based an polyconjugated matrices and graphitized carbon species, is currently a very

popular topic in the field of material science. PANI-graphite polymer composites are regarded as promising material for use in lithium batteries, super capacitors, actuators and sensors etc. Conjugated polymer PANI was prepared as a product of oxidative polymerization of aniline. The reaction temperature was in the range 0-10°C. Polyaniline chloride was filtered, washed with double distilled water and dried at 45^0 C for 24 hrs and then treated with 3% aqueous ammonia. Polymer composite based on polyaniline (PANI) and graphite were prepared using powder technology whereby the polymer and filler powders were mixed at room temperature in 1:2 ratio.

2.3. Irradiation of Polymers by Swift Heavy Ion Beams

2.3.1. 15 UD Pelletron Accelerator at Inter University Accelerator Centre (IUAC), New Delhi.

A schematic diagram of IUAC Pelletron accelerator is shown in Figure 2.2. The IUAC Pelletron accelerator is 15 UD tandem Van de Graff electrostatic accelerator [20]. It is capable of accelerating any ion from proton to uranium (except the inert gases) in the energy range from a few tens of MeV to a few hundreds of MeV, depending on the ion species. The accelerator is installed in vertical geometry in a stainless steel tank which is 26.5 meter high and has 5.5 meter diameter. In the middle of the tank there is a high voltage terminal which can hold potential from 4 to 16 MV. The terminal is connected to the tank vertically with ceramic titanium accelerating tubes. The tank is filled with high dielectric constant SF_6 gas at 6-7 atmospheric pressure to insulate the high voltage terminal from the tank wall. A potential gradient is maintained through the accelerating tubes from the ground potential, and from the terminal to the ground potential at the bottom of the tank. Negative ions of suitable energy from source of negative ions by Cesium Sputtering (SNICS) ion source are injected into the accelerator and are accelerated towards the positive terminal. In the first stage of acceleration, the singly charged negative ions from the ion source are accelerated from ground potential to the terminal at high positive potential V. The energy gained in the process is eV. The beam is then made to pass through a stripper foil where the ions are stripped off the electrons

thereby making them positive ions. The average charge of the ion depends upon the type of the ion and the terminal voltage.

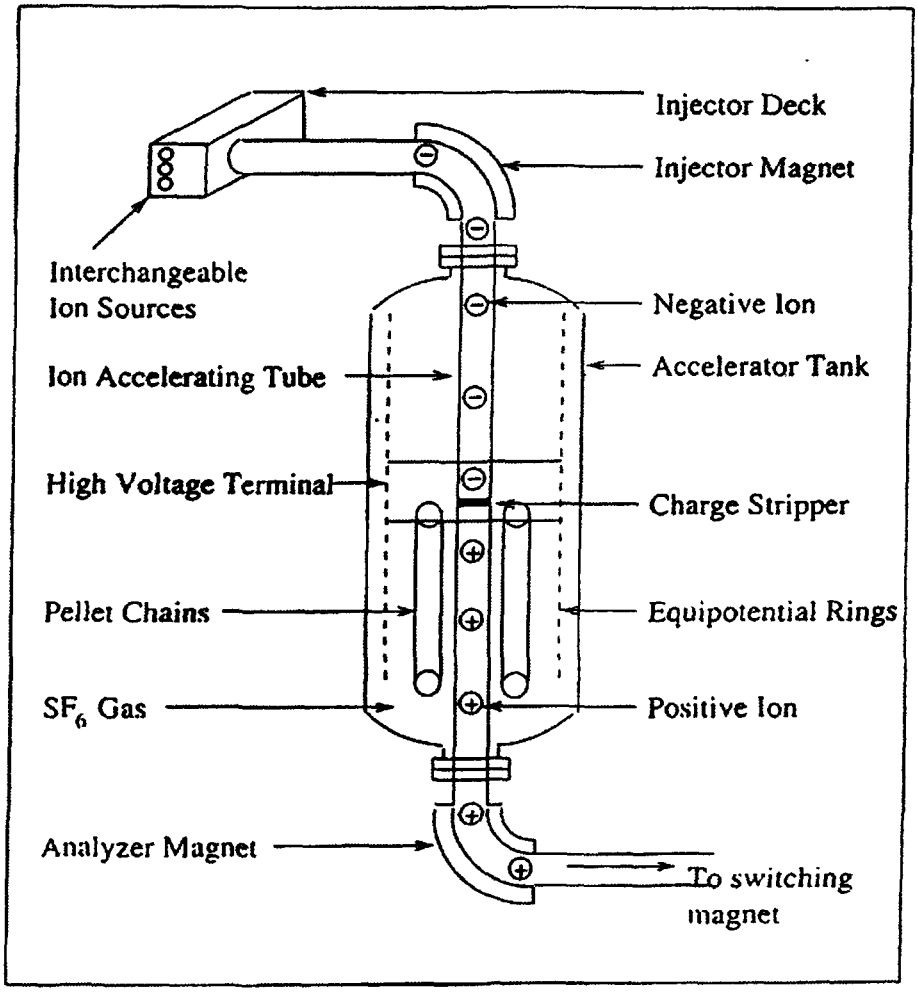

Figure 2.1: A schematic diagram of NSC Pelletron Accelerator

If q is the charge state on the positive ions after passing through the stripper foil, the energy gained by accelerating it from the terminal to the ground potential should be qeV. Thus after passing through the two stages of the acceleration, the final energy of the ion in electron volts is given by

$$E = (q+1)\ V \qquad (2.1)$$

These high-energy ions are then passed through the analyzing magnet and energy slit which selects the particular ions of the desired energy. The beams of ions are then directed towards the desired experimental area with the help of a seven port-switching magnet.

2.3.2. Chamber for high fluence irradiation at IUAC

This high vacuum chamber (38 cm diameter) has a facility for temperature controlled (liquid cooled) multiple sample holders having provision for linear movement of 120 mm and a rotation of 360^0 shown in photograph 2.1. A vacuum of 10^{-7} m bar is maintained by using a diffusion pumping system filled with a LN_2 trap. A remote controlled target holder can be positioned perpendicular to the beam line for irradiation. Various samples can be irradiated in an experiment using bellow-sealed linear movement of the holder by 140mm. Material science beam line is used for ion fluence up to ~ 10^{13} ions/cm^2. For irradiation one has to observe whether ion beam is falling at the desired place on the quartz or not, only after that the beam is allowed to fall on the samples to be irradiated. The rectangular ladder used to fix up seven samples contains four faces and auto control switches can change its position. A CCTV camera was also attached to one of the ports of chamber for viewing the sample position. XY scanner can scan the beam on the target for uniform irradiation.

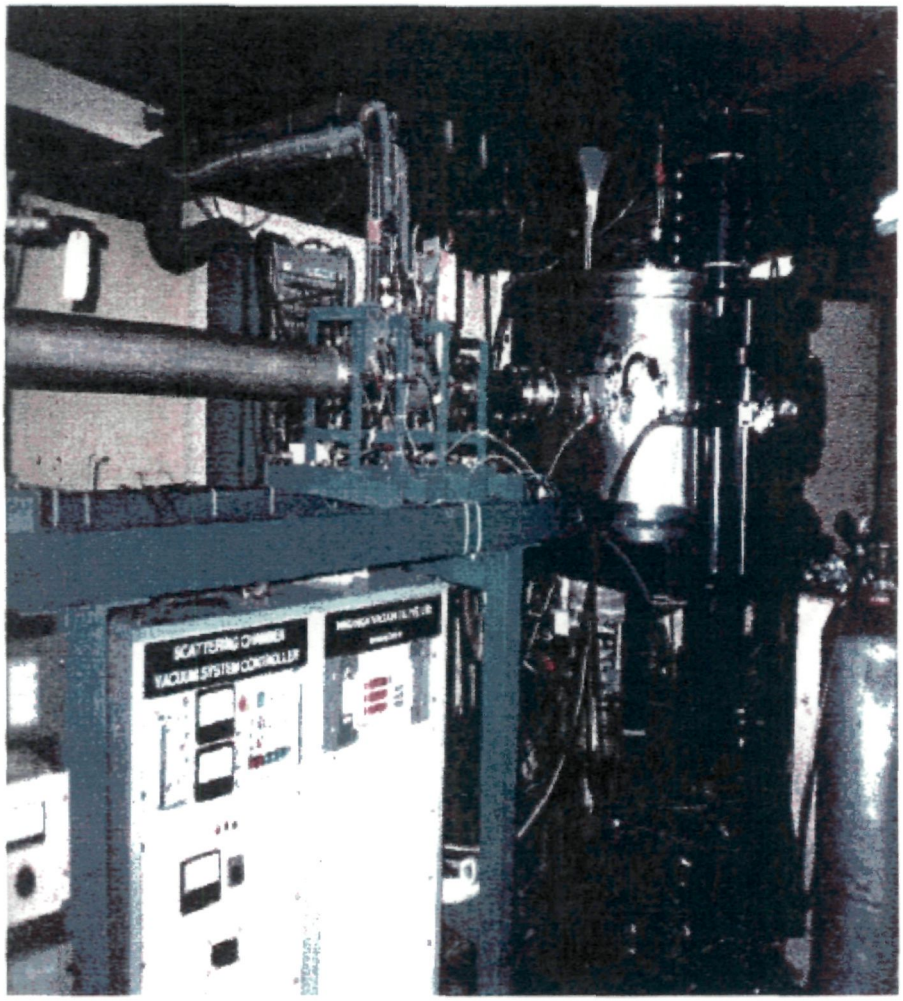

Photograph 2.1: General Purpose Scattering Chamber installed at 15^0 beam line at Inter University, Accelerator Center, New Delhi

2.4 Characterization Techniques

2.4.1 Positron Annihilation Spectroscopy

2.4.1.1 Positron

Positron was discovered by Anderson [21] on 2nd August, 1932 from the length of the tracks in the Wilson cloud chamber. Anderson concluded that he had observed the particle with same mass as that of electron but of opposite charge i.e. +e. Hence Positron is the anti particle of the electron.

2.4.1.2 Positron Annihilation

The damage caused by the passage of energetic ion modifies the free volume properties of the polymeric material. The concept of free volume has significant importance for the gas permeation properties of polymeric membranes as well as for other related subjects of polymer science. The positron annihilation lifetime spectroscopy is capable of probing free volumes directly. The atomic scale free volume holes are detected on the basis that the positronium (Ps) atoms are formed and localized in the free volume holes [22]. The ortho-positronium (o-Ps) lifetime has a strong correlation with the size of the free volume.

Now a days, Positron annihilation has become established as a useful tool in the field of material science and is successfully applied for the investigation of defect structures present in metals, alloys and technologically relevant materials such as polymers. Positron-electron pair is unstable and annihilates by emitting two γ-photons of energy 511 KeV each in opposite direction, since the linear momentum is to be conserved.

Positron annihilation is undertaken to the study of Fermi surface of the metals and alloys and also it has been found that positron annihilation is quite sensitive to the lattice defects and is a common technique used in the study of lattice defects, phase transitions and liquid alloys. Positron electron pair can also be formed as a quasi-stationary state called positronium. It is analogues to the hydrogen atom. Positronium is found in the Para state called Para-positronium (p-Ps) and ortho state called ortho-positronium (o-Ps). Para-Ps will decay through two γ- photons and the ortho-Ps will decay by three γ-photons. Ps is generally not formed in metals. Positron annihilation lifetime spectroscopy provides direct information about the dimension, content and hole size distribution of the free volume in polymers. The Positron annihilation technique has also made its entry in the field of semiconductor technology and the positron annihilation measurement techniques (lifetime, Doppler-broadening and angular correlation) integrate a large number (often~10^6) of annihilation events. Hence today this technique has become established as a useful tool in material science and has been successfully applied for the investigation of defects structures present in technologically relevant materials like polymers.

2.4.2 Positron Annihilation Lifetime Spectroscopy (PALS)

The Positron annihilation Spectroscopy is one of the most important tools for the study of defect in solids. Almost all experiments use the properties of the two-gamma annihilation reaction.

$$e^+ + e^- \rightarrow 2\gamma \qquad (2.2)$$

when a positron with an energy of few hundreds of KeV, e.g. from nuclear decay from radio-isotopes such as ^{22}Na enters molecular solids, it interacts with the molecules through elastic collision processes. It reaches the thermal energy in a few picoseconds by a succession of ionizing collisions, electron hole excitation and phonon interactions. For the period of thermalization and at nearly thermalized stage, a positron captures an electron from the surrounding medium and forms an atom of positronium (Ps). Thus the

bound state of positron-electron pair is formed similar to a hydrogen atom. Therefore, during its lifetime, the positron may exist in both positron and Ps states in molecular solids. The polymeric materials have local free volumes which have the radius of few Å. These are the favorable sites where the positron and Ps atoms are localized before annihilation [23, 24]. It is schematically shown in the Figure 2.2. In the polymeric material, the positron has following two possible states at the time of annihilation

(i) Free (delocalized) and /or localized positron state

(ii) Free and /or localized Ps state.

The localization sites are free volume holes which are more favorable sites than the bulk for positrons and Ps. The Positron Annihilation Spectroscopy probes only free volume regions and is not interfered by the bulk properties of the polymeric material [26]. The ground state of Ps atom has two spin states: (i) Singlet, $1\ ^1S_0$ state, or an anti parallel spin state, called para-positronium. (p-Ps) (ii) triplet, $1\ ^3S_0$ state or a parallel spin state, called ortho-positronium (o-Ps). The energy splitting is only 8.4×10^{-4} eV, the singlet state being the lower one. Accordingly, in the absence of ortho-para conversion, ¼ of the positronium atoms are in the singlet state and ¾ in triplet state.

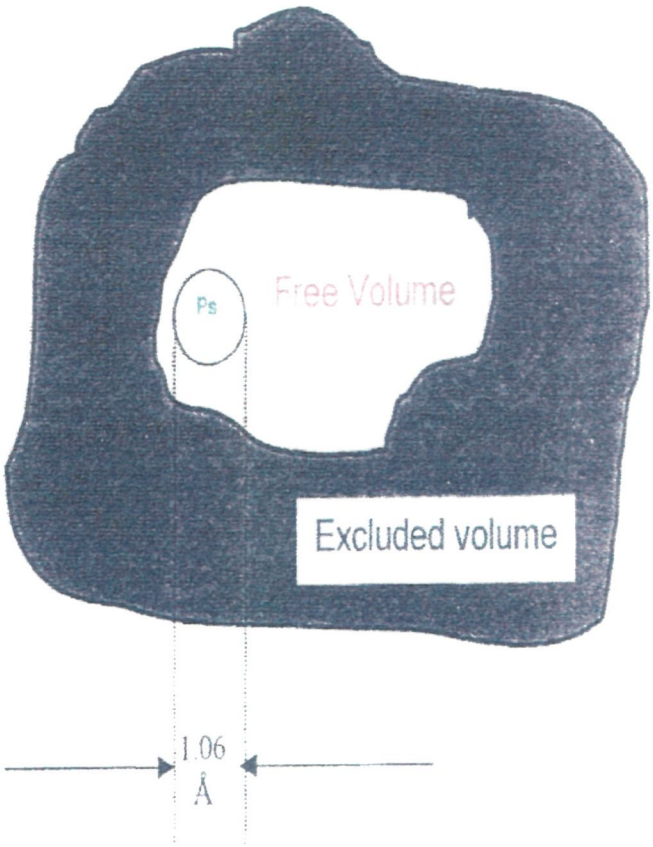

Figure 2.2: Schematic view of Ps localization in free volume holes in a Polymeric material [25]

The para-positronium in free space annihilates with mean life of 125 ps, by emitting 2γ-rays of 511 KeV each in opposite directions whereas o-Ps annihilates in vacuum with mean life of 142ns by emitting 3γ-rays (continuous energy spectrum). The o-Ps lifetime in condensed matter is considerably smaller than the vacuum value of 142 ns, because of the pick-off annihilation of positron by surrounding electrons of appropriate spin orientations (anti-parallel one) via two-quantum emission. The lifetime of the o-Ps confined in the local free volume of the polymers lies typically between 2 to $5x10^{-9}$ s. [24, 27-31].

The positron lifetime can be registered as a time difference between the emissions of 1.27 MeV γ-quantum generated almost simultaneously with the positron in ^{22}Na isotope which is the most commonly used positron source and one of the 0.511 MeV annihilation γ-quanta Figure 2.3.

The lifetime spectrum of polymeric material is conventionally described by a sum of discrete exponentials:

$$N(t) = \sum_{n} I_i e^{-\lambda_i t} \qquad (2.3)$$

where n is the number of exponential terms, I_i and λ_i representing the number of positrons (intensity) and the annihilation rate respectively for the annihilation from the i_{th} state. The positron annihilation rate, λ_i is the reciprocal of positron mean lifetime, τ_i. The PAL spectrum is fitted by a finite number of component terms, n, using the computer codes [29, 32]. For polymers n=3 is selected to fit the observed lifetime spectrum. A typical positron lifetime spectrum in polytetrafluroethelene, commercially known as Teflon is shown in Figure 2.4. The three components which appear in the lifetime spectrum are attributed to the annihilation of p-Ps, free positrons (not Ps) and o-Ps. The shortest component, τ_1 = 0.13±0.03 ns with intensity I_i = 7-20 %, is attributed to p-Ps. The intermediate component, τ_2 =0.4-0.5 ns and the intensity I_2 = 40-60 %, is attributed to the direct annihilation of positrons. The longest component, τ_3 = 2-5 ns and intensity between 10-30 %, is attributed to o-Ps annihilation in free volumes. The o-Ps lifetime is found to sensitively depend on the size of the free volume [34-35].

2.4.3 Positron Annihilation Spectroscopy in Polymers

Positron Annihilation Spectroscopy (PAS) has become established as a useful tool as almost certainly the most valuable and winning technique for the direct assessment of the free volume in polymers. PAS is capable of determining the local hole size and free volume fractions in polymers without interfering significantly with the bulk of the polymers. PAS has also been developed to be a quantitative probe of the free volume. It also gives detailed information on the distribution of free volume hole size in the range from 1 to 10 Å. The annihilation of positrons in condensed matter like polymers provides a unique way of obtaining information about the internal structure of material. This information is transmitted through γ-rays, emitted when the positron annihilates in the material. The internal structure of the material may be probed by measuring three fundamentally different quantities:

- Angular correlation between emitted γ-rays,
- The energy distribution of the γ-rays
- The lifetime distribution of Positron.

Thus the Positron Annihilation Spectroscopy is a family of three experimental techniques:

- Angular Correlation of Annihilation Radiation (ACAR)
- Doppler Broadening Spectroscopy (DBS)
- Positron Annihilation Lifetime Spectroscopy (PALS)

These three methods of positron annihilation are shown in Figure 2.3. Because energy and momentum are conserved in the annihilation process, the two γ – rays resulting from the usual electron–positron pair annihilation each have an energy equal to the rest-mass energy of an electron or positron (m_oc^2 = 511 keV) ± ΔE where ΔE is an energy shift. The two γ–rays nearly propagate in opposite directions ± an angular deviation θ, as shown in Figure 2.3 the deviations ΔE and θ arise from the net momentum of the annihilating positron-electron pair. However, since the positrons have only thermal energies just prior to annihilation, the values of ΔE and θ corresponded only to the momenta of the annihilating electrons. All these techniques have recently been applied to polymers. In the present study PALS has been used to investigate modifications in free volume holes in the polymers induced by the ion bombardment.

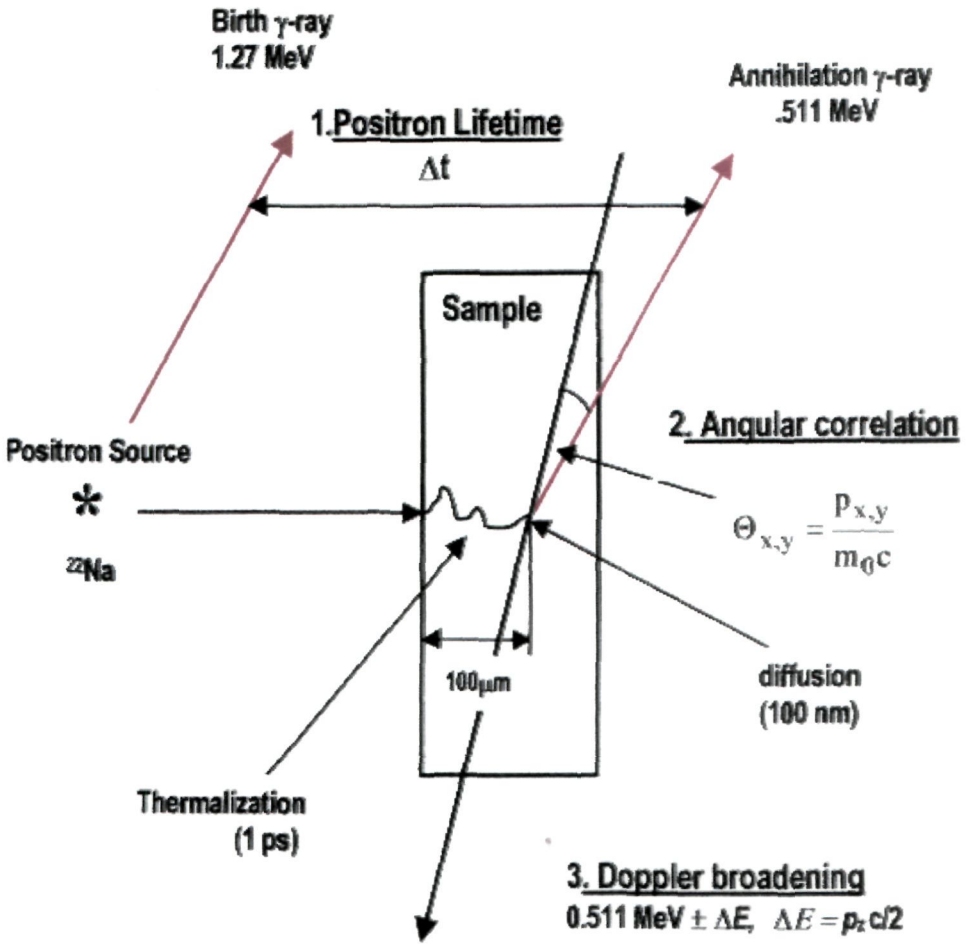

Figure 2.3: Three methods of positron annihilation.

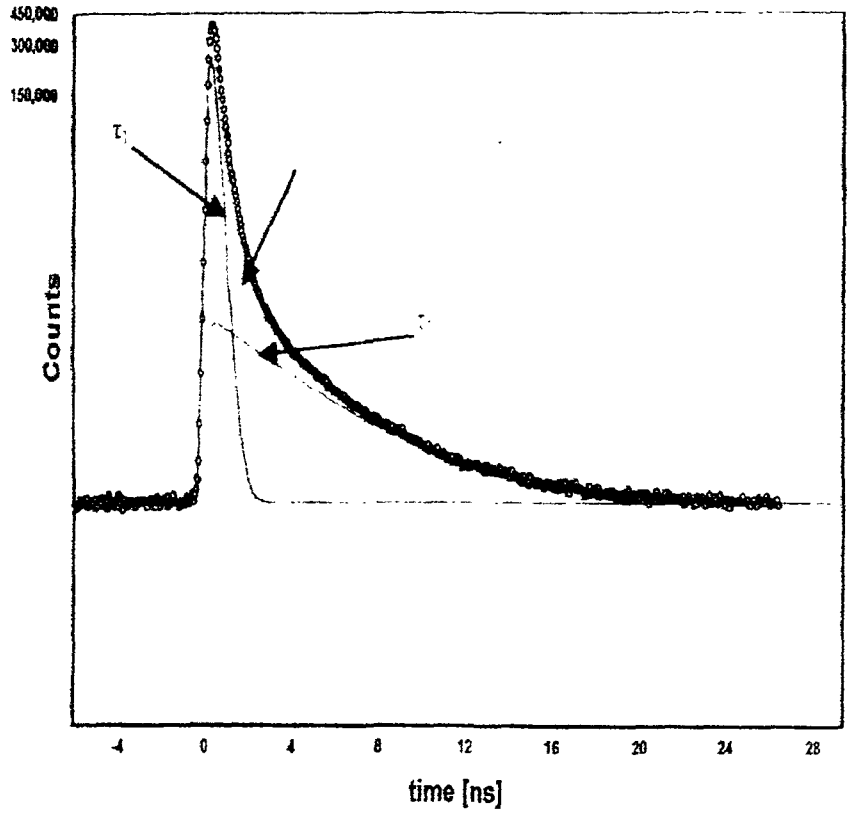

Figure 2.4: A typical lifetime spectrum of Teflon (Polytetrafluroethelene) [36]

2.4.4. Nano Scale-Void detection by PAL measurements

o- Ps lifetime which is due to annihilation by pick-off process is determined by the overlap of Ps wave function with bulk electrons of surrounding medium and the o-Ps lifetime becomes dependent on the trap size. Thus, PAL method can used to probe the free volume in amorphous media. The relation between free volume size and the o- Ps decay rate, λ_3, is given by Tao-Eldrup model [20,37], assuming that the Ps is trapped in a spherical hole with radius $R_o = R + \Delta R$ having an infinite potential barrier. This simple model for Ps confined in a spherical box is schematically shown in Figure 2.5. Tao-Eldrup model treats the o-Ps atom as a single scalar particle with twice the electron mass trapped in an infinite spherical potential well in the ground state. In the central portion of the well the o-Ps atom is assumed to have an infinite lifetime (the finite 142 ns vacuum lifetime is ignored) and with in a distance ΔR from the walls of the walls of the well the o-Ps atom is assumed to have the spin-averaged Ps lifetime. The overall annihilation rate is calculated by averaging the annihilation rate over the volume of the pore using the square of the normalized o-Ps wave function as a weighting factor. Since lifetime is ignored, the calculated annihilation rate is actually the pick-off annihilation rate due to interactions with electrons in the walls of the well. Using this model the annihilation rate due to interactions with electrons in the walls of the well. Using this model the annihilation rate of o-Ps trapped in a pore of radius $R + \Delta R$ is given by λ where $\lambda = (1+\lambda_1+\lambda_3)/4$ is the spin averaged vaccum annihilation rate and λ_1, λ_3 are the singlet and triplet vacuum annihilation rates. This model has one free parameter, ΔR, which is determined to be 1.66 Å by fitting to data taken in well characterized small pore materials such as zeolites [38] and has been shown to be quite material independent.

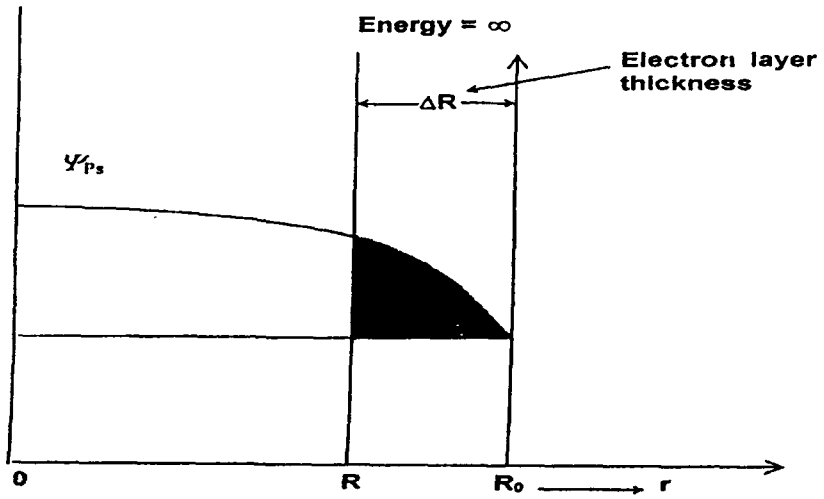

Figure 2.5: A schematic diagram for a semi-empirical quantum model for Ps localized in a spherical box with a radius R, which includes the radius of free volume hole R_o, and a uniform electron layer with a thickness R. The ground state Ps wave fuction is schematically shown and the annihilation rate is proportional to the overlap between the Ps and electron densities as shown in the shades are [26].

This treatment neglects both the finite o-Ps lifetime in the central portion of the well and the possibility that excited states in the well may be populated. For pores, 1 nm in radius at room temperature both these effects can be ignored since typical pick-off annihilation rates of order 0.5 ns^{-1} are much larger λ_3 and since the energy gap between the ground state and first excited state, of order 140 MeV, is larger as compared to kT. Assuming that the annihilation rate of o-Ps inside the electron layer is 2 ns^{-1}, which is the spin averaged annihilation rate of p-Ps and o-Ps and is also very close to annihilation rate of Ps [26], the o-Ps lifetime as a function of free volume radius R is given by.

$$\tau_3 = \frac{1}{\lambda_3} = \frac{1}{2}\left[1 - \frac{R}{R_0} + \frac{1}{2\pi} Sin\left(\frac{2\pi R}{R_0}\right)\right]^{-1} \qquad (2.4)$$

where $R_o = R + \Delta R$

The correlation between, τ_3, and free volume (spherical) is shown in Figure 2.6.

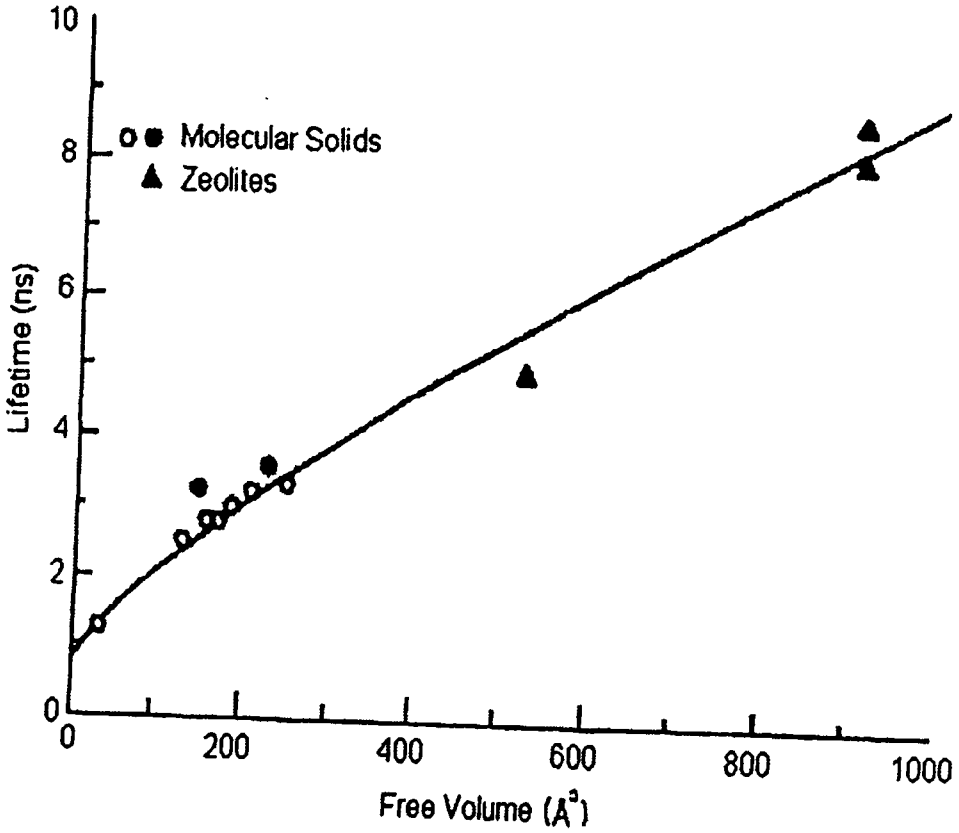

Figure 2.6: A correlation curve between the observed o-Ps lifetime and the volume of the free volume holes. The solid line is the best fit using equation 1.4 with ΔR=1.656 Å. The data points are the measured o-Ps lifetimes in molecular systems with known pore size [38].

2.4.5 Meaning of Positron Annihilation Spectroscopy (PAS)

Two types of information can be obtained from the positron annihilation experiments. First related to the electron density at the annihilation site and the other related to momentum distribution of the electrons. Angular correlation or Doppler broadening experiments gives information regarding to the distribution of electron momenta. The experiment of two gamma to three-coincidence ratio gives the information regarding the fraction of positrons which are annihilating after positronium formation. The same is also obtained by lifetime measurement method. The electron density distribution is substantially affected by defects, present in the crystal and the mean lifetime of positron is sensitive to electron density. Thus the lifetime measurement method is commonly employed for these studies. There are mainly four reasons for the rapid growth of Positron Annihilation Spectroscopy.

(i) Positron can provide unique information on a wide variety of problems in condensed matter physics

(ii) Positron annihilation can be applied in the field of non-destructive testing of the material as the information is carried out of the material by the penetrating annihilation radiation

(iii) In recent years Positron Annihilation Spectroscopy has provided a unique probe to study the size and number distribution of the sub nanometer cavities

(iv) Now a days, equipment is not very expensive and is commercially available.

2.4.6 Positron Sources

More than 200 positron- emitting nuclides are known of which about a dozen can be used as sources in positron annihilation experiments [39]. A large majority of investigations on solids by positrons has been done with 22Na or 58Co positron sources, mainly because of their low production costs and relatively convenient half-lives. Table 2.2 lists many of the relevant properties of the commonly used isotopes [40].

The significant properties of a positron emitting nuclide are:

(a) Positron capitulate

(b) End point energy

(c) Half life

(d) Ease of production

The significance of the positron capitulate is trivial. The end point energy is in two respects, the first being the positron penetration in the sample 'X' (2.5)

$$X = 1/\mu + \text{In } I(o)/I(x) \qquad (2.5)$$

where X is the penetration distance in the sample, $\mu+$ is the absorption coefficient,

I (0) is the initial positron density I (X) is the positron density at x after a beam of positron initial density I (0) traversed a thickness x of a given sample (and the second the percentage of positrons annihilating in the source). One can thus expect by virtue of the end-point energies that the most energetic positron can penetrate the sample to a depth of about 1 mm, although some positrons will stop or return to and annihilate at or near the surface of the sample.

Half-life of the nuclide should be large enough to be able to perform a series of measurements with the same source. However there is no need for a half –life larger than a few years. The energy of the start gamma should be significantly higher than that of the annihilation gamma rays to make the recognition easy and prevent spectrum distortion. Table 2.1 shows the end point energy, half-life and positrons per decay for several isotopes. For lifetime or Doppler measurements, the simplest way to guide the positron into the samples is to use a sandwiched configuration.The source should be very thin so that only a small fraction of the positrons annihilate in the source. Radioactive material can be deposited directly on the samples or consist of a single radioactive metal foil. In our experiment we used the radioactive isotope ^{22}Na. The decay scheme of ^{22}Na is shown in figure 2.2. ^{22} Na decays through positron emission and by electron capture to the first excited state (at 1274 KeV) of ^{22}Ne. The excited state goes to the ground state by the emission of 1274 –KeV gamma ray with a half life-time $\tau_{1/2}$ of $3x10^{-12}$ s. Thus positron emission is almost simultaneous with the emission of 1274 KeV gamma ray while the positron annihilation is accompanied by two511-KeV gamma rays. The measurements of

the time interval between the emission of 1274 KeV gamma ray and 511-KeV gamma rays can yield the lifetime 'τ' of positron annihilation.

2.4.7 Source Corrections

The amount of positrons annihilating in the source (10-15%) is related to the geometry of the sandwich configuration, the thickness and density of the foil include, and of the specific sample for which the measurements are made. The samples enter into the consideration because the positron may reflect at the sample source interface. These annihilation contribute additional lifetime components to the lifetime spectrum. In order to obtain suitable values of lifetimes and their intensities in samples to be studied it is important to make correction foe these components as precisely as possible. The correction should be measured using defect free reference samples. Berolaccini and Zappa [41] have given an empirical formula for the foil intensity as:

$$I_{foil}(\%) = 0.324xZ^{0.93}xD^{3.45/Z\,0.44} \qquad (2.6)$$

where Z is the sample atomic number and D is the foil thickness in mg/cm^2. At high Z values (>40) this formula overestimates the foil intensities.

2. 4.8 Commonly used positron-emitting isotopes

Table – 2.1

Isotope	Half life	β^+-decay(in%)	Maximum energy or end point energy	Application in lifetime studies
^{22}Na	2.6 Y	90	0.54	Yes
^{58}Co	71 d	15	0.47	Yes
^{44}Ti	47 Y	94	1.47	Yes
^{64}Cu	12.7 h	19	0.66	No
^{68}Ge	257d	88	1.90	No
^{57}Ni	36 h	46	0.85	Yes
^{90}Nb	14.6 h	53	1.50	No
^{55}Co	18.2 h	77	1.50	Yes

2.5 Ultraviolet Visible (UV-Vis.) Spectroscopy

Absorption methods involve determination of the reduction in power suffered by a beam of radiation as a consequence of passing through the absorbing medium. When an electromagnetic radiation in UV-Vis region (200-800 nm) falls on the target material, a part of the incident radiation is absorbed by the atoms leading to the transition of the orbital shell electrons. Ultraviolet visible (UV-Vis.) spectroscopy is the powerful analytical tool which gives an idea about the value of optical band-gap energy (E_g) and thus provides an important tool for investigation. In fact Ultraviolet and visible (UV-Vis.) absorption spectroscopy is the measurement of the attenuation of a beam of light with wavelength after it passes through a sample or after reflection from a sample surface. The short wavelength limit for simple UV-Vis Spectrometers is 180nm due to absorption of ultraviolet wavelength below 180nm by the atmospheric gases. The absorbance A, is related to the input and output intensities according to the Beer-Lambert Law [42] which is shown in equation [2.7]

$$\frac{I}{I_o} = e^{-A} \tag{2.7}$$

The absorbance, A, Can be divided by the path length, l to yield absorption coefficient [45] α which quantities quantifies the absorbance per meter, thus taking film thickness into account [2.6]

$$\alpha(\lambda) = 2.303 \frac{A}{l} \tag{2.8}$$

The absorption of light energy by polymeric materials in the ultraviolet or visible radiation region corresponds to excitation of outer electrons. When an atom or molecule absorbs energy, electrons are promoted from their ground state to a higher energy state (excited state).

Figure 2.7 depicts this excitation process which is quantized. The electromagnetic radiation that is absorbed has energy equal to the energy difference between the excited and ground states. The order of the energy changes are of 125 to 650 kJ/mole.

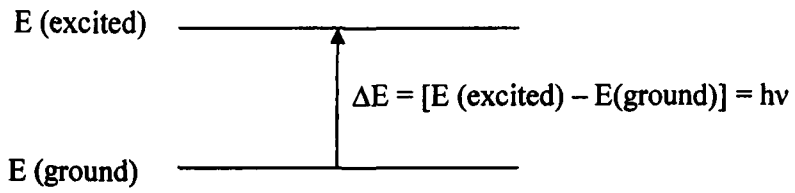

Figure 2.7: The excitation process

In a molecule, the atoms can rotate and vibrate with respect to each other. These vibrations and rotations also have discrete energy levels which can be considered as being packed on the top of each electronic energy level as shown in Figure 2.8. Absorbance of ultraviolet and visible radiation in molecules is restricted to certain functional groups (chromophores) that contain valence electrons of low excitation energy. The spectrum of a molecule containing these chromophores is complex. This is because the superposition of rotational and vibrational transition on the electronic transitions gives s combination of overlapping lines. This appears as a continuous band. The various possible electronic transition in organic molecule are shown in Figure 2.9.

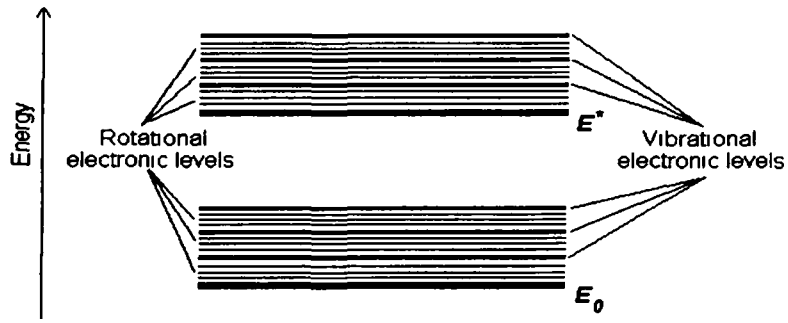

Figure 2.8: Electronic energy level diagram, E_o represents the ground state and E* is the excited state.

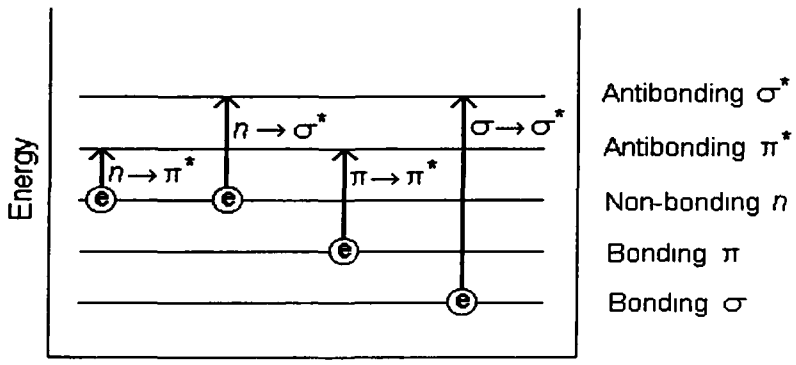

Figure 2.9: Energy level diagram for different electronic transitions

The $\pi \rightarrow \pi^*$ transition requires lesser energy and hence transition of this type appears at longer wavelength. These are the transition of interest in the study of ion-beam induced optical modification in polymers.

Irradiation of polymeric materials results in the shifting of absorption edge from UV towards the visible region. This shift can be correlated with the optical band gap (E_g) using Tauc's expression [44]

$$\omega^2 \varepsilon_2(\lambda) = (h\omega - E_g)^2 \qquad (2.9)$$

where $\varepsilon_2(\lambda)$ is the imaginary part of the complex refractive index, i.e., the optical absorbance and λ is the wavelength. E_g is usually derived from the plot $\varepsilon_2(\lambda)$ versus $1/\lambda$. The intersection of the extrapolated spectrum with abscissa yields the gap wavelength (λ_g), from which gap energy can be derived by

$$E_g = \frac{hc}{\lambda_g} \qquad (2.10)$$

Further, the compounds having double or triple bonds and phenolate or quinonic structures favour cluster formation under suitable ion irradiation. The number of carbon hexagon rings in the cluster 'N' can be found from the Robertson relation [45].

$$E_g = \frac{2\beta}{\sqrt{N}} \text{ eV} \qquad (2.11)$$

Here 2β is the band structure energy of a pair of adjacent π sites and its value is taken as -2.9eV for a six numbered carbon ring. Fink et al have pointed out that the Robertson equation under estimates the cluster size in irradiated polymers. Thus the structure of the cluster was assumed to be like a buck minister fullerene, that is, a C_{60} ring instead of C_6 and the relation emerges:

$$E_g = \frac{34.3}{\sqrt{N}} \text{ e V} \qquad (2.12)$$

where N is the no. of carbon atoms per cluster in the irradiated polymer .Above relation has been used to calculate obtained the no. of carbon atoms per cluster in the irradiated samples.

2.5.1 Instrumentation

The typical ultraviole–Visible spectrometer consists of a light-source, a monochromator and a detector as shown in figure 2.10. The light source is usually a deuterium lamp which emits electromagnetic radiation in the ultraviolet region of the spectrum. A second light source, tungsten lamp is used for wavelengths in the visible region of the spectrum. The monochromator is diffraction grating; its role is to spread the beam of light into its component wavelength. A system of slits focuses the desired wavelength of the sample cell. The light that passes through the sampler cell reaches the detector which required the intensity of the transmitted light (I). The detector is generally a photo multiplier tube, although in modern instruments photodiodes are used.

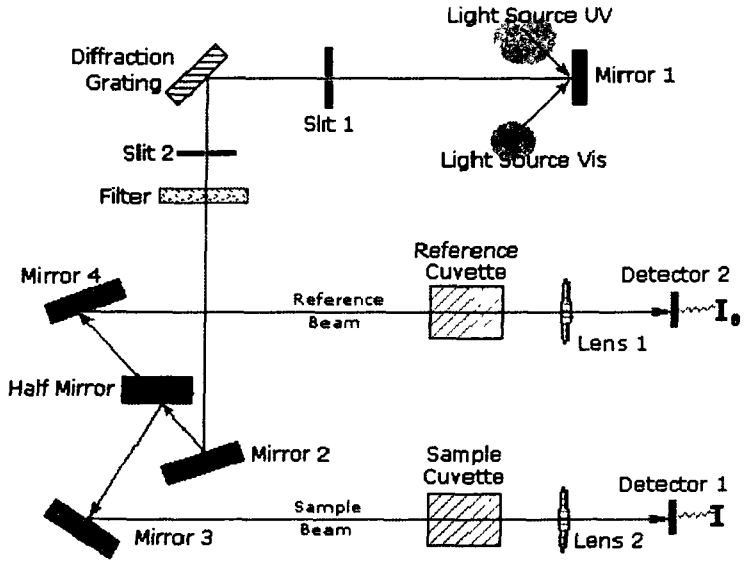

Figure 2.10: Typical Ultraviolet –Visible spectrometer

In a typical double – beam instrument, the light emanating from the light source is split into two beams, the sample –beam and the reference beam. When there is no sample cell in the reference beam, the detected light is taken to be equal to the intensity of light entering the sample (I_o). The spectrum is generally recorded as plot of absorbance versus wavelength.

2.6 X-Ray Diffractions Study (XRD)

X-rays can be used for chemical analysis in three different ways:

- The first method uses the fact that X-rays emitted by an excited element have a wavelength characteristic of that element and the intensity proportional to the number of excited atoms. The excitation can be caused by direct bombardment of the target material with electrons (direct emission analysis and electron probe microanalysis) or by irradiation of material with X-rays of shorter wavelength (fluorescent analysis).
- The second method utilizes the different absorption of X-rays by different materials (absorption analysis).
- The third method involves the diffraction of X-rays by crystals having geometrically periodic arrangement of atoms separated by distance comparable to X-rays wavelength (diffraction analysis). This method is widely used for qualitative identification of crystalline phases. The condition for diffraction of a beam of X-rays from a crystals is governed by the Bragg equation:

$$2d\sin(\theta) = n\lambda \qquad \text{with } \lambda \leq 2d \qquad (2.13)$$

where λ is the wavelength of the X-rays, d is the interplanar spacing for a family of planes; n is the order of the diffraction and θ the incoming diffraction angle.

In thin films, X-rays are diffracted by the oriented crystallites at a particular angle to satisfy the Bragg's condition. Having known the values of θ and λ, one can calculate the interplaner spacing. Schematic view of XRD is shown in0 Figure 2.11

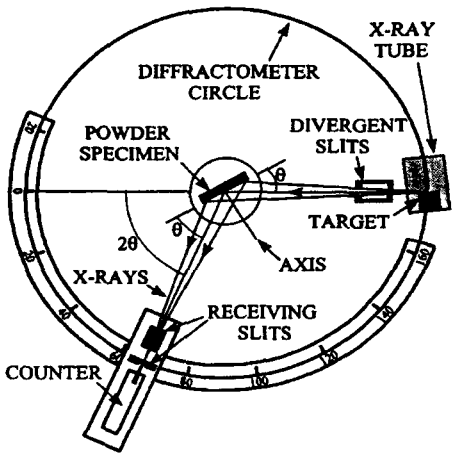

Figure 2.11: A schematic of x-ray diffractometer.

The XRD can be taken in various modes such as θ-2θ scan mode, θ-2θ rocking curve, and ϕ scan shown in figure 2.12.

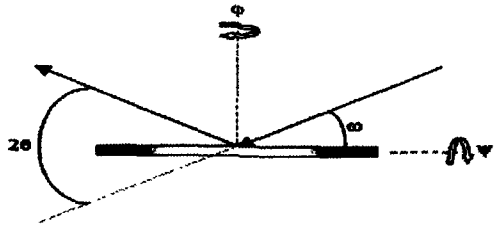

Figure 2.12 An illustration of ϕ-scan x-ray diffraction, where, ω – angle between incident x-rays and sample surface, 2θ – angle between incident x-rays and detector, ψ – sample tilt, φ – in-plane sample rotation, x, y – in-plane displacement of sample, z – vertical displacement of sample.

In the θ-2θ scan mode, a monochromatic beam of X-ray is incident on the sample at an angle of θ with the sample surface. The detector motion is coupled with the x-ray source in such a way that it always makes an angle 2θ with the incident direction of the X-ray beam. The resulting spectrum is a plot between the intensity recorded by the detector and 2θ.Reflection geometry was used in measurements (sample were thin film samples and other possible geometry is the transmission geometry.

The crystallite size in pristine and irradiated polymers was determined by Scherrer formula (2.14).

$$\text{Crystallite size (L)} = \frac{K\lambda}{d \times \cos\theta} \qquad (2.14)$$

where K is the shape factor of the average crystallite (0.9), λ is the wavelength (1.54 Å) for Cu $K\alpha_1$, d is full width at half maxima (FWHM) and θ is the peak position in radian.

In the present work, the XRD pattern for the bulk and thin films of different polymers were recorded at Inter-University Accelerator Centre (IUAC), New Delhi using D8 Advanced Bruker diffractometer with Cu-K_α radiation (λ=1.541838Å) at room temperature by taking 0.020 step size. The cathode was maintained at 30 kV. Diffraction patterns were recorded in the range $20^\circ \leq 2\theta \leq 80^\circ$.

2.7 Fourier Transform Infrared (FTIR) Spectroscopy

Infrared spectroscopy is one of the most powerful analytical techniques which offer the possibility of chemical identification. It involves the twisting, bending, rotating and vibrational motions of atoms in a molecule. Upon interaction with the IR radiation, some portion of the incident radiation is absorbed at particular wavelengths. The multiplicity of vibration occurring simultaneously produces a highly complex absorption spectrum which is uniquely characteristic of the functional groups comprising the molecule and of the overall configuration of the atoms as well.

For IR absorption to occur, two major conditions must be fulfilled:

- Energy of radiation must coincide with the energy difference between the excited and the ground state of the molecule. The radiant energy will then be the absorbed by the molecule, increasing its vibration.
- The vibration must entail a change in electrical dipole moment.

The infra-red spectrum of a compound is essentially thebe superposition of absorption bands of specific functional groups. No two compounds will have same infra-red spectra (except optical isomers). Thus, infra-red spectra is regarded as the fingerprint of a molecule. The higher frequency portion of the infra-red spectra (4000-1300 cm^{-1}) is called the functional group region which shows the absorption arising from stretching vibrations and are useful for identification of the functional groups. The absorption pattern in the region 1400-650 cm^{-1} is unique for a particular compound and hence called fingerprint region. Both the stretching and bending modes of vibration give rise to absorption in this region.

2.8 Electrical Studies

If a polymer contains glacial groups is placed in an electric field, direction of its units and smaller kinetic units will be observed at a definite field – frequency ratios, and this gives rise to values: dielectric constant and tanδ (dissipation factor). Important method that takes place in any dielectric material under the manipulate of electric field is polarization i.e. the limited displacement of bound charges or orientation of dipole

molecules. The dielectric polarization may be judged in terms of the dielectric constant and the dissipation factor (loss angle or tanδ).

The best dielectric materials are those which contain a minimum of charge carriers and potential charge carriers which may be formed by splitting of covalent, atomic or molecular bonds under the influence of the energetic ions. The dielectric response of material provides information about the orientational transnational adjustment of mobile charges present in the dielectric medium in response to an applied electric field. The most important property of dielectric materials is ability to be polarized under the action of the field. The dielectric loss behavior of polymer films is very important because of their possible applications for insulation isolation and passivity in micro-electronic circuits [46]. In general polymers are insulators and commonly used in insulation of electric wires. However, certain classes of polymers have been discovered and used as semiconductor and capacitors with unusual electrical properties.

The electrical conductivity depends on free ions and not only strongly bonded with the macromolecules. Therefore, the conductivity of polymers mostly depends on the presence of low-molecular mass impurities that can serve as source of ions[47]. The conductivity of the polymers approximately lies between 10^{-3} to 10^{-9} $ohm^{-1}cm^{-1}$.

Dielectric constant is mostly used to determine the ability of an insulator to store electrical energy. The dielectric constant is the ratio of the capacitance induced by two metallic plates with an insulator between them to the capacitance of the inefficiency of an insulating material [48]. If the material is to be used for strictly insulating purpose, it would be better to have a lower dielectric constant.

The capacitance (C) and the dielectric loss (tanδ) measurements have been made with the help of variable frequency LCR meter (Hewlett Packard 4284 A) in the frequency range of 1-1000kHz at room temperature. The measured values of capacitance then have been converted into the dielectric constant (ε) by using the formula:

$$\varepsilon = \frac{Cd}{\varepsilon_o A} \qquad (2.15)$$

where d is the thickness of polymer film, A is the area of the electrode plates and ε_0 is the permittivity of free space. AC conductivity is calculated by the relation given below:

$$\sigma_{a.c} = 2\pi f \tan\delta \varepsilon_o \varepsilon_r \qquad (2.16)$$

References

[1] G. Illari et al. Nucl. Instr. and Meth. 143 (1977) 605.

[2] Z. Todorovic. Nucl. Tracks Radiat. Meas. 17(1990)23.

[3] G. Gerlach, K. Baumann, R. Buchhold, A. Nakladal, German Patent D E, 198 53 732 (1998).

[4] R. Buchhold, B. Gassensoren, Dresden University Press, Dresden and Munich, (1999).

[5] M. Guenther, K.Sahre, G. Suchaneck, G.Gerelach K.J. Eichhorn, Surf. Coat. Tech. 482, 142(2001).

[6] J. Sun, Y. Zhang, X. Zhong, X. Zhu, Radiat. Phys. Chem. 44 (1994)655.

[7] A. Oshima, Y. Tabata, H. Kudoh, T. Seguchi, Radiat. Phys-Chem.45 (1994)269.

[8] A. Oshima, S. Ikeda, T.Seguchi, Y. Tabata, Radit. Phys. Chem.49 (1997)581.

[9] E. Katoh, H. Sugisawa, A. Oshima, Y. Tabat, Seguchi, T. Yamuzaki Radiat. Phys. Chem. 54(1999)165.

[10] U. Lappan, U. Geibler, K. Lunkwitz, J. Appl. Polym. Sci. 74(1999)1571.

[11] U. Lappan, U. Geibler, K. Lunkwitz, Radit.Phys.Chem. 59 (2000)451.

[12] R. Mishra, S.P. Tripathy, D. Sinha, K.K. Dwivedi, S. Ghosh, D.T. Khating, M. Muller, D. Fink, Nucl. Instr. and Meth.B, 168 (2000)59.

[13] T. Steckenreiter, E. Balanzat, H. Fuess, C. Trautmann, Nucl. Instr. and Meth.B 131 (1997)159.

[14] C. Liu, Z. Zhu, Y.Jin, Y.Sun, M.hou, Z. Wang, C. Zhang, X. Chen, J. Liu, Buoquan, Nucl. Instr. and Meth.B.,169 (2000)78.

[15] Z. Zhu.,Y.sun, C. Liu, J. Liu, Y. Jin, Nucl. Instr. and Meth.B,193(2002)271.

[16] N. Singh, A. Sharma, D.K. Avasthi, Nucl. Instr. and Meth. B., 206(2003)1120.

[17] Mohamed HFM, A.M.A. El-Sayed, Abd-Elsadek GG., Polymer Degradation and Stability 71(2001)93-97.

[18] J.R. Kulish, H., Franke, A. Singh, R.A. Lessard and J. Knystautas, J. of Appl Phys. 63(1988)2517.

[19] M. Dole (Ed.), The Radiation Chemistry of Macromolecules, Academic Press, New York, Vol.2 (1973).

[20] D. Kanjilal, S. Chopra, M. M. Narayanan, I.S. iyer, V.Jha, R. Joshi, S. K. Datta, Nucl. Instr. and Meth. A 238 (1993)97.

[21] C.D. Anderson, Science 76,238 (1932).

[22] D. M., Shrader, Y.C. Jean, 1988, Positron and positronium Chemistry: Studies in Physics and Theoretical Chemistry (Elsevier, New York).

[23] W. Brant, A. Duspansquir, Eds. Positron Solid State Physics, North Holland Pub. Amsterdam (1983).

[24] N. Naknishi, Y.C. Jean, in Positron and Positronium Chemistry, D. M. Shrader, Y.C. Jean, eds. Elsevier Pub. Amsterdam (1988).

[25] Y. C.Jean, Mater. Sci. Forum, 175-178 (1995)59.

[26] Y. C. Jean Third International Workshop on Positron and Positronium Chemistry, July 16-18, 1990, Milwaukee, USA.

[27] O.E. Mongensen, Positron Annihilation in Chemistry, Springer Verlag, Berlin, 1995.

[28] M. Eldrup, D. Lightbody, J. N. Sherwood, Chem. Phys., 63 (1981)51.

[29] D. Lightbody, J.N. Sherwood, M. Eldrup, Chem.Phys. 93 (1985)475.

[30] Y. C.Jean, Microchem, J. 42 (1990)72

[31] P. Kierkegaard, M. Eldrup, O.E. Mongensen, N. Pedeersen, Compt. Phys. Commun. 23 (1981)307.

[32] J. Kansay, Nucl. Instr. and Meth. A 374(1996)235.

[33] R.B. Gregory, Y. Zhu, Nucl. Instr. and Meth. A 290(1990)172.

[34] M. Eldrup, D. Lightbody, J.N. Sherwood, Chem.Phys. 63(1981)51.

[35] Y.C. Jean, Microchem J 42 (1990)72.

[36] A. Udeno, T. Kawano, S. Tanigawa, M. Ban, M. Kyoto, T. Uozumi, J. Polym. Sci. B: Polym. Phys., 34 (1996)2145.

[37] S. J. Tao, Chem. Phys. 56(1972)5499.

[38] H. Nakanishi, S. J. Wang, Y. C. Jean in Positron Annihilation Studies of Fluids. Ed. S. C. Sharma, World Sci. Singapore (1988)292.

[39] E. A. Lorch; Proc. of the 5th Int. Conf. On Pos. Ann., (Ed. R. Hasigupta) 403 (Sendai, 1979).

[40] E. Browen, J. Dairki, R.E. Doebler, A.A. Slihab-Eldin, L.J. Jardine, J.K. Tuli and A.B. Buryn. "Table of Isotopes" (Edited by C.M. Lederer and V.S. Shirley, eds.) 7th ed. pp.36, 170,196,216. Wiley, New York, (1978).

[41] B. Bergersen and M. J. Stott, Phys. Rev. Lett., 19(1967)307.

[42] W. Kemp, "Spectroscopy of organic compounds", W. H. Freeman, New York, 1991.

[43] S. K. Al-Ani, I. Al-Hassany, Z. Al-Dahan, J. Mat. Sci. 30 (1995)3720.

[44] J. Tauc, R. Grigorovici, A. Vancu, Phys. Stat. Sol. 15(1966)627.

[45] J. Robertson, E.P. O'Reilly, Phys. Rev.,B 35 (1987) 2946.

[46] Z. M. Dang, Y. Shen and C.W. Nan , Appl. Phys. Lett. 81(2002)4814.

[47] S. Sindhu, M. R. Anantharaman, B. P. Thampi, K. A. Malini, P. Kurian, Bull. Material Science. 25(2002)599.

[48] C. Kittel, "Introduction to Solid State Physics" , John Wiley & Sons (Asia), Singapore, (1996)

Chapter-III

Chapter III

POSITRON LIFETIME AND DOPPLER BROADENING STUDIES OF POLYMERS

3.1 Introduction

An energetic ion passing through the polymeric material looses energy by nuclear stopping and /or electronic stopping. The outcomes of the ion irradiation on the polymers include electronic excitations, phonons, ionization, ion pair formation and chain scission. Various gaseous molecular species may be released during irradiation. Most prominent emission is hydrogen followed by less abundant heavier molecular species which are scission products from the pendant side groups and chain and segments and their reaction products. Cross-linking occurs when two free dangling ions or radical pairs unite, whereas double or triple bonds are formed if two neighboring radicals in the same chain unite. Magnitude of scission and cross-linking depends largely upon the energy loss mechanism. Nuclear stopping is supposed to be responsible for scission and electronic stopping is responsible for cross-linking although both the processes can cause cross linking as well as scission [1].

Ion induced modifications of the polymeric materials have been attempted in a variety of ways using the ion energies from few hundred KeV to few hundered MeV. From the lightest ions like H^+, He^+ to heavy ions Au^+ and U^+ have been employed for the modification of polymeric materials. Most of ion beam experiments are related to the implantation modification of polymers. These are mostly focused on the study of conductivity changes resulting from ion implantation [2]. Ion implantation has also been used to improve the surface, optical and gas permeation properties of polymers. Availability of heavy ion accelerators has given new impetus to the field of ion induced modifications. Ion induced modifications in physical and chemical properties and the potential areas of its application are discussed in detail by Lee [3].

The ion path in a polymeric material is described by a cylindrical trajectory defined by the physical core of radius r_c (the approximately limiting distance from the particle trajectory at which electronic excitation occurs initially), and halo or penumbra with radius r_p (outer most cylindrical boundary of δ-rays or secondary electrons emitted along the path of swift heavy ion) [4]. Another distance which lies between physical core and penumbra is called chemical radius, r_{ch}. It defines a range where a chemical reaction occurs. r_{ch} is thus determined by the diffusion and reaction rates of active chemical species such as radicals, cations , anions, electrons and other activated chemical species. Shapes and sizes of track entities are first defined and then followed by the formation of active chemical species, diffusion and their interaction via chemical and columbic forces. Some chemical species may recombine and neutralize in a dense chemical sea while some may diffuse out to the halo region and mix up with the species induced by the δ-rays. In most of the chemical reactions, cross-linking and scission take place near r_c where concentration of radicals and ion pairs is high due to slow migration of radicals. The radius of core and hole depends on energy per nucleon. These may be of the order of 1-10 nm and 10-1000nm respectively [5]. The value of r_c and r_p depends on the energy per nucleon of the ion. δ-rays, penumbra r_p, physical core and r_c are pictorially represented in Figure 3.1.

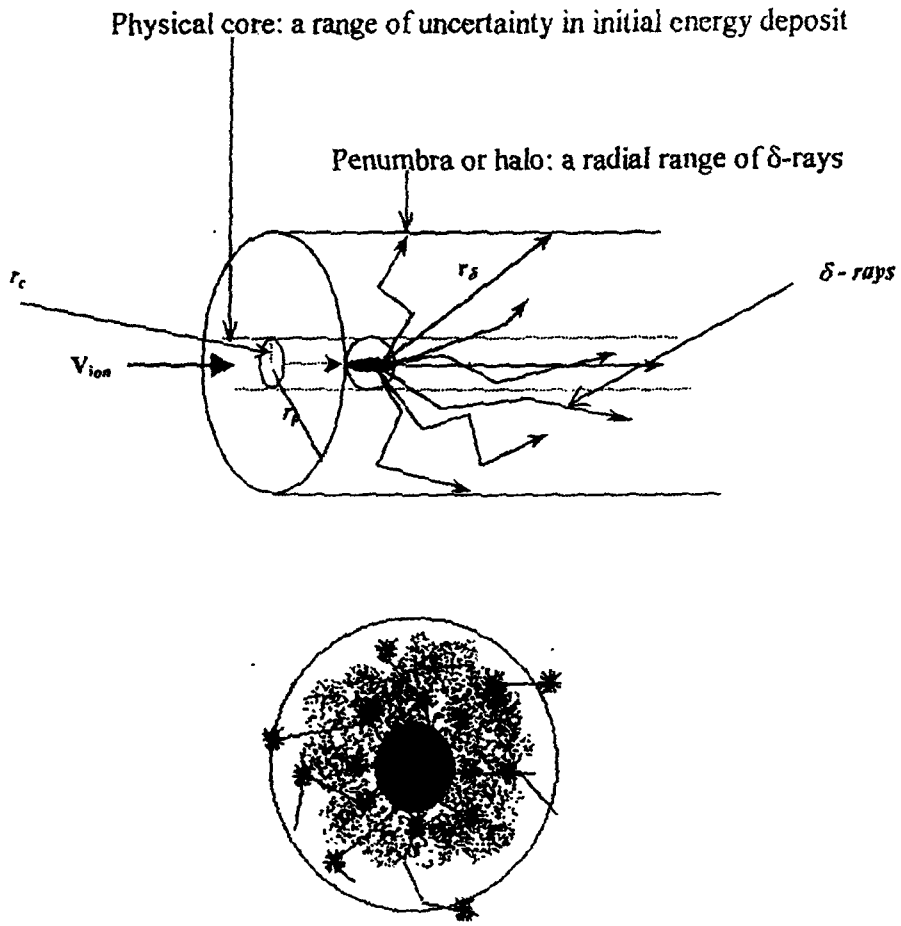

Figure 3.1: Pictorial representation of ion track showing physical core r_c halo r_p and δ- Rays. [6].

Positron annihilation spectroscopy (PAS) has emerged as a unique and potent probe for characterizing the free volume properties of polymers [7]. Unlike other methods used to determine free volume in polymers, PAS is capable of determining the local hole size and free volume fractions in polymers without interacting significantly with the bulk of polymers. PAS has been developed to be a quantitative probe of the free volume. It also gives detailed information on the distribution of free volume hole size in the range from 1 to 10 Å. Positron annihilation lifetime spectroscopy (PALS) is capable of probing free volumes directly. The atomic scale free volume holes are detected on the basis that the positronium (Ps) atoms are formed and localized in the free volume holes [8]. In PAL spectra it is the o-Ps lifetime which is very sensitive to structural changes in the polymer

and is directly correlated to the free volume hole size [9]. PALS is a probe that gives considerable information about the microstructure of materials. It has recently been used on polymers with interesting results [10-12]. In Polymer sample there is substantial pick off annihilation with lifetimes of the order of 1000-2000 ps. This is suggested due to large voids in the polymer structure. The energy transfer due to ion irradiation tends to radical formation, bonds scission and cross-linking, depending essentially on the polymer and linear energy transfer (LET). Dominance of cross linking or scission depends on the polymer and the energy loss per unit path length or linear energy transfer (LET). In case of high LET, spurs overlap, the probability of two radical pairs to be in neighboring chains is increased and cross-linking is facilitated. For low LET spurs develop far apart and independently, the deposited energy tends to be confined in one chain (not in neighboring chain), leading to scission [6]. The scission causes increase in the free volume where as the cross-linking reduces the available free volume [13, 14]. The area occupied by the tracks (diameter of the order 1-10nm) in the sample exposed to low fluences (10^5-10^6ions/cm^2) is of the order of 10^{-6} cm^2. On irradiation on such fluences, average molecular chain length decreases due to scission which eventually results in the increase of the free volume.

At high fluences the area occupied by the tracks becomes comparable to the sample area and overlapping of tracks takes place. At these fluences, however scissioned segments cross-link randomly, increasing the number of free volume holes and decreasing the average free volume. These are schematically shown in Figure 3.2.

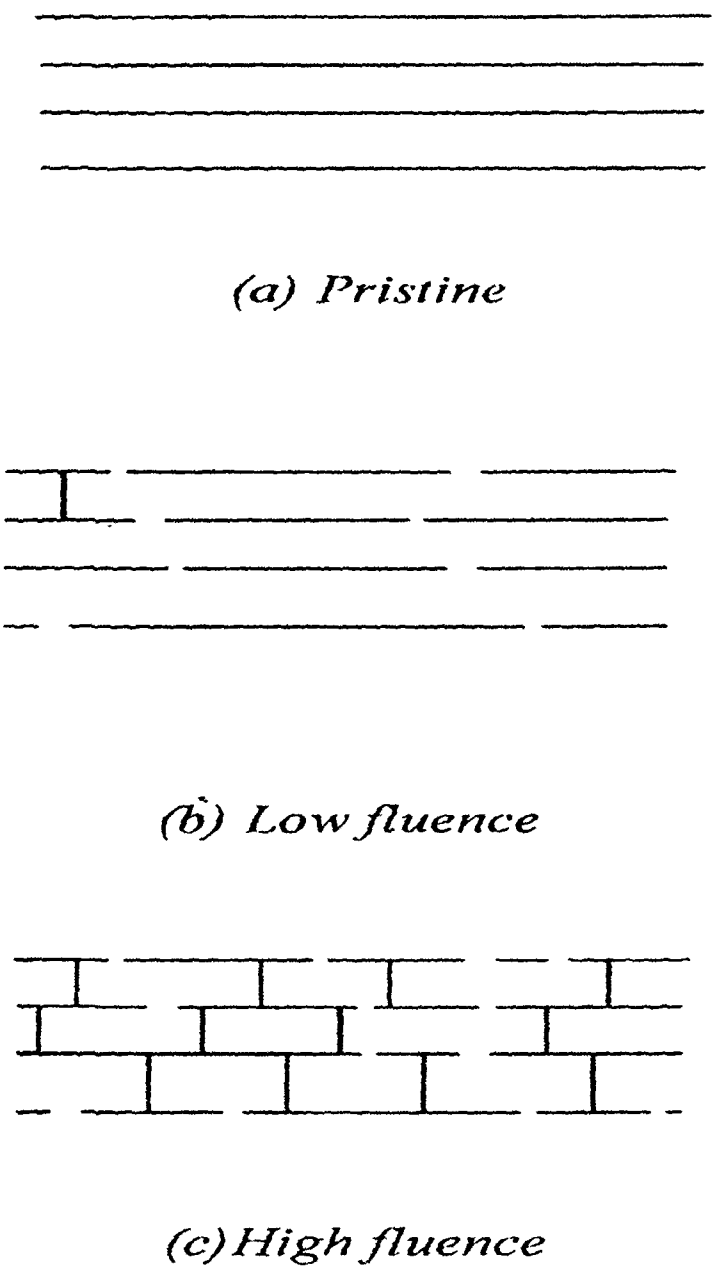

Figure 3.2: Schematic representation of micro structural evolution upon irradiation [15]

Lee (1999) has observed that for low LET, spurs (an energy loss event in a track involving a small energy deposit) develop far apart and independently, the deposit energy leads to be confined in one chain (not in neighboring chain) leading to scission [6]. Trautmann (1999) and Fink (1999) have indicated that scission causes an increase in the free volume where as the cross-linking reduces the available free volume. At high LET spurs overlap, the probability of two radical pairs to be in neighboring chains is increased and cross –linking is facilitated [13,14]. In the present work characterization of free volume properties of polymers modified by Swift Heavy Ions has been carried out through Positron lifetime studies and Doppler broadening studies

3.2 Polymers used for studies

3.2.1 Polymers studied through Positron lifetime studies are

(i) Makrofol-KG Polycarbonate

(ii) Polyethersulphone (PES)

(iii) Polystyrene (PS)

(iv) Polyvinyldifluoride (PVDF)

(v) Polyamide Nylon-6

(vi) Polyamide Nylon-6,6

(vii) Polyethylene Oxide –salt (PEO-salt)

(viii) Lexan Polycarbontae

3.2.2 Following polymers have been studied through Doppler Broadening Spectroscopy (DBS) also

(i) Polyethylene Oxide –salt (PEO-salt)

(ii) Polyamide Nylon-6, 6

(iii) Lexan Polycarbonates

(iv) Polystyrene (PS)

The studies described below modification in free volume properties of various polymers induced by swift heavy ion beams have been carried out through Positron Annihilation Lifetime Spectroscopy and Doppler Broadening Spectroscopy.

3.3 Experimental details

Makrofol-KG polycarbonate, Polyethersulphone (PES), Polystyrene (PS), Polyvinylidene fluoride (PVDF), Polyamide Nylon-6, Polyamide Nylon-6,6 and Lexan polycarbonate polymers were procured from Bayer A.G. Germany, Pershore Moulding limited, England and Good fellow, Cambridge, England.

3.3.1 Irradiation

Swift heavy ion (SHI) irradiation of the polymeric samples was carried out at 15 UD Pelletron Accelerator at Inter University Accelerator Centre (IUAC), New Delhi, India and Variable Energy Cyclotron Centre (VECC), Kolkata, India.

In the present study, five ions of different mass and range were used for irradiation of various types of polymers. Details of irradiated polymers with heavy ions of different energies are presented in Tables-3.3.1 (a) and (b). Details of the Polymers are described in chapter II.

Table-3.1 (a)

Details of heavy ions and polymers irradiated at 15 UD Pelletron Accelerator at Inter University Accelerator Centre, New Delhi, India.

Name of the ion with symbol	Energy MeV/n	Name of the polymer	Name of the manufacturer	Thickness (Approx)
Carbon C^{5+}	70 MeV	Polyamide Nylon-6 (PN-6)	Good Fellow. UK	250 μm
Silicon Si^{8+}	100 MeV	Makrofol-KG (Bisphenol-A Polycarbonate)	Farben Fabri-ken Bayer A.G., Germany	40 μm
Silicon Si^{8+}	100 MeV	Polyethersulphone (PES)	Good Fellow. UK	250 μm
Silicon Si^{8+}	100 MeV	Polystyrene (PS)	Good Fellow. UK	1 mm.
Oxygen O^{6+}	95 MeV	Polyethylene oxide Salt 17%	BDH England	170 μm
Oxygen O^{6+}	95 MeV	Lexan Polycarbonate	Farben Fabri-ken Bayer A.G., Germany	225 μm
Lithium Li^{3+}	50 MeV	Polyamide Nylon-6,6 (PN-6,6)	Good Fellow. UK	250 μm
Lithium Li^{3+}	50 MeV	Polystyrene (PS)	Good Fellow. UK	1 mm.

Table-3.1 (b)

Details of heavy ions and polymers irradiated at Variable Energy Cyclotron Centre (VECC), Kolkata, India.

Name of the ion with symbol	Energy MeV/n	Name of the polymer with chemical composition	Name of the manufacturer	Thickness (Approx)
Neon Ne^{6+}	145 MeV	Makrofol-KG (Bisphenol-A Polycarbonate)	Farbenfabri-ken Bayer A.G., Germany	40 μm
Neon Ne^{6+}	145 MeV	Polyethersulphone (PES)	Good Fellow. UK	250 μm
Neon Ne^{6+}	145 MeV	Polyvinyli dene difluoride (PVDF)	Good Fellow. UK	80 μm

At 15 UD Pelletron Accelerator at Inter University Accelerator Centre, New Delhi, INDIA [Table- 3.1(a)] polymer samples of size 1.5x1.5 cm^2 were mounted on a vacuum shielded vertical sliding ladder and were exposed to 70 MeV C^{5+}, 100 MeV Si^{8+}, 95 MeV O^{6+} and 50 MeV Li^{3+} ion beam in the General Purpose Scattering Chamber (GPSC) under high vacuum (~$4x10^{-6}$ Torr) [16]. Various polymer samples were irradiated to different fluences. In order to expose the whole target area uniformly, the beam was scanned in the X-Y plane.

Polymers samples [Table-3.1(b)] were irradiated by the 145 MeV Ne^{6+} ion beam at Variable Energy Cyclotron Centre (VECC), Kolkata. Irradiation was carried out to the different fluences. XY scanner was used for uniform irradiation of the film. At VECC ion beam was defocused using a magnetic scanning system so that the film may be uniformly irradiated.

3.4. Positron Annihilation Lifetime (PAL) measurements

3.4.1 Positron Lifetime Measurements

The details of Positron Annihilation Spectroscopy have been presented in Chapter II. In the present study Positron annihilation lifetime measurements were made using fast – fast coincidence spectrometer at the UGC-DAE Consortium for Scientific Research, Kolkata Centre and Saha Institute of Nuclear Physics, Kolkata. The fast – fast coincidence set up is shown in the photograph 3.3

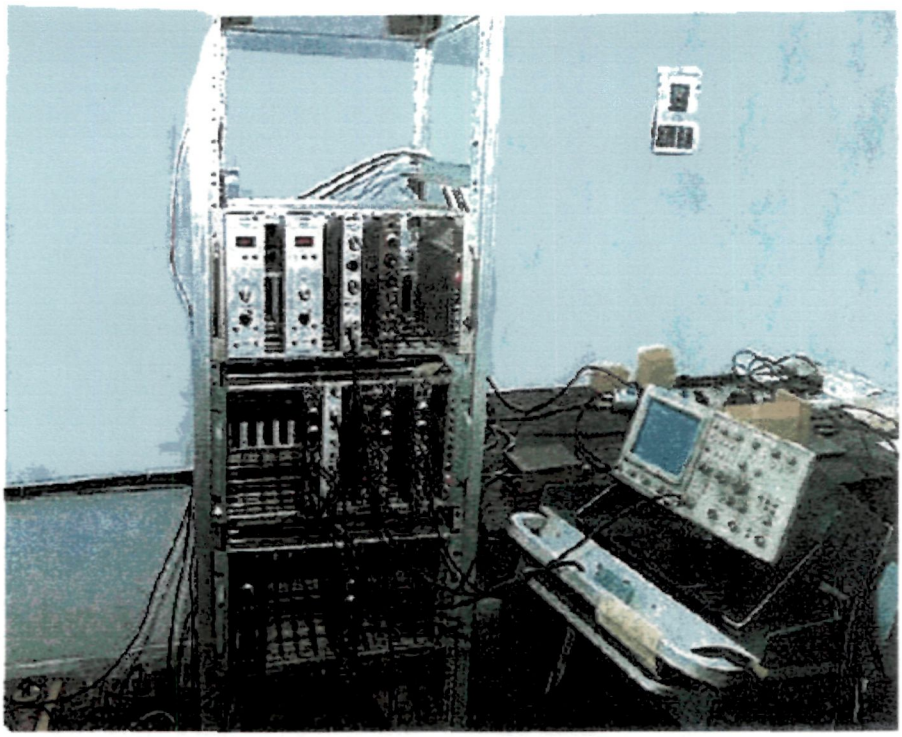

Photograph 3.3: Fast - fast coincidence spectrometer for positron lifetime measurements

The positrons for the lifetime measurements were obtained from the radioactive decay of ^{22}Na isotope which is the most commonly used source of positrons. ^{22}Na decays to the excited state of ^{22}Ne by emission of positron and a neutrino. The decay scheme of ^{22}Na is shown in Figure 3.4.

$$^{22}Na \rightarrow {}^{22}Ne + e^{+} + \gamma \qquad (3.1)$$

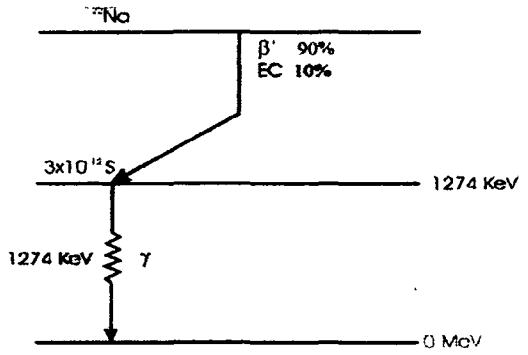

Figure 3.4: Decay Scheme of ^{22}Na

The ground state of ^{22}Ne is reached after 3.7 ps by the emission of γ quantum of 1.27 MeV. Competitive processes with lower probabilities are electron capture (EC) and direct transition to the ground state of Ne [17]. ^{22}Na isotope gives a relatively high positron yield of 90% and has several other advantages. The appearance of 1.27 MeV γ quanta almost simultaneously with the positron emission, the easiness of its handling for laboratory work, comparatively large half-life (2.6 years) and low cost make this isotope the most useful source material in positron research [18]. The positron annihilation lifetime was registered as a time difference between the emissions of the 1.27 MeV γ - quantum generated almost simultaneously with the positron and one of the 0.511 MeV annihilation γ –quanta. Positron source was prepared by evaporating 5 μCi of aqueous $^{22}NaCl$ salt on a thin (~8μm) rhodium foil. The source foil was thin in order to reduce the background of 0.511 MeV annihilation photon. In the present study the samples were in the form of films of different thicknesses. Therefore, the source deposited on rhodium foil was sandwiched between two identical stacks (Figure. 3.5), of layers of the sample film whose total thickness was adequate (~ 400μm) to absorb more than 99%.

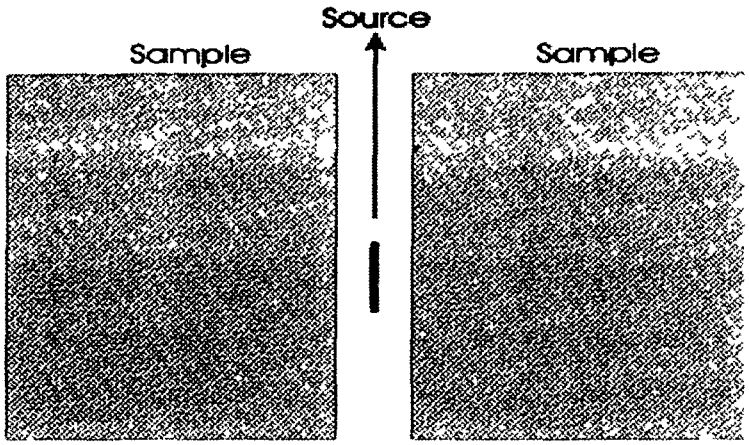

Figure 3.5: Sandwich configuration

of positrons emitted. PAL spectra were obtained using conventional fast-fast coincidence spectrometer whose block diagram is shown in Figure 3.5. Coincidence spectrometer entails monitoring of the signals; 1.28 MeV gamma ray from positron decay of the source as start signal and 0.511 MeV gamma ray from the positron annihilation in the material sample under study as the stop signal. BaF_2 scintillators in truncated conical geometry coupled to Philips XP2020 photo multipliers were used for fast timing. The conical shapes of the scintillators improve the light collection process [19]. The energy resolution is associated mainly with the slow component at 310 nm with decay constant of 620 ns and emitting about 80% of the total light. Apart from the advantages of the fast component, BaF_2 is attractive due to its high atomic number Ba (56) and relative high density of 4.88 g/cm^3 which are favorable properties for high photo peak detection efficiency for gamma rays. ORTEC 583 Constant Fraction Differential Discriminators (CFDD) were used for selecting energy and providing timing signal, independent of the rise time and amplitude of the anode signal from the PM tubes to Time to Amplitude Converter (TAC) (ORTEC 567). The windows of the CFDDs in start and stop arms were adjusted for 1.27 MeV start and 0.511 MeV stop signals respectively.

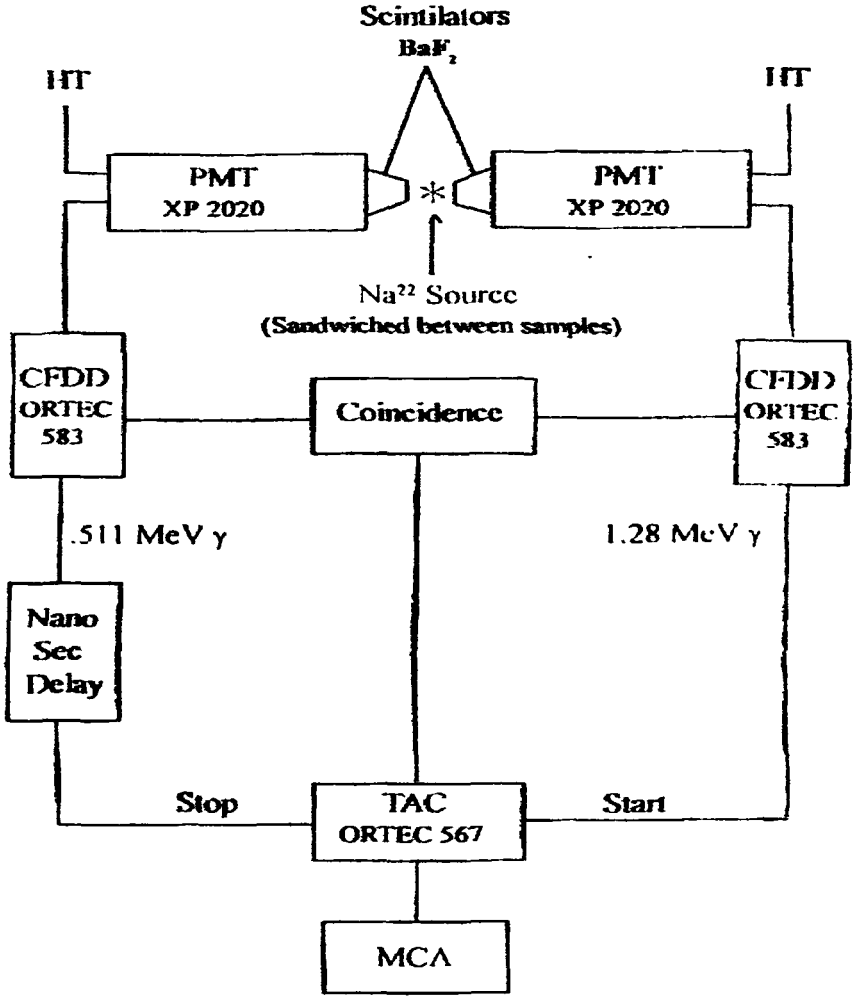

Figure 3.6: The block diagram of the positron lifetime spectrometer

Detection of the 1.27 MeV gamma photon provides the start signal for a TAC. The stop signal is generated by the detection of one of the 0.511 MeV gamma photons obtained from the annihilation of positron. If legitimate gamma-gamma coincidences are observed, a pulse whose amplitude is proportional to the time interval between start and stop signals is sent from the TAC to a multi-channel analyzer (MCA) where it is stored in the appropriate time channel. The uncertainty in the measurement of lifetime was estimated by observing the distribution of time interval when ^{22}Na source is replaced by ^{60}Co which emits two γ-rays almost simultaneously. The prompt curve is shown in Figure 3.7. The full width of this prompt distribution at half maximum was ~280

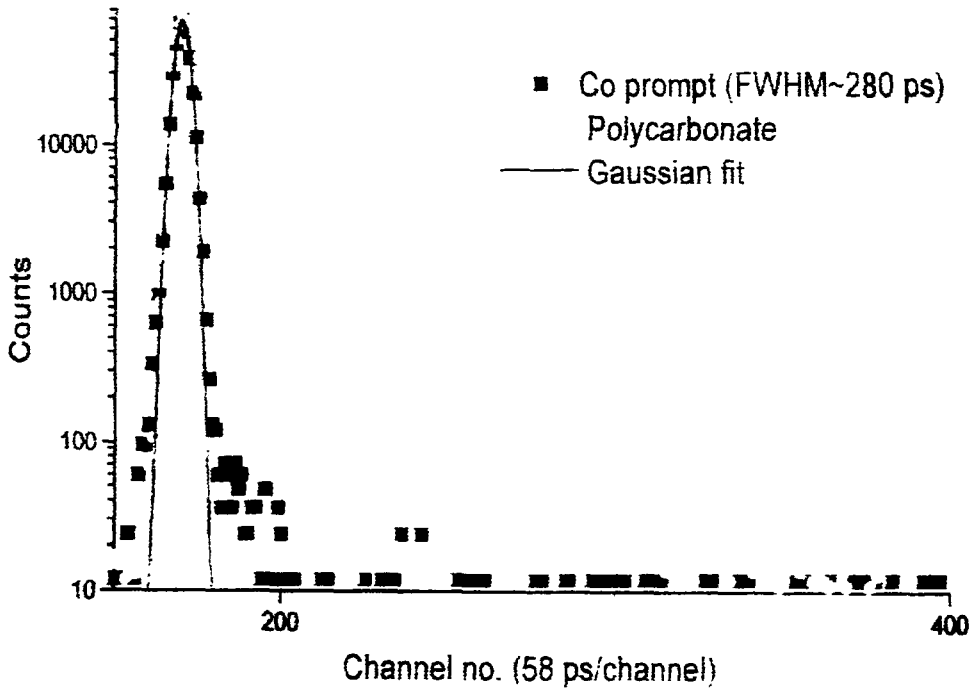

Figure 3.7: Typical lifetime spectra of polycarbonate. The prompt curve represents the instrumental resolution.

3.5 Data acquisition and Analysis

The lifetime spectra for the samples were recorded for ~ 100000 total counts and under the same experimental conditions. The count rate was ~ 8 S^{-1}. ^{60}Co prompt Spectrum at ^{22}Na gate was recorded. The full width at half maximum (FWHM) of this spectrum was ~ 0.280ns. The stability of the spectrometer was ensured by measuring the width of the resolution function (FWHM) at the start and the end of the experiment. The lifetime's spectra of well annealed Aluminum and PI (Kapton) which have only one lifetime component were recorded in the same experimental settings and with the same positron source as a reference spectrum. Good variance and only statistical scatter of the bulk lifetime of reference samples indicate the stability of the spectrometer [20]. It can, therefore, be assumed that the resolution function and the source components are expected to be identical in all spectra. However, the total source contribution may differ due to different positron back-scattering coefficients, The lifetime parameters of source were estimated by assuming the positron lifetime in well annealed Al and Kapton foil, τ = 0.164 ns and τ = 0.385 ns respectively and fixing them during the fitting procedure. The lifetime spectra of some studied unirradiated and irradiated Polymer samples.

Computer code PATFIT [21] was used for spectra analysis. This program allows positron spectrums to be analyzed in terms of discrete components, as well as in terms of continuous sum of decay curves given with a log normal distribution. The program can also carry out a mixed analysis in the sense that some components can be constrained to be discrete whilst others may be treated as continuous. In mixed analysis the longest component is assumed to be continuous because of the fact that shorter components should not give large distributions owing to their origin, while the longest one should reflect the whole distribution. PATFIT decomposes a PAL spectrum into 2-5 terms of negative exponentials. In polymers three lifetime results give the best χ^2 (<1.1) and most reasonable standard deviations [22]. o-Ps annihilation in the spherical free volume can be described by a simple quantum mechanical model of spherical potential well with an electron layer of thickness ΔR. The results of o-Ps lifetime (τ_3), the longest lifetime due to o-Ps pick off annihilation were employed to obtain the mean free volume hole radius by the semi-empirical equation [23,24].

$$\tau_3 = \frac{1}{\lambda_3} = \frac{1}{2}\left[1 - \frac{R}{R_0} + \frac{1}{2\pi} Sin\left(\frac{2\pi R}{R_0}\right)\right]^{-1} \quad (3.2)$$

where

τ_3 is the long lived component (o-Ps lifetime) in ns

R is the hole radius expressed in Å

Ro equals R+ΔR where ΔR is the fitted empirical layer thickness (= 1.66Å)

Average micro- void volume V_f can be computed by

$$V_h = \frac{4}{3}\pi R^3 \quad (3.3)$$

and the fractional volume f_v is given by as

$$f_v = c(\tfrac{4}{3}\pi R^3) \times I_3 \quad (3.4)$$

where c is a structural constant evaluated from an independent isochronal experiment and is determined empirically to be ~ .0018 [25] and I_3 is the intensity of the o-Ps component..

3.6 Results and Discussion

3.6.1 Polyamide Nylon-6 (PN-6)

Polyamide Nylon-6 samples were irradiated by 70 MeV C^{5+} ion beam from 15 UD Pelletron Accelerator to the fluences of $9.3x10^{11}$, $3.7x10^{12}$, $1.8x10^{13}$ and $3.7x10^{13}$ ions/cm^2.The lifetime parameters of the un-irradiated and irradiated samples obtained from the analysis of PAL spectra are presented in Table-3.2a. Table-3.2b shows the results obtained from o-Ps lifetime τ_3 for the values of the free volume hole radius r_h, volume of free holes V_h and fractional free volume f_V for the pristine samples and irradiated with 70 MeV C^{5+} ion beam to different fluences. The variation of V_h and F_v as a function of ion fluence are shown in figures 3.6.1(a) and (b).

Table – 3.2 (a)

Polyamide Nylon-6 irradiated with 70 MeV C^{5+} Lifetime and intensities of unirradiated and irradiated PN-6 polymer

Fluence (ions/cm^2)	τ_1 (ns)	I_1 (%)	τ_2 (ns)	I_2 (%)	τ_3 (ns)	I_3 (%)
Unirradiated	0.20 ± 0.01	35.96 ± 4.24	0.39 ± 0.01	46.30 ± 4.24	1.71 ± 0.01	18.56 ± 0.23
9.3×10^{11}	0.17 ± 0.01	31.18 ± 2.78	0.38 ± 0.01	51.78 ± 2.64	1.69 ± 0.01	18.29 ± 0.19
3.7×10^{12}	0.17 ± 0.01	32.75 ± 1.79	0.37 ± 0.01	50.23 ± 1.01	1.68 ± 0.01	17.89 ± 0.18
1.8×10^{13}	0.17 ± 0.01	32.46 ± 1.791	0.37 ± 0.01	50.52 ± 1.01	1.67 ± 0.01	17.65 ± 0.18
3.7×10^{13}	0.16 ± 0.01	29.28 ± 2.01	0.36 ± 0.01	50.21 ± 1.02	1.62 ± 0.01	17.01 ± 0.18

Table – 3.2 (b)

The lifetime parameters of o-Ps and radius of free volume hole r_h (Å) and free volume V_h (Å^3) fractional free volume (f_V) in PN-6 polymer

Fluence (ions/cm^2)	τ_3 (ns)	I_3 (%)	r_h (Å)	V_h (Å^3)	F_V
Unirradiated	1.71 ± 0.01	18.56 ± 0.23	2.57	71.32	2.38
9.3×10^{11}	1.69 ± 0.01	18.29 ± 0.19	2.55	69.91	2.30
3.7×10^{12}	1.68 ± 0.01	17.89 ± 0.18	2.54	69.66	2.24
1.8×10^{13}	1.67 ± 0.01	17.65 ± 0.18	2.53	69.17	2.20
3.7×10^{13}	1.62 ± 0.01	17.23 ± 0.18	2.48	64.40	1.99

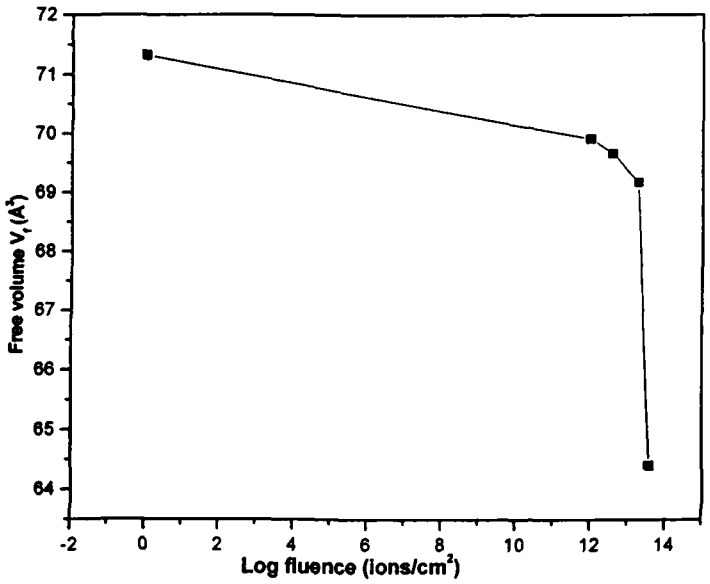

Figure 3.6.1 (a): Variation of average free volume (Å^3) with the fluence (ions/cm^2) in Polyamide Nylon-6, 70 MeV C^{5+} ions irradiated

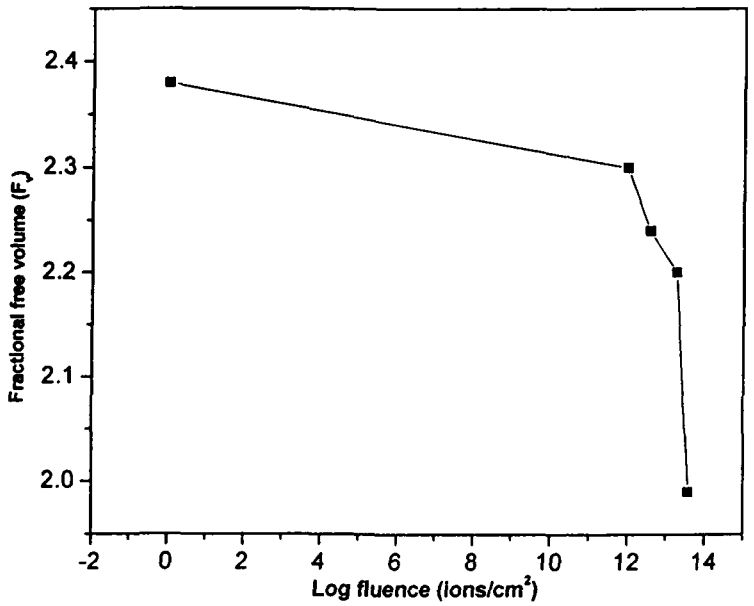

Figure 3.6.1 (b): Variation of fractional free volume with the fluence (ions/cm^2) in Polyamide Nylon-6, 70 MeV C^{5+} ions irradiated

The short lived component τ_1, corresponding to p-Ps is found to vary from 0.16 to 0.20 ns and corresponding intensity shows marginal change with fluences. It is observed that the lowest lifetime τ_1, attributed to p-Ps annihilation is found to be slightly larger than the expected value of $\tau_{1=}$ 0.125 ns and lies between (τ_1 =0.20 - 0.16 ns and I_1=35.96 - 29.28 %). The intermediate component τ_2, attributed to direct annihilation of positrons changes as (τ_2=0.36 - 0.39 ns and I_2 = 46.30-50.21). The intensity of this component is around 50% and shows the marginal variation with increasing fluences. A detailed analysis is difficult because of the possible formation of positron and positronium compounds that may overlap both components. The long lived component (τ_3 = 1.71 – 1.62 ns and I_3 = 18.56 – 17.01 %) is attributed to the o-Ps atoms in free volumes of amorphous regions of polymer via the pick-off annihilation. In PALS, it is the o-Ps lifetime which is directly correlated to the free volume. The intensity of this component contains information about free volume concentration [9].

o-Ps lifetime and, therefore, the average free volume and fractional free volume are found to be decreased due to irradiation at the fluences used in the present experiment. The results of

Lee et al for PMMA on irradiation indicate that high LET produces a high concentration of free radicals over many neighboring molecules, facilitating track overlap and enhancing cross-linking over scission while low LET affects only a simple molecular chain, leading to chain scission. In our earlier PAL measurements [26-31] on polymers (i) irradiated with different swift heavy ions to low fluences (10^5-10^6 ions/cm^2), average free volume has been found to increase with fluence and has been attributed to the chain scission along the tracks and (ii) irradiation to high fluences leads to the decrease in free volume, indicating cross linking of scissioned segments. The scission causes increase in the free volume whereas the cross-linking causes decreases in the free volume [14]. At high fluences the track area where cross-linking is predominant becomes comparable to the sample area. This explains the observed decrease in the o-Ps lifetime.

3. 6. 2 Makrofol-KG (Poly Carbonate)

Makrofol-KG polycarbonate, samples were irradiated with 100 MeV Si^{8+} ion beam to the fluences of 10^{10}, $3x10^{10}$, $1x10^{11}$, $3x10^{11}$, $6x10^{11}$ and 10^{12} ions/cm^2 at 15 UD Pelletron Accelerator at Inter University Accelerator Centre, New Delhi, INDIA and with with 145 MeV Ne^{6+} to the fluences of 10^{10}, 10^{11}, 10^{12} and 10^{13} ions/cm^2 at Variable Energy Cyclotron Centre (VECC), Kolkata, INDIA. A typical PAL spectral for virgin and irradiated samples is shown in Figure 3.6.2 (a). PAL spectra for virgin and irradiated samples were analyzed in terms of three lifetime components, each lifetime corresponding to the average annihilation rate of a positron in a different state.

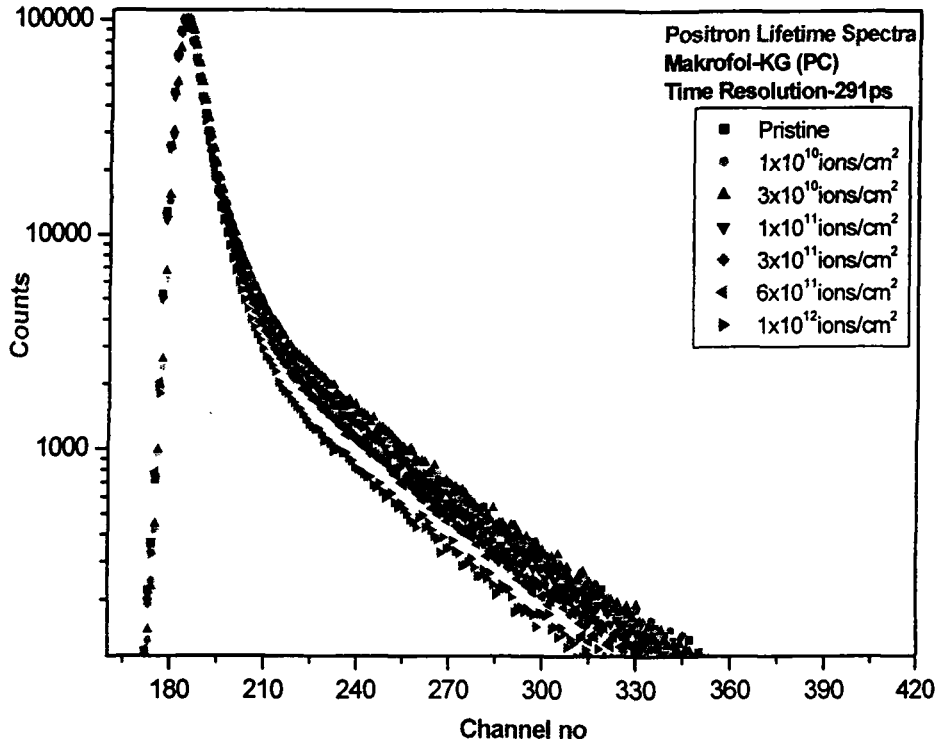

Figure 3.6.2(a): Positron lifetime spectra of pristine and irradiated with 100 MeV Si^{8+} ions Makrofol-KG.

Values of o-Ps lifetime, intensity are presented in Table 3.3-(a). Table-3.3(b) shows the results obtained from o-Ps lifetime τ_3 for the values of the free volume hole radius r_h and volume of free holes V_h and fractional free volume F_v for the pristine samples and irradiated with 100 MeV Si^{8+} ion beam to different fluences. The variation of

3. 6. 2 Makrofol-KG (Poly Carbonate)

Makrofol-KG polycarbonate, samples were irradiated with 100 MeV Si^{8+} ion beam to the fluences of 10^{10}, $3x10^{10}$, $1x10^{11}$, $3x10^{11}$, $6x10^{11}$ and 10^{12} ions/cm^2 at 15 UD Pelletron Accelerator at Inter University Accelerator Centre, New Delhi, INDIA and with with 145 MeV Ne^{6+} to the fluences of 10^{10}, 10^{11}, 10^{12} and 10^{13} ions/cm^2 at Variable Energy Cyclotron Centre (VECC), Kolkata, INDIA. A typical PAL spectral for virgin and irradiated samples is shown in Figure 3.6.2 (a). PAL spectra for virgin and irradiated samples were analyzed in terms of three lifetime components, each lifetime corresponding to the average annihilation rate of a positron in a different state.

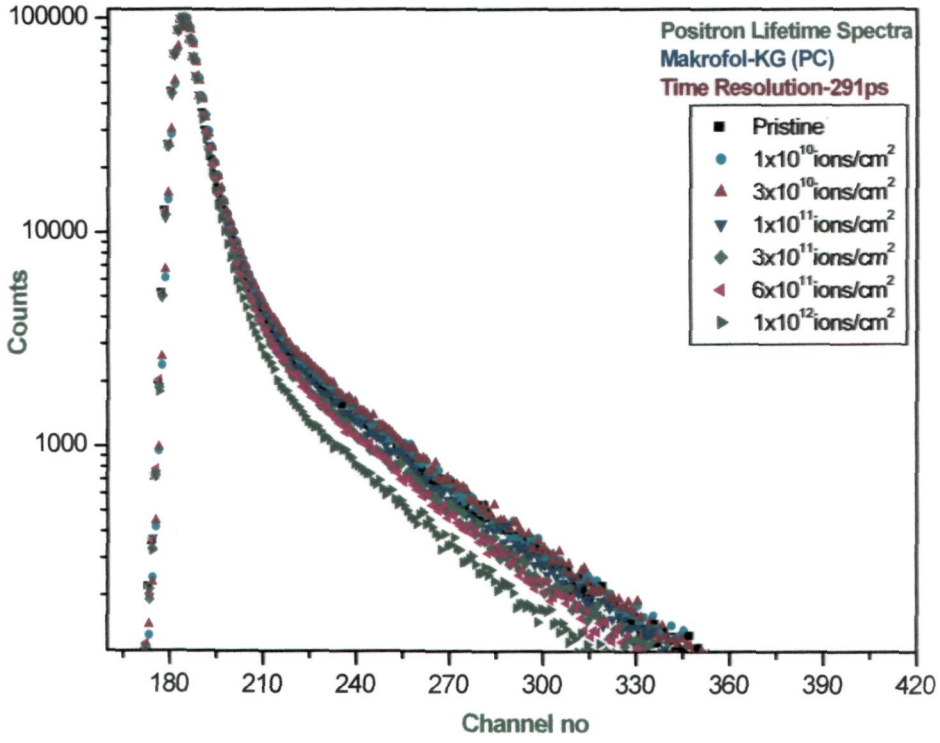

Figure 3.6.2(a): Positron lifetime spectra of pristine and irradiated with 100 MeV Si^{8+} ions Makrofol-KG.

Values of o-Ps lifetime, intensity are presented in Table 3.3-(a). Table-3.3(b) shows the results obtained from o-Ps lifetime τ_3 for the values of the free volume hole radius r_h and volume of free holes V_h and fractional free volume F_v for the pristine samples and irradiated with 100 MeV Si^{8+} ion beam to different fluences. The variation of

V_h and F_v as a function of ion fluence are shown in Figures 3.6.2 (b) and (c). In PALS, it is the o-Ps lifetime, which is directly correlated to the free volume. The intensity of this component contains information about free volume concentration [9].

The shortest lifetime component τ_1 varies from 0.177 to 0.189 ns and I_1 from 47.85 to 56.93 % and belongs to the annihilation of p-Ps atoms, while the intermediate one (τ_2 = 0.397 – 0.446 ns and I_2 = 26.21 – 3164%) arises from the free annihilation of positrons in the polymer matrix. The long lived component (τ_3 = 2.1348 – 2.2368 ns and I_3 = 13.053 – 21.498 %) is attributed to the o-Ps atoms in free volumes of amorphous regions of polymer via the pick-off annihilation, which is very sensitive to the structural changes in the polymer.

Table – 3.3 (a)

Makrofol-KG Polycarbonate (PC) irradiated with 100 MeV Si^{8+} Lifetime and intensities of unirradiated and irradiated

Fluence (ions/cm^2)	**τ_1 (ns)**	**I_1 (%)**	**τ_2 (ns)**	**I_2 (%)**	**τ_3 (ns)**	**I_3 (%)**
Pristine	0.177 ± 0.005	47.85 ± 2.03	0.426 ± 0.013	30.65 ± 1.91	2.2368 ± 0.01	21.498 ± 0.17
$1x10^{10}$	0.179 ± 0.005	47.90 ± 2.00	0.424 ± 0.013	30.67 ± 1.89	2.2244 ± 0.01	21.427 ± 0.16
$3x10^{10}$	0.178 ± 0.005	45.62 ± 2.21	0.413 ± 0.013	31.64 ± 2.10	2.2098 ± 0.010	22.546 ± 0.17
$1x10^{11}$	0.189 ± 0.005	53.78 ± 2.06	0.446 ± 0.016	26.21 ± 1.93	2.2083 ± 0.01	20.009 ± 0.18
$3x10^{11}$	0.177 ± 0.005	52.27 ± 2.23	0.413 ± 0.013	30.19 ± 2.12	2.1755 ± 0.01	17.540 ± 0.16
$6x10^{11}$	0.176 ± 0.005	51.26 ± 2.15	0.415 ± 0.013	31.57 ± 2.04	2.1431 ± 0.01	17.169 ± 0.16
10^{12}	0.178 ± 0.005	56.93 ± 2.56	0.397 ± 0.013	30.02 ± 2.47	2.1348 ± 0.01	13.054 ± 0.15

Table – 3.3 (b)

The lifetime parameters of o-Ps and radius of free volume hole r_h (Å), free volume V_f (Å^3) and fractional free volume (f_V)

Fluence (ions/cm^2)	**τ_3 (ns)**	**I_3 (%)**	**r_h (Å)**	**V_h (Å^3)**	**F_V**
Pristine	2.2368 ± 0.01	21.498 ± 0.17	3.063	120.370	4.658
1x10^{10}	2.2244 ± 0.01	21.427 ± 0.16	3.053	119.194	4.598
3x10^{10}	2.2098 ± 0.010	22.546 ± 0.17	3.041	117.795	4.781
1x10^{11}	2.2083 ± 0.01	20.009 ± 0.18	3.039	117.562	4.234
3x10^{11}	2.1755 ± 0.01	17.540 ± 0.16	3.011	114.343	3.610
6x10^{11}	2.1431 ± 0.01	17.169 ± 0.16	2.983	111.182	3.445
10^{12}	2.1348 ± 0.01	13.054 ± 0.15	2.976	110.401	2.603

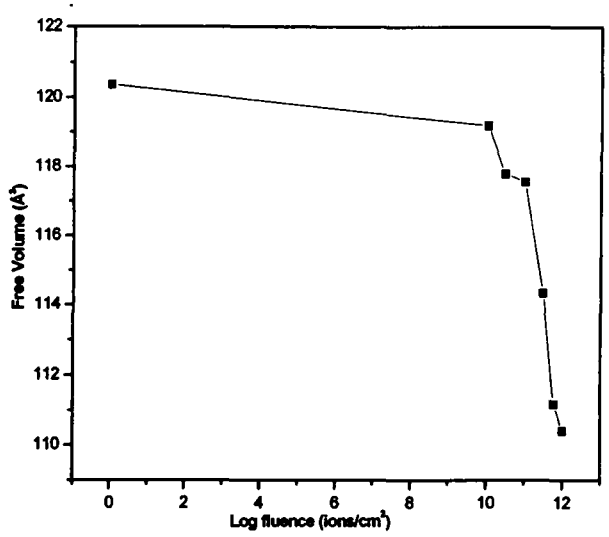

Figure 3.6.2 (b): Variation of average free volume ($Å^3$) with the fluence (ions/cm^2) in Makrofol-KG, 100 MeV Si^{8+} ions irradiated

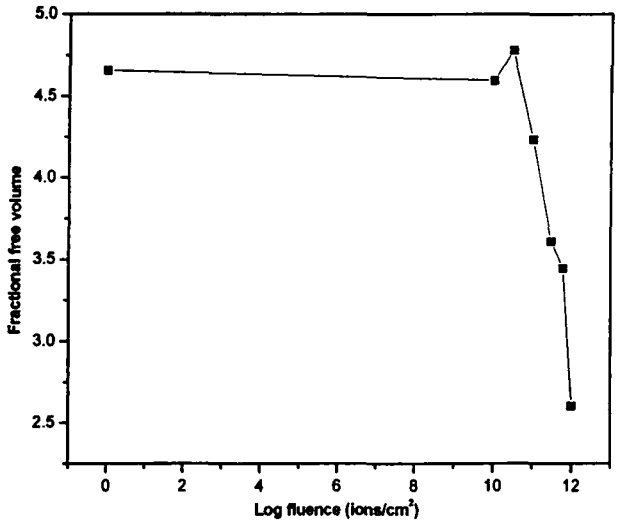

Figure3.6.2 (c): Variation of fractional free volume with the fluence (ions/cm^2 in Makrofol-KG, 100 MeV Si^{8+} ions irradiated

Values of lifetime and intensity obtained from the analyses of PAL spectra of Makrofol-KG samples for pristine and irradiated with 145 Ne^{6+} ion beam are presented in Table3.4 (a). Table-3.4 (b) shows the results obtained from o-Ps lifetime τ_3 for the values of the free volume hole radius r_h and volume of free holes V_h. Figures 3.6.2 (d) and (e) shows the variation of fee volume V_f and fractional free volume F_v with the ion fluence.

Table – 3.4 (a)

Makrofol-KG Polycarbonate (PC) irradiated with 145 MeV Ne^{6+} Lifetime and intensities of unirradiated and irradiated samples

Fluence (ions/cm^2)	τ_1 (ns)	I_1 (%)	τ_2 (ns)	I_2 (%)	τ_3 (ns)	I_3 (%)
Un-irradiated	0.176 ± 0.010	46.613 ± 2.22	0.409 ± 0.010	34.469 ± 2.11	2.218 ± 0.010	18.418 ± 0.17
10^{10}	0.174 ± 0.010	45.124 ± 2.18	0.405 ± 0.010	34.045 ± 2.01	2.214 ± 0.010	20.831 ± 0.16
10^{11}	0.178 ± 0.010	45.817 ± 2.21	0.414 ± 0.010	31.637 ± 2.11	2.210 ± 0.010	22.546 ± 0.17
10^{12}	0.165 ± 0.010	40.922 ± 2.27	0.388 ± 0.010	36.207 ± 2.16	2.196 ± 0.010	21.872 ± 0.16
10^{13}	0.166 ± 0.010	42.702 ± 2.35	0.384 ± 0.010	38.380 ± 2.25	2.090 ± 0.010	16.118 ± 0.16

Table- 3.4 (b)

The lifetime parameters of o-Ps and radius of free volume hole r_h (Å) and free volume V_f (Å^3) fractional free volume (f_V)

Fluence (ions/cm^2)	τ_3 (ns)	I_3 (%)	r_h (Å)	V_F (Å^3)	F_v
Unirradiated	2.218 ± 0.010	18.418 ± 0.17	3.048	118.590	4.038
10^{10}	2.214 ± 0.010	20.831 ± 0.16	3.044	118.143	4.429
10^{11}	2.210 ± 0.010	22.546 ± 0.17	3.041	117.795	4.780
10^{12}	2.196 ± 0.010	21.872 ± 0.16	3.029	116.410	4.583
10^{13}	2.090 ± 0.010	16.118 ± 0.16	2.937	106.118	3.613

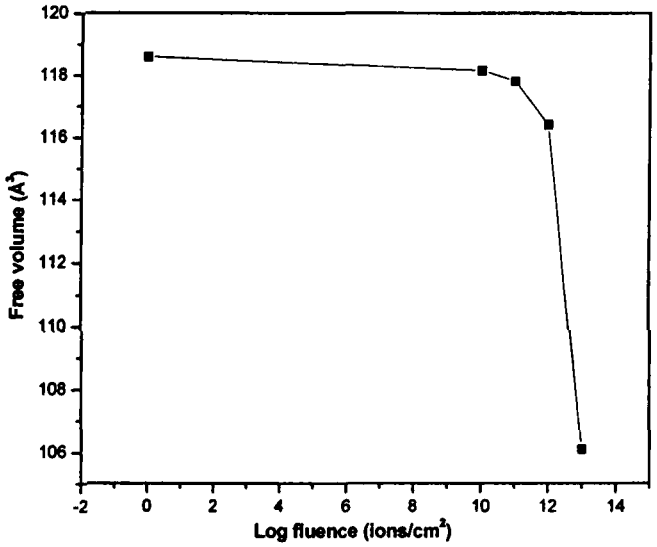

Figure3.6.2 (d): Variation of average free volume ($Å^3$) with the fluence ($ions/cm^2$) in Makrofol-KG, 145 MeV Ne^{6+} ions irradiated

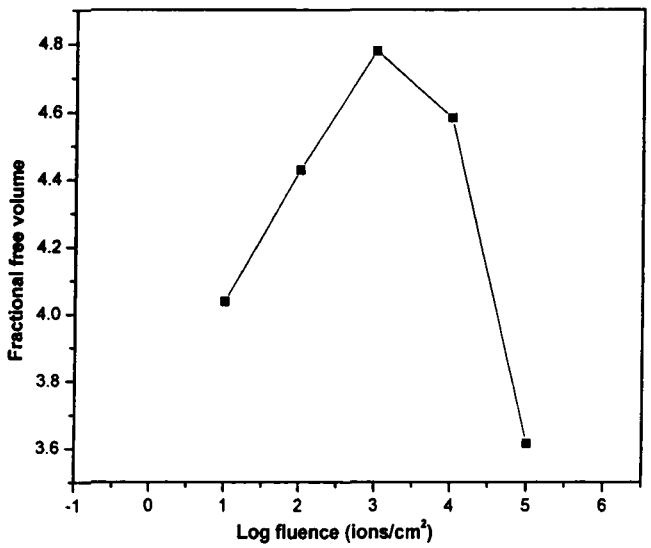

Figure 3.6.2 (e): Variation of fractional free volume with the fluence ($ions/cm^2$ in Makrofol-KG, 145 MeV Ne^{6+} ions irradiated

The analyses gives (τ_1 = 0.165 – 0.178 ns and I_1 = 40.92 – 46.61 %) belonging to the annihilation of p-Ps atoms and intermediate one (τ_2 = 0.384 – 0.414 ns and I_2 = 31.63 – 38.38 %) arising from the free annihilation of positrons in the polymer matrix. The longest lived component attributed to the o-Ps atoms in free volumes of polymer via e pick-off annihilation gives (τ_3 = 2.090 – 2.218 ns and I_3 = 16.11 – 22.54 %) . o-Ps lifetime is directly correlated to the free volume whereas the intensity of this component contains information about free volume hole concentration. o-Ps lifetime and, therefore, the average free volume and fractional free volume are found to be decreased due to irradiation at the fluences used in the present experiment. The decrease in τ_3 is related to the change in the free volume as a result of the formation of new bonds or cross-linking. This decrease in τ_3 implies some shrinking of inner and inner-chain of free volume holes (i.e. impact structure was attained). V_h is found to decrease from 118.59 to 106.11Å^3 with a decrease 0f 10.52% at 10^{13} ions/ cm^2. Kobayashi et al., 1994 have attributed the small decrease in free volume in PEEK due to electron irradiation, to intermolecular cross-linking. The dominance of scission or cross-linking due to ion irradiation depends essentially on the polymer and energy loss per unit path length or linear energy transfer (LET). For low LET, spurs develop for apart and independently; the deposited energy tends to be confined in one chain (not in neighboring chain) leading scission [27, 28, and 31]. In case of high electronic LET, spurs overlap, the probability of two radical pairs to be in neighboring chains is increased and cross-linking is facilitated. The scission causes increase in the free volume whereas the cross-linking causes decreases in the free volume [14]. At high fluences the track area where cross-linking is predominant becomes comparable to the sample area. This explains the observed decrease in the o-Ps lifetime.

The results of Lee et al., 1999 for PMMA on ion irradiation indicate that high LET produce a high concentration of free radicals over many neighboring molecular chains, facilitating track overlap and enhancing cross-linking over scission while low LET affects only a simple molecular chain, leading to chain scission.

In our earlier PAL measurements [27-32] on polymers (i) irradiated with different swift heavy ions to low fluences (10^5-10^{69} ions/cm^2), average free volume has been found to increase with fluence and has been attributed to the chain scission along the tracks and

(ii) irradiation to high fluences leads to the decrease in free volume, indicating cross linking of scissioned segments.

In the present case I_3 is found to decrease with ion fluence and more generally speaking, cross-linking resulting in a loss in the number of those free spaces where Ps formed in either the crystalline or amorphous phases can be responsible for this. It is to be noted that, on the basis of the spur model, one may further hypothesize that cross-linking would result in decrease in the diffusive properties of either e^+ or e^-, resulting in a lesser probability for Ps formation.

The cross-linking as an essential phenomenon is known to be the most effective process in polystyrene, PN-6 and CR-39 polymers as bombarded with high energy particles [27,31 and 33] due to the free radical recombination and various degradations, possibly resulting in the changes in amorphousity. For low LET, spurs develop far apart and independently; the deposited energy tends to be confined in one chain (not in neighboring chain) leading to scission [6, 14]. In case of high electronic LET, spurs overlap, the probability of two radical pairs to be in neighboring chains is increased and cross-linking is facilitated. The scission causes increase in the free volume whereas the cross-linking causes decrease in the free volume [26-31,6]. At high fluences the track area where cross-linking is predominant becomes comparable to the sample area. This may explain the observed decrease in the o-Ps lifetime as observed in the present case.

3.6.3 Polyethersulphone (PES)

Polyethersulphone (PES) , samples were irradiated with 100 MeV Si^{8+} ion beam to the fluences of $1x10^{10}$,$1x10^{11}$,10^{12}, and $5x10^{12}$ ions/cm^2 at 15 UD Pelletron Accelerator at Inter University Accelerator Centre, New Delhi, India and with 145 MeV Ne^{6+} ion beam to the fluences of 10^{12} and 10^{13} ions/cm^2 at Variable Energy Cyclotron Centre (VECC), Kolkata, India.

The lifetime spectra of pristine and 100 MeV Si^{8+} ions irradiated Polyethersulphone (PES) is shown in fig 3.6.3 (a).

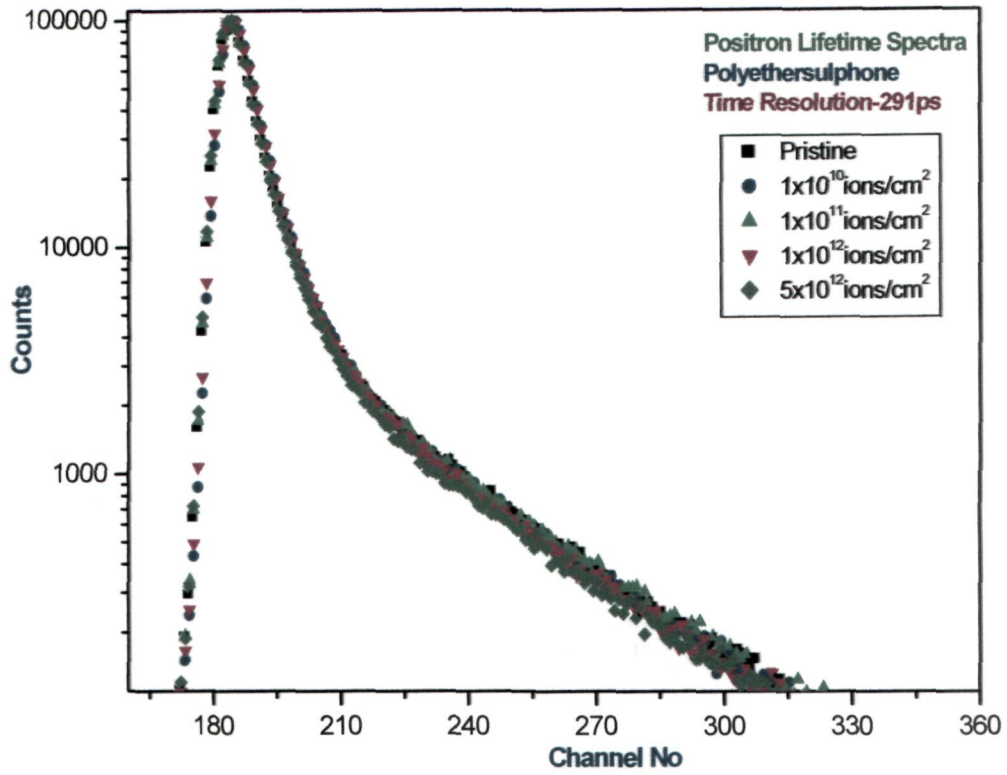

Figure 3.6.3(a): Positron lifetime spectra of Pristine and irradiated with 100 MeV Si^{8+} ions Polyethersulphone (PES)

The positron lifetimes and intensities are presented in Table-3.5 (a) obtained from PATFIT. Table-3.5 (b) presents the values of the free volume hole radius r_h and volume of free holes V_h for the pristine samples and irradiated with 100 MeV Si^{8+} ion beam to different fluences. Figures 3.6.3 (b) and (c) shows the variation of free volume V_h and fractional free volume F_v with the ion fluence.

Table – 3.5 (a)

Polyethersulphone (PES) irradiated with 100 MeV Si^{8+}. Lifetime and intensities of unirradiated and irradiated Polyethersulphone (PES)

Fluence (ions/cm^2)	τ_1 (ns)	I_1 (%)	τ_2 (ns)	I_2 (%)	τ_3 (ns)	I_3 (%)
Pristine	0.161 ± 0.006	44.427 ± 2.55	0.370 ± 0.010	39.527 ± 2.44	1.906 ± 0.011	16.047 ± 0.17
$1x10^{10}$	0.165 ± 0.005	48.028 ± 2.46	0.377 ± 0.011	36.918 ± 2.36	1.899 ± 0.012	15.054 ± 0.16
$1x10^{11}$	0.183 ± 0.005	53.671 ± 2.39	0.416 ± 0.015	30.586 ± 2.27	1.951 ± 0.013	15.743 ± 0.19
10^{12}	0.193 ± 0.004	60.023 ± 2.19	0.444 ± 0.017	26.863 ± 2.06	1.992 ± 0.015	13.115 ± 0.15
$5x1x10^{12}$	0.202 ± 0.004	62.22 ± 1.91	0.479 ± 0.018	24.279 ± 1.77	1.998 ± 0.016	13.503 ± 0.21

Table – 3.5 (b)

The lifetime parameters of o-Ps and radius of free volume hole (R), free volume and fractional free volume (f_V) in Polyethersulphone (PES).

Fluence (ions/cm^2)	τ_3 (ns)	I_3 (%)	R (Å)	V_f (Å^3)	F_V
Pristine	1.906 ± 0.011	16.047 ± 0.17	2.768	88.833	2.565
$1x10^{10}$	1.899 ± 0.012	15.054 ± 0.16	2.762	88.257	2.392
$1x10^{11}$	1.951 ± 0.013	15.743 ± 0.19	2.810	92.938	2.633
10^{12}	1.992 ± 0.015	13.115 ± 0.15	2.848	96.760	2.308
$5x10^{12}$	1.998 ± 0.016	13.503 ± 0.21	2.854	97.373	2.366

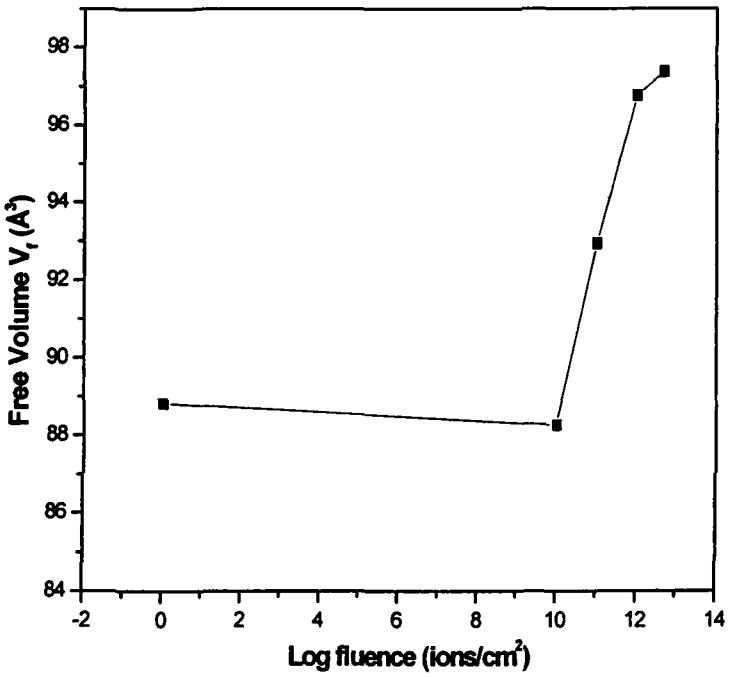

Figure3.6.3 (b): Variation of average free volume (Å^3) with the log fluence (ions/cm^2) in Polyethersulphone (PES) 100 MeV Si^{8+} ions irradiated.

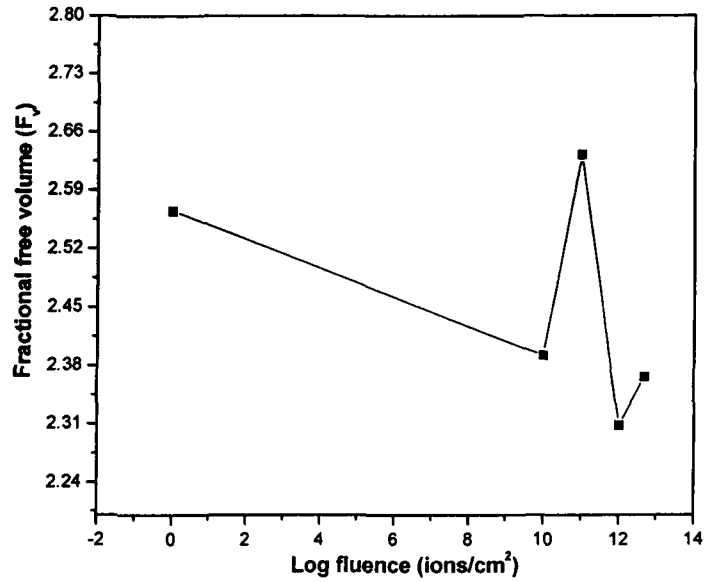

Figure 3.6.3 (c): Variation of fractional free volume with the log fluence (ions/cm^2) in Polyethersulphone (PES) 100 MeV Si^{8+} ions irradiated

From the analyses of the spectra we obtain (τ_1 = 0.161 – 0.193 ns and I_1 = 44.427 – 60.023 %) , (τ_2 = 0.370 – 0.444 ns and I_2 = 39.527 – 26.863 %) and (τ_3 = 1.906 – 1.992 ns and I_3 = 16.047 – 13.115 %).

The positron lifetimes and intensities for Polyethersulphone are presented in Table-3.6(a). Table-3.6(b) shows the results obtained from o-Ps lifetime τ_3 for the values of the free volume hole radius r_h and volume of free holes V_h for the pristine samples and irradiated with 145 MeV Ne^{6+} ion beam to the fluences of 10^{12} and 10^{13} ions/cm^2. Figures 3.6.3(d) and 3.6.3(e) shows the variation of fee volume V_h and fractional free volume F_v with the ion fluence.

Table 3.6 (a)

Polyethersulphone (PES) irradiated with 145 MeV Ne^{6+} Lifetime and intensities of un-irradiated and irradiated.

Fluence (ions/cm^2)	**τ_1 (ns)**	**I_1 (%)**	**τ_2 (ns)**	**I_2 (%)**	**τ_3 (ns)**	**I_3 (%)**
Unirradiated	0.187 ± 0.005	55.17 ± 2.66	0.412 ± 0.015	31.31 ± 2.54	1.96 ± 0.01	13.52 ± 0.18
10^{12}	0.175 ± 0.006	50.32 ± 2.80	0.382 ± 0.002	41.09 ± 2.70	1.95 ± 0.01	8.58 ± 0.14
10^{13}	0.161 ± 0.006	44.43 ± 2.55	0.370 ± 0.010	39.53 ± 2.44	1.91 ± 0.01	16.05 ± 0.17

Table 3.6 (b)

The lifetime parameters of o-Ps and radius of free volume hole r_h (Å) and free volume V_f (Å^3) fractional free volume (f_V)

Fluence (ions/cm^2)	**τ_3 (ns)**	**I_3 (%)**	**r_h (Å)**	**V_f (Å^3)**	**(Fv)**
Unirradiated	1.96	13.523	2.8180	93.72	2.2812
10^{12}	1.95	8.588	2.8090	92.82	1.4349
10^{13}	1.91	16.046	2.7710	89.11	2.5736

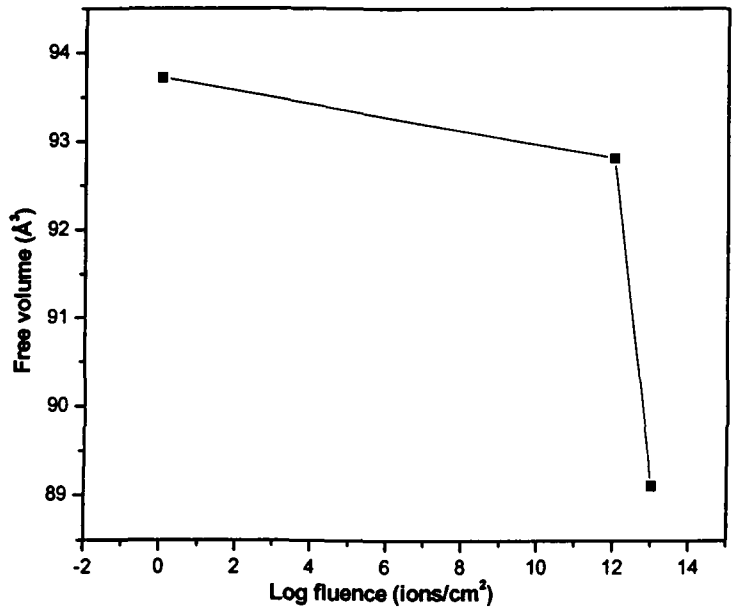

Figure 3.6.3(d): Variation of average free volume ($Å^3$) with the fluence ($ions/cm^2$)

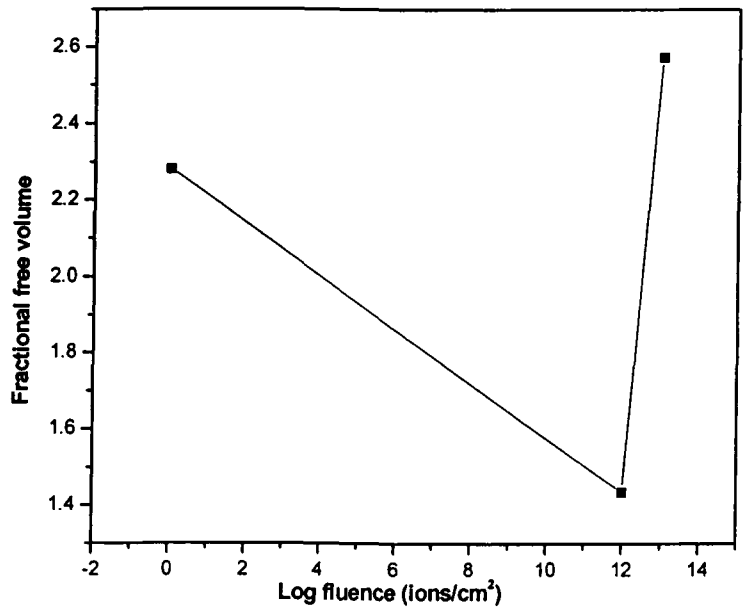

Figure3.6.3 (e): Variation of fractional free volume with the fluence ($ions/cm^2$)

PAL spectra of pristine and irradiated with 145 MeV Ne^{6+} ion beam, analyzed in terms of three lifetime components provides the shortest lifetime component (τ_1 = 0.161 – 0.187 ns and I_1 = 44.43 – 55.17 %) belonging to the annihilation of p-Ps atoms, while the intermediate one (τ_2 = 0.370 – 0.412 ns and I_2 = 39.53 – 31.31 %) arises from the free annihilation of positrons in the polymer matrix. The long-lived component (τ_3 = 1.91 – 1.96 ns and I_3 = 16.05 – 13.52 %).

The energy transfer by the ion irradiation leads to radical formation, bond scission and cross-linking of polymer chains. The dominance of scission or cross-linking depends essentially on the polymer and energy loss per unit path length or linear energy transfer (LET). The decrease in τ_3 is related to the change in the free volume as a result of the formation of new bonds or cross-linking. The average free volume of PES has been found to increase with the ion fluence and has been attributed to chain scission along the track in case of si^{8+} ion beam irradiation. The decrease in τ_3 is related to the change in the free volume as a result of the formation of new bonds or cross-linking. Ne^{6+} ion beam irradiation of PES films is found to decrease the free volume from 93.72 $Å^3$ to 89.11$Å^3$.

3.6.4 Polystyrene (PS)

The positron lifetime spectra of conducting Polystyrene pristine and irradiated with 100 MeV Si^{8+} ion beam from 15 UD Pelletron Accelerator at IUAC, New Delhi to the fluences of 10^{11}, 10^{12} and 10^{13} ions/cm^2 and $5x10^{10}$, and the fluences 10^{11},$5x10^{11}$, 10^{12}, $5x10^{11}$ and $3.5x10^{13}$ ions/cm^2 for irradiated with 50MeVLi^{3+} ion beam were analyzed in terms of three lifetime components. Values of the positron lifetimes and intensities for Polystyrene are presented in Table-3.7(a). Table-3.7(b) shows the results obtained from o-Ps lifetime τ_3 for the values of the free volume hole radius r_h and volume of free holes V_h and fractional free volume F_v The variation of V_h and F_v as a function of ion fluence are shown in Figures 3.6.4 (a) and (b).

Table – 3.7 (a)

Polystyrene (PS) irradiated with 100 MeV Si^{8+} Lifetime and intensities of unirradiated and irradiated

Fluence (ions/cm^2)	τ_1 (ns)	I_1 (%)	τ_2 (ns)	I_2 (%)	τ_3 (ns)	I_3 (%)
Pristine	0.170 ± 0.006	43.019 ± 2.16	0.4056 ± 0.012	32.568 ± 2.05	1.906 ± 0.011	16.047 ± 0.17
$1x10^{11}$	0.169 ± 0.007	40.520 ± 2.62	0.3809 ± 0.011	37.921 ± 2.53	1.899 ± 0.012	15.054 ± 0.16
$1x10^{12}$	0.175 ± 0.007	42.099 ± 2.56	0.3957 ± 0.013	33.887 ± 2.45	1.951 ± 0.013	15.743 ± 0.19
$1x10^{13}$	0.149 ± 0.007	35.330 ± 2.17	0.3635 ± 0.010	39.076 ± 2.07	1.998 ± 0.016	13.503 ± 0.21

Table – 3.7 (b)

The lifetime parameters of o-Ps and radius of free volume hole r_h (Å) and free volume V_h (Å^3) fractional free volume (f_V).

Fluence (ions/cm^2)	τ_3 (ns)	I_3 (%)	r_h (Å)	V_f (Å^3)	Fv
Pristine	2.26 ± 0.008	25.59 ± 0.150	3.083	122.72	5.65
10^{11}	2.25 ± 0.009	24.41 ± 0.166	3.075	121.77	5.35
10^{12}	2.23 ±0.010	21.56 ± 0.152	3.058	119.76	4.65
10^{13}	2.22 ± 0.009	24.01 ± 0.165	3.049	118.70	5.12

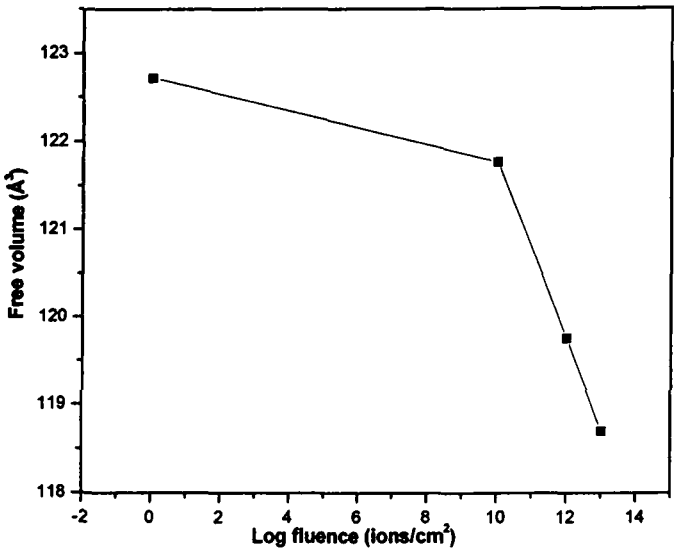

Figure 3.6.4 (a): Variation of average free volume ($Å^3$) with the fluence (ions/cm^2) in Polystyrene (PS) 100 MeV Si^{8+} ions irradiated

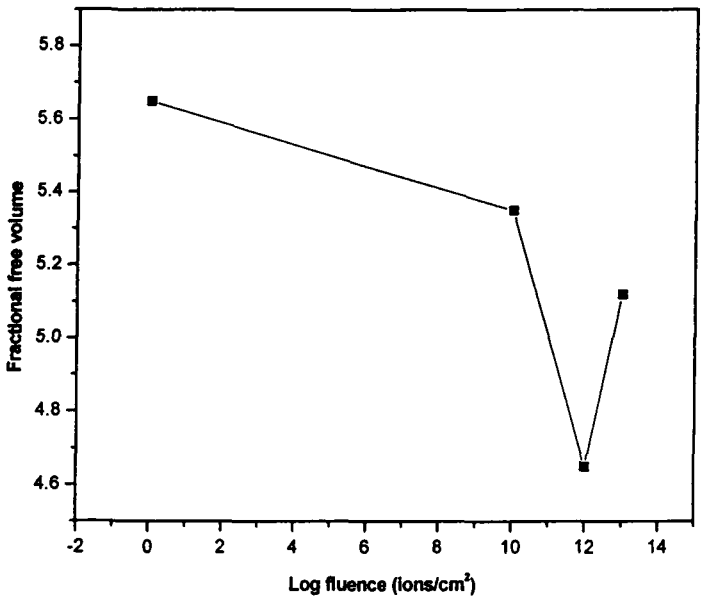

Figure 3. 6. 4 (b): Variation of fractional free volume with the fluence (ions/cm^2) in Polystyrene (PS) 100 MeV Si^{8+} ions irradiated

The shortest lifetime component (τ_1= 170-.149 ns and I_1= 43.019 – 35.330%), the intermediate one (τ_2 = 0.4056 – 0.3635 ns and I_2 = 32.568 – 39.076 %) and the longest-lived component (τ_3 = 1.906 – 1.998 ns and I_3 = 16.047 – 13.503 %) were obtained from PATFIT analyses. o-Ps lifetime and, therefore, the average free volume and fractional free volume are found to be decreased due to irradiation at the fluences used in the present experiment. At these high fluences the track area where cross-linking is predominant becomes comparable to the sample area. This explains the observed decrease in the o-Ps lifetime.

The results for 50 MeV Li^{3+} ion beam irradiated Polystyrene lifetime spectra are presented in Table-3.8(a). The lifetime component obtained from the analyses are: the shortest: (τ_1= 0.132-0.136 ns and I_1= 25.9 – 27.80%), the intermediate one (τ_2 = 0.331 – 0.353 ns and I_2 = 45.5 – 47.8 %) and the longest-lived component (τ_3 = 2.099 – 2.056 ns and I_3 = 28.2 – 24.9%). Table-3.8(b) presents the data obtained from o-Ps lifetime τ_3 for the values of the free volume hole radius r_h, volume of free holes V_h and F_v along with the S-parameter obtained from Doppler Broadening Spectra (DBS) for the pristine and irradiated samples. The variation of V_h and F_v as a function of ion fluence is shown in Figures 3.6.4 (c), (d) and (e).

Table – 3.8 (a)

Polystyrene (PS) irradiated with 50 MeV Li^{3+} Lifetime and intensities of unirradiated and irradiated Polystyrene.

Fluence (ions/cm^2)	τ_1 (ns)	I_1 (%)	τ_2 (ns)	I_2 (%)	τ_3 (ns)	I_3 (%)
Pristine	.132 ± .004	25.9 ± 1.1	.331 ± .004	45.5 ± 1.0	2.099 ± 0.02	28.2 ± 0.2
$5x10^{10}$	.120 ± .004	24.2 ± 1.1	.325 ± .004	46.8 ± 1.0	2.098 ± 0.02	28.6 ± 0.2
$1x10^{11}$	.126 ± .004	25.7 ± 1.1	335 ± .004	45.7 ± 1.0	2.110 ± 0.02	28.2 ± 0.2
$5x10^{11}$	.126 ± .004	25.3 ± 1.1	.331 ± .004	45.9 ± 1.0	2.096 ± 0.02	28.4 ± 0.2
$1x10^{12}$	.136 ± .004	27.6 ± 1.1	.344 ± .004	44.2 ± 1.0	2.113 ± 0.02	27.7 ± 0.2
$5x10^{12}$	.128 ± .004	25.7 ± 1.1	.338 ± .004	46.0 ± 1.0	2.109 ± 0.02	27.4 ± 0.2
$1x10^{13}$	.125 ± .004	26.4 ± 1.1	.343 ± .004	47.8 ± 1.0	2.108 ± 0.02	25.4 ± 0.2
$3.5x10^{13}$	.136 ± .004	27.8 ± 1.1	.353 ± .004	47.8 ± 1.0	2.056 ± 0.02	24.9 ± 0.2

Table – 3.8 (b)

The lifetime parameters of o-Ps and radius of free volume hole (R). free volume, fractional free volume (f_V) and S-parameter in Polystyrene (PS).

Fluence (ions/cm^2)	τ_3 (ns)	I_3 (%)	r_h (Å)	V_f (Å^3)	Fv	S-Parameter
Pristine	2.099 ± 0.01	28.2 ± 0.3	2.945	106.970	5.43	0.4585
$5x10^{10}$	2.098 ± 0.01	28.6 ± 0.3	2.943	106.752	5.45	0.4565
$1x10^{11}$	2.110 ± 0.01	28.2 ± 0.3	2.956	107.795	5.47	0.4549
$5x10^{11}$	2.096 ± 0.01	28.4 ± 0.3	2.942	106.644	5.45	0.4593
$1x10^{12}$	2.113 ± 0.01	27.7 ± 0.3	2.957	108.283	5.34	0.4594
$5x10^{12}$	2.109 ± 0.01	27.4 ± 0.3	2.953	107.844	5.32	0.4597
$1x10^{13}$	2.108 ± 0.01	25.4 ± 0.3	2.952	107.735	4.93	0.4600
$3.5x10^{13}$	2.056 ± 0.01	24.9 ± 0.26	2.906	102.776	4.44	0.4581

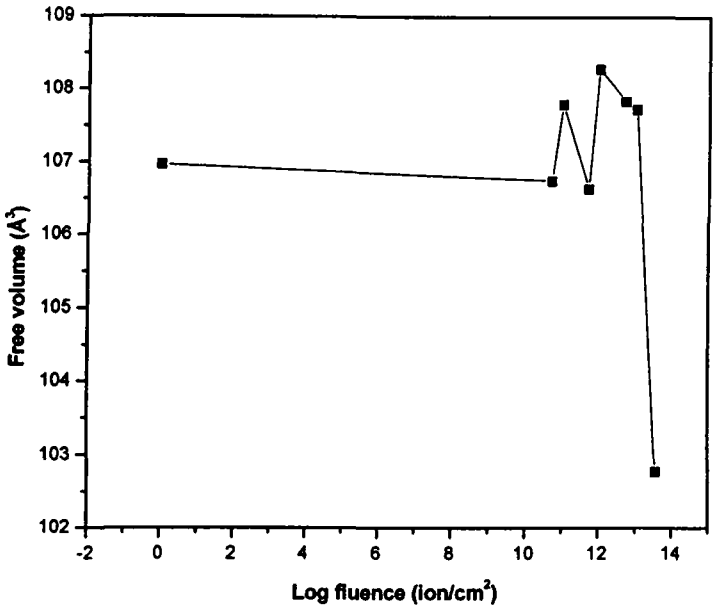

Figure 3.6.4 (c): Variation of average free volume ($Å^3$) with the fluence (ions/cm^2) in Polystyrene (PS), 50 MeV Li^{3+} ions irradiated

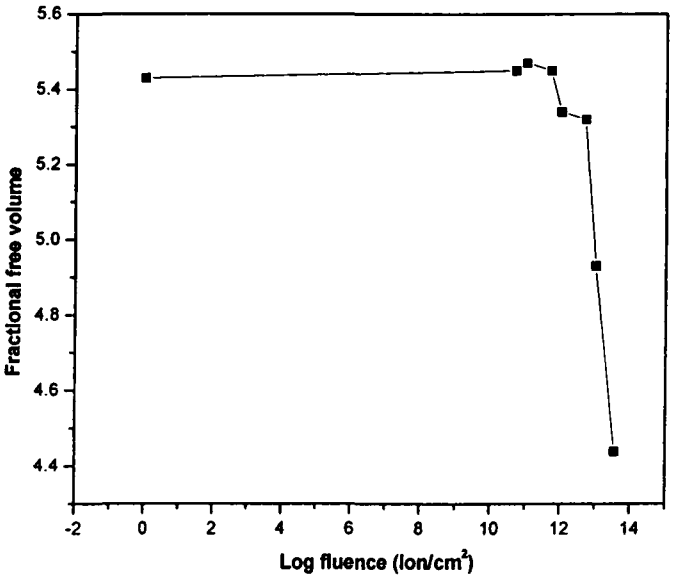

Figure 3.6.4 (d): Variation of fractional free volume with the fluence log (ions/cm^2)

Free volume values change slowly with ion fluence with a decrease at the highest fluence of $3.5x10^{13}$ ions/cm^2. The decrease in τ_3 implies some shrinking of inner and inter-chains of free volume holes (i.e. the impact structure was attained). The free volumes are found to decrease from 107 to 103 Å^3. o-Ps intensity I_3 remains constant up to $5x10^{11}$ ions/cm^2 and then decreases regularly. This decrease in I_3 that reflects a decrease in the number of free volume holes may be interpreted on the process of cross-linking. The cross-linking, as an essential phenomenon, is known to be most effective process in polystyrene as bombarded with high energy particles [32] due to free radical recombination and various degradation possibly resulting in change in amorphousity towards crystallinity. An increase in crystallinity for the polystyrene composite is effectively observed in the irradiation process where the decrease in I_3 with dose is thus ascribed to this effect [33]. The values of S-parameter as given in Table 3.4 (b) shows a minor decrease with increasing fluence. Figure 3.6.4 (e) shows the variation of S-parameter with the fluence.

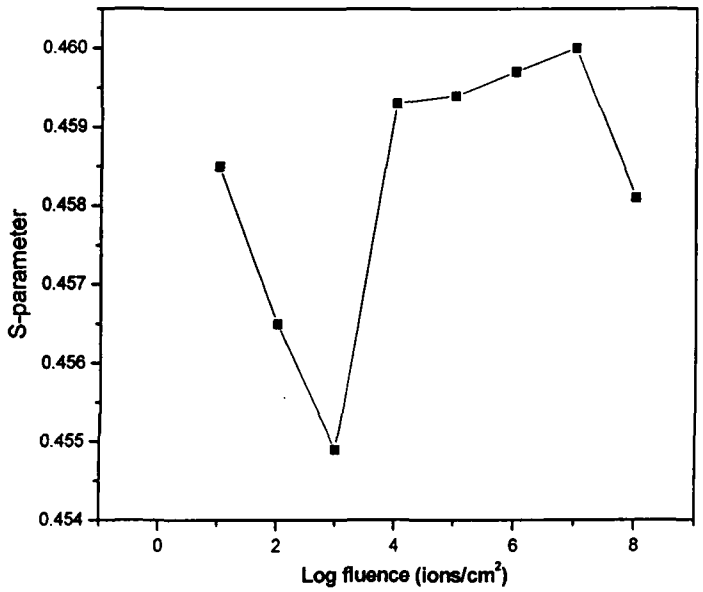

Figure 3.6.4 (e): Variation of S-parameter with the log fluence (ions/cm^2)

3.6.5 Polyethylene-Oxide Salt 17% (PEO-Salt 17%)

Solution-cast films of PEO(BDH, England) and of complexes with NH_4ClO_4 (Fluka AG, 99.5% purity) were prepared in salt concentration of 17% and 19%. Pure PEO is non conducting while its complex $PEO_{(1-x)}$ $(NH_4ClO_4)_x$ with weight fraction x =17%, 19% is an ion conducting polymer.

The three lifetime components decomposed from the positron lifetime spectra arises from the annihilation of para positronium (p-Ps), free positron annihilation and ortho positronium pick off process (o-Ps)[34, 10]. The intensity of o-Ps (I_3) is proportional to the probability of positronium (Ps) formation. In the past it has been related to the concentration of free volume holes in the polymers [35]. However, it was found that I_3 is also affected by a number of other non structural variables [28, 36-42].

The positrons lifetimes and intensities for PEO complex are presented in Table-3.9(a). Table-3.9(b) shows the results for the values of the free volume hole radius r_h, volume of free holes V_h and fractional free volume F_v for the samples irradiated with 95 MeV O^{6+} ion beam to different fluences The variation of V_h, F_v and S-parameter as a function of ion fluence are shown in Figures 3.6.5(a),(b) and (c).

Table 3.9 (a)

Polyethylene Oxide irradiated with 95 MeV O^{6+} Lifetime and Intensities of unirradiated and irradiated

Fluence (ions/cm^2)	τ_1 (ns)	I_1 (%)	τ_2 (ns)	I_2 (%)	τ_3 (ns)	I_3 (%)
Unirradiated	0.147 ± 0.003	39.50 ± 1.2	0.392 ± 0.006	45.3 ± 1.1	1.702 ± 0.012	15.2 ± 0.19
10^{10}	0.145 ± 0.003	39.3 ± 1.2	0.391 ± 0.006	45.7 ± 1.1	1.685 ± 0.012	15.0 ± 0.19
10^{11}	0.147 ± 0.004	38.4 ± 1.4	0.382 ± 0.007	45.9 ± 1.3	1.623 ± 0.012	15.6 ± 0.21
10^{12}	0.145 ± 0.003	37.2 ± 1.2	0.371 ± 0.005	48.8 ± 1.1	1.820 ± 0.011	14.0 ± 0.13
10^{13}	0.141 ± 0.003	36.3 ± 1.2	0.369 ± 0.005	48.6 ± 1.1	1.876 ± 0.011	15.0 ± 0.14

Table 3.9 (b)

The lifetime parameters of o-Ps and radius of free volume hole r_h (Å). free volume hloe V_h(Å^3) fractional free volume (F_V) and S-parameter

Fluence (ions/cm^2)	τ_3 (ns)	I_3 (%)	r_h (Å)	V_h(Å^3)	Fv	S Parameter
Unirradiated	1.702 ± 0.012	15.2 ± 0.19	2.565	70.677	1.933	0.4059 ± .0010
10^{10}	1.685 ± 0.012	15.0 ± 0.19	2.544	68.955	1.861	0.4035 ± .0010
10^{11}	1.623 ± 0.012	15.6 ± 0.21	2.481	63.955	1.795	0.4040 ± .0010
10^{12}	1.820 ± 0.011	14.0 ± 0.13	2.684	80.975	2.040	0.4026 ± .0010
10^{13}	1.876 ± 0.011	15.0 ± 0.14	2.739	86.055	2.323	0.4018 ± .0010

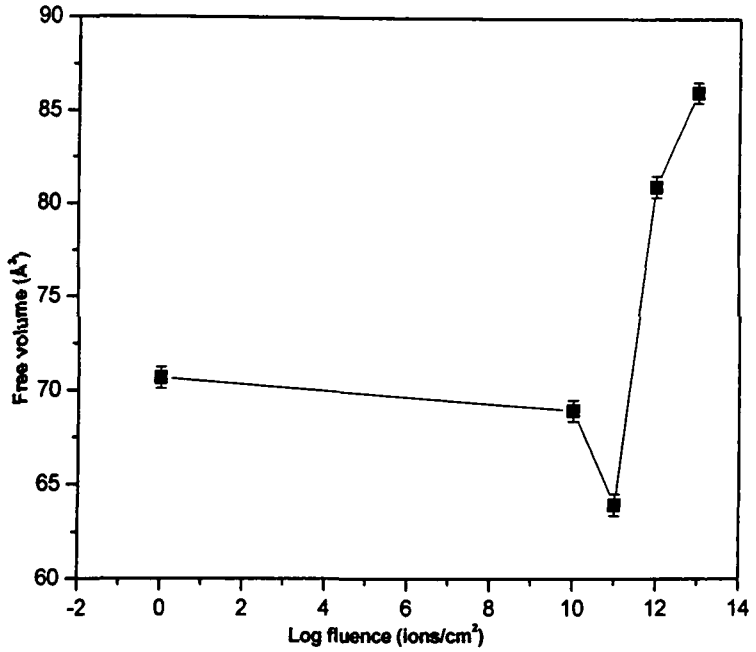

Figure 3.6.5 (a): Variation of average free volume ($Å^3$) with the fluence (ions/cm^2).

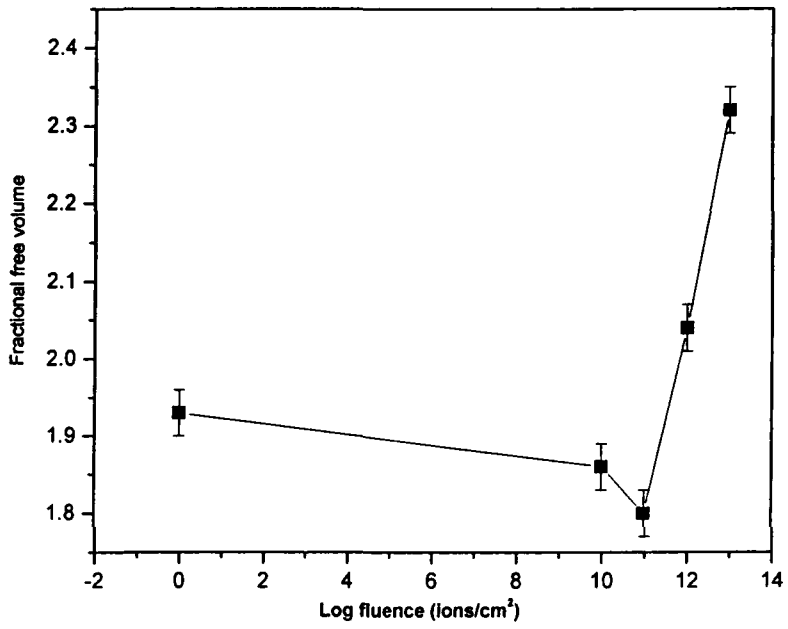

Figure 3.6.5 (b): Variation of fractional free volume with the fluence (ions/cm^2).

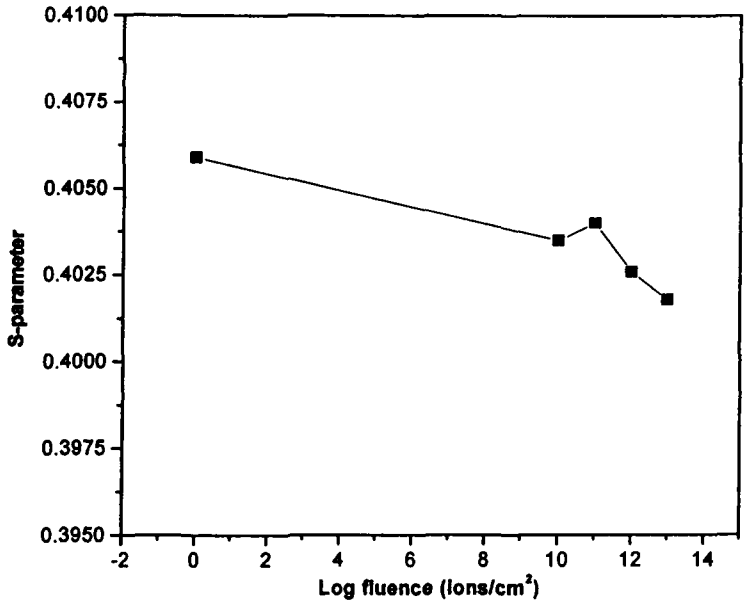

Figure 3.6.5 (c): Variation of S-parameter with the log fluence (ions/cm^2)

From the above Tables, it can be observed that the o-Ps lifetime τ_3 decreases for the fluences 10^{10} and 10^{11} ions/cm^2 and then increases for 10^{12} and 10^{13} ions/cm^2. This is contrary to our earlier measurements [28,30] on CR-39 polycarbonate irradiated with ^{40}Ar and ^{197}Au ions to low fluences of 10^5 ions/cm^2 and Makrofol-N polycarbonate irradiated with C ions to 10^6 ions/cm^2 where free volume was found to increase with fluences and has been attributed to chain scission along the track. The results on CR-39 polycarbonate, polystyrene and polyamide nylon-6 [28, 32] irradiated with C ions to the higher fluences indicated the facilitation of cross-linking [29]. The modification (scission or cross-linking) due to ion irradiation depends essentially on the polymer and energy loss per unit length or linear energy transfer (LET). The intensity of the o-Ps lifetime component I_3 shows almost no change up to 10^{12} ions/cm^2 and then a slight decrease at 10^{13} ions/cm^2. Values of S parameter are given in Table 2 Generally the production of more and more vacancy-type defects during increased dose of irradiation should have caused an increase of the S parameter. On the contrary, the S parameter continuously decreased due to the irradiation. The initial decrease of the longer lifetime τ_3 indicated a decreasing free volume and could support the initial fall of S as well. This should have happened if free volume defects of sizes relatively smaller than the initially present ones are freshly

created during the irradiation. However, the nearly constant intensity I_3 does not support such a possibility. The intermediate lifetime τ_2 continuously decreases and levels off to a constant at the largest dose of irradiation while its intensity I_2 shows the opposite trend, indicating that vacancy cluster-type defects less than the sizes of free volume defects are created during the irradiation. Since such defects, owing to their smaller sizes, do not favor the formation of positronium (the origin of τ_3), the peak of the Doppler broadened line shape no more becomes sharper and the S parameter decreases accordingly.

3.6.6 Polyvinylidene fluoride (PVDF)

The positron lifetime spectra PVDF samples irradiated with 145 MeV Ne^{6+} ions to different fluences were analyzed in terms of three lifetime components the values of which are obtained as: the shortest lifetime component (τ_1=.1885-.1818 ns and I_1 = 50.1352 – 46.9824%), the intermediate one (τ_2 = .4218 - .4180 ns and I_2 = 41.3900 – 40.5544%) and the longest lived component (τ_3 = 2.2859-2.2813 ns and I_3 = 12.4632-10.1712%).

The positron lifetimes and intensities for PVDF are presented in Table -3.10(a). Table-3.10(b) shows the results obtained from o-Ps lifetime τ_3 for the values of the free volume hole radius r_h and volume of free holes V_h and fractional free volume F_v for the pristine samples and irradiated with 145 MeV Ne^{6+} ion beam to different fluences. The variations of V_h and F_v as a function of ion fluence are shown in Figures 3.6.6(a) and (b).

Table 3.10 (a)

PVDF irradiated with 145 MeV Ne^{6+} Lifetime and Intensities of unirradiated and irradiated

Fluence	Lifetime τ_1 (ns)	Lifetime τ_2 (ns)	Lifetime τ_3 (ns)	Intensity I_1(%)	Intensity I_2(%)	Intensity I_3(%)
Pristine	0.1818 ± 0.0055	0.4218 ± 0.0096	2.2859 ± 0.0157	46.9824 ± 2.1079	40.5544 ± 2.0190	12.4632 ± 0.1360
10^{10}	0.1867 ± 0.0054	0.4330 ± 0.0102	2.2680 ± 0.0158	48.1555 ± 2.0869	39.2284 ± 1.9929	12.6161 ± 0.1430
10^{11}	0.1854 ± 0.0054	0.4207 ± 0.0098	2.2813 ± 0.0179	49.7848 ± 2.2233	40.0440 ± 2.1396	10.1712 ± 0.1276
10^{12}	0.1885 ± 0.0056	0.4180 ± 0.0097	2.2486 ± 0.0204	50.1352 ± 2.3728	41.3900 ± 2.2921	8.4749 ± 0.1227

Table- 10(b)

The lifetime parameters of o-Ps and radius of free volume hole (R), free volume V_h and fractional free volume (f_V) PVDF

Fluence (ions/cm^2)	Lifetime τ_3 (ns)	Intensity I_3(%)	R (Å)	V_h (Å^3)	F_v
Unirradiated	2.2859 ± 0.0157	12.4632 ± 0.1360	3.104	125.268	2.82
10^{10}	2.2680 ± 0.0158	12.6161 ± 0.1430	3.090	123.581	2.81
10^{11}	2.2813 ± 0.0179	10.1712 ± 0.1276	3.076	121.909	2.24
10^{12}	2.2486 ± 0.0204	8.4749 ± 0.1227	3.065	120.606	1.85

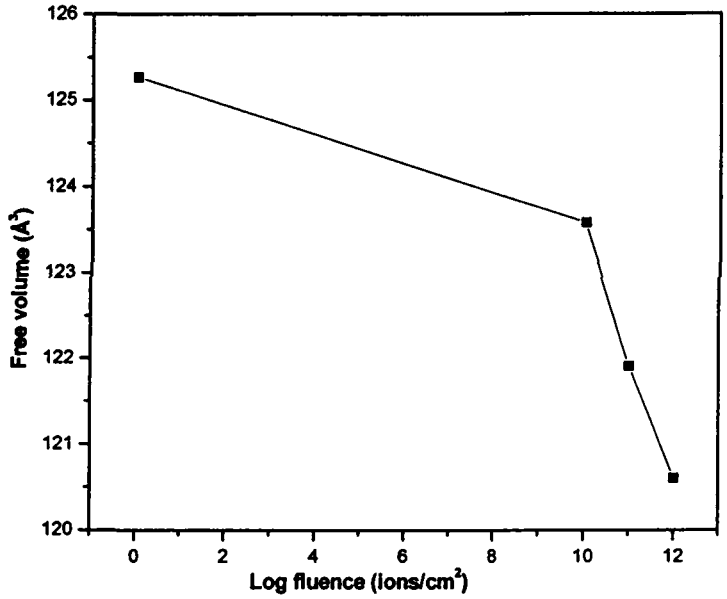

Figure3.6.6 (a): Variation of average free volume ($Å^3$) with the fluence (ions/cm^2) in Polyvinylidene fluoride (PVDF) 145 MeV Ne^{6+} ions irradiated.

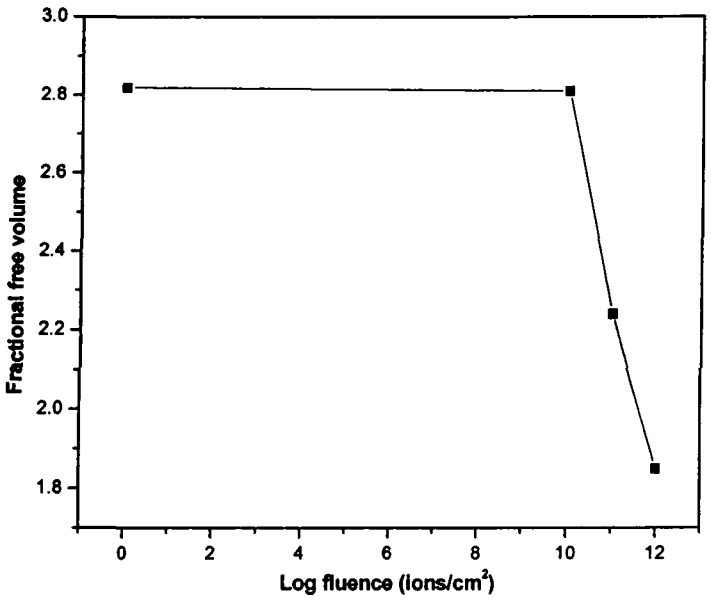

Figure 3.6.6 (b): Variation of fractional free volume with the fluence (ions/cm^2) in Polyvinylidene fluoride (PVDF) 145 MeV Ne^{6+} ions irradiated.

The decrease in the τ_3 is related to change in the free volume as a result of the formation of new bonds or cross-linking. This decrease in τ_3 implies some shrinking of inner and inter – chains of free volume.

3.6.7 LEXAN polycarbonate

Lexan Polycarbonate (PC) films were irradiated with 95 MeV O^{6+} at Pelletron accelerator. The analyses of the PAL spectra gives: the short-lived component (τ_1= 91-105 ps and I_1 = 24.8 – 20.8%), the intermediate component (τ_2 = 0.415 – 0.428ns and I_2 = 31.0 – 47.5%) Detailed analysis of these two compounds is very difficult because of the possible formation of positron and positronium compounds that contribute to both of them. The long-lived component due to pick-off annihilation of the o-Ps in free volume holes is (τ_3=2.021- 1.957ns and I_3= 44.2 – 31.7%). The lifetime τ_3 is the mean value of the o-Ps lifetimes in the free volume holes of different sizes. On the other hand, the intensity (I_3) is proportional to the number of these free volume holes. The positron lifetimes and intensities for pristine and irradiated LEXAN polycarbonate films are presented in Table-3.11(a). Table-3.11(b) shows the results obtained from o-Ps lifetime τ_3 for the values of the free volume hole radius r_h , volume of free holes Vh and fractional free volume Fv along with the S-parameter obtained from Doppler Broadening Spectra(DBS). The variations of free volume , fractional free volume and S-parameter are shown in Figures 3.6.7 (a),(b) and (c)

Table – 3.11 (a)

Lexan Polycarbonate (PC) irradiated with 95 MeV S O^{6+} Lifetime and intensities of unirradiated and irradiated Lexan Polycarbonate.

Fluence (ions/cm^2)	τ_1 (ns)	I_1 (%)	τ_2 (ns)	I_2 (%)	τ_3 (ns)	I_3 (%)
Pristine	.091±4	24.8±0.7	.415±9	31.0±0.6	2.021±0.01	44.2±0.3
$1x10^{10}$	.091±4	24.3±0.7	.417±9	30.6±0.6	2.026±0.01	45.0±0.3
$1x10^{11}$	.088±3	26.9±0.6	.429±9	29.7±0.5	2.030±0.01	43.4±0.3
$1x10^{12}$	.088±4	26.0±0.6	.426±9	31.2±0.5	2.011±0.01	42.8±0.3
$1x10^{13}$	.092±4	23.8±0.6	.427±6	43±0.5	1.976±0.01	33.2±0.3
$2x10^{13}$	.105±3	20.8±0.7	.428±6	47.5±0.6	1.957±0.01	31.7±0.26

Table – 3.11 (b)

The lifetime parameters of o-Ps and radius of free volume hole radius r_h (Å) and fractional free volume (f_V) in Lexan Polycarbonate

Fluence (ions/cm^2)	τ_3 (ns)	I_3 (%)	R(Å)	V_f (Å^3)	Fv	S parameter
Pristine	2.021±0.01	44.2±0.3	2.875	99.48	7.91	0.4629
$1x10^{10}$	2.026±0.01	45.0±0.3	2.879	99.96	8.09	0.4535
$1x10^{11}$	2.030±0.01	43.4±0.3	2.883	100.34	7.84	0.4572
$1x10^{12}$	2.011±0.01	42.8±0.3	2.865	98.53	7.59	0.4586
$1x10^{13}$	1.976±0.01	33.2±0.3	2.833	95.25	5.69	0.4500
$2x10^{13}$	1.957±0.01	31.7±0.3	2.816	93.48	5.33	0.4489

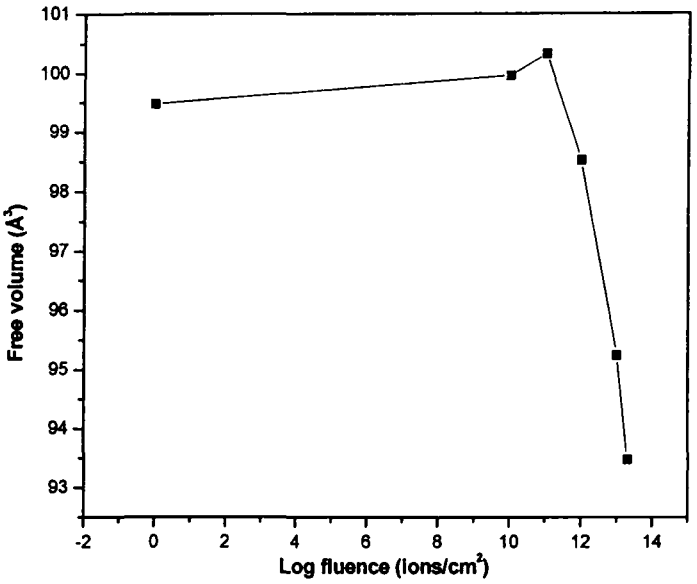

Figure 3.6.7 (a): Variation of average free volume ($Å^3$) with the fluence (ions/cm^2) in Lexan Polycarbonate, 95 MeV O^{6+} ions irradiated

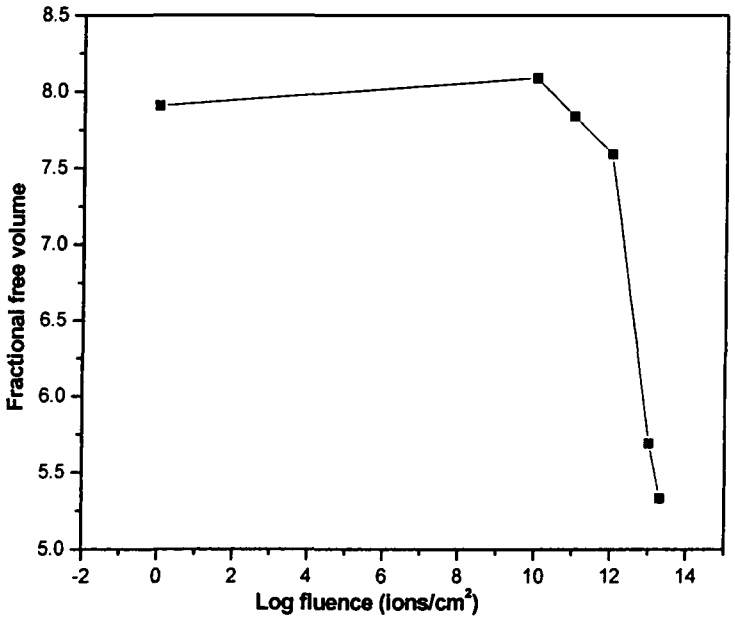

Figure 3.6.7 (b): Variation of fractional free volume with the fluence (ions/cm^2) in Lexan Polycarbonate, 95 MeV O^{6+} ions irradiated.

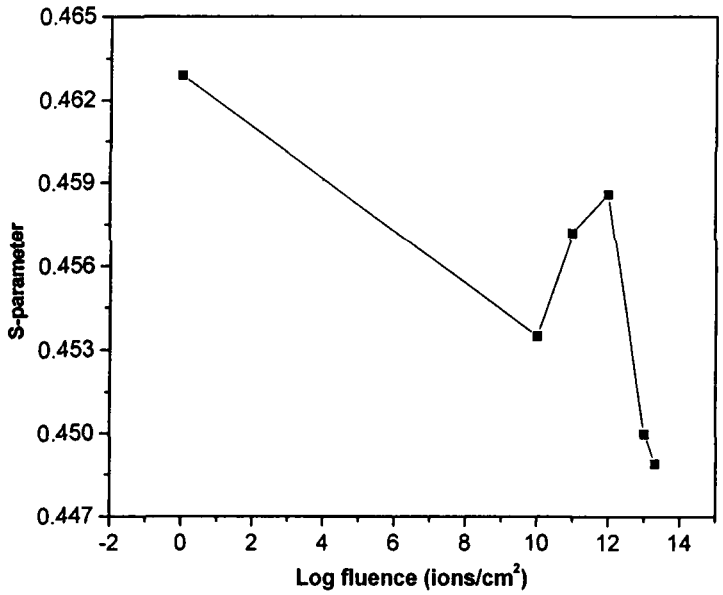

Figure 3.6.7 (c): Variation of S-parameter of LEXAN polycarbonate

Free volume is found to decrease with the fluence. S parameter obtained from DBS remains constant up to the fluence of 10^{12} ions/cm^2 and then falls. With the increase in the fluence, scissioned segments crosslink randomly, resulting into the decrease of average free volume due to overlapping of tracks.

3.6.8 Polyamide Nylon-6,6

Polyamide Nylon-6,6 samples were irradiated by 50 MeV Li^{3+} ion beam from 15 UD Pelletron Accelerator to different fluences. The lifetime parameters obtained from the analyses of PAL spectra are presented in Table-3.12 (a). Table 3.12(b) shows the values of free volume hole radius r_h, volume of free holes V_h results obtained from o-Ps lifetime τ_3 for the values of the free volume hole radius r_h and for the pristine samples and irradiated. The variation of V_h and fractional free volume Fv along with the S-parameter obtained from Doppler Broadening Spectra (DBS). The variation of V_h , F_v and S-parameter as a function of ion fluence are shown in Figures 3.6.8(a),(b) and (c).

Table –3.12 (a)

Polyamide Nylon-6,6 (PN-6,6) irradiated with 50 MeV Li^{3+} Lifetime and Intensities of unirradiated and irradiated.

Fluence (ions/cm^2)	**τ_1 (ns)**	**I_1 (%)**	**τ_2 (ns)**	**I_2 (%)**	**τ_3 (ns)**	**I_3 (%)**
Pristine	0.151±.004	31.8±1.1	0.357±.005	47.0±1.0	1.638±0.01	21.2±0.3
$5x10^{10}$	0.139±004	27.6±1.1	0.340±.005	50.8±1.0	1.621±0.01	21.7±0.3
$1x10^{11}$	0.140±004	27.7±1.1	0.339±.005	50.2±1.0	1.619±0.01	22.0±0.3
$1x10^{12}$	0.120±004	25.0±1.1	0.329.005	53.3±1.0	1.629±0.01	21.6±0.3
$5x10^{12}$	0.136±004	28.7±1.1	0.340±.005	50.1±1.0	1.630±0.01	21.2±0.3
$1x10^{13}$	0.147±004	30.1±1.1	0.346±.005	48.7±1.0	1.617±0.01	21.2±0.3
$3.5x10^{13}$	0.133±004	26.8±1.1	0.335±.005	51.7±1.0	1.615±0.01	21.5±0.3

Table – 3.12 (b)

The lifetime parameters of o-Ps and radius of free volume hole r_h (Å), free volume V_h , fractional free volume (f_V) and S-parameter in Polyamide Nylon-6, 6.

Fluence (ions/cm^2)	**τ_3 (ns)**	**I_3 (%)**	**r_h (Å)**	**V_f (Å^3)**	**Fv**	**S-parameter**
Pristine	1.638±0.01	21.2±0.3	2.4969	65.194	2.48	0.4429±.001
$5x10^{10}$	1.621±0.01	21.7±0.3	2.4786	63.771	2.49	0.4429±.001
$1x10^{11}$	1.619±0.01	22.0±0.3	2.4764	63.602	2.51	0.4433±.001
$1x10^{12}$	1.629±0.01	21.6±0.3	2.4872	64.438	2.50	0.4420±.001
$5x10^{12}$	1.630±0.01	21.2±0.3	2.4883	64.523	2.46	0.4436±.001
$1x10^{13}$	1.617±0.01	21.2±0.3	2.4742	63.432	2.42	0.4436±.001
$3.5x10^{13}$	1.615±0.01	21.5±0.26	2.4721	63.271	2.44	0.4415±.001

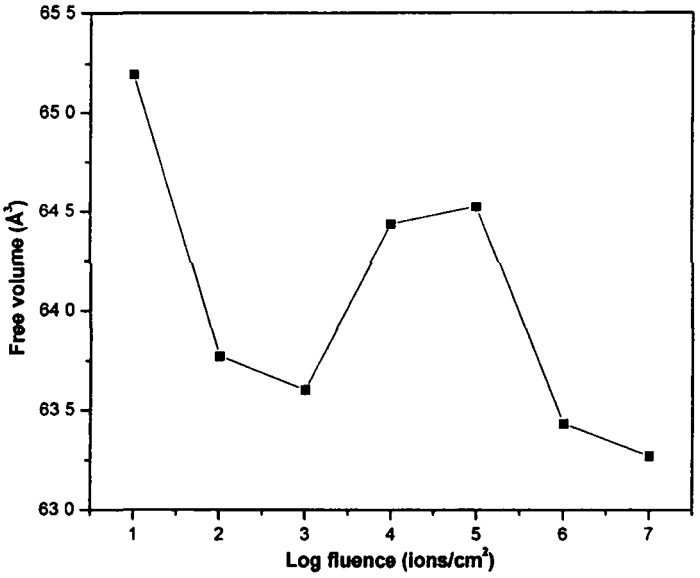

Figure 3.6.8 (a): Variation of average free volume ($Å^3$) with the fluence (ions/cm^2) in Polyamide Nylon-6,6 Polymrer, 50 MeV Li^{3+} ions irradiated.

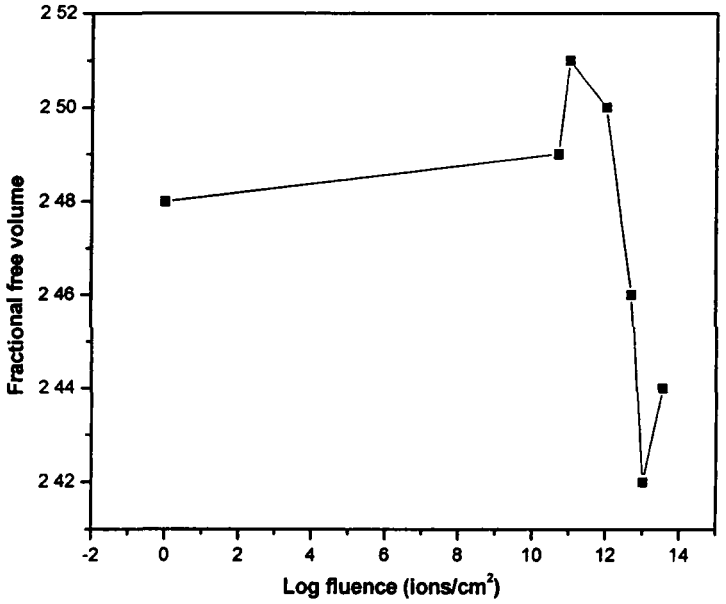

Figure 3.6.8 (b): Variation of fractional free volume with the fluence (ions/cm^2) in Polyamide Nylon-6,6 polymer, 50 MeV Li^{3+} ions irradiated.

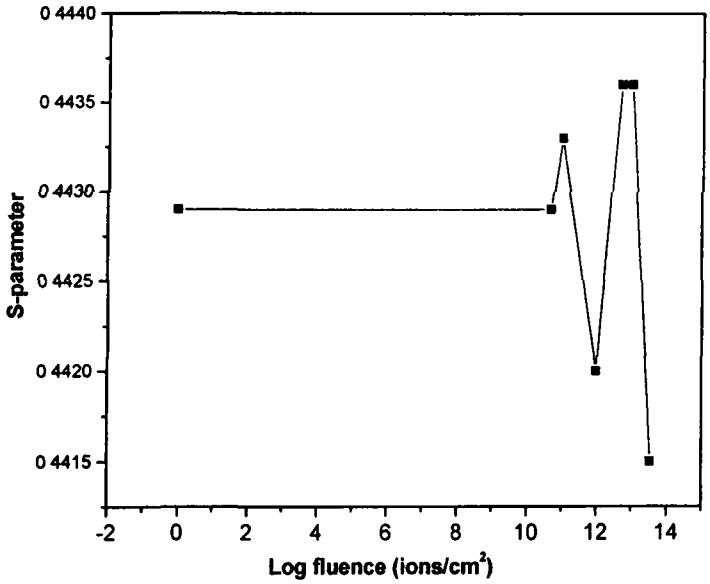

Figure 3.6.8 (c): Variation of S-parameter with the log fluence (ions/cm^2).

Various life time components obtained from the analyses of the PAL spectra are (τ_1= .151-.133 ns and I_1 = 31.8 – 26.8%), (τ_2 = 0.357 – 0.335ns and I_2 = 47.0 – 51.7%) and (τ_3=1.638- 1.615ns and I_3= 21.2 – 21.5%). The lifetime (τ_3) is the mean value of the o-Ps lifetimes in the free volume holes of different sizes and it and free volume show erratic behavior and lastly decreases with the fluence. S parameter obtained from DBS remains almost constant. With the increase in the fluence, scissioned segments crosslink randomly, resulting into the decrease of average free volume due to overlapping of track.

References

[1] Cowie, J. M., 1973, Polymer: Chemistry and Physics of Modern Materials, Intertext Books, Billings Worcester, Great Britain.

[2] C.J. Sofield, S. Sugden, J. Ing, L.B. Bridwell, Y.Q. Wang, Vacuum, 44 (1993)285.

[3] E.H. lee, Chapter 17 in Polyimides, in: K. Mittal, M.Ghosh (Eds.), Fundamental Aspects and Technological Applications, Marcel Dekker, (1996) 471-503.

[4] J. L. Magee, A. Chattergee, Chapter 4, in: G. R. Freeman, (Eds.) Kinetics of nonhomogeneous processes, Wiley, New Yourk, 1987.

[5] Trautmann, C., 1998, Ion beam irradiation of polymers. Article Presented in Workshop at NSC, New Delhi, unpublished.

[6] Lee, E.H., 1999. Ion beam modification of polymeric materials-fundamental principles and application. Nucl. Instr. Meth.B 151, 29-41

[7] Y. C. Jean 1995. Positron Spectroscopy of Solids. Eds. Dupasquir, A. and Mills Jr. A. P. IOS Pub. Amsterdam, 563.

[8] D. M. Shrader, Y.C. Jean, 1988, Positron and Positronium Chemistry: Studies in Physics and Theoretical Chemistry. Elsevier Scientific Publications, Amsterdam.

[9] Y. C. Jean1990. Free volume hole properties of polymers probed by positron annihilation spectroscopy. 3rd Int. Workshop on positron and positronium chemistry.1.

[10] O.E. Mogensen, Positron Annihilation in chemistry, Springer, Berlin, 1995

[11] Stevens, J.R., in: R.A. fava (Ed.), Method Exp. Phys., Vol.16 A, Academic, New York (1980) 371 [12] M. Forsyth, P. Meakin, D.R. Macfarlane, A.J. Hill, J. Phys., Condens. Matter 7 (1995)7601.

[13] Trautmann, C., Schwartz. K., Steckenreiter. T., Specificity of ion induced damage. Nucl. Instr. Meth. B 156(1999)162.

[14] D.Fink, M. Muller, S. Ghosh, K. K.Dwivedi, J. Vacik, V. Hantowicz, J. Cervena., Y. Kobayshi, K. Hirata, New ways of polymeric ion track characterization. Nucl. Instr.Meth.B156, 170(1999)176.

[15] Lee. E.H., G.R. Rao, L.K. Mansur, Mat. Sci. Forum 248-249(1997)135.

[16] D. Kanjilal, S. Chopra, M. M. Narayanan, I.S. iyer, V.Jha, R. Joshi, S. K. Datta, Nucl. Instr. and Meth. A 238 (1993)97.

[17] C.M. Lederer, V.S. Shirley (Eds.): table of Isotopes, 7th Ed., John Wiley & Sons, New York (1978).

[18] D.V. Lang, J. Appl. Phys. 45(1974)3014.

[19] P.Sen, Positron and Positronium Chemistry, Ed. Y.C. Jean, world Scientific (1990)109.

[20] B. Somieski, T. E. M. Staab, R. Krause-Rehbrg, Nucl. Instr. and Meth. A, 381 (1996) 128.

[21] P. Krkegaard, M. Eldrup, O.E. Mogensen, N. Pedersen, Compt. Phys. Commun. 23 (1981) 307.

[22] Jean, Y.C., Dai, G.H., Free volume hole distribution of polymers probed by positron annihilation spectroscopy. Nucl. Instr.Meth. B 79(1993) 356.

[23] H. Nakanishi, S. J. Wang, Y.C. Jean, 1988. Positron Annihilation Studies of Fluids. Editor. Sharma., S.C., World. Sci. Pub., Singapore 292.

[24] G. Dlubek, Ch. Hubner, and S. Eichler, Nucl.Instr. and Meth. B142 (1998)191

[25] Y.Y. Wang., H. Nakanishi, Y.C. Jean, J. Polym. Sci. B: Polym Phys., 28(1990)1431.

[26] Rajesh Kumar, B. K. Nath, D. Das and Rajendra. Prasad. Indian. J. Physics 78A(2) (2004) 221.

[27] Rajesh Kumar, Rajendra Prasad, Radiat. Meas. 40(2005)750.

[28] Rajesh Kumar, S. Rajguru, D. Das., Rajendra Prasad. Radiat. Measu. 36 (2003)151.

[29] R. Kumar, B. K. Nath, D. Das, Rajendra Prasad, Ind. J. Phys. 78A 2,(2004a) 221-223.

[30] R. Kumar, A.K. Mahur, K. K. Dwivedi, D. Das and Prasad, Rajendra., Ind .J. Phys., 78A 2,(2004b) 225-227.

[31] Rajesh Kumar, S.A.Ali, A. K. Mahur, D.Das, A.H.Naqvi, H. S. Virk, Rajendra Prasad, Nucl.Instr. Meth.B244(2006)257.

[32] S. Klaumunzer, S. Zhu, Q. Q., W. Schnabel, G. Schumacher. Nucl. Inst. and Meth. B 116(1996)154-158.

[33] H. Nakanishi, Y. C. Jean, 1990 In; Y.C. Jean (Ed.), Positron and positronium Chemistry , World Science Singapore.

[34] Y. C. Jean, Microchem. J.42, (1990) 72; in Y.-J. He, B.-S. Cao, Y. C. Jean (Eds.),Positron Annihilation, Proceedings of the 10th International Conference on Positron Annihilation, Mater. Sci. Forum Vols.175–178, (1995)59.

[35] V.P. Shantarovich, J.Radioanal. Nucl .Chem.210 (1996)357.

[36] C. Wastlund, F.H.J. Maurer, Polymer39 (1998)2897.

[37] M. Welander, F.H.J. Maurer, Mater. Sci. Forum 105-110(1992)1811;

[38] D. Cangialosi, H. Schut, M. Wübbenhorst, J. van Turnhout, A. van Veen, Radiat. Phys. Chem. 68(2003)507.

[39] C.L. Wang, K. Hirata, J. Kawahara, Y. Kobayashi, Phys. Rev. B,58(1998)14864;

[40] A. Alba Garcia, L.D.A. Siebbeles, H. Scout, A. van Veen, Radiat.Phys. Chem. 68(2003)515

[41] J. Zrubcova, J. Kristiak, W. B. Pedersen, N.J. Pedersen, M. Ederlup, Mater. Sci. Forum 363(2001)359.

[42] F.H.J. Maurer, M. Schimidt, Radiat. Phys. Chem. 58(2000)509.

Chapter-IV

Chapter IV

In this chapter, the results of characterization of optical and chemical modifications induced by swift heavy ions in polymers through Ultraviolet–Visible (UV-Vis) spectroscopy and Fourier Transform Infrared (FT IR) spectroscopic analyses are presented.

4.1 Characterization of Optical Modification through UV-Visible Spectroscopy

Ultraviolet-Visible (UV-Vis) spectroscopy gives an idea about the value of optical band gap energy (E_g) and thus is an important tool for investigation. The absorption of light energy by polymeric materials in UV and Visible regions involves promotion of electrons in σ, π and η orbitals from the ground state to higher energy states which are described by molecular orbitals [1]. The damage produced by ion beam interaction with polymer leads to the formation of new defects and new charge states. UV-Vis spectroscopy performed in the wavelength range 200 – 1100 nm by SHIMADZU, UV-1601 PC (Japan) UV-Visible spectrophotometer has been used for the study of new bands formed due to ion irradiations.

4.2 Irradiation

In our present study, modification in various types of polymers irradiated by four type of ions of different mass and range has been characterized. Details of irradiated polymers and irradiating heavy ions of different energies are presented in Tables 4.1 (a) and 4.1(b).

Swift heavy ion (SHI) irradiation of the polymeric samples were carried out at 15 UD Pelletron Accelerator at Inter University Accelerator Centre (IUAC), New Delhi, India and Variable Energy Cyclotron Centre (VECC), Kolkata, India. Various types of polymers samples of various fluences were irradiated by 100 MeV Si^{8+} ion beam. In the second run the samples of different polymers were irradiated by 145 MeV Ne^{6+} ion beam

to the fluence of 10^{10} to 10^{13} ions/cm^2. In the third run the samples of various polymers were irradiated by 95 MeV O^{6+} ion beam to the fluence of 10^{10} to 10^{13} ions/cm^2. In the last fourth run the samples of different fluences and different thickness were exposed to 50 MeV Li^{3+} ion beam to the fluence 10^{10} to $2x10^{13}$ ions/cm^2 as per the scheme described in chapter II. The various polymers details are described in Tables - 4.1(a) and 4.1 (b).

Table 4.1 (a); Polymers samples of size 1.5x1.5 cm^2 were mounted on a vacuum shielded vertical sliding ladder and were exposed to 100 MeV Si^{8+}, 95 MeV O^{6+} and 50 MeV Li^{3+} ion beam in the General Purpose Scattering Chamber (GPSC) under high vacuum (~$4x10^{-6}$ Torr) from 15 UD Pelletron accelerators at Inter University Accelerator Centre, New Delhi, India [2]. The samples were irradiated to the different fluences. In order to expose the whole target area uniformly, the beam was scanned in the X-Y plane.

Table 4.1(b); Polymers samples were irradiated by 145 MeV Ne^{6+} ion beam at Variable Energy Cyclotron Centre (VECC), Kolkata. Irradiation was carried out to different fluences. At VECC ion beam was defocused using a magnetic scanning system so that the film may be uniformly irradiated. Also X-Y scanner was used for uniform irradiation of the samples.

Table-4.1 (a)

Details of heavy ions and polymers for irradiation at Inter University Accelerator Centre, New Delhi, in the present investigation

Name of the ion with symbol	Energy MeV/n	Name of the polymer	Name of the manufacturer	Thickness
Silicon Si^{8+}	100 MeV	Makrofol-KG (Bisphenol-A Polycarbonate)	Farben Fabri-ken Bayer A.G., Germany	40 μm
Silicon Si^{8+}	100 MeV	Makrofol-N (Bisphenol-A Polycarbonate)	Farben Fabri-ken Bayer A.G., Germany	30 μm
Silicon Si^{8+}	100 MeV	Polyethersulphone (PES)	Good Fellow. UK	250 μm
Silicon Si^{8+}	100 MeV	Polytetrafluoroethylene (PTFE)	Good Fellow. UK	100 μm
Silicon Si^{8+}	100 MeV	Polypropylene (PP)	Good Fellow. UK	50 μm
Silicon Si^{8+}	100 MeV	Polymethylmethacrylate (PMMA)	Good Fellow. UK w	125 μm
Oxygen O^{6+}	95 MeV	Polyethylene oxide Salt 17%	BDH England	170 μm
Oxygen O^{6+}	95 MeV	Polyethylene oxide Salt 19%	BDH England	170 μm
Oxygen O^{6+}	95 MeV	Lexan Polycarbonate	Farben Fabri-ken Bayer A.G., Germany	225 μm
Oxygen O^{6+}	95MeV	Low density Polyethylene-oxide (LDPE)	Good Fellow. UK	50 μm
Oxygen O^{6+}	95MeV	Polyvinylidene fluoride (PVDF)	Good Fellow. UK	80 μm
Lithium Li^{3+}	50 MeV	Polyamide Nylon-6,6 (PN-6,6)	Good Fellow. UK	250 μm
Lithium Li^{3+}	50 MeV	Polystyrene (PS)	Good Fellow. UK	1 mm.
Lithium Li^{3+}	50 MeV	Low density Polyethylene-oxide (LDPE)	Good Fellow. UK	50 μm

Table-4.1 (b)

Details of heavy ions and polymers for irradiation at Variable Energy Cyclotron Centre (VECC), Kolkata, in the present investigation

Name of the ion with symbol	Energy MeV/n	Name of the polymer	Name of the manufacturer	Thickness
Neon Ne^{6+}	145 MeV	Makrofol-KG (Bisphenol-A Polycarbonate)	Farben Fabri-ken Bayer A.G., Germany	40 μm
Neon Ne^{6+}	145 MeV	Polyethersulphone (PES)	Good Fellow U K	250 μm
Neon Ne^{6+}	145 MeV	Polymethyl methacrylate (PMMA)	Good Fellow U K	125 μm
Neon Ne^{6+}	145 MeV	Polytetrafluoro ethylene (PTFE)	Good Fellow U K	100 μm
Neon Ne^{6+}	145 MeV	Polypropylene (PP)	Good Fellow UK	50 μm
Neon Ne^{6+}	145 MeV	Polyvinylidene fluoride (PVDF)	Good Fellow UK	80 μm

4.3 UV-Vis spectroscopy/optical response

Ultraviolet-visible spectroscopy gives an idea about the value of optical band-gap of virgin and irradiated polymer samples energy (E_g) and thus provides an important tool for investigation. The absorption of light energy by polymeric materials in the ultraviolet and visible regions involves promotion of electrons in σ, π and n-orbitals from the ground state to higher energy states which are described by molecular orbitals [1]. The electronic transitions ($\rightarrow$) that are involved in the ultraviolet and visible regions are of the following types:

$$\sigma \rightarrow \sigma^*, \; n \rightarrow \pi^*, \text{ and } \pi \rightarrow \pi^*.$$

Many of the optical transitions which result from the presence of impurities have energies in the visible part of the spectrum; consequently the defects are referred to as colour centers [3]. Ion beam interaction with polymers generates damage, which leads to the formation of new defects and new charge states resulting in the modification of optical

properties. In the present study, significant changes of different amounts have been observed in optical response of the polymers after irradiation with Si^{8+} ,Ne^{6+}, O^{6+} and Li^{3+}ions of energies 100 MeV, 145 MeV, 95 MeV and 50 MeV respectively.

The absorption spectra of virgin and irradiated polymer samples were recorded with UV-Vis spectrophotometer are presented in Figs. 4.10 to 4.30. It is observed that optical absorption increases with increasing fluence and this absorption shifts from UV-Vis towards the visible region for all irradiated polymer samples as the fluence increases. The increase in absorption with irradiation may be attributed to the formation of a conjugated system of bonds due to bond cleavage and reconstruction [4].

The optical absorption method can be used for the investigation of the optically induced transitions and can provide information about the bond structure and energy gap in crystalline and non-crystalline materials [5]. The shift in absorption edge is correlated with the optical band gap $E_g = hc / \lambda_g$, where h is Planck constant and c the velocity of light. The wavelength λ_g is determined using Tauc's expression [6].

$$\omega^2\varepsilon_2(\lambda) = (h\,\omega - E_g)^2 \qquad (4.1)$$

where ε_2 (λ) is the optical absorbance, λ, the wavelength and $\omega = 2\pi\upsilon$ is the angular frequency of the incident radiation. Solving the Equation 4.1 one gets

$$\sqrt{\varepsilon_2}/\lambda = h/2\pi\lambda - E_g/2\pi c \qquad (4.2)$$

Therefore the plot of $\sqrt{\varepsilon_2}/\lambda$ vs $1/\lambda$ must be a straight line with an intercept of $-E_g/2\pi c$. If θ is the inclination of the straight line with X-axis, the slope should be $\tan\theta$ and we have

$$\frac{h}{2\pi} = \frac{E_g / 2\pi c}{1/\lambda_g} \qquad (4.3)$$

where $1/\lambda_g$ represents the abscissa of the point of intersection of the straight line with the X-axis and

$$E_g = \frac{hc}{2\pi} \tag{4.4}$$

The number of carbon hexagonal rings in the cluster 'N' can be found from the Robertson relation [7].

$$E_g = \frac{2\beta}{\sqrt{N}} \text{ eV} \tag{4.5}$$

Here 2β is the band structure energy of a pair of adjacent π sites and its value is taken as -2.9 eV for a six numbered carbon ring. Fink et al.[8] have pointed out that the Robertson equation underestimates the cluster size in irradiated polymers. Thus the structure of the cluster was assumed to be like a buck minister fullerene, that is, a C_{60} ring instead of C_6 and the relation emerges:

$$E_g = \frac{34.3}{\sqrt{N}} \text{ eV} \tag{4.6}$$

Where N is the no. of carbon atoms per cluster in the irradiated polymer. Above relation has been used to calculate the no. of carbon atoms per cluster in the irradiated samples.

4.3.1 Response of Makrofol-KG

Makrofol-KG polycarbonate samples were irradiated with 100 MeV Si^{8+} ions from Pelletron accelerator and 145 MeV Ne^{6+} ions from Variable Energy Cyclotron to the fluences of and respectively. Figures 4.1 and 4.2 show the optical absorption spectra of pristine and 100 MeV Si^{8+}, and 145 MeV Ne^{6+}ions irradiated Makrofol-KG (PC) samples at different fluences.

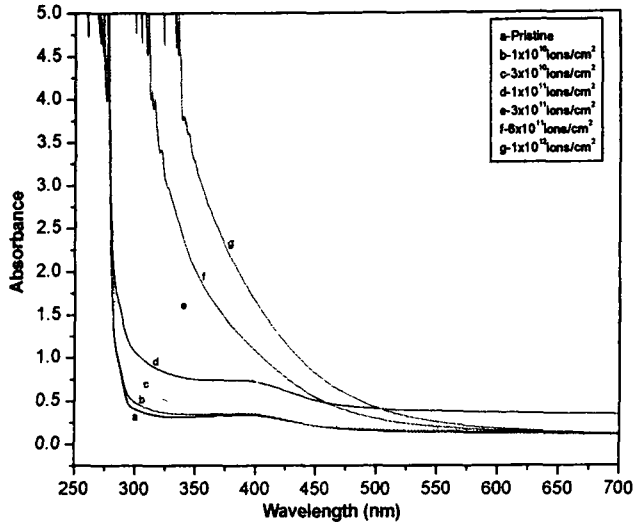

Figure 4.1: Optical absorption spectra of Makrofol-KG (PC) polymer irradiated with 100 MeV Si^{8+} ions beam

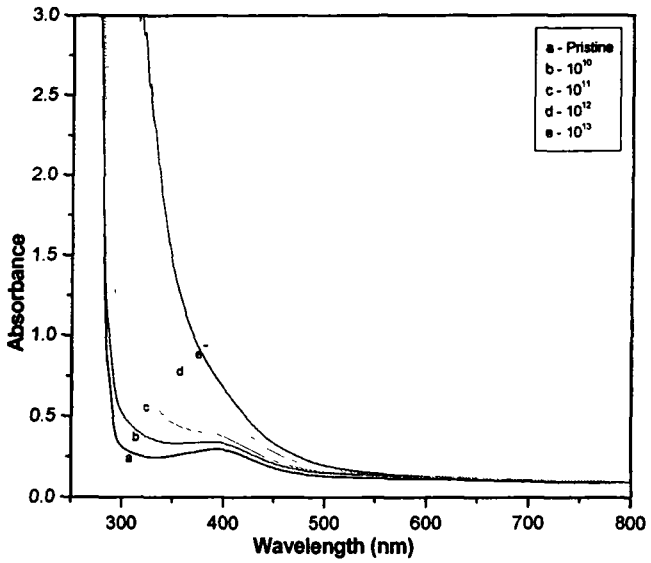

Figure 4.2: Optical absorption spectra of Makrofol-KG (PC) polymer irradiated with 145 MeV Ne^{6+} ion beam.

The values of absorption edges are increasing with increasing the fluences. The E_g values show a decreasing trend with increasing the ion dose for samples irradiated by both kinds of ions. The cluster size for the Si^{8+} irradiated samples is found to lie between 62- 187 atoms, while it lies between 62- 139 atoms for Ne^{6+} ions irradiated samples. The cluster size in the pristine polymer corresponds to the grain structure of the polymer due to the complexity of its monomeric units. Tables- 4.2 and 4.3 present the values of absorption edge λ_g, band gap E_g and the number of carbon atoms N per conjugation length.

Table – 4.2

Variation of absorption edge (λ_g), energy gap (E_g) and number of carbon atoms (N) per conjugation length in pristine and Si^{8+} irradiated samples of Makrofol-KG (PC) at different fluences.

Fluence (ions/cm^2)	**Absorption edge (λ) (nm)**	**Band gap energy E_g (eV)**	**(N)**
0	285.10	4.36	62
1×10^{10}	291.80	4.30	64
3×10^{10}	291.86	4.26	65
1×10^{11}	294.03	4.23	66
3×10^{11}	315.42	3.94	76
6×10^{11}	418.20	2.97	133
1×10^{12}	495.48	2.51	187

Table – 4.3

Variation of absorption edge (λ_g), energy gap (E_g) and number of carbon atoms (N) per conjugation length in pristine and Ne^{6+} ion irradiated samples of Makrofol-KG Polycarbonate to different fluences.

Fluence (ions/cm^2)	**Absorption edge λ_g (nm)**	**Band gap energy E_g (eV)**	**N**
0	285.10	4.36	62
10^{10}	308.43	4.04	72
10^{11}	309.78	4.01	73
10^{12}	411.50	3.02	129
10^{13}	426.69	2.91	139

In Si ion irradiated samples the optical band gap energy remains almost constant upto the dose of 3 x 10^{11} ions/cm^2 after which it decreases gradually with increase in dose while in Ne^{6+} irradiated samples the optical band gap decreases slowly up to the dose of 10^{12} ions/cm^2 after which it decreases fast. Band gap decreases ~43% in case of Si ion irradiated samples at higher fluence of 1 x 10^{12} and ~33% at the higher fluence of 10^{13} ions/cm^2 in Ne ion irradiated PC. The variation of energy gap is shown in figure 4.3 for both the ions. On heavy ion irradiation and higher fluences polymeric restructuring process due to predominant cross linking leads to formation of free radicals [8] as confirmed by Sinha et al. [9] that the free radical formation takes place in PADC (Acrylics) by gamma irradiation at higher doses. This causes a significant reduction in energy band gap. Thus the decrease in energy band gap in present case can be correlated to the formation of free radicals. We find that the cluster size to be larger (~187 atoms for Silicon and ~139 atoms for Neon irradiation). This may be due to the fact that heavy ions of Silicon and Neon create more damage in the carbon chain inside the polymer. The variation in optical energy band gap of Makrofol-KG with ion fluence for the two ion beams has been presented in figure 4.3.

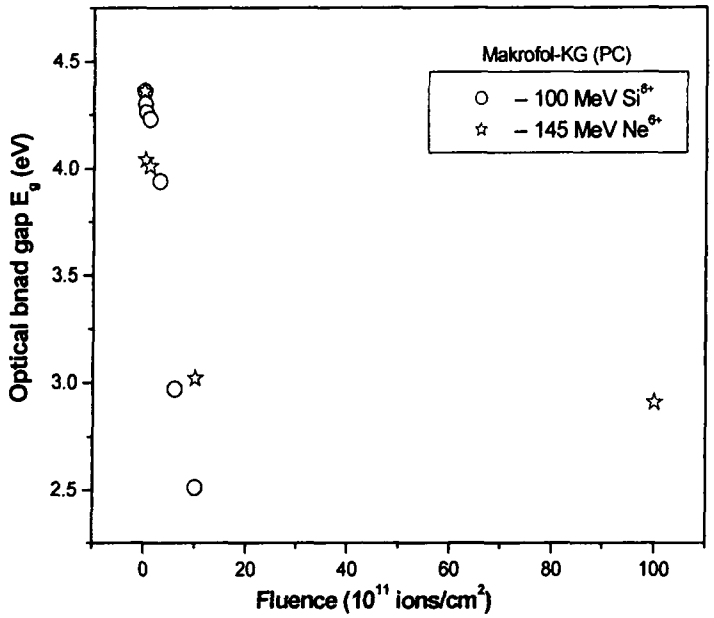

Figure 4.3; The variation of optical – gap energy of Makrofol-KG with different ion fluences

4.3.2. Response of Makrofol-N

The optical absorption spectra of Makrofol-N (PC) pristine and irradiated samples with 100 MeV Si^{8+} ions to the fluences of 10^{10}, $3x10^{10}$, 10^{11}, $3x10^{11}$, $6x10^{11}$ and 10^{12} ions/cm^2 are shown in Figure 4.4. The values of absorption edges, optical band gap energies and cluster size N are given in Table- 4.4

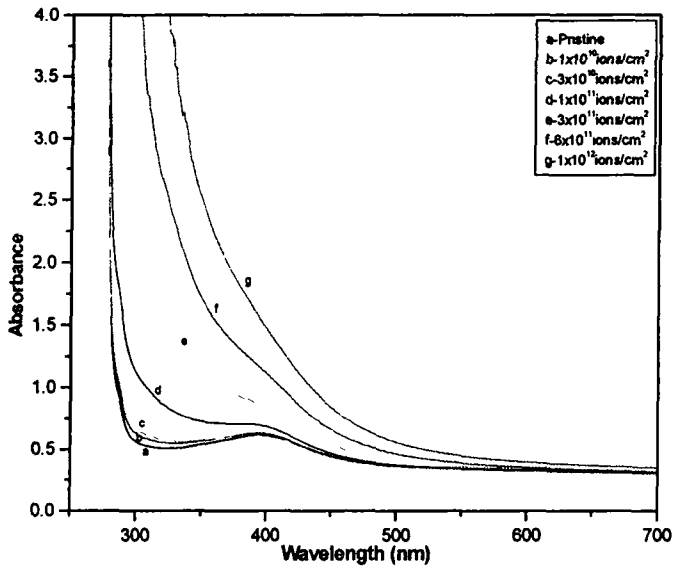

Figure 4.4: Optical absorption spectra of Makrofol- N Polycarbonate irradiated With 100 MeV Si^{8+} ions beam

Table – 4.4

Variation of absorption edge (λ_g), energy gap (E_g) and number of carbon atoms (N) per conjugation length in pristine and irradiated samples of Makrofol-N (PC) at different fluences.

Fluence (ions/cm^2)	Absorption edge (λ_g) (nm)	Band gap energy (eV)	N
0	285.45	4.36	62
10^{10}	287.32	4.32	63
$3x10^{10}$	288.83	4.30	64
10^{11}	296.92	4.19	67
$3x10^{11}$	300.38	4.13	69
$6x10^{11}$	325.95	3.81	81
10^{12}	449.81	2.76	154

The pristine sample shows the absorption edge at 285.45 nm, with corresponding optical band gap energy 4.36 eV. After irradiation, a strong increase in absorbance in the visible region along with gradual shifting of the optical absorption edge from UV to visible region was clearly observed with the increase of ion fluence. At the highest fluence of 10^{12} ions/cm^2 the absorption edge got shifted to 449.91 nm, with corresponding optical band gap as 2.76 eV. Thus, there is decrease of approximately 37% in the optcal band gap at higher fluence 10^{12} ions/cm^2. The variation in optical energy band gap of Makrofol-N with ion fluence for the two ion beams has been presented in Figure 4.5.

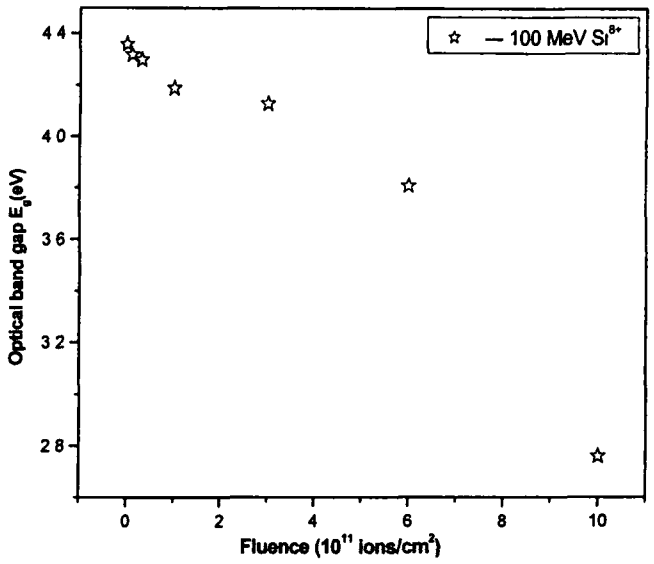

Figure 4.5: Variation of optical band gap energy with different ion fluences in Makrofol-N (PC)

Earlier studies [4, 9 and 10] have indicated that the carbon enriched domains created in polymers during irradiation are responsible for the decrease in band gap. The cluster size for the silicon irradiated samples is found to lie between 62 and 154 atoms. The cluster size in the pristine polymer corresponds to the grain structure of the polymer due to the complexity of its monomeric units. The decrease in present case can be correlated to the formation of free radicals due to predominant cross linking leading to the formation of free radicals [8] resulting from heavy ion irradiation.

4.3.3 Response of Polyethersulphone (PES)

Absorption studies with UV-Vis spectrophotometer were carried out on samples of aromatic polymer, polyether-sulphone (PES) samples (1.5x1.5 cm^2} ,pristine and irradiated with 100MeV Si^{8+} ions to the fluences of 1x 10^{10}, 1x 10^{11}, 1x10^{12} and 5 x 10^{12} ions/cm^2 and with 145 MeV Ne^{6+} ions to the fluences of 10^{12} and 10^{13} ions/cm^2. The optical absorption spectra are shown in Figures 4.6 and 4.7.

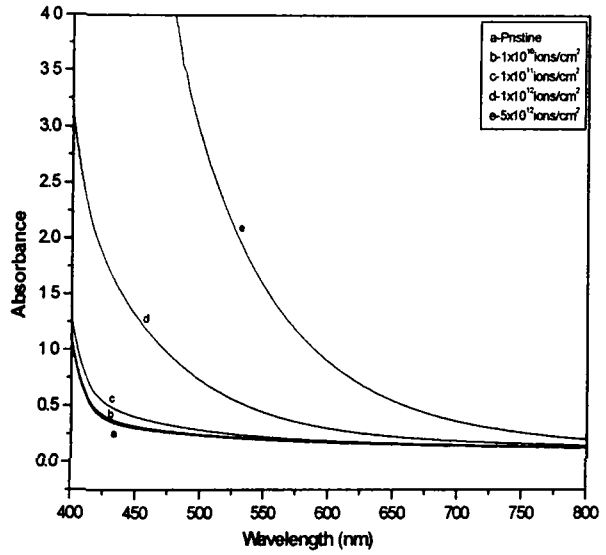

Figure 4.6: Optical absorption spectra of Polyether sulphone (PES) irradiated with 100 MeV Si^{8+} ion beam.

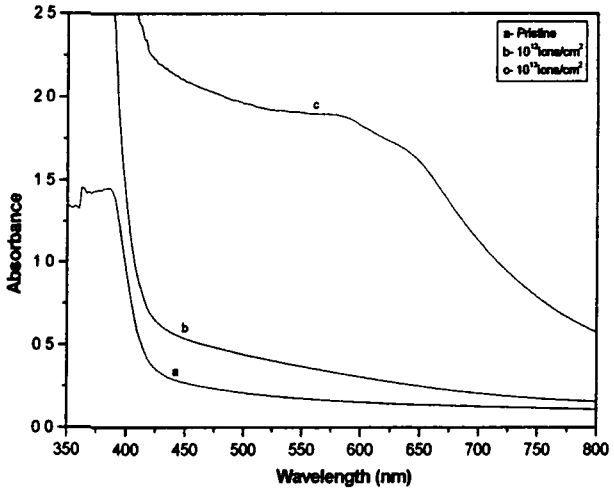

Figure 4.7: Optical absorption spectra of Polyethersulphone (PES) irradiated with 145 MeV Ne^{6+} ion beam

Figures 4.6 and 4.7 show a sharp decrease with increasing wavelength up to ~ 425 nm, followed by a plateau region. It is evident that optical absorption increases with increasing fluence and this absorption shifts from UV-Vis towards the visible region for irradiated samples. The values of λ_g and the corresponding results of energy gap (E_g) and

the number of carbon atoms per conjugation length (N) for pristine as well as irradiated samples are reported in Table 4.5 and 4.6.

Table - 4.5

Variation of absorption edge (λ_g), energy gap (E_g) and number of carbon atoms (N) per conjugation length in pristine and Si^{8+} ion irradiated samples of PES to different fluences.

Fluence (ions/cm^2)	Absorption edge λ_g (nm)	Band gap energy E_g (eV)	N
0	463.22	2.68	164
$1x10^{10}$	497.21	2.50	188
$1 x 10^{11}$	498.30	2.49	190
$1 x 10^{12}$	681.05	1.82	355
$5x10^{12}$	762.19	1.63	443

Table – 4.6

Variation of absorption edge (λ_g), energy gap (E_g) and number of carbon atoms (N) per conjugation length in pristine and Ne^{6+} ion irradiated samples of PES to different fluences.

Fluence (ions/cm^2)	Absorption edge λ_g (nm)	Band gap energy E_g (eV)	N
0	463.22	2.68	164
$1 x 10^{12}$	698.03	1.78	371
$1x 10^{13}$	771.54	1.61	454

The increase in absorption may be attributed to the formation of a conjugated system of bonds due to bond cleavage and reconstruction [4]. For Si ions optical band gap decreases by almost 39 % at the highest fluence of 5 x 10^{12} ions/cm^2. For Ne ion irradiation to the fluence of $1x10^{13}$ ions/cm^2, the optical band gap decreases by almost 40%. Previous studies [10-13] on different polymers have indicated that the carbon enriched domains created in polymers during irradiation are responsible for the decrease in band gap. It is observed that energy gap decreases with the increase in ion fluence. Optical band gap decreases by almost the same amount for both the ions irradiation. It is found that cluster size increases with transferred energy density for both the ions. The variation of optical band gap is shown in Figure 4.8.

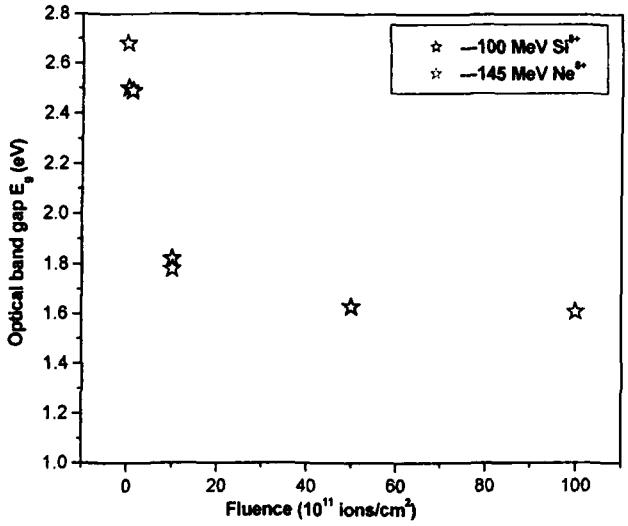

Figure 4.8: Variation of optical band gap energy with different ion fluences of Polyethersulphone (PES)

4.3.4 Response of Polypropylene (PP)

Polypropylene (PP) in the form of flat films of thickness 50 μm was procured from Good Fellow, Cambridge Ltd. England (U.K.). The specimens of the size (1.5 x 1.5 cm^2) were prepared for irradiation. Samples were mounted on a vertical vacuum shield ladder and irradiated in General Purpose Scattering Chamber (GPSC) by 100 MeV Si^{8+} ion beam from 15 UD Pelletron accelerator at Inter University Accelerator Centre, New Delhi to the fluences of 1 x 10^{10}, 3 x 10^{10}, 1 x 10^{11}, 3 x 10^{11}, 6 x 10^{11} and 1 x 10^{12} ions/cm^2. Irradiation with 145 MeV Ne^{6+} ion beam was carried out at Variable Energy Cyclotron Centre,(VECC) Kolkata to the fluences of 10^8, 10^{10}, 10^{11}, 10^{12} and 10^{13} ions/cm^2. The ion beam was defocused using a magnetic scanning system so that the film may be uniformly irradiated. The beam current was kept below (10 nA) to suppress thermal decomposition. Optical, modifications are characterized by UV-Vis spectroscopy analyses. Ultraviolet-Visible (UV-VIS) spectroscopy is performed in the wavelength range 200 – 800 nm by SHIMADZU, UV-1601 PC (Japan) UV-Visible spectrophotometer.

The formation of new bands due to ion irradiations has been studied by UV-Visible spectroscopy. The results of absorption studies with UV-Vis spectrophotometer

carried out on pristine and irradiated Polypropylene (PP) samples are shown in figures 4.9 and 4.10. Figure 4.9 shows the optical spectra for PP polymer samples after irradiation *with* Si^{8+} *ions to the fluences of* 1×10^{10}, 3×10^{10}, 1×10^{11}, 3×10^{11}, 6×10^{11} *and* 1×10^{12} ions/cm^2 and figure 4.10 shows the optical absorption spectra of PP polymer samples pristine and after irradiation with Ne^{6+} ion to the fluences of 10^8, 10^{10}, 10^{11}, 10^{12} and 10^{13} ions/cm^2 respectively.

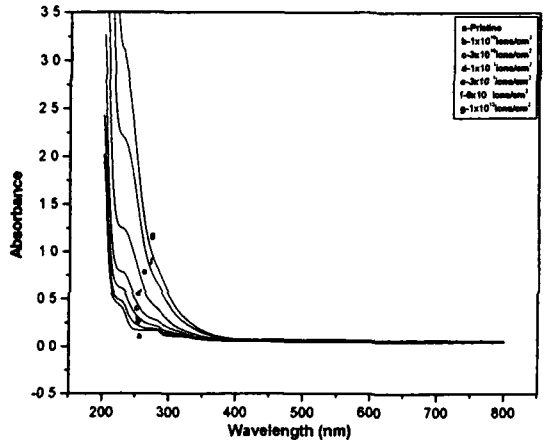

Figure 4.9: Optical absorption spectra of Polypropylene (PP) polymer, pristine and irradiated with 100 MeV Si^{8+} ion beam

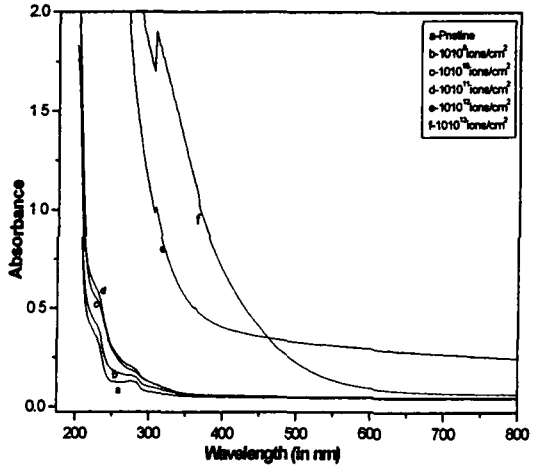

Figure 4.10: Optical absorption spectra of Polypropylene (PP) polymer, pristine and irradiated with 145 MeV Ne^{6+} ion beam

The optical absorption spectrum of the pristine sample shows a sharp decrease in absorbance with increasing wavelength followed by a plateau region for both the ions. It is observed that optical absorption increases with increasing fluence and this absorption shifts from UV-Vis towards the visible region for irradiated samples. The increase in absorption may be attributed to the formation of a conjugated system of bonds due to bond cleavage and reconstruction [1].

The damage of sharpness decreases with increasing dose which indicates towards the increased damage in the films as the fluence is increased. Optical absorption method can be used for the investigation of the optically induced transitions and can provide information about the bond structure and energy gap in crystalline and non crystalline matter [4]. The values of λ_g and the corresponding results of energy gap (E_g) and the number of carbon atoms per conjugation length (N) for pristine as well as irradiated samples are presented in Tables 4.7 and 4.8.

Table – 4.7

Variation of absorption edge (λ_g), energy gap (E_g) and number of carbon atoms (N) per conjugation length in pristine and 100 MeV Si^{8+} ion irradiated samples of PP to different fluences.

Fluence (ions/cm^2)	Absorption edge λ_g (nm)	Band gap energy E_g (eV)	N
0	225.32	5.52	38
10^{10}	227.43	5.47	39
$3x10^{10}$	233.85	5.32	41
$1x10^{11}$	242.78	5.12	44
$3x10^{11}$	246.10	5.05	46
$6x10^{11}$	260.38	4.77	51
$1x10^{12}$	286.79	4.33	62

Table - 4.8

Variation of absorption edge (λ_g), energy gap (E_g) and number of carbon atoms (N) per conjugation length in pristine and145 MeV Ne^{6+} ion irradiated samples of PP to different fluences.

Fluence (ions/cm^2)	Absorption edge λ_g (nm)	Band gap Energy (eV)	N
0	228.27	5.45	39
10^8	229.6+8	5.41	40
10^{10}	232.11	5.36	41
10^{11}	233.57	5.32	42
10^{12}	352.65	3.53	94
10^{13}	458.87	2.71	160

It is observed that energy gap decreases with the increase in ion fluence. Optical band gap decreases by almost 21 % at the highest fluence of 1 x 10^{12} ions/cm^2 for Si^{8+} ion irradiation whereas for Ne^{6+} ion irradiation the change is 50% at the highest fluence of 10^{13} ions/cm^2 Earlier studies [10-14] have indicated that the carbon enriched domains created in polymers during irradiation are responsible for the decrease in band gap. The variation of optical band gap is shown in figure 4.11.

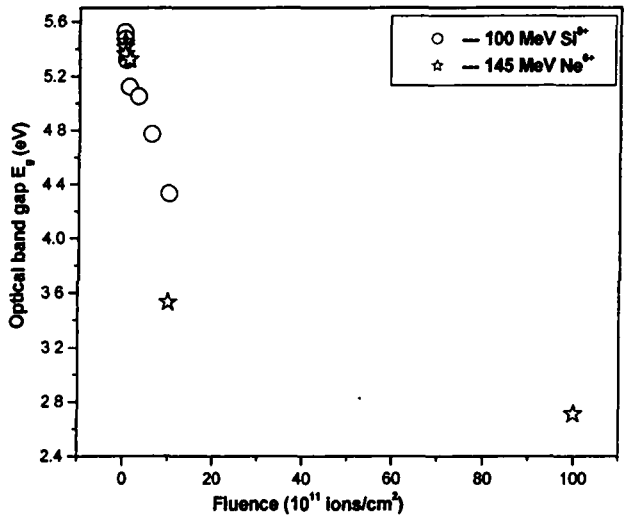

Figure 4.11: Variation of optical band gap energy with different ion fluences of Polypropylene (PP)

4.3.5 Response of Polyethylene terephthalate (PET)

A representative plot of absorption as a function of wavelength for the samples of PET films irradiated with 100 MeV Si^{8+} ions to the fluences of 10^{10}, 10^{11} and 10^{12} ions/cm^2 is shown in Figure 4.12.

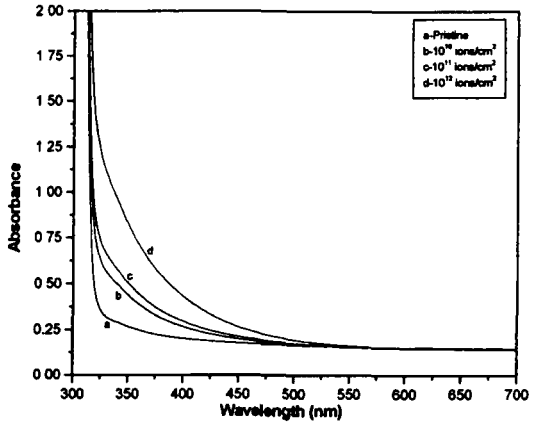

Figure 4.12: Optical absorption spectra of Polyethylene terephthalate (PET) polymer irradiated with 100 MeV Si^{8+} ion beam

A clear shift in the absorption edge towards the red end of the spectrum is observed. The values of absorption edges λ_g, optical band energy gap E_g and number of carbon atoms per cluster (N) presented in table 4.9

Table – 4.9

Variation of absorption edge (λ_g), energy gap (E_g) and number of carbon atoms (N) per conjugation length in pristine and Si^{8+} ion irradiated samples of PET to different fluences.

Fluence (ions/cm^2)	Absorption edge λ_g(nm)	Band gap energy E_g(eV)	(N)
0	321.44	3.86	79
10^{10}	323.58	3.84	80
10^{11}	326.24	3.81	81
10^{12}	328.12	3.78	82

The value of optical gap energy (E_g) shows a decreasing trend with increasing ion fluence. Optical band gap decreases almost 2.07% at the highest fluence of 10^{12} ions/cm^2. This fact is further corroborated as the number of carbon atoms per cluster obtained in the

work too shows dependence with the increase in the ion fluence. Variation with fluence in optical band gap is shown in Figure 4.13.

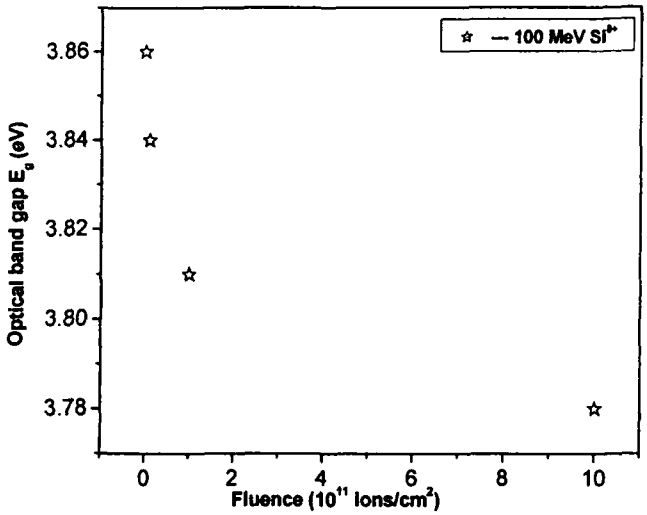

Figure 4.13: Variation of optical band gap energy with different ion fluences of Polyethylene trephthalate (PET)

4.3.6 Response of Polytetrafluoroethylene (PTFE)

Figures 4.14 and 4.15 present the absorption spectra of pristine and 100 MeV Si^{8+} ions irradiated samples to the fluences of 10^{10}, 10^{11}, 10^{12} and 10^{13}ions/cm^2 and 145 MeV Ne^{6+} ions irradiated samples to the fluences of (10^{10}, 10^{11} and10^{12} ions/cm^2) respectively.

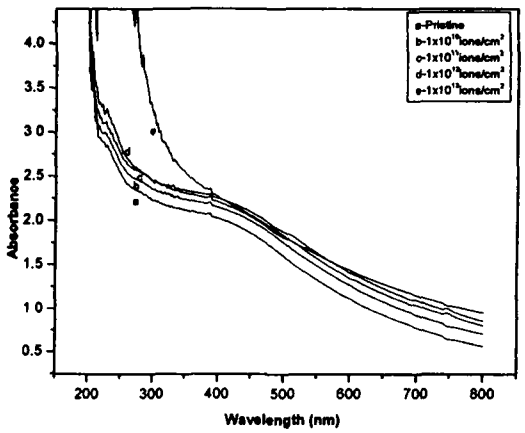

Figure 4.14: Optical absorption spectra of Polytetrafluoro ethylene (PTFE) polymer irradiated with 100 MeV Si^{8+} ion beam.

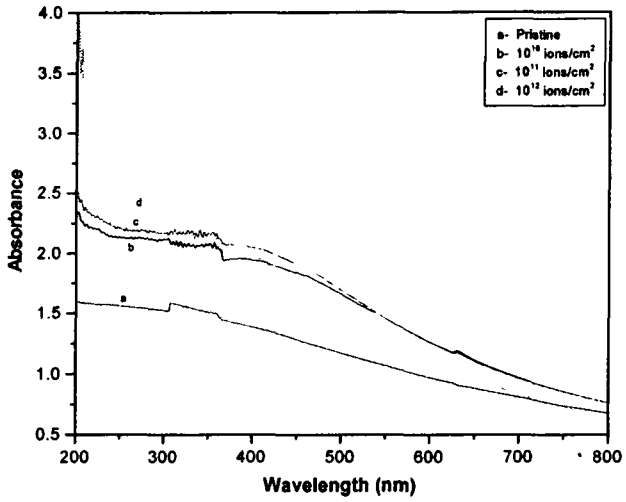

Figure 4.15: Optical absorption spectra of PTFE polymer irradiated with 145 MeV Ne^{6+} ion beam.

The values of absorption edge and corresponding optical energy gap and number of carbon atoms per cluster are given in Tables- 4.10 and 4.11.

Table – 4.10

Variation of absorption edge (λ_g), energy gap (E_g) and number of carbon atoms (N) per conjugation length in pristine and Si^{8+} ion irradiated samples of PTFE at different fluences.

Fluence (ions/cm^2)	Absorption edge λ_g (nm)	Band gap energy (eV)	(N)
0	556.01	2.23	236
10^{10}	565.97	2.19	245
10^{11}	582.21	2.13	259
10^{12}	585.81	2.12	261
10^{13}	594.38	2.09	269

Table - 4.11

Variation of absorption edge (λ_g), energy gap (E_g) and number of carbon atoms N per conjugation length in pristine and Ne^{6+} ion irradiated samples of PTFE to different fluences.

Fluence (ions/cm^2)	Absorption edge (λ_g) (nm)	Band gap energy (eV)	No. of carbon atoms (N)
0	556.01	2.23	236
10^{10}	592.00	2.10	266
10^{11}	609.11	2.04	283
10^{12}	664.70	1.87	336

The pristine sample shows absorption edge (λ_g) as 556 nm, which corresponds to optical energy gap of 2.23 eV. The pronounced shift in absorption edge is observed with 100 MeV Si^{8+} ion beam, and optical edge shifs to 594.38 nm, at the fluence 10^{13} ions/cm^2. For the 145 MeV Ne^{6+} ions irradiated PTFE, optical edge shift to 664.70 nm, at the fluence of 10^{12} ions/cm^2. At the highest fluence of ~10^{13} ions/cm^2 maximum decrease in energy gap of almost 6.27 % has been found for Si^{8+} ions irradiated PTFE polymer samples and decrease of about 16.14% is found in PTFE samples irradiated with 145 MeV Ne^{6+} ions. The variation of optical band gap is shown jn Figure 4.16. Carbon enriched domains created in polymers during irradiation may be responsible for the decrease in band gap as indicated by earlier studies [8,14] and [10-13]. The optical absorption method can be used for the investigation of the optically induced transitions and can provide information about the bond structure and energy gap in crystalline and non-crystalline materials [4].

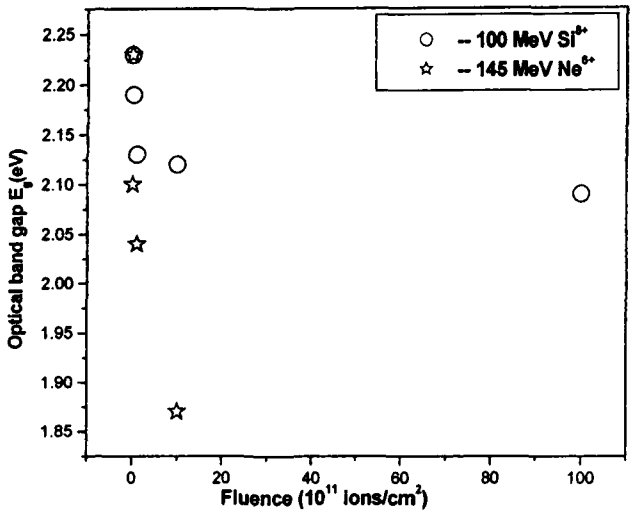

Figure 4.16: Variation of optical – gap energy with different ion fluences of Polyetetrafluoroethylene (PTFE)

4.3.7 Response of Polymethyle methacrylate (PMMA)

Optical absorption spectra of pristine and 100 MeV Si^{8+}, 145 MeV Ne^{6+} and 50 MeV Li^{3+} ions irradiated PMMA film samples to different fluences are presented in Figures 4.17, 4.18 and 4.19.

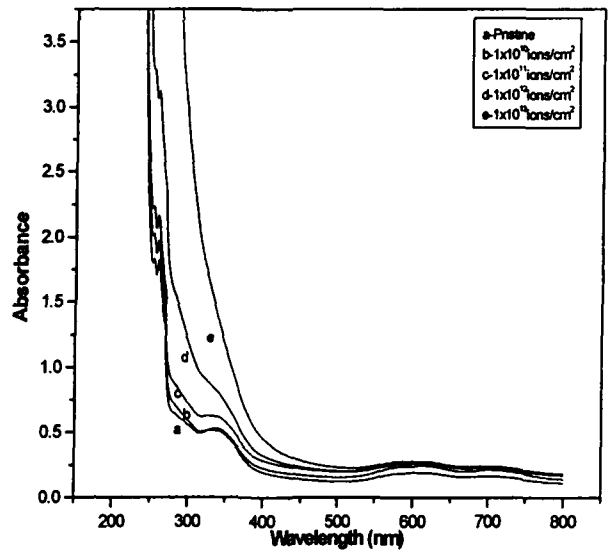

Figure 4.17: Optical absorption spectra of Polymethyl methacrylate (PMMA) polymer irradiated with 100 MeV Si^{8+} ion beam.

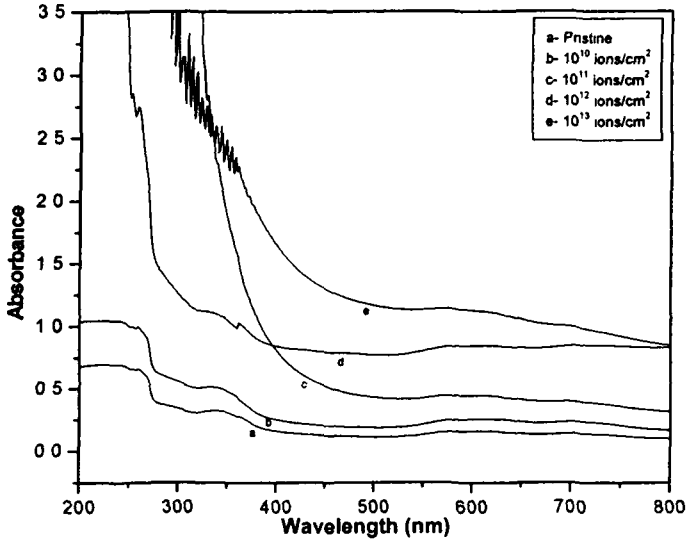

Figure 4.18: Optical absorption spectra of Polymethylmethacrylate (PMMA) Polymer irradiated with 145 MeV Ne^{6+} ion beam

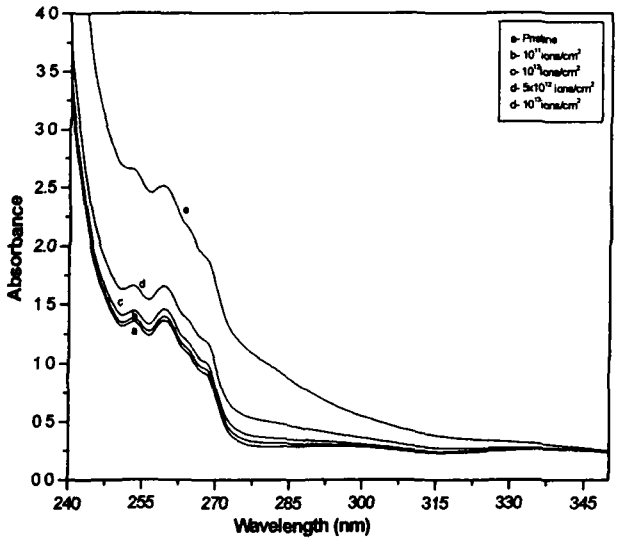

Figure 4.19: Optical absorption spectra of PMMA polymer irradiated with 50 MeV Li^{3+} ion beam.

Figures show a sharp decrease in absorbance in pristine samples with increasing wavelength, followed by a plateau region. Figures 4.12 – 4.14(b-e) show the optical spectra for PMMA polymer samples after irradiation to the different fluences. It is observed that optical absorption increases with increasing fluence and the absorption shifts from UV-Vis towards the visible region for irradiated samples as the fluence increases. The increase in absorption may be attributed to the formation of a conjugated system of bonds due to bond cleavage and reconstruction [4]. The values of absorption edges λ_g, the corresponding optical band gap (E_g) and number of carbon atoms per cluster N are given in Tables 4.12, 4.13 and 4.14.

Table – 4.12

Variation of absorption edge (λ_g), energy gap (E_g) and number of carbon atoms (N) per conjugation length in pristine and Si^{8+} ion irradiated samples of PMMA to different fluences.

Fluence (ions/cm^2)	Absorption edge λ_g (nm)	Band gap energy (eV)	N
0	399.24	3.11	122
10^{10}	404.06	3.07	124
10^{11}	414.84	2.99	131
10^{12}	422.22	2.94	136
10^{13}	426.41	2.91	138

Table – 4 .13

Variation of absorption edge (λ_g), energy gap (E_g) and number of carbon atoms (N) per conjugation length in pristine and Ne^{6+} ion irradiated samples of PMMA to different fluences.

Fluence (ions/cm^2)	Absorption edge λ_g (nm)	Band gap energy (eV)	N
0	395.57	3.14	119
10^{10}	430.77	3.05	126
10^{11}	455.76	2.73	158
10^{12}	544.97	2.22	239
10^{13}	598.59	2.08	272

Table - 4.14

Variation of absorption edge (λ_g), energy gap (E_g) and number of carbon atoms N per conjugation length in pristine and Li^{3+} ion irradiated samples of PMMA to different fluences.

Fluence (ions/cm^2)	Absorption edge λ_g (nm)	Band gap energy E_g (eV)	N
0	388.68	3.19	116
$5x10^{10}$	396.49	3.13	120
10^{11}	405.65	3.06	126
10^{12}	423.59	2.93	137
10^{13}	461.99	2.69	163

It can be observed that energy gap decreases with the increase in ion fluence for all the three kind of ions. Optical band gap decreases by almost 6.4% for Si^{8+} ion irradiation to the highest fluence whereas for Ne^{6+} ion irradiation the change is 34% at the highest fluence of 10^{13} ions/cm^2 and decrease in band gap 16% for the sample irradiated to Li^{3+} ions at the highest fluence of 10^{13} ions/cm^2. The cluster size for the silicon irradiated samples is found to lie between 122-138 atoms and for the Neon irradiated it lies between 119-172 atoms, while it lies between 116-163 atoms for the lithium irradiated samples. Carbon enriched domains created in polymers during irradiation may be responsible for the decrease in band gap as indicated by earlier studies [8, 10-13]]. The optical band gap variation with fluences is shown in figure 4.20 for the ions.

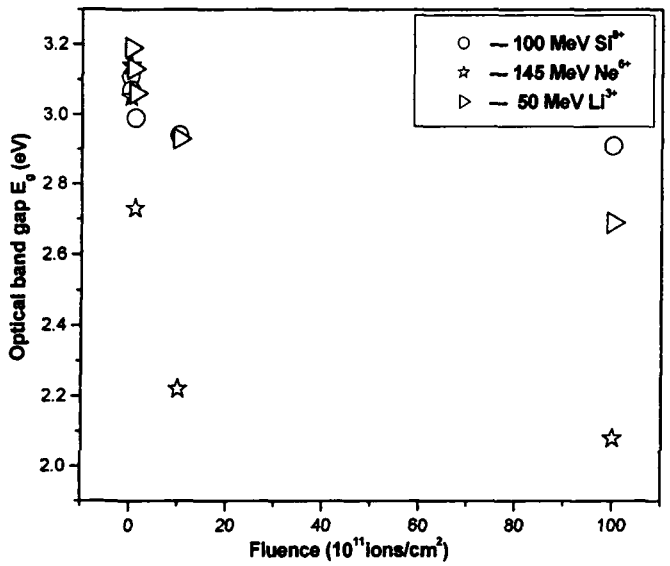

Figure 4.20: Variation of optical band gap energy with different ion fluences of Polymethylemethacrylate (PMMA)

4.3.8 Response of Low Density Polyethylene (LDPE)

Figure 4.21 shows the UV-Vis absorption spectra of pristine and 95 MeV O^{6+} ion irradiated LDPE samples at different fluences. The values of absorption edges and the corresponding optical band gap energies, number of carbon atoms per cluster(N) are given in Table 4.15.

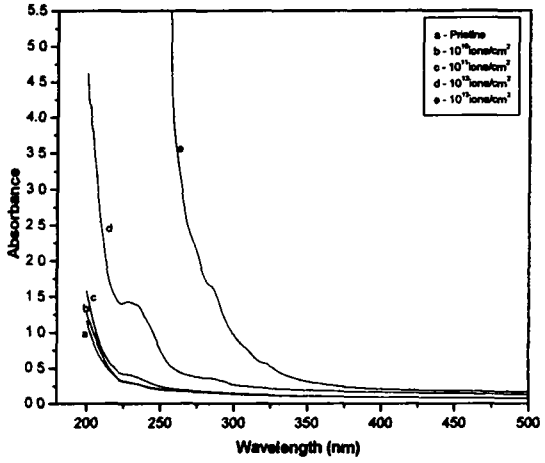

Figure 4.21: Optical absorption spectra of LDPE polymer irradiated with 95 MeV O^{6+} ion beam.

Table - 4.15

Variation of absorption edge (λ_g), energy gap (E_g) and number of carbon atoms N per conjugation length in pristine and O^{6+} ion irradiated samples of LDPE to different fluences.

Fluence (ions/cm^2)	Absorption edge λ_g (nm)	Band gap energy E_g(eV)	N
0	240.30	5.17	44
10^{10}	248.23	5.00	47
10^{11}	255.25	4.87	50
10^{12}	273.12	4.55	57
10^{13}	380.72	3.27	110

The pristine LDPE sample shows absorption edge at 240.30 nm, with corresponding optical band gap of 5.17 eV. After irradiation, a strong increase in absorbance in the visible region along with gradual shifting of the optical absorption edge from UV to visible region was clearly observed with the increase of ion fluence. At the highest fluence 10^{13} ions/cm^2, the absorption edge got shifted to 380.32 nm, with corresponding optical band gap as 3.27 eV. It can be observed that energy gap decreases with the increase in ion fluence. Optical band gap decreases by almost ~37% for O^{6+} ion irradiation. The decrease in optical band gap is generally attributed to the formation of carbon-enriched domains created in polymers during irradiation. The ion irradiation has lead to pronounced coloration effects, starting from the transparent pristine film to yellowish and then dark brown at the highest fluence.

We got similar effects with 50 MeV Li^{3+} ion irradiation to $5x10^{10}$, 10^{11}, 10^{12} and 10^{13} ions/cm^2 as shown in Figure 4.22.

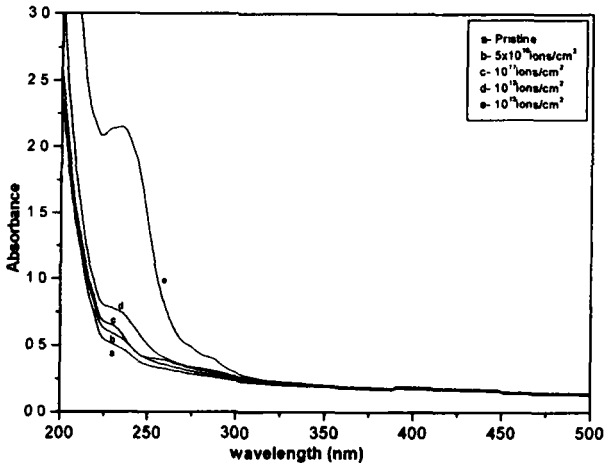

Figure 4.22: Optical absorption spectra of LDPE polymer irradiated with 50 MeV Li^{3+} ion beam.

The values of absorption edges and the corresponding optical band gap energies, numbers of carbon atoms per cluster (N) are given in table 4.16.

Table - 4. 16

Variation of absorption edge (λ_g), energy gap (E_g) and number of carbon atoms N per conjugation length in pristine and Li^{3+} ion irradiated samples of LDPE to different fluences.

Fluence (ions/cm^2)	Absorption edge λ_g (nm)	Band gap energy E_g(eV)	N
0	238.57	5.21	43
$5x10^{10}$	243.22	5.11	45
10^{11}	255.41	4.87	50
10^{12}	261.61	4.75	52
10^{13}	343.05	3.62	90

A similar trend of shift in the absorption has been noticed as 238.57 nm. In this case the ion irradiation has shifted the absorption edge to 343.05 nm, with corresponding optical band gap energy as 3.62 eV, at the highest fluence of 10^{13} ions/cm^2. So, the optical energy gap got decreased by nearly 31%. In similarity to results of 95 MeV O^{6+} ion irradiation, the colour has changed from yellowish to dark brown with increase in ion fluence. The cluster size for the various LDPE samples irradiated with 95 MeV O^{6+} ions

varies from 44 to 110 while for 50 MeV Li^{3+} ion irradiated samples the cluster size varies from 43 to 90. The cluster size in pristine polymer refers to the density fluctuations in the polymer structure. These carbonaceous clusters are responsible for the conductivity in irradiated polymers. Variation in optical band gap of LDEPE with the fluences for both the ions is shown in figure 4.23.

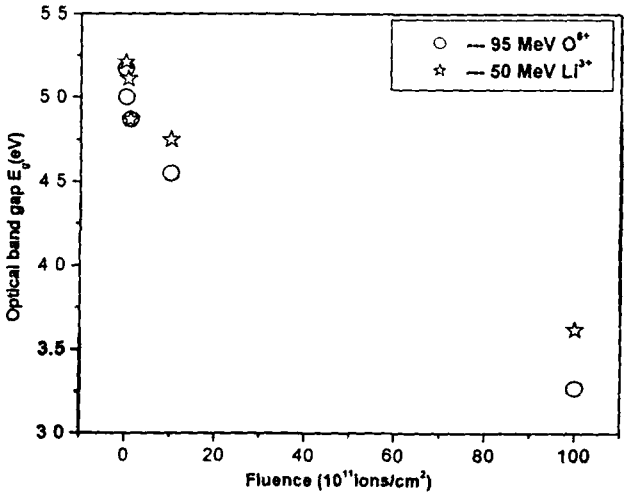

Figure 4.23: Variation of optical – gap energy with different ion fluences of Low Density Polyethylene (LDPE)

4.3.9 Response of Polyethylene oxide - Salt (17% & 19%)

The UV-Vis spectra recorded for the O^{6+} ion beam irradiated Polyethylene oxide - Salt (17% & 19%) samples are shown in Figures 4.24 and 4.25 respectively.

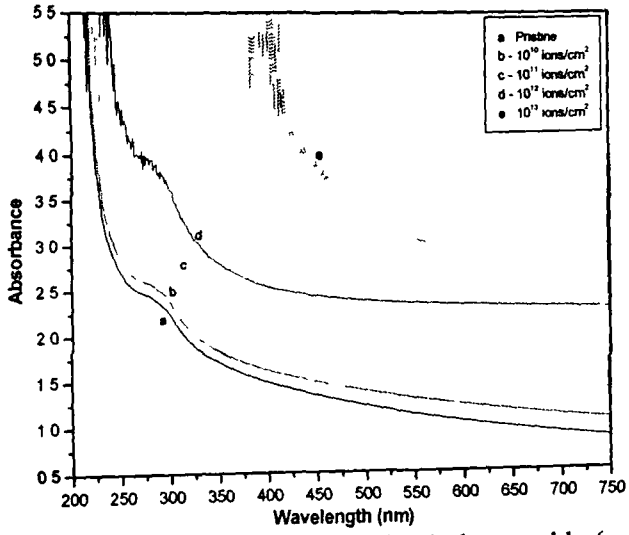

Figure 4.24: Optical absorption spectra of of Polyethylene-oxide (salt) PEO-17% polymer irradiated with 95 MeV O^{6+} ion beam.

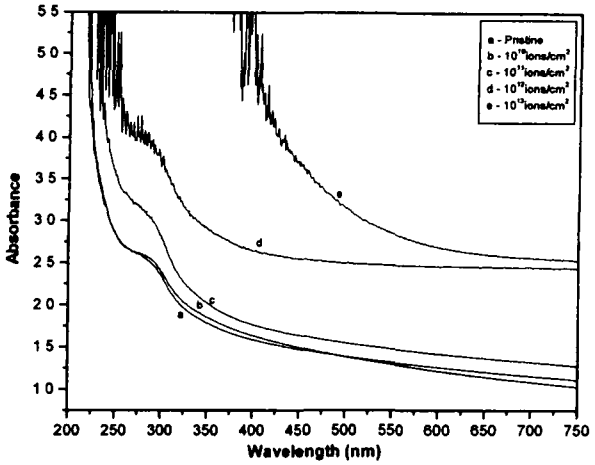

Figure 4.25: Optical absorption spectra of Polyethylene-oxide (salt) PEO-19% polymer irradiated with 95 MeV O^{6+} ion beam.

A shift of absorption edge towards longer wavelength with increasing ion fluence can be readily observed for both salt percentages. The optical absorption spectrum of pristine samples (figures 4.22 & 4.23) curve (a) shows a sharp decrease with increasing wavelength up to ~230 nm, followed by a plateau region for both kind of salt percentages. In figures 4.24 & 4.25 curve (b-e) shown are the optical spectra of Polyethylene oxide - Salt (17% & 19%) after irradiation to the fluences of 10^{10} - 10^{13} ions/cm^2 for both the cases. The values of absorption edges and the corresponding optical band gap energies and number of carbon atoms per conjugation length (N) are given in Tables 4.17 & 4.18.

Table - 4.17

Variation of absorption edge (λ_g), energy gap (E_g) and number of carbon atoms N per conjugation length in pristine and Si^{8+} ion samples of PEO-17% irradiated to different fluences.

Fluence (ions/cm^2)	Absorption edge λ_g (nm)	Band gap energy E_g (eV)	N
0	424.00	2.93	137
10^{10}	434.31	2.86	144
10^{11}	517.98	2.84	146
10^{12}	721.35	2.15	255
10^{13}	865.26	1.60	460

Table - 4.18

Variation of absorption edge (λ_g), energy gap (E_g) and number of carbon atoms (N) per conjugation length in pristine and O^{6+} ion samples of PEO-19% irradiated to different fluences.

Fluence (ions/cm^2)	Absorption edge λ_g (nm)	Band gap energy E_g (eV)	N
0	462.98	2.68	164
10^{10}	474.71	2.61	173
10^{11}	517.98	2.39	206
10^{12}	578.94	1.72	398
10^{13}	781.10	1.44	567

It is evident that the optical absorption increases with increasing fluence and the absorptions shift from UV-Vis towards the visible region for irradiated samples. It is observed that energy gap decreases with increase in ion fluence. Optical band gap decreases by almost 45.39% at the highest fluence in Polyethylene oxide - Salt 17% while , total change in optical band gap at the highest fluence in Polyethylene oxide - Salt 19% is almost 46.26%. The cluster size for oxygen ion irradiated Polyethylene oxide - Salt 17% samples is found to lie between 137-460 atoms, while it lies between 164- 567 for Polyethylene oxide - Salt 19% irradiated with oxygen ion beam. The variation of optical band gap with fluence for both the PEO-complexes is shown in Figure 4.24.

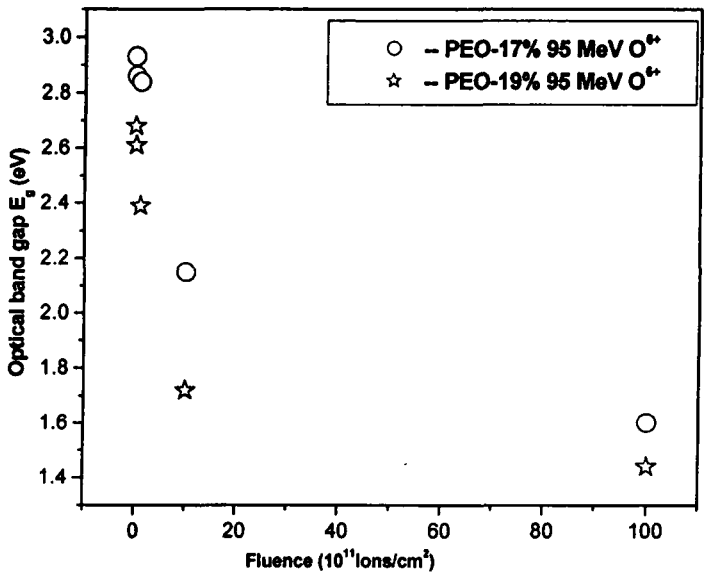

Figure 4.26: Variation of optical band gap energy with different ion fluences of Polyethylene-oxide (PEO)

4.3.10 Response of LEXAN Polycarbonate

In LEXAN polycarbonate the formation of new bands have been studied by UV-Visible spectroscopy. Figure 4.27 shows the absorption spectra of pristine and irradiated LEXAN Polycarbonate samples.

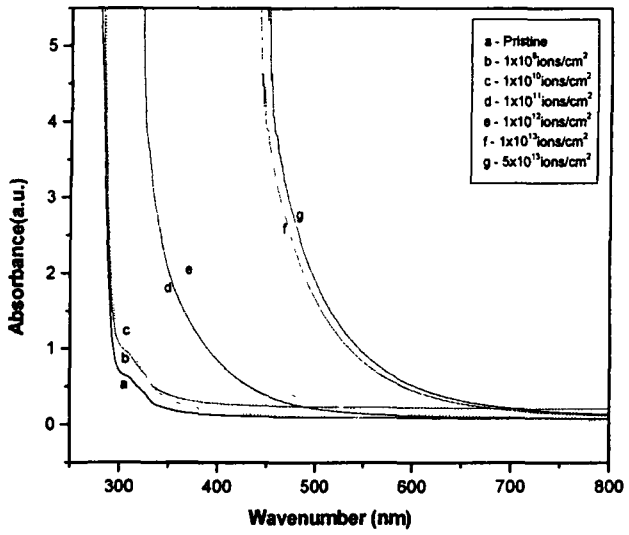

Figure 4.27: Optical absorption spectra of LEXAN polycarbonate polymer irradiated with 95 MeV O^{6+} ion beam.

The value of absorption edge (λ_g) and the corresponding optical band-gap (E_g) and number of carbon atoms per conjugation length is given in the Table 4.19.

Table - 4.19

Variation of absorption edge (λ_g), energy gap (E_g) and number of carbon atoms N per conjugation length in pristine and O^{6+} ion irradiated samples of LEXAN (PC) to different fluences.

Fluence (ions/cm^2)	Absorption edge λ_g (nm)	Band gap energy (eV)	N
0	301.81	4.12	69
10^8	306.80	4.05	72
10^{10}	312.25	3.98	74
10^{11}	349.17	3.56	93
10^{12}	385.84	3.22	113
10^{13}	492.98	2.52	185
$2x10^{13}$	530.20	2.34	215

The value of E_g decreases with increase of fluence. It is clear that the optical band gap energy of the pristine PC is found to be 4.12 eVwhich starts decreasing for PC after irradiation up 10^8 ions/cm^2 to a dose of 2 x 10^{13} ions / cm^2 and reaches a minimum of 2.34 eV. Figure 4.28 shows the variation in band gap energy (E_g) with fluence The radicals contribute to the polymeric restructuring process which leads to conductivity [9] as confirmed by Sinha et al. [8] that the free radical formation takes place in PADC (Acrylics) by gamma irradiation at higher doses. The decrease in present case can be correlated to the formation of free radicals.

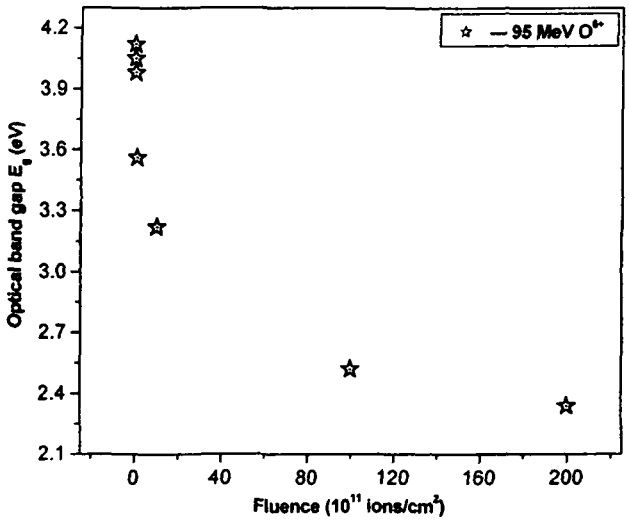

Figure 4.28: Variation of optical band gap energy with different ion fluences of LEXAN Polycarbonate

4.3.11 Response of Polyvinylidene fluoride (PVDF)

Figure 4.29 presents the results of absorption studies with UV-Vis spectrophotometer carried on pristine Polyvinylidene fluoride (PVDF) and irradiated samples with Ne^{6+} ions to the fluences of 10^{10}, 10^{11},10^{12}, and 10^{13} ions/cm^2 and figure 4.30 shows the optical absorption spectra of pristine and irradiated PVDF samples with O^{6+} ion to the fluences of 10^{10}, 10^{11}, 10^{12} and 10^{13} ions/cm^2.

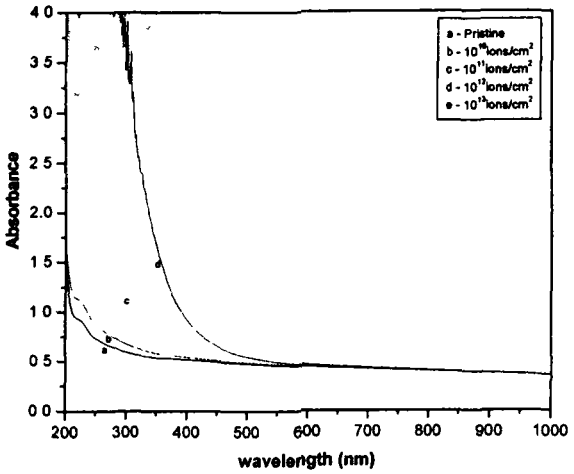

Figure 4.29: Optical absorption spectra of PVDF polymer irradiated with 145 MeV Ne^{6+} ion beam.

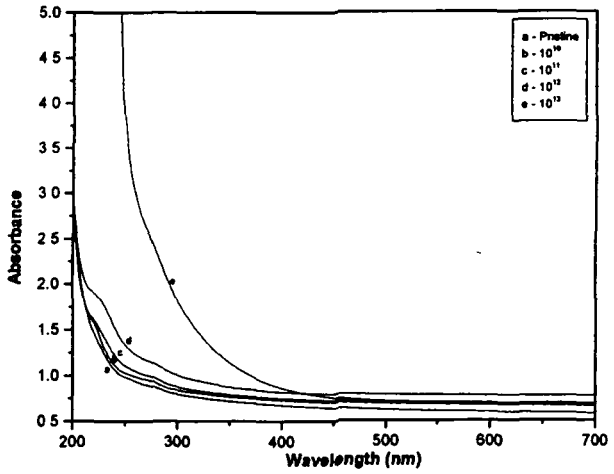

Figure 4.30: Optical absorption spectra of PVDF polymer irradiated with 95 MeV O^{6+} ion beam.

The optical absorption spectrum of the pristine sample shows a sharp decrease with increasing wavelength followed by a plateau region. It is evident that optical absorption increases with increasing fluence and this absorption shifts from UV-Vis towards the visible region for irradiated samples. The increase in absorption may be attributed to the formation of a conjugated system of bonds due to bond cleavage and reconstruction [4]. The values of λ_g and the corresponding results of energy gap (E_g) and the number of carbon atoms per conjugation length (N) for pristine as well as irradiated samples are presented in tables 4.20 & 4.21.

Table - 4.20

Variation of absorption edge (λ_g), energy gap (E_g) and number of carbon atoms N per conjugation length in pristine and irradiated with 145 MeV Ne^{6+} ions PVDF samples to different fluences.

Fluence (ions/cm^2)	Absorption edge λ_g (nm)	Band gap energy E_g (eV)	N
0	339.49	3.66	88
10^{10}	356.42	3.49	97
10^{11}	406.65	3.06	126
10^{12}	574.89	2.16	252
10^{13}	772.08	1.61	454

Table - 4. 21

Variation of absorption edge (λ_g), energy gap (E_g) and number of carbon atoms (N) per conjugation length pristine and irradiated with of 95 MeV O^{6+} ions PVDF samples to different fluences

Fluence (ions/cm^2)	Absorption edge λ_g (nm)	Band gap energy E_g (eV)	N
0	339.49	3.66	88
10^{10}	382.80	3.25	111
10^{11}	433.79	2.87	143
10^{12}	466.55	2.66	166
10^{13}	472.41	2.63	170

The energy gap decreases with the increase in ion fluence. Optical band gap decreases by almost 56 % at the highest fluence of 10^{13} ions/cm^2 for Ne^{6+} ion irradiation whereas for O^{6+} ion irradiation the change is 28.14% at the highest fluence of 10^{13} ions/cm^2. The variation of optical band gap is shown in Figure 4.31.

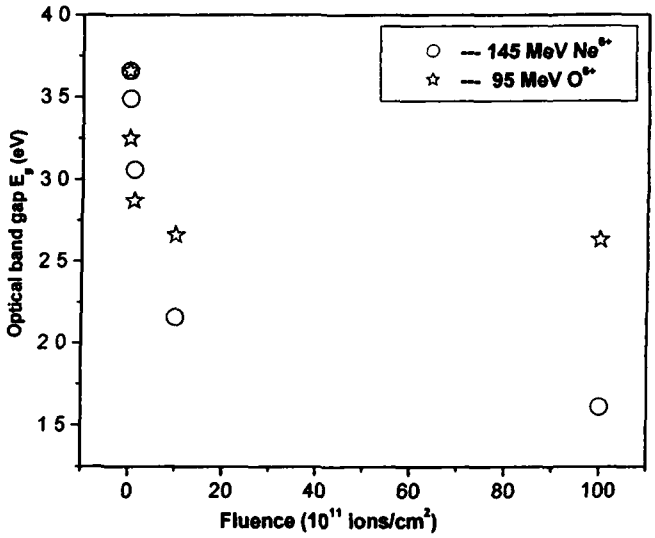

Figure 4.31: Variation of optical band gap energy with different ion fluences of PVDF

4.3.12 Response of Polyamide Nylon-6, 6 (PN-6, 6)

Ion beam interaction with polymer generates damage which leads to the formation of new defects and new charge states. The results of absorption studies with UV-Vis spectrophotometer carried out on pristine and irradiated samples of Polyamide Nylon-6, 6 (PN-6, 6) with 50 MeV Li^{3+} ion beam at different fluences are illustrated in Figure 4.32.

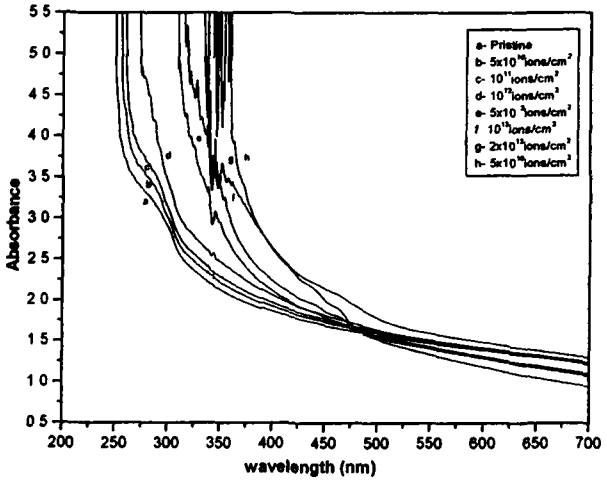

Figure 4.32: Optical absorption spectra of PN-6,6 polymer irradiated with 50 MeV Li^{3+} ion beam.

The optical absorption spectrum of the pristine sample figure 4.32 curve (a) shows a sharp decrease with increasing wavelength up to ~427 nm followed by a plateau region. (curves b-f) in Figure 4.32 show the optical spectra for PN-6,6 polymer samples after irradiation to the fluences of 10^{10} to $5x10^{13}$ ions/cm^2, respectively. Optical absorption increases with increasing fluence and this absorption shifts from UV-Vis towards the visible region for irradiated samples. The value of λ_g and the corresponding results of energy gap (E_g) and the number of carbon atoms per conjugation length (N) for pristine as well as irradiated samples are reported in Table- 4.4.1.

Table - 4.22

Variation of absorption edge (λ_g), energy gap (E_g) and number of carbon atoms N per conjugation length in pristine and Li^{3+} ion irradiated samples of PN-6, 6 to different fluences.

Fluence (ions/cm^2)	Absorption edge λ_g (nm)	Band gap energy E_g (eV)	N
0	427.03	2.91	139
10^{10}	433.47	2.87	143
10^{11}	437.07	2.84	146
10^{12}	470.94	2.63	170
$5x10^{12}$	518.03	2.39	206
10^{13}	563.28	2.21	241
$2x10^{13}$	700.67	1.77	376
$5x10^{13}$	738.32	1.68	417

Optical band gap decreases by almost 42.26% at the highest fluence of $5x10^{13}$ ions/cm^2. Variation of optical band gap is shown in Figure 4.33.

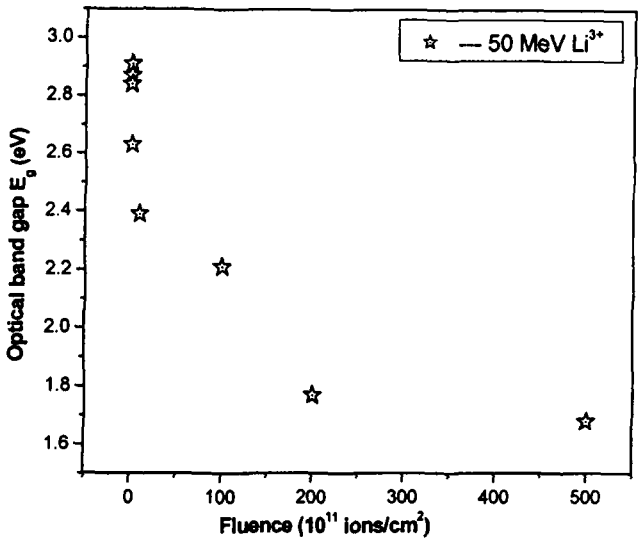

Figure 4.33: Variation of optical band gap energy with different ion fluences of Polyamide Nylon-6,6 (PN-6,6)

4.4 Characterization of Chemical Modification through FTIR Spectroscopy

Infrared red spectroscopy is one of the most powerful analytical techniques which offers the possibility of chemical identification. In a polymer the FTIR spectrum provides the useful information about its chemical structure s it involves the twisting , bending, rotational and vibrational motions of atoms in a molecule. The higher frequency region of the infra red spectra (4000-1300 cm^{-1}) is called the functional group region which shows the absorption arising from stretching vibrations and is useful for identification of the functional groups. The absorption pattern in the region 1400-650 cm^{-1} is unique for particular compound and hence called the fingerprint region. Both the stretching and bending modes of vibration give rise to absorption in this region. Ion irradiation brings about significant modifications in a polymer, owing to process like chain scission, cross-linking, desorption of gasses, formation of double and triple bonds etc. Thus such modification will be reflected in the spectrum of irradiated polymer. So, this technique has been found very useful for the study of radiation-induced modifications in polymers.

The present study of FTIR spectroscopy in polymers has been carried out through NEXUS 670 FTIR E.S.P. at Inter University Accelerator Centre, New Delhi.

4.4.1 FTIR Spectroscopy of Makrofol-KG Polycarbonate

(a) Irradiated with 145 MeV Ne^{6+} ions

The IR spectra of the Makrofol-KG polycarbonate samples, virgin and irradiated with 145 MeV Ne^{6+} to the fluences of 10^{10}, 10^{11}, 10^{12} and 10^{13} ions/cm^2 at Variable Energy Cyclotron Centre (VECC), Kolkata, India are shown in Figure 4.34. The wave numbers for characteristic peaks along with their interpretations are given in Table 4.23.

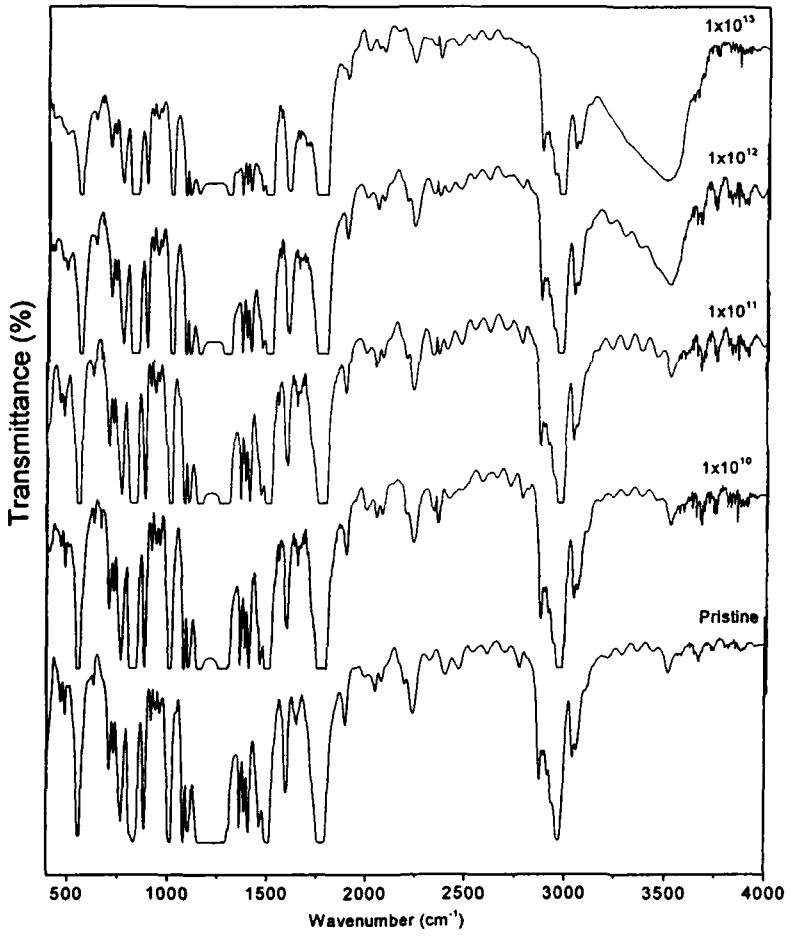

Figure 4.33 FTIR spectra of Makrofol-KG Polycarbonate irradiated with 145 MeV Ne^{6+} ion beam (a) Virgin (b) 10^{10} (c) 10^{11} (d) 1x 10^{12} (e) 10^{13}.

Table - 4.23

Identification of absorption bands in Makrofol-KG irradiated with 145 MeV Ne^{6+} ions corresponding to their wave numbers ($1/\lambda$).

Peak	$1/\lambda$ (cm^{-1})	Identification
1	2974	CH_3 stretching vibrations
2	1774	C=O stretching vibrations
3 4	1600 1500	C=C phenyl ring stretching vibrations
5	1395	Symmetric in plane bending of CH_3 group
6	1162	Anti-symmetric stretching of C-O-C links
7	832 1012	C-H para out of plane aromatic bending vibrations C-H para in plane aromatic bending vibrations
8	762	C-H & C-C vibrations

It is observed that there is no change over all structure of the polymer. On irradiation at the highest fluences of 10^{12} and 10^{13} ions/cm^2 a peak corresponding to 3500cm^{-1} appeared and its intensity increased with the ion fluence along with decrease in the absorption intensity of the band at 1774 cm^{-1} representing C=O stretching changed with ion fluence. This indicates that chain scission may be taking place at the carbon dioxide/carbon monoxide and formation of hydroxyl group. H atom required for its formation coming perhaps from the isopropyl group, as the absorption around 2974 cm^{-1} which arises due to CH_3 symmetric stretch decrease in intensity with increase in ion fluence. The Corroboration of chain scission can be deduced from the decrease in the intensity of absorption bands around 1162cm^{-1} attributed to C-O stretch. The decrease intensity of absorption bands at 832 and 1012 cm^{-1} corresponds to para out of plane aromatic C-H wag of two adjacent H atoms and para in plane aromatic C-H bands. This lends credence to the fact that substantial changes are taking place in the environment around the phenyl ring, which perhaps is affecting the wagging nature [15]. Contrary to

the bands mentioned above the bands at 1600 and 3500 show increasing absorbance with the ion fluence. The increase of the hydroxyl bond suggests an increase of the end group of macromolecules. This is consistent with the results observed by Lück [16], which indicate that under irradiation, the macromolecular weight decreases and the etchability of the irradiated PC film increases. Alkyne's formation in FTIR analysis is an important feature of the polymer degradation by SHI bombardment.

(b) Irradiated with 100 MeV Si^{8+}ions

Makrofol-KG polycarbonate, samples of 40 μm thickness were irradiated with 100 MeV Si^{8+} ion beam to the fluences of 10^{10}, $3x10^{10}$, $1x10^{11}$, $3x10^{11}$, $6x10^{11}$ and 10^{12} ions/cm^2 at 15 UD Pelletron Accelerator at Inter University Accelerator Centre, New Delhi, India. Figure 4.34 shows various absorption bands of the PC foils irradiated with of Si ions to different fluences along with those of pristine sample. The Infrared absorption peaks of functional groups of PC [17] are present in spectra. Fink and coworkers [18] used low energy Ar ions to carry out IR studies on polycarbonate whereas Varda Rajulu et al. [19] have used 60 MeV Si beam for modifying the chemical structure of polymers, like polypropylene, polyimide and polymethyl methacrylate / polystyrene blend. In the pristine foil, the absence of the absorption band around 3500 cm^{-1} shows the absence of terminal hydroxyl group indicating high molecular weight of the polymer under study. This polymer is synthesized by transestrification of diphenyl carbonate with bisphenol A with the elimination of phenol as side product.

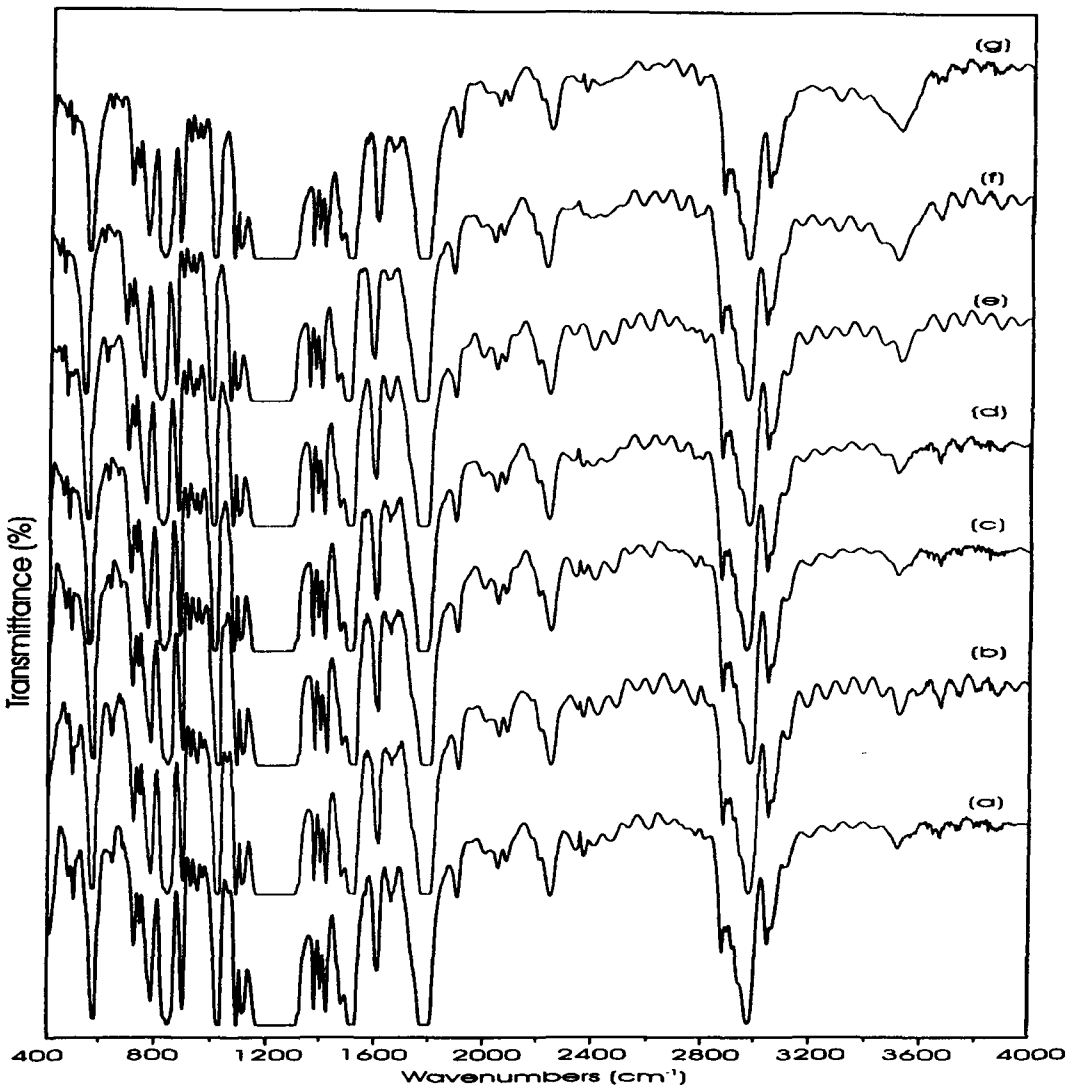

Figure 4.34: FTIR spectra of Makrofol-KG Polycarbonate irradiated with 100 MeV Si^{8+} ion beam (a) Virgin (b) $1x10^{10}$ (c) $3x10^{10}$ (d) $1x\ 10^{11}$ (e) $3x\ 10^{11}$ (f) $6x10^{11}$ and (g) $1x\ 10^{12}$ ions/cm^2.

Therefore, it is expected that the initial concentration of hydroxyl group will monotonously decrease with the increase in the chain length of the polymer. There is almost no change in the spectra up to the fluence of $1x10^{11}$. On irradiation to the fluence of $6x10^{11}$and $1x10^{12}$ ions/cm^2 the intensity of the 3500 cm^{-1} peak along with the intensity of the band at 1770 cm^{-1} representing C = O stretch changed with the ion fluence. This indicates that chain scission may be taking place at the carbonate site with probable elimination of carbon dioxide / carbon monoxide and formation of hydroxyl group. H atom required for its formation, coming perhaps from the isopropyl group, as the absorption around 2970 cm^{-1} which arises due to CH_3 symmetric stretch, decrease in intensity with increase in ion fluence. The Corroboration of chain scission can be deduced from the decrease in the intensity of absorption bands around 1160cm^{-1} attributed to C-O stretch. The decrease in intensity of absorption bands at 830 and 1018 cm^{-1} corresponds to para out of plane aromatic C-H wag of two adjacent H atoms and para in plane aromatic C-H bands. This lends credence to the fact that substantial changes are taking place in the environment around the phenyl ring which perhaps is affecting the wagging nature. Contrary to the bands mentioned above, the bands at 1600 and 3500 show increasing absorbance with the ion fluence. The increase of the hydroxyl bond suggests an increase of the end group of macromolecules. This is consistent with the results observed by Lück [16], which indicate that under irradiation, the macromolecular weight decreases and the etchability of the irradiated PC film increases. Alkyne's formation in FTIR analysis is an important feature of the polymer degradation by SHI bombardment.

4.4.2 FTIR – Spectroscopy of Makrofol-N Polycarbonate(MFN) irradiated with 100 MeV Si^{8+} ions

Makrofol-N polycarbonate samples of thickness 30 μm were irradiated with 100 MeV Si^{8+} ion beam to the fluences of 10^{10}, $3x10^{10}$, $1x10^{11}$, $3x10^{11}$, $6x10^{11}$ and 10^{12} ions/cm^2 at 15 UD Pelletron Accelerator at Inter University Accelerator Centre, New Delhi, India. Figure 4.35 shows the FTIR spectra for pristine as well as irradiated with 100 MeV Si^{8+} ions to different fluences.

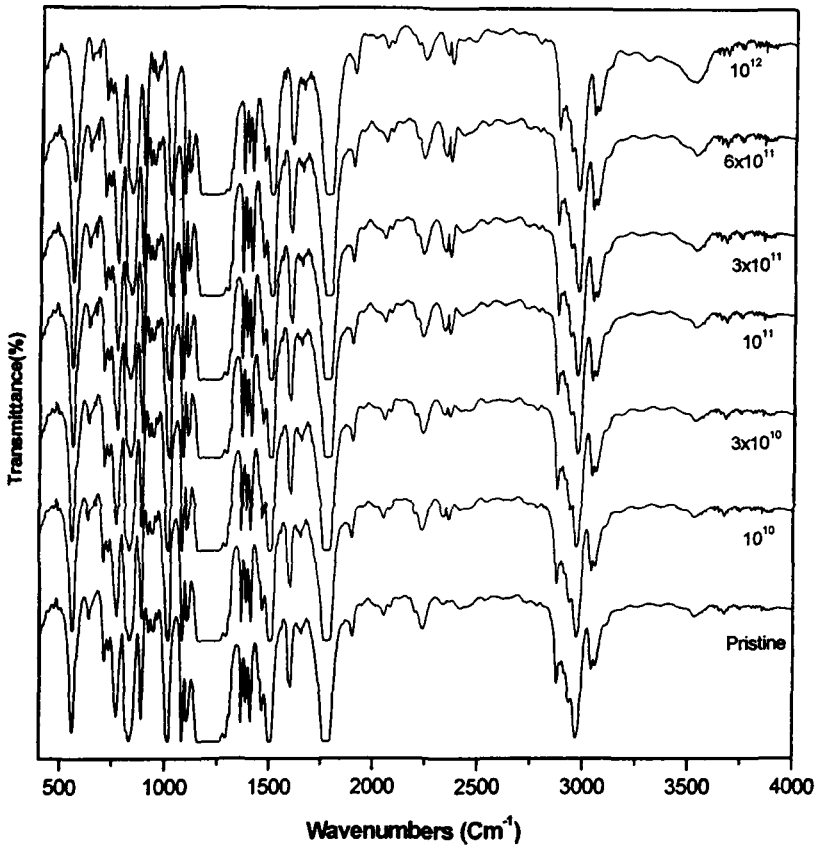

Figure 4.35: FTIR spectra of Makrofol-N (MFN) Polycarbonate irradiated with 100 MeV Si^{8+} ion beam (a) Virgin (b) $1x10^{10}$ (c) $3x10^{10}$ (d) $1x\ 10^{11}$ (e) $3x\ 10^{11}$ (f) $6x10^{11}$ and (g) $1x\ 10^{12}$ ions/cm^2.

The absorption bands as obtained from pristine spectrum are identified and given in table 4.24.

Table - 4.24

Identification of absorption bands in Makrofol-N (MFN) irradiated with 100 MeV Si^{8+} ions corresponding to their wave numbers ($1/\lambda$).

Peak	$1/\lambda$ (cm^{-1})	Identification
1	2976	CH_3 stretching vibrations
2	1772	C=O stretching vibrations
3	1500-1600 (1607)	C=C phenyl ring stretching vibrations
4	1393	Symmetric in plane bending of CH_3 group
5 6	1151 1103	Anti-symmetric stretching of C-O-C stretching of ester group
7	1015	C-O stretching vibrations
8	832	C-H para out of plane aromatic bending vibrations
9	768	Out of phase skeletal vibration of C-H deformation
10	3061	C-H stretching vibration of aromatic compounds

No change is observed in over all structure of the polymer but minor change in intensities were observed at highest fluence. On irradiation, with the increasing fluences a peak corresponding to $3525cm^{-1}$ appeared and its intensity increased with the ion fluence along with the decrease in the absorption intensity of the band at 1772 cm^{-1} representing C=O stretching. This indicates that chain scission may be taking place at the carbon dioxide/carbon monoxide and formation of hydroxyl group. It is found that the absorption bands, characteristics of all above functional groups decline, confirming their destruction by irradiation. This functional group vanishes gradually as irradiation proceeds. This might be attributed to breaking of chemical bonds and formation/emission of low molecule gases and radicals due to irradiation [20].

4.4.3 FTIR – Spectroscopy of Polytethersulphone (PES)

(a) Irradiated with 100 MeV Si^{8+} ions

Polyethersulphone (PES) samples thickness of 250 μm were irradiated with 100 MeV Si^{8+} ion beam to the fluences of $1x10^{10}$, $1x10^{11}$, 10^{12}, and $5x10^{12}$ ions/cm^2 at 15 UD Pelletron Accelerator of Inter University Accelerator Centre, New Delhi, India. Figure 4.36 shows the FTIR spectra of pristine and irradiated with 100 MeV Si^{8+} ions to the different fluences. Many results of FTIR analysis show that the main evidence of chemical degradation of the irradiated polymer by swift heavy ions are: the intensity decrease of the infrared bands, characteristics of the different chemical functional groups and creation of triple bonds.

Important absorption bands have been observed in FTIR spectra. C-H stretching vibration occurs in the range 3066-2868 cm^{-1}. Overtones and combinations bonds due to C-H out of plane deformations occurs in the region 2000-1675 cm^{-1}[21]. –C=C stretching vibrations of benzene ring occurs in the region 1428-1625 cm^{-1}. –C=C- stretching vibrations at 1625 cm^{-1} decreases on increasing the ion fluence. C-H in plane deformation vibration appears at 967 and 1011 cm^{-1}. The intensity of the bands also decreases on increasing ion fluence. In the pristine PES, SO_2 scissoring is observed at 635cm^{-1}. The deformation vibration of C-O-C occurs at ~500 cm^{-1} which also disappears at higher fluence of $5x10^{12}$ ions/cm^2. The absorption band due to the symmetric stretching of C-O-C and aryl sulphone appears in the region 1125-1400 cm^{-1}.

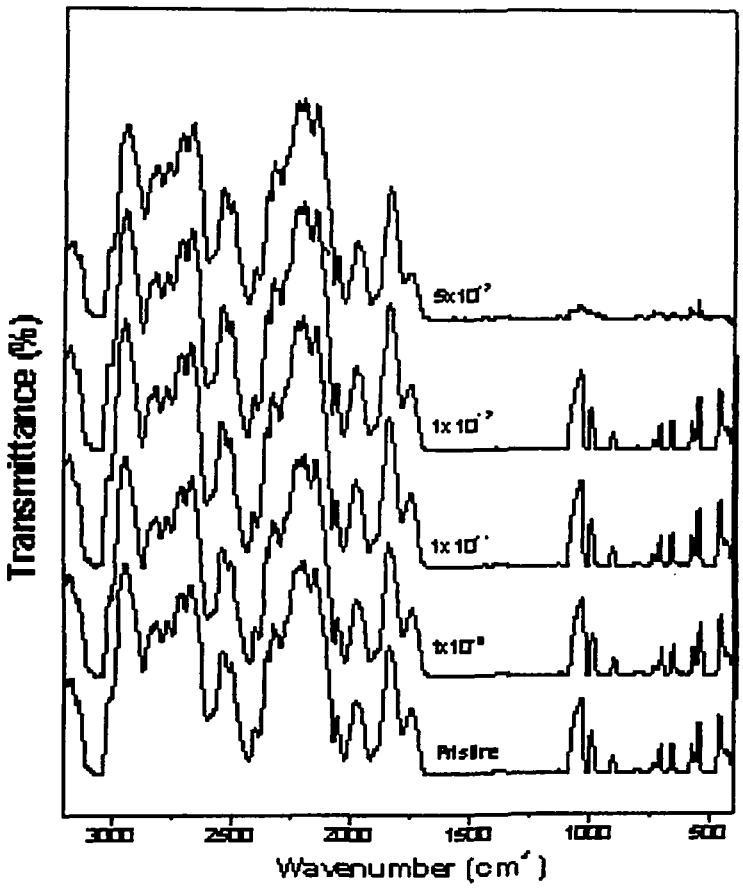

Figure 4.36: FTIR: Spectra of Polyethersulphone (PES) irradiated with 100 MeV Si^{8+} ions

(b) Irradiated with 145 MeV Ne^{6+} ions

Polyethersulphon(PES) samples were irradiated with 145 MeV Ne^{6+} ion beam to the fluences of 10^{12} and 10^{13} ions/cm^2 at Variable Energy Cyclotron Centre (VECC), Kolkata, India. Figure 4.37 shows the spectra of pristine and irradiated 145 MeV Ne^{6+} ions up to the fluences 10^{12} 1nd 10^{13} ions/cm^2 of PES samples. The absorption bands obtained from the pristine spectrum are identified as 2871-3068 cm^{-1} and at 1640-2000 cm^{-1} overtones and combination bonds due to C-H out of plane deformation. The –C=C stretching vibrations of benzene ring at 1430-1625 cm^{-1} and C-H in plane deformation vibration at 942 and 1014 cm^{-1} decreases on increasing the ion fluence.

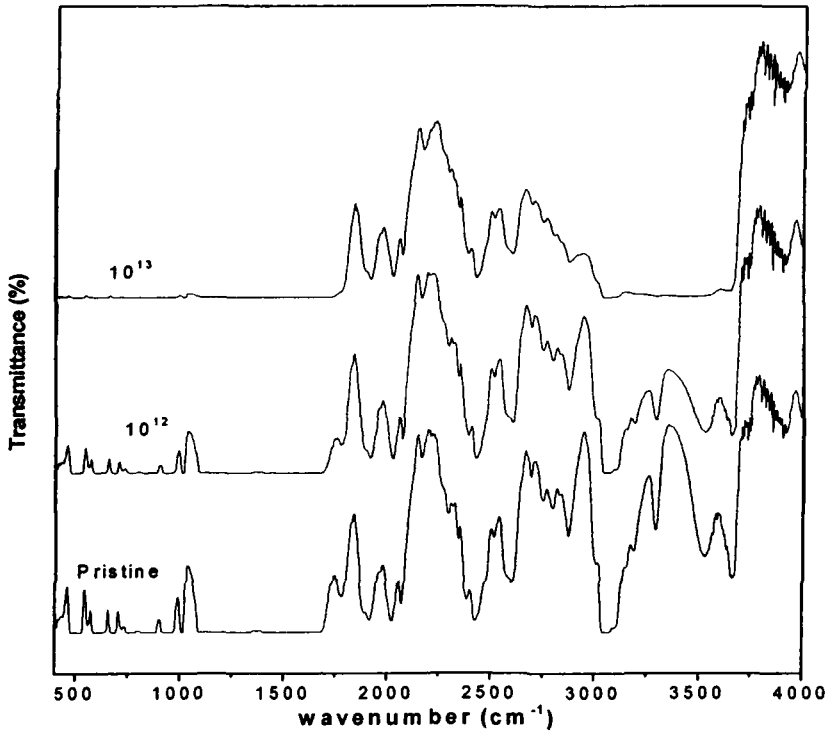

Figure 4.37: FTIR Spectra of Polyethersulphone (PES) irradiated with 145 MeV Ne^{6+} ions.

The intensity of SO_2 scissoring at 616 cm^{-1} and deformation vibration of C-O-C ~500 cm^{-1} also decreases on increasing ion fluence and finally disappear at 10^{13} ions/cm^2. Spectrum corresponding to the fluence 10^{13} ions/cm^2 indicates a very significant change in the structure of polymer. This might be due to the breakage of bonds in the structure as well as formation of unsaturated structure. Further at this fluence, the surface becomes dark brown as seen with naked eyes.

4.4.4 FTIR – Spectroscopy of Polyethylene Terephthalate (PET) irradiated with 100 MeV Si^{8+} ions.

PET samples of thickness 50 μm were irradiated with 100 MeV Si^{8+} ion beam to the fluences of 10^{10}, $3x10^{10}$,$1x10^{11}$,$3x10^{11}$and $3x10^{13}$ ions/cm^2 at 15 UD Pelletron Accelerator at Inter University Accelerator Centre, New Delhi, India

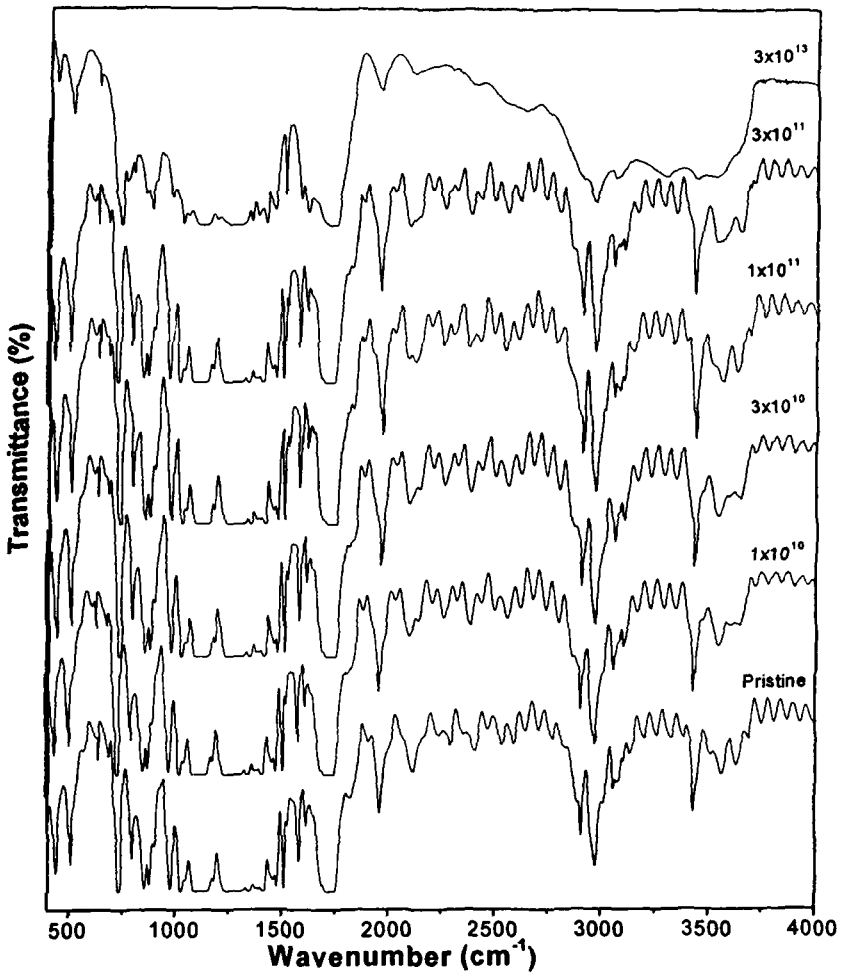

Figure 4.38: FTIR: Spectra of Polyethylene trephthalate (PET) irradiated with 100 MeV Si^{8+} ions

Figure 4.38 shows the FTIR spectra of pristine and 100 MeV Si^{8+} ions irradiated PET samples. From the FTIR spectra over all decrease in the intensity of typical bandsis observed. We observed the changes of absorption bands for the methylene group in 3914-2970, 1679-1576 and 638-511 cm^{-1} regions [22]. The changes in this spectrum in the regions 1762-1670 and 1670-1601 cm^{-1} are assigned to the bands of the carbonyl group [8-11]. Main absorption bands are obtained from the pristine spectrum, are identified and given in Table 4.25. There is no change in over all structure of the polymer up to the fluence of $3x10^{11}$ ions/cm^2 . The spectrum corresponding to $3x10^{13}$ ions/cm^2 revealed that the materials get degraded through bond breakage and significant change in the structure of the polymer can be observed.

Table - 4.25

Identification of absorption bands in PET irradiated with 100 MeV Si^{8+} ions corresponding to their wave numbers (1/λ).

Peak	1/λ (cm^{-1})	Identification
1	2965	C-H stretching of CH_2 group
2	1732	C=O stretching vibrations
3	1340	C-C stretching of phenyl ring vibrations Para substituted benzene ring
4	1017	C-O-C stretching of ester group
6	870	C-H deformation of phenyl ring, Vibration band of para substituted benzene rings
7	729	Ring deformation of phenyl ring, Bending vibration of CH_2

4.4.5 FTIR – Spectroscopy in Polytetrafluoroethylene (PTFE) irradiated with 100 MeV Si^{8+} ions

The PTFE sample of thickness 100 μm were irradiated with 100 MeV Si^{8+} ion beam to the fluences of 10^{10}, 10^{11}, 10^{12} and 10^{13} ions/cm^2 at 15 UD Pelletron Accelerator at Inter University Accelerator Centre, New Delhi, India. The FTIR spectra of pristine and irradiated to different fluences shown in figure 4.39.

It observed from the spectra, that there is no change in over all structure of polymer. The spectrum corresponding to 10^{13} ions/cm^2 showed to new extra peaks at

983cm^{-1} and 1717 cm^{-1}. Absorption bands at 983cm^{-1} is assumed to arise from $-CF_3$ side groups and band at 1717cm^{-1} is assigned to –CF=CF The absorbance peaks from 1000 cm^{-1} to 1300 cm^{-1} are contributions of the C-F stretching vibrations [23]. The structure of polymer (given in chapter 2) might be visualized as polyethylene with all its hydrogen atoms substituted by fluorine, where C-F coupling was less covalent than C-C coupling due to more electro negativity of fluorine. This made the C-C bond relatively less probable towards cleavage.

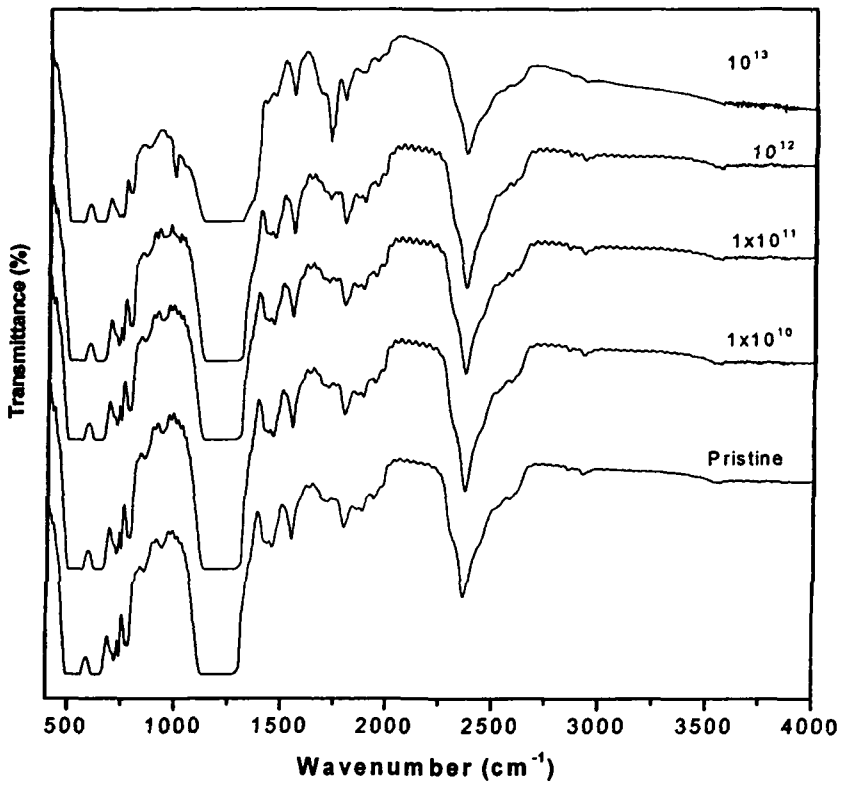

Figure 4.39 FTIR: Spectra of Polytetrafluoroethylene (PTFE) Polycarbonate irradiated with 100 MeV Si^{8+} ions

4.4.6 FTIR Spectroscopy of Polypropylene (PP) irradiated with 145 MeV Ne^{6+} ions.

The samples of Polypropylene (PP) of thickness 50 μm were irradiated with 145 MeV Ne^{6+} ions to the fluences of 10^8, 10^{10}, 10^{11}, 10^{12} and 10^{13} ions/cm^2. FTIR spectra of pristine and irradiated polypropylene shown in Figure 4.40.

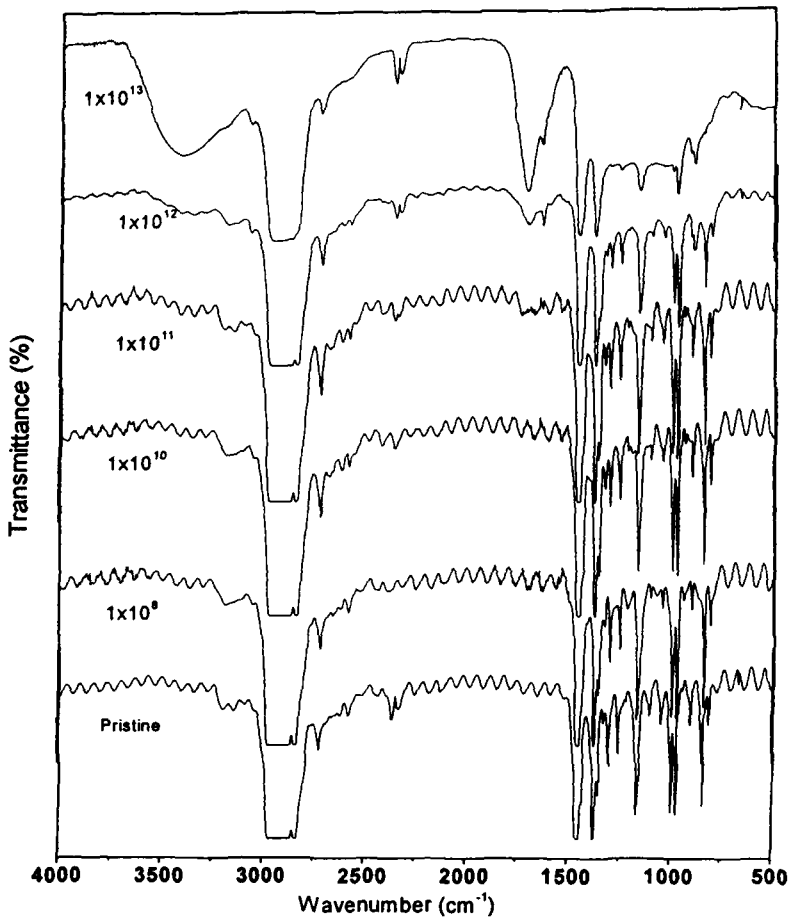

Figure 4.40: FTIR Spectra of Polypropylene (PP) irradiated with 145 MeV Ne^{6+} ions

The FTIR spectrum of the pristine PP sample reveals strong absorption in the range 2832-2973 cm^{-1} due to sp^3 C-H stretching of CH_3 & CH_2 along with strong bands near 1454 and 1381 cm^{-1} due to bending absorption of CH_2 and CH_3 groups, respectively, which are characteristics of polypropylene.

Spectra of Irradiated polypropylene show that with the increase in ion fluence, there appears a new band at 3424 cm^{-1} which is attributed to O-H stretching. Presence of a band at 1701 cm^{-1} indicates the presence of C=O bonds. The presence of these bands suggests the reaction of the polymer with atmospheric moisture on swift heavy ion irradiation leading to formation of O-H and C-H groups. Another importance observation is thr growth of a band near 3312cm^{-1} on irradiation, which is characteristic of sp-hybridized C-H stretching mode of alkyne group. An additional sp^2 hybridized C-H stretching occurs at 3072cm^{-1}, along with =C-H out of plane bending at 915 cm^{-1} and

C=C stretch at 1639 cm^{-1} suggests the formation of unsaturations in the polymer chains (double bonds). Some indication of it can be found in the presence of absorbance in 3500cm^{-1} region. The 996 cm^{-1} peak disappears on high fluence irradiation. 1164 cm^{-1} band is also affected showing that 3/1 helix structure gets somewhat affected by Ne^{6+} irradiation though H^{+} irradiation does not do so [24].

4.4.7 FTIR – Spectroscopy in Polyvinylidene fluoride (PVDF) irradiated with 145 MeV Ne^{6+} ions.

Polvinylidene fluoride (PVDF) is a semi crystalline polymer with piezoelectric properties and chemical inertness. PVDF samples of thickness 80 μm were irradiated with 145 MeV Ne^{6+} ions to the fluences of 10^{10}, 10^{11}, 10^{12} and 10^{13} ions/cm^2. Figure 4.421shows the FTIR spectra of Polyvinylidene fluoride (PVDF) samples; pristine and irradiated with 145 MeV Ne^{6+} ions to different fluences.

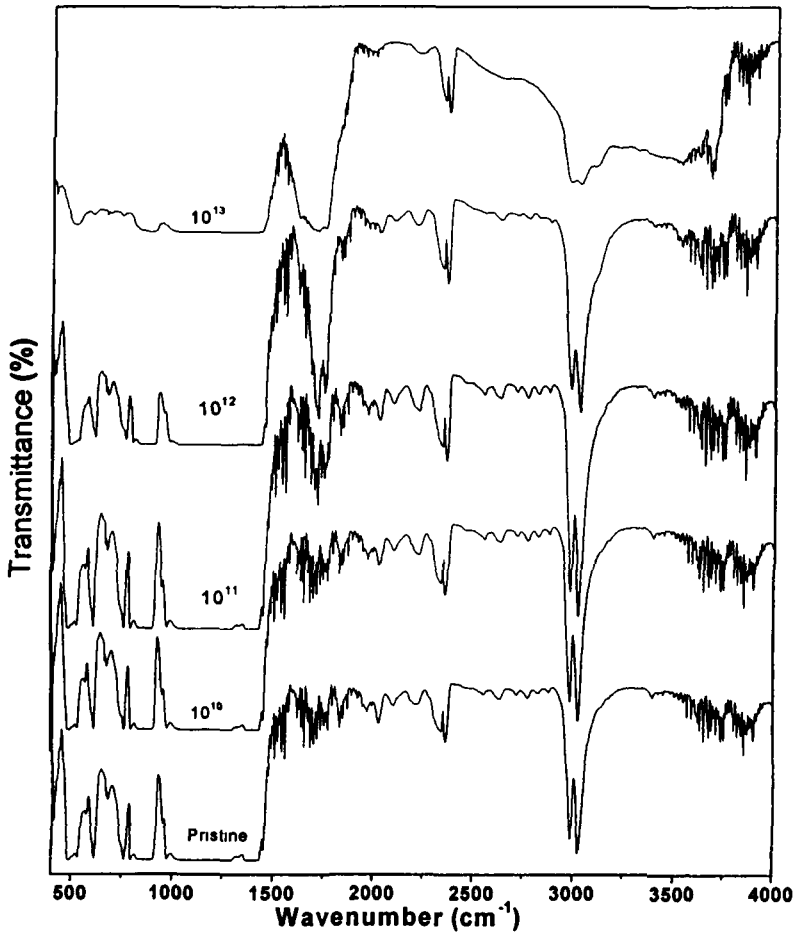

Figure 4.41: FTIR: Spectra of (PVDF) irradiated with 145 MeV Ne^{6+} ions.

The ion energy deposition breaks the carbon – hydrogen and carbon –fluorine chemical bonds, produces a high rate of molecular emission of hydrogen and hydrofluoric acid and transforms the residual material in a carbon amorphous film [25]. The symmetric and asymmetric stretching vibration of the CH_2 group in the pristine samples are located, respectively at 2980 cm^{-1}(ν_s CH_2) and 3021cm^{-1} ($\nu_a CH_2$). All the chemical groups with a CH bond have valence vibration located in this region. Figure 4.41 shows the modification of the 3800-2400 cm^{-1} region as the ion fluence increases and the decrease of the intensity of the PVDF CH_2 bands. Significant changes are observed in the region 800-400 cm^{-1}.The bands observed at 512, 613 and 760 cm^{-1} are characteristic of the crystalline α phase [26,27]. Figure shows almost total disappearance of these crystalline bands as the ion fluence increases for Ne^{6+} ions radiation. From these spectra it can be concluded that amorphization is completed at 10^{13} ions/cm^2. The bands appear at 1700-1710 cm^{-1} by C=C stretching vibrations of –CF=CH-CF_2- [28-31] at the fluence 10^{12} & 10^{13} ions/cm^2 . This defect results from the evolving of HF. Conjugated double bonds are responsible for the broadening of the band 1700-1710 cm^{-1} band on its lower frequency side. UV absorption measurements demonstrate their creation after radiati on with ionizing radiation [32,33]. Main chain scission occurs as seen by the existence of alkyne groups.

4.4.9: FTIR – Spectroscopy in Low Density Polyethylene (LDPE) irradiated with 50 MeV Li^{3+} ions.

Low density polyethylene samples of thickness 50 μm were irradiated with 50 Mev Li^{3+} ions to the fluences of $5x10^{10}$, 10^{11}, 10^{12} and 10^{13} ions/cm^2. Figure 4.42 shows the FT-IR spectra of pristine and irradiated LDPE to different ion fluences. It reveals strong band 2838-2972 cm^{-1}, due to sp^3 C-H stretching of methylene group both symmetric and anti symmetric along with strong bands near 1466 and 1376 cm^{-1} due to bending absorption of methylene and methyl groups respectively. The prominent band present at 722cm^{-1}, is known as long chain band and it indicates the rocking vibrational mode of long chain of methylene groups.

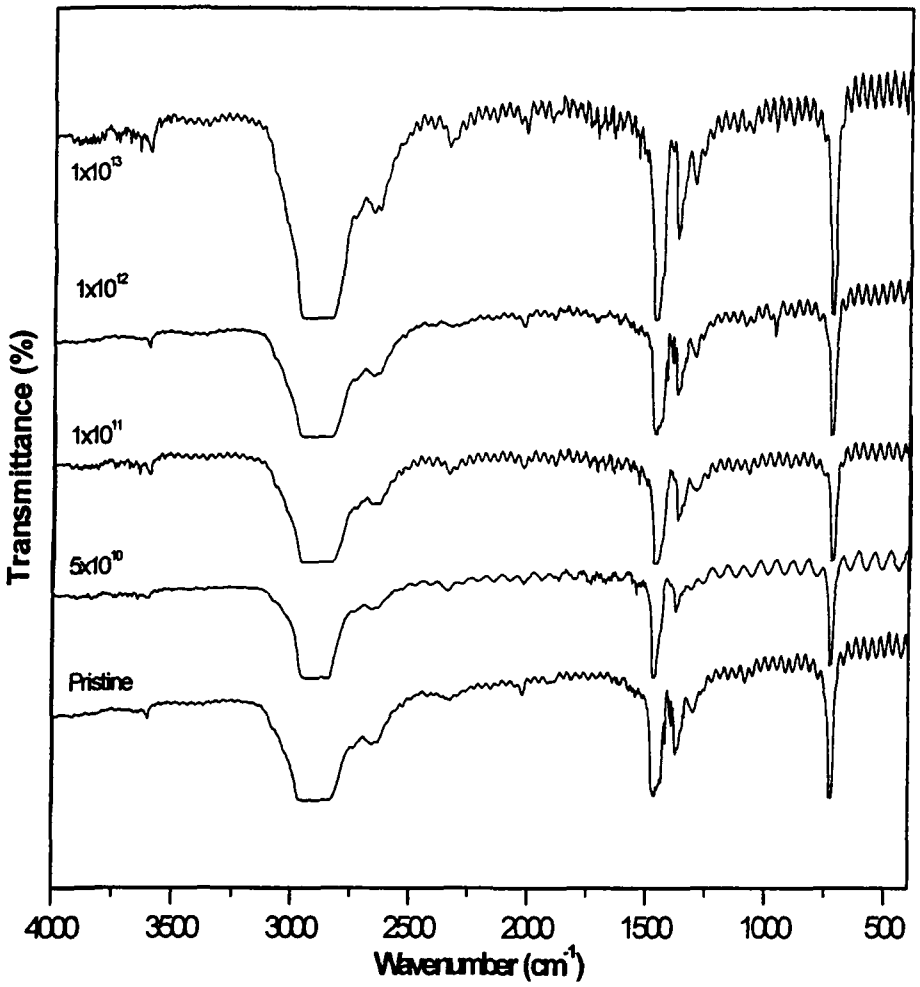

Figure 4.42: FTIR: Spectra of LDPE pristine and irradiated with 50MeV Li^{3+} ions

The irradiation induces modifications in the polymer and a number of new chemical bonds are produced. The formation of double bonds is represented by sp^2 C-H stretching peak (=C-H) at 3086 cm^{-1}, along with absorption band for mono substituted alkenes (1640 cm^{-1}), di-, tri-,tetra-substituted alkenes (1652-1671 cm^{-1}). Mono substituted double bonds (vinyl) gives two strong bands at 988cm^{-1} and 911 cm^{-1} for alkyl-substituted alkenes. The presence of band at 962 cm^{-1} at the fluence 10^{12} and 10^{13} ions/cm^2 suggests the presence of transvinyledene as in chain unsaturation. Increase in the intensity of the absorption band associated with vinyl group ($-CH_2=CH_2$) on irradiation suggests the increase of conjugation. An increase in the number of conjugate polymer chains (C=C bond) will result in the increase of free electrons in appropriate activation process. This might have been responsible for decreasing optical energy gap in the irradiated polymers

as observed in UV-Vis. Analysis. Optical density increases due to the formation of cross-links and conjugated double and triple bonds by irradiation [33]. The presence of triple bonds is suggested by C-H stretching at 3311cm^{-1} and bending absorption at 630cm^{-1}.

The above change may be due to bond cleavage and bond reconstruction. The predominant radiation effect in polyethylene is cross-linking. Significant in-chain defects created are trans-vinylene unsaturations and conjugated double bonds (diene). Chain scission occurs with the formation of methyl end groups, Vinyl end groups formation was also detected. Similar effects were observed earlier in swift heavy ion irradiated polyethylene [34].

4.4.9 FTIR Spectroscopy in PMMA pristine and irradiated with 145 MeV Ne^{6+} ions.

Parts of each sample were irradiated by 145 MeV Ne^{6+} ion beam at Variable Energy Cyclotron Centre (VECC), Kolkata, India to the fluences of 10^{10}, 10^{11}, 10^{12}, 10^{13} ions/cm^2. The nature of chemical modification can be studied through characterization of the vibration modes, determined by infrared spectroscopy. Fig. 4.43 (a-e) shows the IR spectra of pristine and irradiated PMMA. The symmetric and asymmetric stretching, scissions or bending and wagging of CH_3 and CH_2 group frequencies were observed in the pristine as well as in all the irradiated PMMA samples. The peak positions in the pristine and the irradiated PMMA samples remained almost constant indicating that the $\frac{3}{1}$ helical structure of the polymer was not destroyed after ion irradiation. Fig. 2 indicates the general decrease in intensity of the peaks of the irradiated samples as compared to pristine sample. However, the increase in absorbance at ~ 1300 cm^{-1} after ion irradiation at the fluence of 10^{12} ions/cm^2 can be attributed in part by the formation of CH_2 groups via radiation induced cross linking mechanism [24, 35) The increase in this particular band indicates the increase in crystallinity of PMMA [36].

An absorption band can be seen as a broad peak in the range of 3000-2800 cm^{-1}. This can be identified as C-H stretching vibrations. The band around 3000 cm^{-1} corresponding to CH_2 does not show any major change. The peak around 1720 cm^{-1}, corresponding to

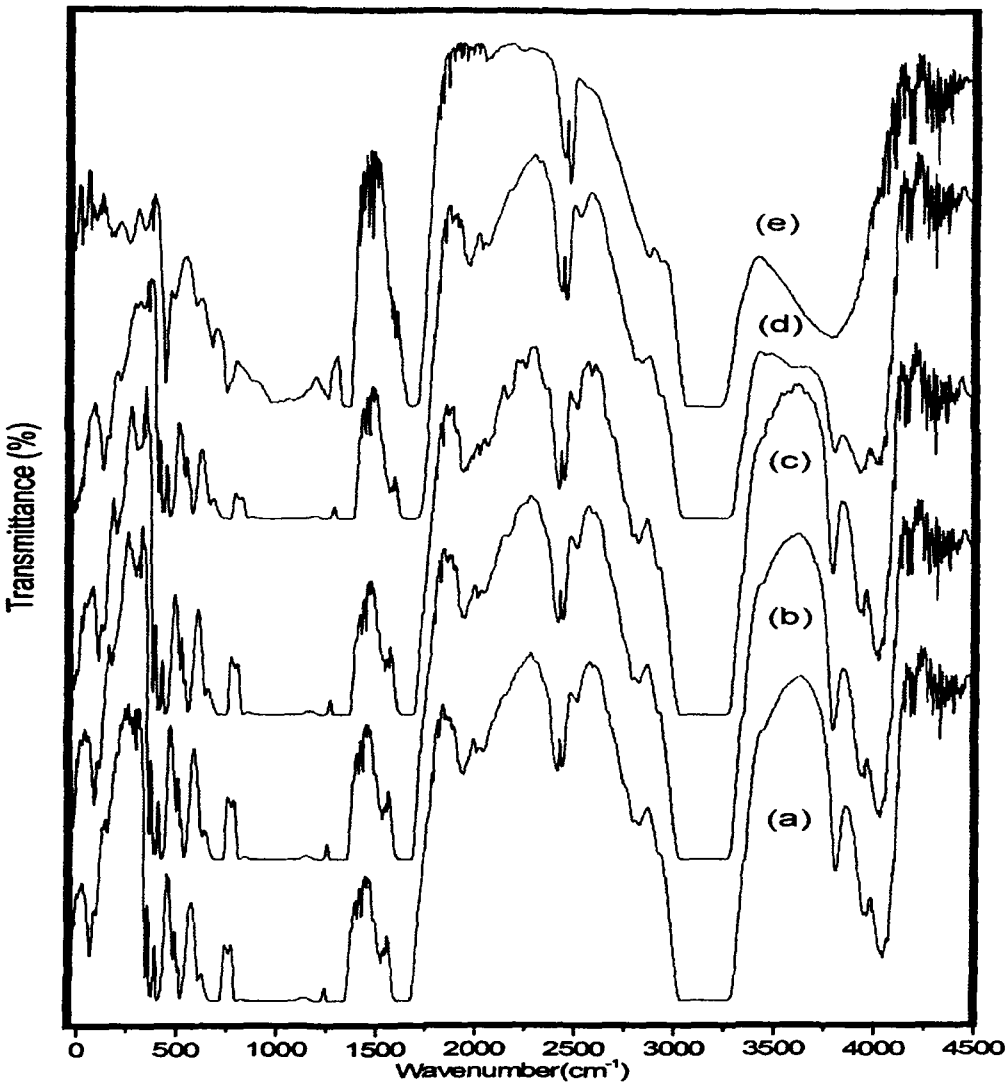

Figure4.43: FTIR spectra of PMMA polymer (a) Virgin; and irradiated 145 MeV Ne^{6+} ions (b) 10^{10} (c) 10^{11} (d) 10^{12} (e) 10^{13} ions/cm^2

C = O vibrations in the pristine sample appears to be slightly shifted towards lower values in the irradiated samples. A regular trend in the variation of the peak positions is not observed with the increase of the fluence.

Irradiation of PMMA polymer did change the absorption intensity of the C – H vibration peak and the broad bump slowly forms more pronounced peaks with increasing fluence. In the 3200 – 3600 cm^{-1} region the formation of O- H bonds can be observed as a function of irradiation fluence. Indication for the formation of -C = C- double bonds are given by rise of vibrations at 1640 cm^{-1}.

References

[1] R. John Dyer, Applications of absorption spectroscopy of organic compounds (NJ: Prentice-Hall Inc.)(1994).

[2] D. Kanjilal, S. Chopra, M. M. Narayanan, I.S. iyer, V.Jha, R. Joshi, S. K. Datta, Nucl. Instr. and Meth. A 238 (1993)97.

[3] A. K. Srivastava, H. S. Virk, J. Polym. Mater. **17** (2000)325.

[4] L. S. Farenzena, R.M. Papaléo, A. Hallén, Araújo de., M. A., R.P. Livi, B.U.R. Sundqvist, Nucl. Instr. Meth. **B105** (1995) 134.

[5] R. Mishra, S.P. Tripathy, D. Sinha, K.K. Dwivedi, S. Ghosh, D.T. Khating, M. Muller, D. Fink, Nucl. Instr. and Meth.B.,**168** (2000)59.

[6] J. Tauc, R. Grigorovici, A. Vancu, Physica Status Solidi, **15(2)** (1996) 627.

[7] J. Robertson, E.P. O'Reilly, Phys. Rev.,B **35** (1987) 2946.

[8] D.Fink, W.H.Chung, R. Klett, A. Schmoldt, J. Cardoso, R. Mntiel, H. Vazquez, L. Wang, F. Hosoi, H. Omichi,P. Goppelt-Langer, Radiat. Eff. Defe. Solid. **133**(1995)193.

[9] D. Sinha, T. Phukan, S. P. Tripathy, R. Mishra, K. K. Dwievedi, Radiat. Meas. 34(2001)109.

[10] A. Saha, V. Chakaraborty, S. N. Chintalpudi, Nucl. Instr. and Meth. B 168 (2000)245.

[11] D. Fink, R. Klett, L.T. Chaddertan, J. Cardosa, R. Montiel, M.H. Vazquez, A. Karanovich, Nucl. Instr. and Meth., B 111,303(1996).

[12] H. S. Virk, P. S. Chandi, A. K. Srivastava, Nucl. Instr. and Meth., B 183 (2001) 329.

[13] T. Phukan, D. Kanjilal, T. D. Goswami, H. L. Das, Radiat. Meas., 36,611(2003).

[14] R. Kumar, U. De, R. Prasad, Nucl. Instr. and Meth. B 248 (2006)279.

[15] A. Srivastava, T.V. Singh, S. Mule, C. R. Rajan, S. Ponrathnam, Nucl. Instr. and Meth.B 192(2002) 402.

[16] H. B. Lück, Nucl. Instr. and Meth.B 200(1982)517.

[17] C. Gagnadre, J. L. Decossas, J. C. Vareille, Nucl. Instr. and Meth. B 73(1993) 48.

[18] D. Fink, M. Muller, L. T. Chadderton, P. H. annington, R. G. Ellimam, D. C. McDonaldt. Radiat. Eff. Def. Solids, 132, (1994)313.

[19] A. Varada Rajulu, R. Lakshminarayana Reddy, D.K. Avasthi, K. Ashokan, Radiat. Eff. & Defects Solids, 152 (2000) 57.

[20] A. Biswas, S. Lotha, D. Fink, J.P. Singh, D.K. Avasthi, B.K. Yadav, S. K Bose, D.K. Khating, Nucl. Instr. and Meth. B 159(1999) 40.

[21] G. Socrates, Infrared Characteristics Group Frequencies, John Wiley & Sons, New York, 1980.

[22] R.M Silverstein, G. C. Bassler, T.C. Morill, Spectrometric Identification of Organic Compounds, Wiley, New York, 1990, Chapter 3.

[23] N. L Alpert, W.E. Keiser, and H. A. Szymanski IR –Theory and Practice of Infrared Spectroscopy. A Plenum/Rosetta edition, Published by Plenum Publishing Corporation, New York. (1970) 184-300

[24] R. Mishra, S.P. Tripathy, K. K. Dwivedi, D. T. Khating, S. Ghosh, M. Muller and D. Fink, Rdiat. Measure, 33(2001)845

[25] L. Calcagno, G. Compagini and G. Foti, Nucl. Instr. and meth. B65(1990)338.

[26] M. Kobayashi, K. Tashiro and M. Tadokoro, Macromolecules,8 (1975)158.

[27] F. J. Boerio and J.L. Koenig, J. Polym. Sci. A-2,9(1971)1517.

[28] M. Hagiwara, G. Ellinghorst, and D.O. Hummel, Makromol, Chem.,178 (1977)2913.

[29] A. M. Guzman, J. D. Carlson, J. E. Bares and P.P. Pronko, Nucl. Instr. Meth.B7/8 (1985)468.

[30] G. Socrates , Infrared Characteristics Group Frequencies, John Wiley & Sons, New York, 1975.

[31] J. Brandrup and E.H. Immergut, Polymer Handbook, Interscience Publishers, New York, 1975.

[32] K. Makuuchi, M. Asano, and T. Abe, J. Polym. Sci., Polym. Chem. Ed., A14, (1976)617.

[33] A. Fina , A. Le Moël, J. P. Duraud, M.T.Valin, C.Le Gressus, E. Balanzat, J.M. Ramillon, and C. Darnez, Nucl. Instr. and Meth., B42(1989)69.

[34] E. Balanzat , N. Betz, S. Bouffard, Nucl. Instr. and Meth. B 105(1-4) (1995)46.

[35] Alpert, N.L., Keiser, W.E., Szyma nsky, H.A., 1970. IR-Theory and practice of Infrared Spectroscopy, A Plenum?Rosetta edition. Plenum Publishing Corporation, New York, 184-300.

[36] Heinen, W.,1959. Infrared determination of the crystallinity of polypropelene. J. Polym. Sci. 38, 545-547.

Chapter-V

Chapter V

STRUCTURAL AND ELECTRICAL MODIFICATIONS IN POLYMERS

5.1 Introduction

In this chapter, the experimental results in terms of the structural and electrical modifications by swift heavy ion irradiation. Interaction of the Swift Heavy Ions with a polymer may results in cross-linking of the molecular chains, chain scission, destruction and degradation of the macromolecules with the simultaneous formation of the molecules of smaller chain lengths and change in number and nature of bonds. A large number of polymer's properties depend on its molecular structure and super molecular structure. The changes in the properties of a polymer subjected to irradiation results from the changes in its structure. These changes lead to modifications in the the structural, electrical, surface roughness and thermal properties of polymers affecting its glass transition temperature, melting temperature, crystallinity etc.[70].

5.2 Characterization of modification in structural properties through XRD Analyses.

X-ray diffraction (XRD) provides a fast and reliable tool for routine mineral identification. Experiments have shown that the polymeric samples studied here are widely used materials falling in the class of the majority of polymers materials consisting of crystalline and amorphous regions in different proportions. Polymers can be modified by ion irradiation. XRD has been performed with the following limited objectives and no attempt has been made to determine the complete structure of the polymeric samples. Thus any modification of the polymer structure upon irradiation is reflected in its diffraction pattern. In this section, results of X-ray diffraction analysis of pristine and ion irradiated polymers have been presented. XRD measurements for the polymer films were carried out at Inter-University Accelerator Centre (IUAC), New Delhi using D8 Advanced Bruker diffractometer with Cu-K_α radiation (λ=1.541838Å) at room temperature by taking 0.020 step size. The cathode was maintained at 30 kV. Diffraction patterns were recorded in the range $20^\circ \leq 2\theta \leq 80^\circ$.

The condition for diffraction of a beam of X-rays from a crystal is governed by the Bragg equation:

$$2d\sin(\theta) = n\lambda$$

where, d is the spacing between layers of atoms, λ is the wavelength of X-rays used and θ is the angle of incidence of the X-rays.

The crystallite size in pristine and irradiated polymers was determined by Scherrer formula [equation].

$$\text{Crystallite size (L)} = \frac{K\lambda}{d \times \cos\theta} \qquad (5.1)$$

where K is the shape factor of the average crystallite (0.9) usually equal to 1, λ is the wavelength (1.54 Å) for Cu $K\alpha_1$, d is full width at half maxima (FWHM) and θ is the peak position in radian.

5.3 Results and Discussion of XRD Analyses

5.2.1 Polymetylemethacrylate (PMMA)

The polymer PMMA is a complex polymer widely used in ion beam lithography and in semiconductor industry. This polymer falls in the category of polymer materials that consist mainly of amorphous regions with some crystalline region in different proportions. Heavy ion irradiation was carried out under a vacuum of ~ 10^{-6} torr by 145 MeV Ne^{6+} ions from Variable Energy Cyclotron Centre, Kolkata, India using a low beam current (~15 nA) to the ion fluences of 10^{10}, 10^{11}, 10^{12}, 10^{13} ions/cm^2. XRD measurements have been carried out with the limited objectives of the study of variation of intensity of the XRD peaks with ion fluence to observe loss of crystallinity with irradiation and no attempt has been made to determine the complete structure of the polymeric sample. Figure 5.1 presents the XRD pattern for pristine PMMA film and also for those irradiated with Ne ions to various fluences.

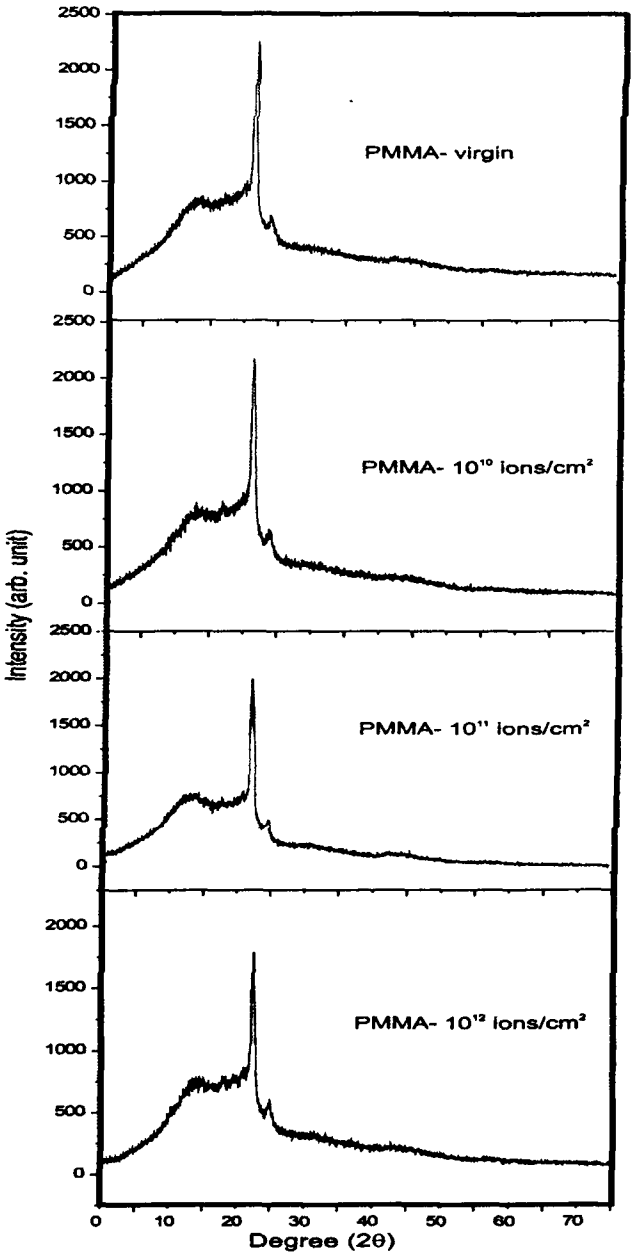

Figure 5.1: X-ray diffraction pattern of PMMA polymer irradiated with Ne ions

The diffraction patterns show a sharp peak at 21.66° and few low intensity peaks, indicating the crystallinity. The diffraction pattern of pristine sample shows partial crystallinity. The most intense peak occurs at $2\theta = 21.66°$. The irradiated samples also exhibit identical diffraction pattern. Diffraction pattern of virgin PMMA sample also shows a broad peak around 14° indicating that polymer is mainly amorphous in nature. A sharp peak at 21.66° with lattice spacing d = 4.10 indicating the crystallinity. Although the intensity of this diffraction peak decreases with ion fluence, no significant shift of the peak position is observed. This implies that the lattice parameters do not change significantly. Similar pattern has been observed by Zhu et al. (2002) in PET irradiated with 35 MeV/u Ar ions, by Liu et al.(2000) in PET irradiated with high energy heavy ions (Ar, Kr and Xe) and our earlier study (Kumar et al., 2006) on PES irradiated with 70 MeV C-ions.

The average crystal size, more commonly known as particle size L, is related to b, the full width at half maximum (FWHM) of the peak (in radian) by the well known Scherer formula $L = \lambda / (b. \cos\theta)$, where λ is the wavelength of the X-ray used. Calculations show that L is 97.69 Å for the virgin or un-irradiated polymer and 93.38 Å for irradiation to 10^{13} ions/cm^2. This implies that average crystallinty size L is reduced by about 4.41% on irradiation to a fluence of 10^{13} ions/cm^2.

5.3.2 Low Density Polyethylene (LDPE)

The diffraction pattern of the pristine LDPE sample is presented in Figure 5.2. Three peaks are observed but very pronounced peak is observed at the position $2\theta = 21.398°$ which indicate that the polymer is semi crystalline in nature. Figure 5.2 shows diffraction patterns of 95 MeV O^{6+} ion irradiated LDPE.

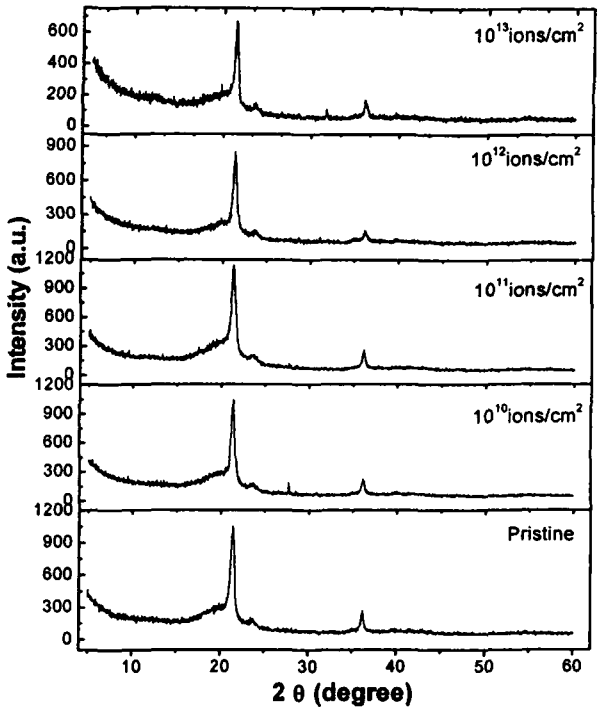

Figure 5.2: XRD spectra of LDPE films: pristine and irradiated with 95 MeV O^{6+} ions

It has been observed that in very pronounced peak, there is decrease in peak intensity and increase in the full width half maximum (FWHM) upon ion irradiation. This observation suggests that ion irradiation has lead to increase in disorder of the polymer. According to Hosemann's theory of Para crystals [174], semi-crystalline polymers point out two types of distortions as compared to ideal, well-ordered crystalline cell. First class distortions are exhibited by crystalline cell, in which long-range order exists and structural units show statistical fluctuations in their position as compared to those of ideal crystalline cell, resulting in increase in the peak intensity in X-ray diffractograms. The crystallites size of pristine and irradiated LDPE calculated by Scherer equation [176] are reported in Table- 5.1.

Table-5.1

FWHM and crystallite size of pristine and 95 MeV Ne^{6+} ion irradiated LDPE samples

Samples Fluence (ions/cm^2)	2θ (degree)	FWHM (b)	Crystallite Size (Å)
Pristine	21.398	0.41108	196.66
10^{10} ions/cm^2	21.405	0.53307	151.59
10^{11} ions/cm^2	21.401	0.55777	144.94
10^{12} ions/cm^2	21.410	0.57940	139.53
10^{13} ions/cm^2	21.339	0.64781	124.78

The crystallite size in pristine LDPE found to be 196.66 Å. As the ion fluence increases, crystallite size decreases and at the highest fluence of 10^{13} ions/cm^2, it decreases by nearly 36.55%.

5.3.3 Polyvinylidene fluoride (PVDF)

Thin films of commercial PVDF film (procured from Good Fellow, Cambridge, England) samples were irradiated with 95 MeV O^{6+} ion beam at 15 UD Pelletron Accelerator at Inter University Accelerator Centre (IUAC), New Delhi, India, to the fluences of 10^{10}, 10^{11}, and 10^{12} ions/cm^2.

Figure 5.3 shows the XRD pattern for Polyvinylidene fluoride(PVDF) samples, pristine and irradiated with 95 MeV O^{6+} ion beam. The diffraction pattern of PVDF pristine polymer indicates that the polymer is amorphous in nature and shows broad peak at 2θ= 19.134° for the pristine sample. It increased and shifted to 2θ = 19.392° after irradiation to the highest fluence of 10^{12} ions/cm^2. However, the change in intensity and the shift in angular position can be defined by change in lattice spacing [23]. The broadening of peak suggests an evolution of the polymer towards a more disordered state and also a change in crystallite size on irradiation by the ions. The average crystal size, more commonly known as particle size L.

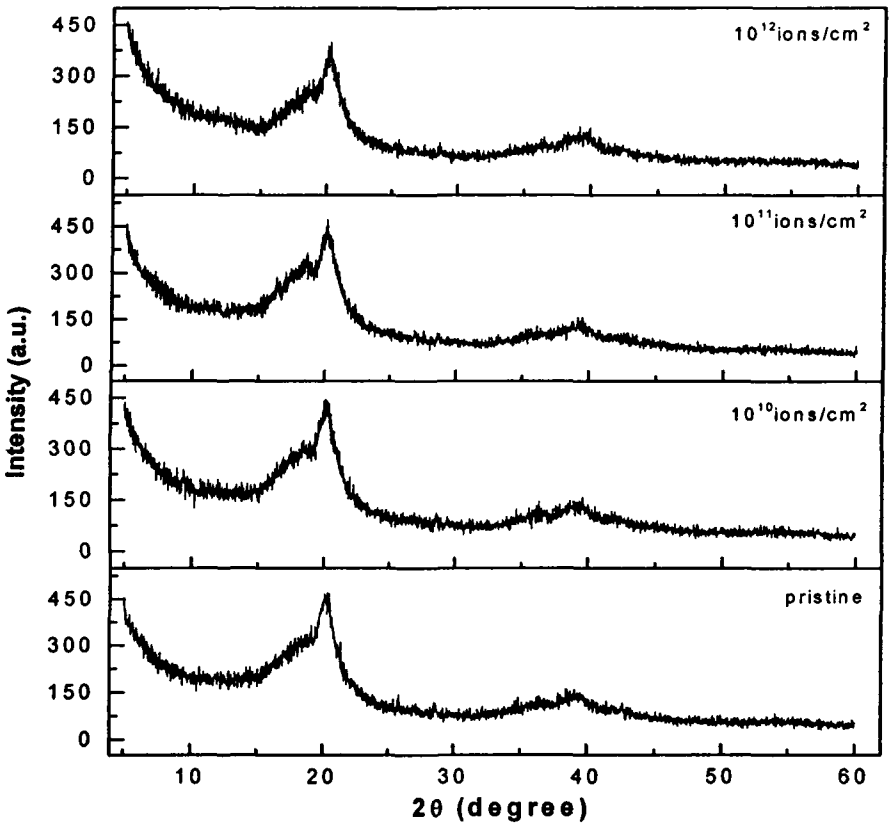

Figure 5.3: XRD spectra of pristine and irradiated PVDF with 95 MeV O^{6+} ions

The crystallites size of pristine and irradiated PVDF calculated by Scherer equation [176] are reported in table 5.2.

Table-5.2

FWHM and crystallite size of pristine and 95 MeV Ne^{6+} ion irradiated PVDF samples

Samples Fluence (ions/cm^2)	**2θ (degree)**	**FWHM (b)**	**Crystallite Size (Å)**
Pristine	19.134	3.458	23.295
10^{10} ions/cm^2	19.150	3.917	20.573
10^{11} ions/cm^2	19.357	4.742	16.994
10^{12} ions/cm^2	19.392	5.900	13.657

The crystallite size for pristine PVDF sample is found to be 23.295Å. As the ion fluence increases, crystallite size decreases to 13.657 Å at the highest fluence of 10^{12} ions/cm^2, by nearly 41.37%.

5.3.4 Makrofol-KG Polycarbonate

Makrofol-KG samples were irradiated with 100 MeV Si^{8+} ion beam to the fluences of 10^{11}, 10^{12} and 10^{13} ions/cm^2. Figure 5.4 shows the diffraction pattern of the pristine and irradiated samples of Makrofol-KG.

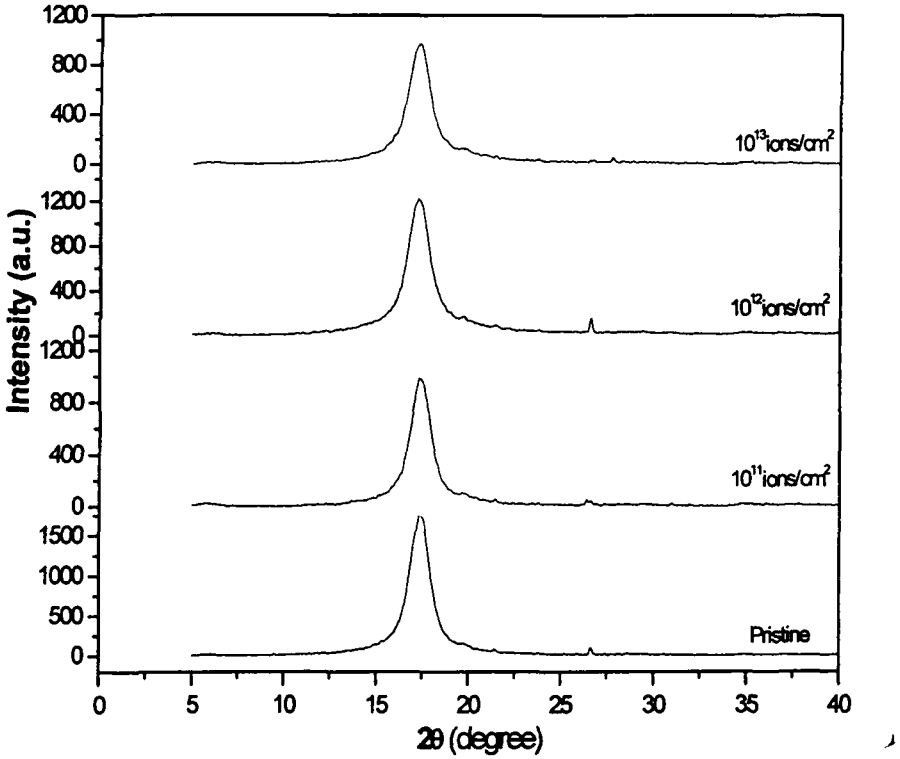

Figure 5.2: XRD spectra of pristine and irradiated Makrofol-KG with 95 MeV O^{6+} ions

The crystallite size corresponding to the diffraction peaks of the pristine and irradiated polymer samples were calculated using Scherer equation and the results are presented in Table -5.3. Peak at the position 2θ = 17.378° indicates the semi-crystalline nature of the polymer. After irradiation the peak shifted to 2θ= 17.303° at the highest fluence of 10^{13} ions/cm^2. The crystallite size for pristine Makrofol-KG is found to be 64.648Å.

Table-5.3

FWHM and crystallite size of pristine and 100 MeV Si^{8+} ion irradiated PC

Samples Fluence (ions/cm^2)	2θ (degree)	FWHM (b)	Crystallite Size (Å)
Pristine	17.378	1.240	64.808
10^{10} ions/cm^2	17.368	1.243	64.647
10^{11} ions/cm^2	17.254	1.260	63.766
10^{12} ions/cm^2	17.303	1.294	62.094

As the ion fluence increases, crystallite size decreases to 62.094 Å at the highest fluence of 10^{13} ions/cm^2, a reduction of nearly 3.95%.

5.3.5 Polypropylene (PP)

The diffraction patterns of the pristine and irradiated with 100 MeV Si^{8+} ion beam polypropylene samples to the fluences of 10^{10}, 10^{11}, $3x10^{11}$ and 10^{12} ions/cm^2 are presented in Figures 5.5 (a & b). Five peaks observed in the diffraction pattern of the pristine and irradiated samples clearly indicate that polypropylene is semicrystalline in nature. There occurs a decrease in the peak intensity and increase in the full width half maximum (FWHM) as the fluence increases. The crystallite size corresponding to five peaks of the pristine and irradiated polymer samples were calculated using Scherer equation (5.1) and the results are reported in Table 5.4

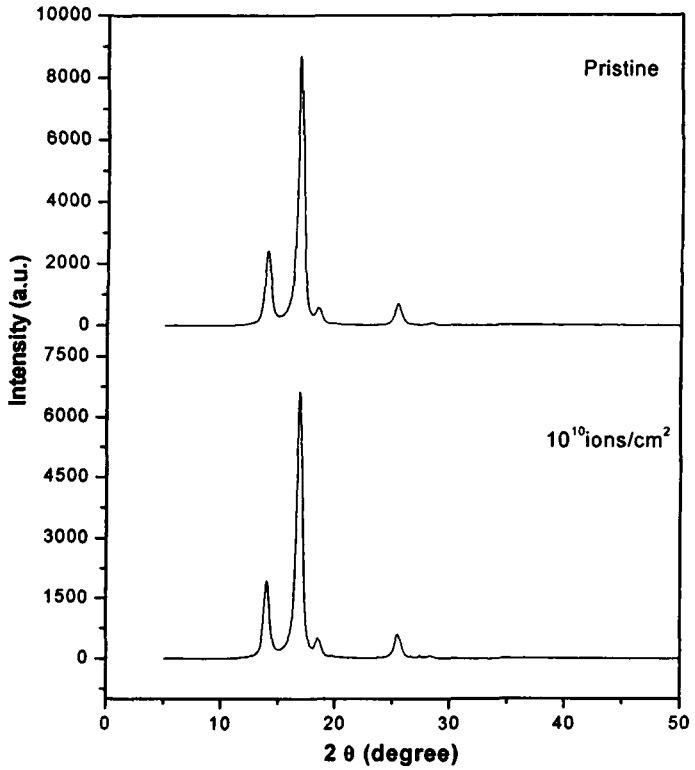

Figure 5.5(a): XRD spectra of pristine and irradiated PP with 100 MeV Si^{8+} ions

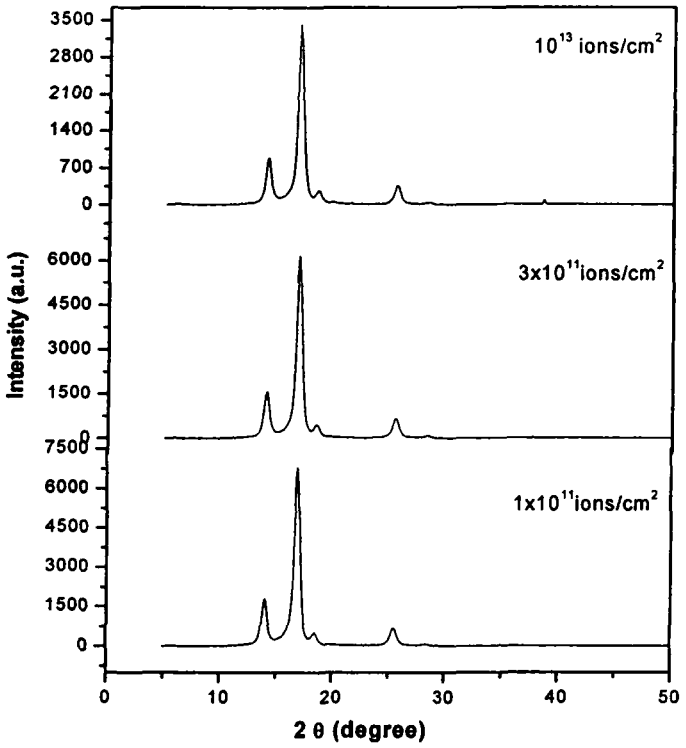

Figure 5.5(b): XRD spectra of pristine and irradiated PP with 100 MeV Si^{8+} ions

Table-5.4

FWHM and crystallite size of pristine and 100 MeV Si^{8+} ion irradiated

Samples	Peak position	2θ (degree)	FWHM (b)	Crystallite Size (Å)
Pristine	1	14.079	0.496	161.620
	2	16.937	0.578	144.156
	3	18.540	0.478	168.641
	4	25.580	0.632	127.548
	5	28.437	0.579	141.751
10^{10} ions/cm^2	1	14.010	0.527	153.097
	2	16.937	0.564	142.623
	3	18.540	0.509	158.369
	4	25.580	0.629	129.707
	5	28.437	0.537	152.838
10^{11} ions/cm^2	1	14.079	0.532	150.683
	2	16.937	0.571	141.174
	3	18.540	0.467	172.613
	4	25.647	0.654	124.762
	5	28.365	0.608	134.962
$3x10^{11}$ ions/cm^2	1	14.079	0.542	147.88
	2	16.937	0.553	145.459
	3	18.538	0.507	158.995
	4	25.577	0.615	132.659
	5	28.365	0.558	147.055
10^{12} ions/cm^2	1	14.079	0.558	143.647
	2	16.798	0.571	140.845
	3	18.470	0.519	154.879
	4	25.440	0.631	129.256
	5	28.437	0.517	158.750

5.2.6 Polytetrafluoroethylene (PTFE)

The effect of heavy ion irradiation on high crystalline PTFE (at room temperature) has to be smaller than an amorphous PTFE (in the melt). Additionally further qualitative changes will be expected by irradiation of molten PTFE. Lappan et al [27] have studied the behavior of PTFE on such special irradiation conditions. In the present study PTFE samples were irradiated with 100 MeV Si^{8+} ion beam to the fluences of 10^{10},10^{11},10^{12}, and 10^{13} ions/cm^2 at 15 UD Pelletron Accelerator at Inter University Accelerator Centre, New Delhi, India. The structure of the pristine and irradiated to different fluences PTFE samples were analyzed by X-ray diffraction studies. Diffracion spectra are shown in Figure 5.6 and various parameters assigned with the peaks are presented in Table - 5.5.

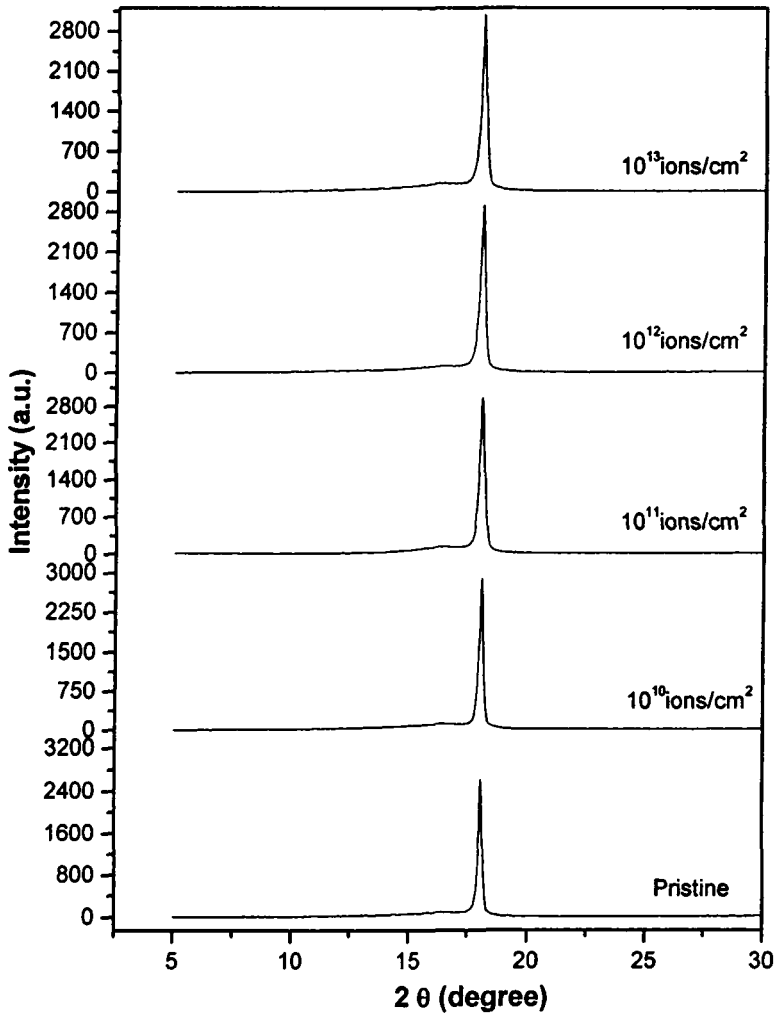

Figure 5.6: XRD spectra of pristine and irradiated PTFE with 100 MeV Si^{8+} ions

Table-5.5

FWHM and crystallite size of pristine and 100 MeVSi^{8+} ion irradiated PTFE

Samples Fluence (ions/cm^2)	2θ (degree)	FWHM (b)	Crystallite Size (Å)
Pristine	18.052	0.224	359.612
10^{10} ions/cm^2	18.061	0.226	356.430
10^{11} ions/cm^2	18.062	0.236	341.327
10^{12} ions/cm^2	18.041	0.251	320.928
10^{13} ions/cm^2	18.044	0.256	314.660

The results showed that the intensity of the main peak at 2θ =18.052° for the pristine sample shows a minor reduction in intensity and shifting to 2θ =18.044 for the sample irradiated to highest fluence of 10^{13} ions/cm^2. Crystallite size of pristine PTFE is found to be 359.612 Å. As the ion fluence increases, crystallite size decreases to 314.660 Å at the highest fluence of 10^{13} ions/cm^2, a reduction of nearly 12.5%.

5. 2. 7 Polyaniline graphite (PANI-GRP)

Polyaniline graphite (PANI-GRP) composite samples were irradiated with 50 MeV Li^{3+} ion beam to the fluences of 10^{11}, 10^{12}, 10^{13}, and $2x10^{13}$ ions/cm^2 at 15 UD Pelletron Accelerator at Inter University Accelerator Centre, New Delhi, India. The XRD spectra of pristine and irradiated samples are shown in Figure 5.7 and various parameters assigned with the peaks are presented in Table - 5.6.

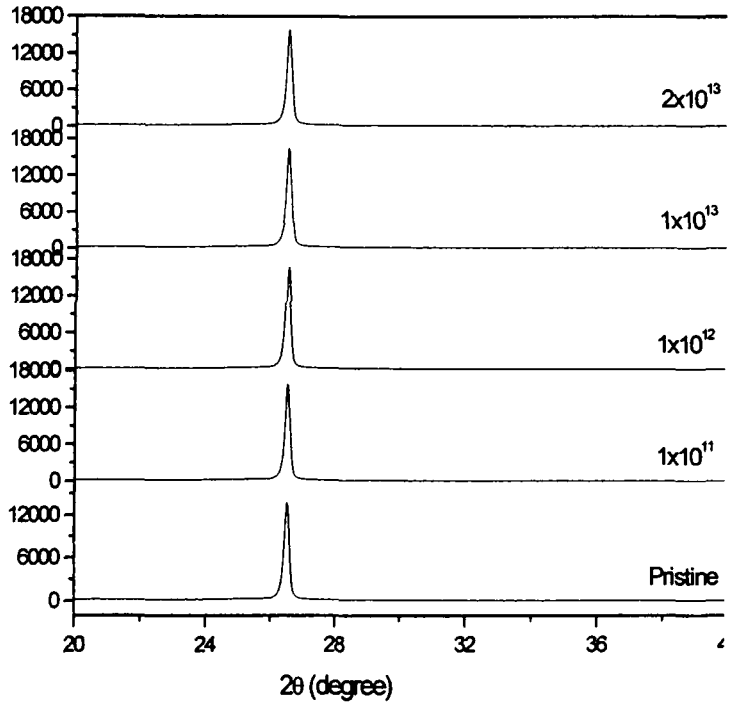

Figure 5.7: XRD spectra of pristine and irradiated (PANI-Grp) with 50 MeV Li^{3+} ions.

Table-5.6

FWHM and crystallite size of pristine and 50 MeVLi^{3+} ion irradiated

Samples Fluence (ions/cm^2)	**2θ (degree)**	**FWHM (b)**	**Crystallite Size L(Å)**
Pristine	26.526	0.1679	485.875
10^{11} ions/cm^2	26.523	0.1736	469.925
10^{12} ions/cm^2	26.522	0.1786	456.289
10^{13} ions/cm^2	26.524	0.1790	455.755
$2x10^{13}$ ions/cm^2	26.521	0.1806	451.967

The crystallite size of pristine Polyaniline graphite composite is found to be 485.875 Å. As the ion fluence increases, crystallite size decreases to 451.967 Å at the highest fluence of $2x10^{13}$ ions/cm^2. It decreases by nearly 6.98%.

5.4 Characterization of modification in Electrical Properties through Dielectric Measurements.

The best dielectric materials are those which contain a minimum of charge carriers and potential charge carriers and which may be formed by splitting of covalent, atomic or molecular bonds under the influence of the energetic ions. The dielectric response of material provides information about the orientational translational adjustment of mobile charges present in the dielectric medium in response to an applied electric field. The most important property of dielectric materials is the ability to be polarized under the action of the field. The dielectric loss behavior of polymer films is very important because of their possible applications for insulation, isolation and passivation in micro-electronic circuits (Dang et al 2002). In general polymers are insulators and commonly used in insulation of electric wires. However, certain classes of polymers have been discovered and used as semiconductor and capacitors with unusual electrical properties. The dielectric polarization may be judged in terms of the dielectric constant and the dissipation factor (loss angle or tanδ).

The dielectric constant of the samples was determined by measuring the capacitance of the samples. Simultaneously the loss factor was also measured. Capacitance (C_p) and dielectric loss (tan δ) measurements were carried out using a parallel plate configuration of electrodes on both sides of PC film using a LCR meter (Hewlett-Packard 4284) in the frequency range of 1-1000 kHz at room temperature. The measured values of capacitance then have been converted into the dielectric constant(ε') by using the formula

$$\varepsilon' = Cd/\varepsilon_o A$$

where d is the thickness of polymer film, A is the area of the electrode plates and ε_o is the permittivity of free space. AC conductivity, $\sigma_{a.c}$ is calculated by the relation given below

$$\sigma_{a.c} = 2\pi f \tan\delta . \varepsilon_o . \varepsilon_r \qquad (2.13)$$

where f is the frequency and tanδ. Is the dielectric loss.

5.5 Results and Discussion of Dielectric Constant measurements

5.4.1 Makrofol-KG Polycarbonate

40 μm thick Makrofol-KG bisphenol-A PC films, manufactured by a casting process were obtained from Bayer AG, Lever Kussen, Germany. The Makrofol-KG PC films (1.5 x 1.5 cm^2) were mounted on a vertical vacuum shield ladder and irradiated in General Purpose Scattering Chamber (GPSC) by 100 MeV Si^{8+} ion beam from 15 UD Pelletron accelerator at Inter University Accelerator Centre (IUAC), New Delhi to the fluences of 1 x 10^{10}, 3 x 10^{10}, 1 x 10^{11}, 3 x 10^{11}, 6 x 10^{11} and 1 x 10^{12} ions/cm^2. 145 Mev Ne^{6+} ion beam irradiation was carried out at Variable Energy Cyclotron Centre,(VECC), Kolkata to the fluences of 10^{10}, 10^{11}, 10^{12} and 10^{13} ions/cm^2. The ion beam was defocused using a magnetic scanning system so that the film may be uniformly irradiated. The beam current was kept below (10 nA) to suppress thermal decomposition. To expose the whole target area uniformly the beam was scanned in the X-Y plane. The ranges, as estimated by SRIM - 2003 of the incident ions was more than the thickness of the PC film.

Figures 5.8 and 5.9 illustrate the dielectric response of 100 MeV Si^{8+} ion and 145 MeV Ne^{+6} ion irradiated Makrofol –KG PC samples respectively along with that of pristine samples.

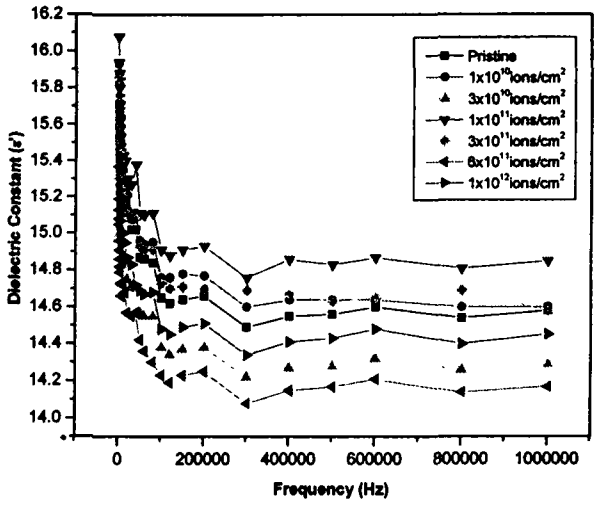

Figure 5.8: Frequency variation of dielectric constant for Si^{8+} (100 MeV) ion beam irradiated Makrofol-KG Polycarbonate

Significant changes have been observed in dielectric response of Makrofol -KG PC after irradiation. It is evident from the Figure 5.8 and 5.9 that dielectric constant increases with the fluence and at a particular fluence does not show any change in the frequency range of 300-1000 kHz for Si ion irradiated samples and in the range of 200-1000 KHz for Ne ion irradiated sample for all the ion fluences studied.

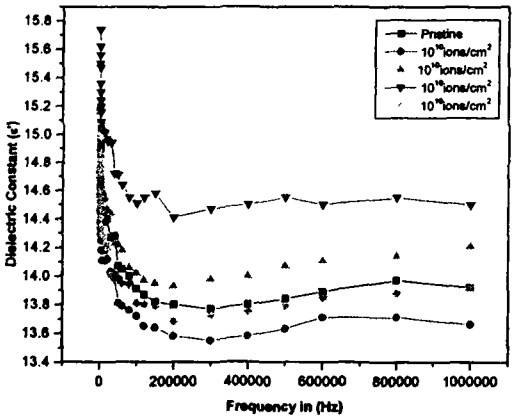

Figure 5.9: Frequency variation of dielectric constant for Ne^{6+} (145 MeV) ion beam irradiated Makrofol-KG Polycarbonate

The motion of free charge carriers may be assumed constant at these frequencies which indicate the uniform motion of defects responsible for ion migration through the polymer. Ion migration in solids is assumed to be dependent on the hoping rate i.e the jumping frequency of the ions which has a unique value for an ion. Therefore, the nearly constant value of dielectric constant may be due to the presence of some ionic species in excess than others.

At lower frequencies a rapidly decreasing trend is observed. In this region the slow migration of charge carriers may be assumed to be the cause for the decreasing of the dielectric constant. With the increase in frequency the charge carrier migrations through the dielectric get entrapped in the defect site and induce opposite charge in its vicinity.

The variation of dielectric loss presented in Figures 5.10 and 5.11 shows random behavior. It increases up to about 70 KHz for both the ions followed by a decrease up to 200 KHz.

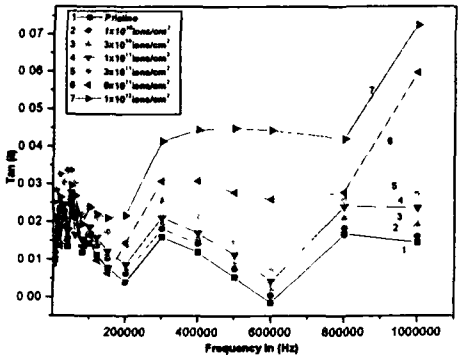

Figure 5.10: Frequency variation of dielectric loss for Si^{8+} (100 MeV) ion beam irradiated and Pristine Makrofol-KG polycarbonate.

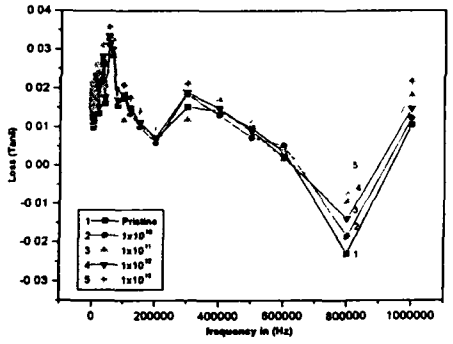

Figure 5.11 Frequency variation of dielectric loss for Ne^{6+} (145 MeV) ion beam irradiated and Pristine Makrofol-KG polycarbonate.

The variations with ion fluences are visible only at higher frequencies in the range 600-1000 KHz for Si^{8+} ion and 200-1000 KHz for Ne^{6+} ions. This indicates a small change in the dissipation factor of the polymer with ion irradiation although the change depends on the ion. It may thus be concluded that irradiation has changed the dielectric constant with out affecting the dielectric losses only slightly in the polymer. The change in dielectric loss tangents in Makrofol-KG are found to be higher for Ne^{6+} as compared to Si^{8+} ion.

5.5.2 Makrofol-N (Polycarbonate) Makrofol-N, films of thickness 30 μm. PC films(1.5x1.5cm^2) were irradiated by 100 MeV Si^{8+} ion beam to the fluences of 1 x 10^{10}, 3 x 10^{10}, 1 x 10^{11}, 3 x 10^{11}, 6 x 10^{11} and 1 x 10^{12} ions/cm^2. Dielectric constant of pristine and ion irradiated samples was determined by measuring the capacitance of the samples. Simultaneously the loss factor was also measured.

Figure 5.12 presents the dielectric response of 100 MeV Si^{8+} ion irradiated Makrofol–N PC samples along with that of pristine samples.

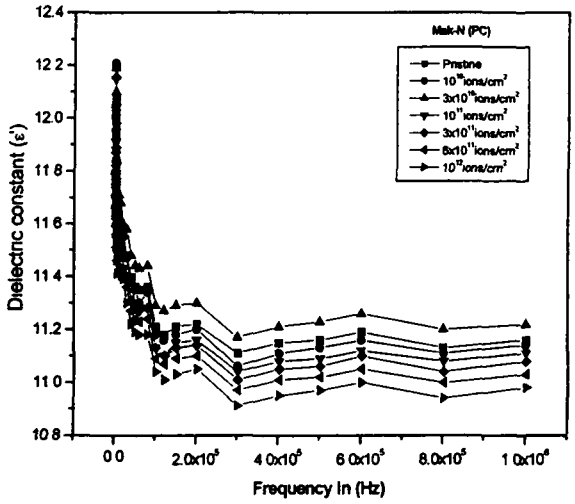

Figure 5.12: Frequency variation of dielectric constant for 100 MeV Si^{8+} ion beam irradiated Makrofol-N (PC).

On irradiation dielectric response of Makrofol-N PC changes significantly. The effect of irradiation is almost the same as observed in Makrofol KG PC. It is evident that dielectric constant increases with the fluence and at a particular fluence it does not show any change with the frequency in the frequency range of 300-1000 kHz. This happens at all the ion fluences. The motion of free charge carriers may be assumed constant at these frequencies which indicate the uniform motion of defects responsible for ion migration through the polymer. Ion migration in solids is assumed to be dependent on the hoping rate i.e. the jumping frequency of the ions which has a unique value for an ion. Therefore, the nearly constant value of dielectric constant may be due to the presence of some ionic species in excess amount. At lower frequencies a rapidly decreasing trend is observed. In this region the slow migration of charge carriers may be assumed to be the cause of

observed decrease in dielectric constant. With increase in frequency the charge carriers, migrating through the dielectric get entrapped in the defect site and induce opposite charge in its vicinity. The variation of dielectric loss presented in Figure5.13 shows random behavior. It increases up to about 70 kHz followed by a decrease up to 200 kHz.

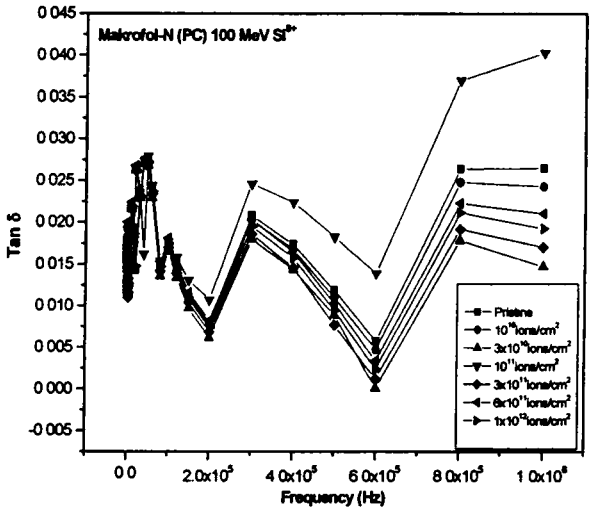

Figure5.13: Frequency variation of dielectric loss for Si^{8+} (100 MeV) ion beam irradiated and Pristine Makrofol-N polycarbonate.

The variations with ion fluences are visible only at higher frequencies in the range 600-1000 kHz. This indicates a small change in the dissipation factor of the polymer with ion irradiation. It may thus be concluded that irradiation changes the dielectric constant without affecting the dielectric losses, only slightly in the polymer.

5.4.3 Polyethersulphone (PES)

Polyethersulphone (PES) is finding extensive use in electronics due to its excellent dielectric property. There are few measurements which report the effects of low and highions on PES(Wang et al 1991, Bridwell et al,1991). Polyethersulphone (PES) , samples were irradiated with 100 MeV Si^{8+} ion beam to the fluences of $1x10^{10}$,$1x10^{11}$,10^{12}, and $5x10^{12}$ ions/cm^2 at 15 UD Pelletron Accelerator at Inter University Accelerator Centre, New Delhi, INDIA and with 145 MeV Ne^{6+} ion beam to the fluences of 10^{12} and 10^{13} ions/cm^2 at Variable Energy Cyclotron Centre (VECC), Kolkata. A.C. conductivity measurements were performed for pristine and irradiated PES

samples for different fluences and different ions. Figures 5.14 and 5.15 show the A. C. conductivity vs. log frequency plot for pristine and irradiated PES for 100 MeV Si^{8+} ions and 145 MeV Ne^{6+} ions.

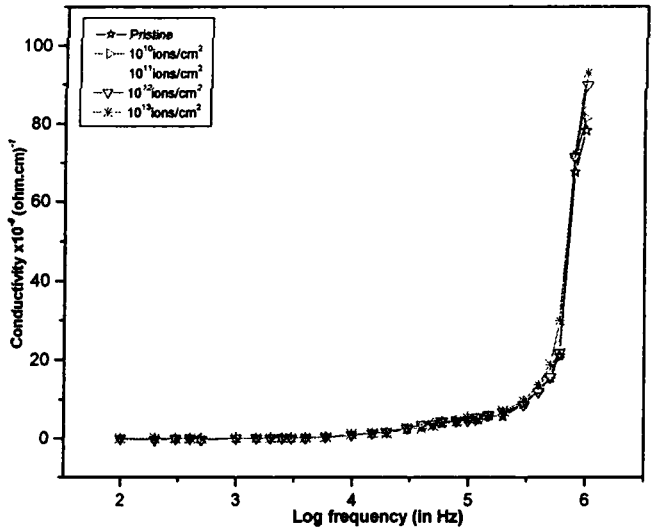

Figure 5.14: AC conductivity versus log frequency plot for pristine and 100 MeV Si^{8+} ions irradiated Polyethersulphone (PES)

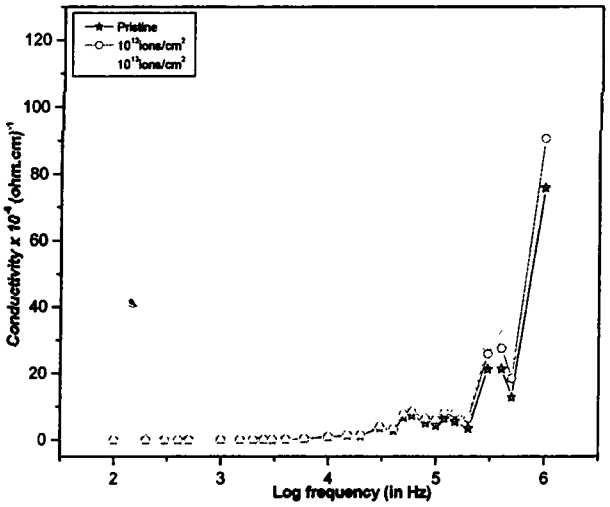

Figure 5.15: AC conductivity versus log frequency plot for pristine and 145 MeV Ne^{6+} ions irradiated Polytethersulphone (PES).

It is observed that a sharp increase in conductivity in pristine as well as irradiated samples. It is also observed that conductivity shows more increase as fluence increases for Ne^{6+} ions in comparison to Si^{8+} ions. Due to irradiation the increase in conductivity at

a given frequency may be attributed to scissoring of polymer chains, resulting in an increase of free radicals, unsaturation, etc. An a. c. field of sufficiently high frequency may cause a net polarization which is out of phase with field. This results in a. c. conductivity and it appears at frequencies greater than that at which traps are filled or emptied (Jonscher 1977; singh et al2004b)

Figures 5.16 and 5.17 show the plot of dielectric constant (ε') versus log frequency at room temperature for pristine and irradiated PES samples.

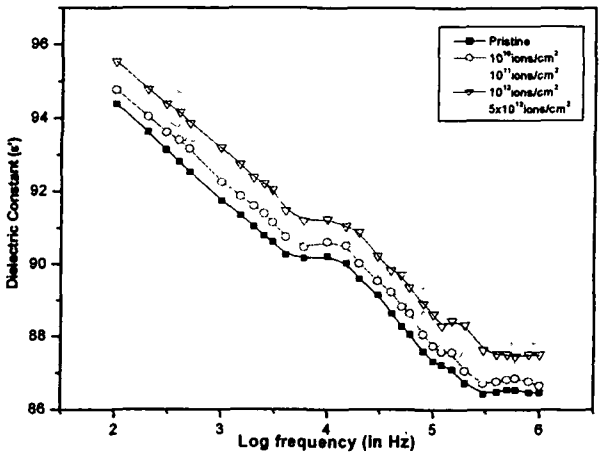

Figure 5.16: Plot of dielectric constant versus log frequency for pristine and irradiated with 100 MeV Si^{8+} ions of Polyethersulphone (PES)

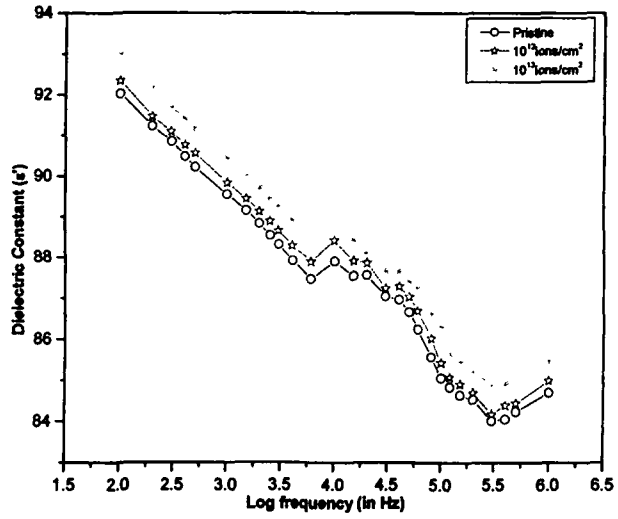

Figure 5.17: Plot of dielectric constant versus log frequency for pristine and 145 MeV Ne^{6+} ions irradiated Polytethersulphone (PES).

At lower frequencies a rapidly decreasing trend in dielectric constant is observed. In this region the slow migration of charge carriers may be assumed as the cause for the decreasing of the dielectric constant. The dielectric constant decreases at higher frequencies and increases with fluence. As the frequency increases the charge carriers migrate through the dielectric and get trapped against a defect site and induce an opposite charge in its vicinity. At these frequencies for both the ions , the polarization of trapped and bound charges can not take place and hence the dielectric constant decreases. Figures 5.18 and 5.19 shows a plot of tanδ (dissipation factor) versus log frequency for pristine and 100 MeV Si^{8+} ions and 145 MeV Ne^{6+} ions irradiated samples.

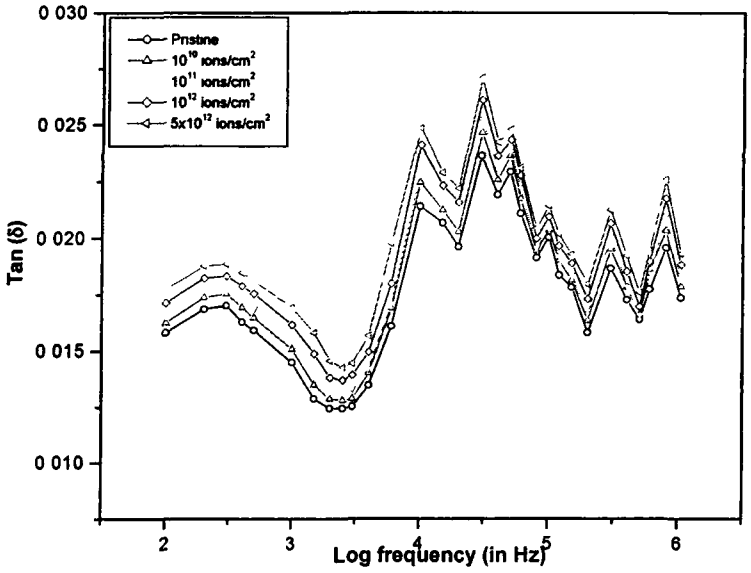

Figure 5.18: Variation of tanδ with log frequency for pristine and 100 MeV Si^{8+} ions irradiated Polyethersulphone (PES).

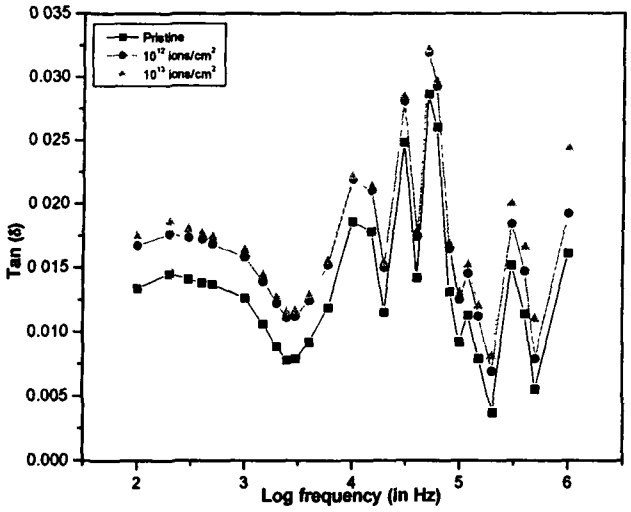

Figure 5.19: Variation of tanδ with log frequency for pristine and 145 MeV Ne^{6+} irradiated Polytethersulphone (PES)

It is observed from the figures that the loss factor increases moderately with fluence for both the ions. The increase in loss factor with fluence may be due to scissoring of polymer chains, resulting in an increase in of free radicals..

5.4.4 Polypropylene (PP)

Polypropylene film samples were irradiated with 100 MeV Si^{8+} ions to the fluences of 1×10^{10}, 3×10^{10}, 1×10^{11}, 3×10^{11}, 6×10^{11} and 1×10^{12} ions/cm^2 and with 145 MeV Ne^{6+} ions to the fluences of 10^8, 10^{10}, 10^{11}, 10^{12} and 10^{13}. Figures 5.20 and 5.21 show the dependence of conductivity of PP films on log frequency at room temperature for pristine and irradiated samples for both the ions.

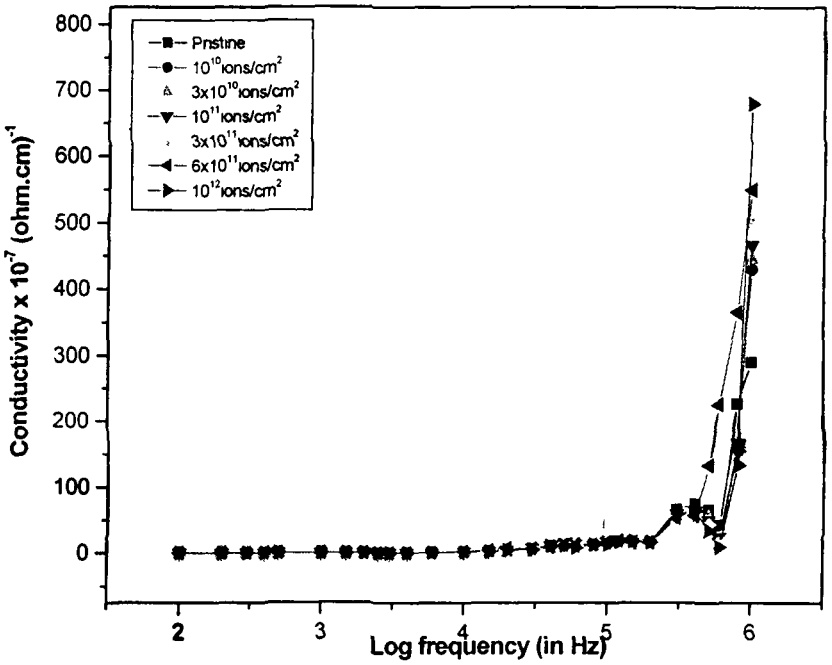

Figure 5.20: AC conductivity versus log frequency plot for pristine and 100 MeV Si^{8+} ions irradiated Polypropylene (PP)

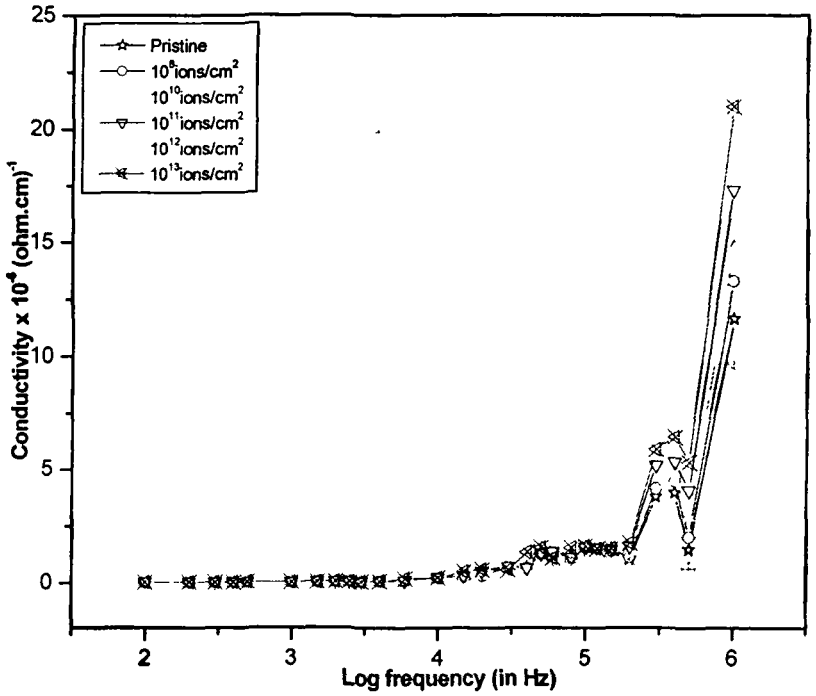

Figure 5.21: AC conductivity versus log frequency plot for pristine and 145 MeV Ne^{6+} ions irradiated Polypropylene (PP).

A sharp increase in conductivity has been observed at nearly 200 kHz for both the ions. It is also observed that conductivity increases as fluence increases. The increase in conductivity due to irradiation may be attributed to scissoring of polymers chains. When a.c. field of sufficiently high frequency is applied to a metal polymer/ metal structure, it may cause a net polarization, which is out of phase with the field. This results in a.c. conductivity.

Figures 5.22 and 5.23 show the plot of dielectric constant (ε') versus log frequency at room temperature for pristine and irradiated PP samples.

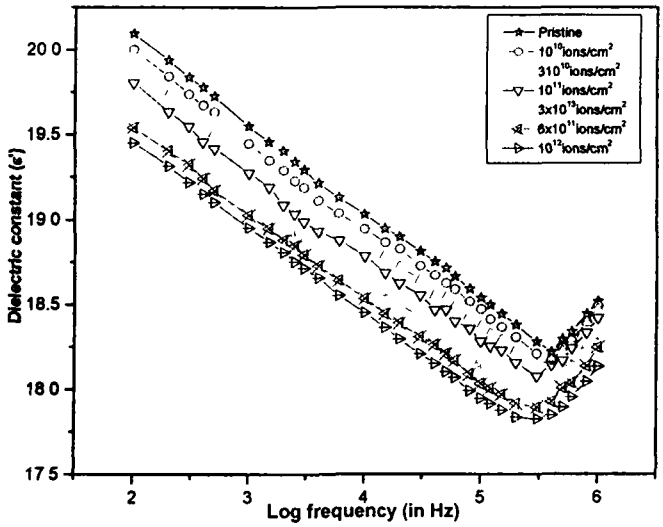

Figure 5.22: Plot of dielectric constant versus log frequency for pristine and 100 MeV Si^{8+} ions irradiated Polypropylene (PP).

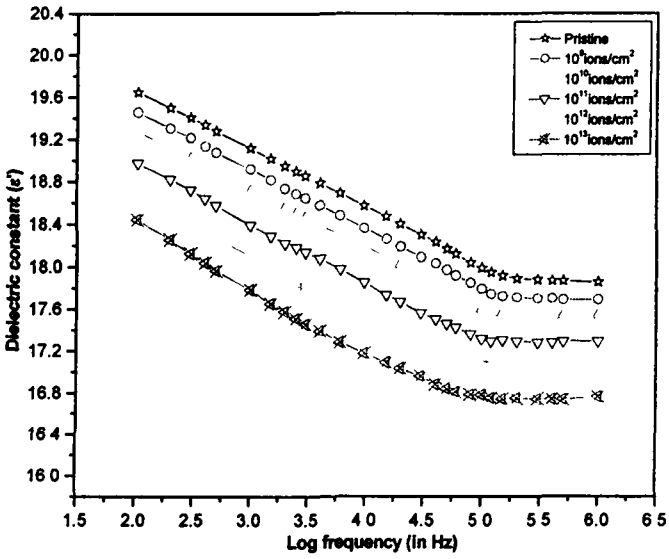

Figure 5.23: Plot of dielectric constant versus log frequency for pristine and 145 MeV Ne^{6+} ions irradiated Polypropylene (PP)

Dielectric constant at lower frequencies shows a rapidly decreasing trend. The dielectric constant decreases also at higher frequencies but slowly and it also increases with fluence. The effect of irradiation shows almost the same pattern as seen in PES.

References

[1] A. Biswas, S. Lotha, D. Fink, J. P. Singh, D. K. Avasthi, B. K. Yadav, S. K. Bose, D. T. Khating, A.M. Avasthi, Nucl. Instr. and Meth. B159(1-2)(1999)40.

[2] Z. Zhu,Y.Sun C. Liu, J, Liu and Y Jin Nucl. Instr, and Meth, B 193(2002)271.

[3] C. Liu, Z. Zhu, Y. Jin, Y. Sun, M. Hou, Z. Wang , X. Chen, C. Zhang, Jie, J. Liu, B. Li, Y. Yanbin, Nucl. Instr. Meth. B 166-167(2000.)641.

[4 Rajesh Kumar, U. De, Rajendra Prasad, Nucl. Instr. Meth. B 248(2006) 279-283.

[5] R. Hosemann, Journal Polymer Science C 20 (1967)11.

[6] P. Scherrer, Gott. Nachar, 2 (1918)98.

[7] A. M. Guzman, J. D. Carlson, J. E. Baras, P.P. Pronko, Nucl. Instr. and Meth. B 7-8 (1985) 468.

[8] U. Lappan, U. Geibler, K. Lunkwitz, Radit.Phys.Chem.59(2000)451.

[9] Z. M. Dang, Y. Shen and C.W. Nan, Appl. Phys. Lett. 81(2002)4814

[10] Y. Q. Wang, L. B. Bridwell, R. E. Giedd and M. J. Marphy, Nucl. Instr. Meth. B56/57 (1991)660.

[11] L. B. Bridwell, R. E. Giedd, Y. Q. Wang, S.S. Mohite, T. Jahnke, I. M. Brown, C.J. Bedell and C.J. Sofield, Nucl. Instr. and Meth B 56-57 (1991)656.

[12] A.K. Joncher, Nature 267(1977)673.

[13] N. L. Singh, A. Sharma , V. Shrinet, A. K. Rakshit and D.K. Avasthi Bull. Mater. Sci. 27(2004b) 263.

List of Publications

In Journals

1. Free Volume Study of 70 MeV carbon ion induced modification in Polymers through positron annihilation.
   Rajesh Kumar, S. Asad Ali, D. Das, A. H. Naqvi, H. S. Virk and R. Prasad
   Nucl. Instr. and Meth. B 244 (2006)257-260.
2. Characterization of optical modification in PES due to irradiation with Si^{8+} and Ne^{+6} ion.
   Rajesh Kumar, S. Asad Ali, U. De, and Rajendra Prasad
   Asian Journal of Chemistry 18, No. 5 (2006) 3365-3370.
3. Modification in Makrofol-N Polycarbonate by SHI
   Rajesh Kumar, S. Asad Ali, D. K. Awasthi and Rajendra Prasad
   Chem. Environ. Res.15 [3&4] (2006) 251-256.
4. Positron lifetime studies of the dose dependendence of nanohole free volumes in ion- irradiated conducting poly-(ethylene-oxide)-salt polymers
   Rajesh Kumar, Udayan De, P.M.G. Nambissan, Minakshi Maitra, S. Asad Ali, T. R. Middya, S. Tarafdar, F. Singh, D. K. Awasthi and Rajendra Prasad.
   Nucl. Instr. and Meth. B 266(2008) 1783-1787.
5. Study of Optical Band Gap and Carbonaceous Clusters in Swift Heavy Ion Irradiated Polymers with UV-vis Spectroscopy
   Rajesh Kumar, S. Asad Ali, A.K. Mahur, H. S. Virk, F. Singh, S. A. Khan, D. K. Awasthi
   Nucl. Instr. and Meth. B 266(2008) 1788-1792.
6. Studies of the o-Ps Lifetime and Free Volume in Ion Irradiated Makrofol-KG Polycarbonate by Positron Annihilation
   Rajesh Kumar' S. Asad Ali, U. De, A. H. Naqvi S. K. Chaudhary, D. Das, and Rajendra Prasad
   Radiation Measurements 43(2008) S578–S582.
7. Dielectric response of Makrofol–KG Polycarbonate irradiated with 145 MeV Ne^{6+} and 100 MeV Si^{8+} ions
   Rajesh Kumar, S. Asad Ali, Udayan De, D. K. Avasthi and Rajendra Prasad
   Indian Journal of Physics 2008 (In Press).
8. Study of optical band gap and carbon cluster sizes formed in 100 MeV Si^{8+} and 145 MeV Ne^{6+} ion irradiated Polypropylene Polymer
   Rajesh Kumar, S. Asad Ali, A.H. Naqvi, H.S. Virk, Udayan De, D. K. Avasthi and Rajendra Prasad.
   Indian Journal of Physics 2008 (In Press).
9. Si Ion Induced Modification in Makrofol-KG Polycarbonate.
   Rajesh Kumar, U. De, S. Asad Ali, S. A. Khan, D. K. Avasthi and R. Prasad
   Radiation Effects & Defects in Solids (Communicated).
10. Physical and Chemical Response of 145 MeV Ne^{+6} Ion Irradiated (PMMA) Polymer
    Rajesh Kumar, S. Asad Ali, Udayan De, S. G. Prasad, F. Singh and Rajendra Prasad
    Radiation Meas. (Revised Communicated).
11. Si^{+8} ion induced modification in Makrofol-KG Polycarbonate by Positron Annihilation
    Rajesh Kumar, S. Asad Ali, D. Das, Rajendra Prasad
    Radiation Meas.(Communicated)

In Proceedings.

12. Si induced modification in Makrofol-KG polycarbonate
    Rajesh Kumar, S. A. Ali, A. K. Mahur, S.A. Khan, D.K. Awasthi and Rajendra Prasad.
    50th DAE Golden Jubilee Solid State Physics Symp. Proc.,Vol. 50 (2005)469.
13. Study of Radon and its Daughters in Dwellings of Bhatinda near Thermal Power Plant
    Rajesh Kumar, A.K. Mahur, S. Asad Ali, Ashwani Kumar, and R. Prasad
    Nuclear and Radiochemistry Symposium (NUCAR) 2005Proc.
14. o-Ps Lifetime and Free Volume Studies of 100 MeV Si^{8+} Ion Irradiated Polystyrene
    Rajesh Kumar, S. Asad Ali, S. K. Chaudhary, D. Das and Rajendra Prasad
    51st DAE, Solid State Physics Symposium Proc.,Vol. 51 (2006)173.
15. Ne^{6+} ion induced modification in free volume in PES polymer by positron annihilation Lifetime studies
    Rajesh Kumar, S. Asad Ali and Rajendra Prasad
    Proc, Recent Advances in Material Science (Kurukshetra Univ.) 2006.
16. SHI Ion Irradiation Effects on Makrofol-KG Polycarbonate Studied by Positron Annihilation
    Rajesh Kumar, S. Asad Ali, A. K. Mahur, S. K. Chaudhary, D. Das, S. A. Khan, U. De and Rajendra Prasad,
    52nd DAE, Solid State Physics Symposium Proc., Vol. 52 (2007).

Papers Presented/Accepted in International Conferences/Workshop

17. 70 MeV Carbon Ion Induced Modification in Polyethersulphone (PES) through Positron Annihilation Lifetime Studies.
    Rajesh Kumar, S. Asad Ali, H.S. Virk, D.Das and Rajendra Prasad
    14th Int. Conference on Ion Beam Modification of Materials (IBMM, 2004) Monterely, California, USA, September 5- 10, 2004(Accepted).
18. Free Volume Study of SHI Induced Modification in Polyamide Nylon-6 Polymer
    Rajesh Kumar, S. Asad Ali, D. Das, A. H. Naqvi, H. S. Virk and R. Prasad
    Indo German Workshop on Synthesis and Modification of Nano-structured Materials by Energetic Ion Beams at Nuclear Science Centre, New Delhi, India, February 20-25, 2005(Presented)
19. 70 MeV Carbon Induced Modification in CR-39 (DOP) Polycarbonate through Positron Annihilation
    Rajesh Kumar, S. Asad Ali, A. K. Mahur, D. Das, A. H. Naqvi, H. S. Virk and Rajendra Prasad
    Indo German Workshop on Synthesis and Modification of Nano-structured Materials by Energetic Ion Beams at Nuclear Science Centre, New Delhi, India, February 20-25, 2005(Presented)
20. Si Ion Induced Modification in Makrofol-KG Polycarbonate
    Rajesh Kumar, U. De, S. Asad Ali, S. A. Khan, D. K. Avasthi and R. Prasad
    Sixth International Symposium on Swift Heavy Ions in Matter at G.S.I, Germany, May 28-31, 2005 (Accepted).
21. Studies of the o-Ps Lifetime and Free Volume in Ion Irradiated Makrofol-KG Polycarbonate by Positron Annihilation
    Rajesh Kumar, S. Asad Ali, Udayan De, A. H. Naqvi S. K. Chaudhary, D. Das, and Rajendra Prasad.
    23rd International Conference on Nuclear Tracks in Solids in Beijing(China), Sept., 11-15, 2006 (Presented).

22. Physical and Chemical Response of 145 MeV Ne^{6+} Ion Irradiated Poly methyl - Polymethylemethacrylate (PMMA) Polymer
Rajesh Kumar, S. Asad Ali, Udayan De, S. G. Prasad, F. Singh and Rajendra Prasad
23rd International Conference on Nuclear Tracks in Solids in Beijing(China), Sept., 11-15, 2006 (Presented).

23. Positron lifetime studies of the dose dependendence of nanohole free volumes in ion- irradiated conducting poly-(ethylene-oxide)-salt polymers
Rajesh Kumar, Udayan De, P.M.G. Nambissan, Minakshi Maitra, S. Asad Ali, T. R.Middya, S. Tarafdar, F. Singh, D.K. Awasthi and Rajendra Prasad
18th International Conference on Ion Beam Analysis in Hyderabad University, 23 - 28th September, 2007 (Presented).

24. Study of Optical Band Gap and Carbonaceous Clusters in Swift Heavy Ion Irradiated Polymers with UV-vis Spectroscopy
Rajesh Kumar, S. Asad Ali, A.K. Mahur, H. S. Virk, F. Singh, S. A. Khan, D. K. Awasthi and Rajendra Prasad
18th International Conference on Ion Beam Analysis in Hyderabad University, 23-28th September 2007(Presented).

25. Optical, chemical and structural modifications induced by 100 MeV Oxygen ion Irradiation in LEXAN polycarbonate
R. Kumar, S. Asad Ali, U. De, F. Singh, P. K. Kulriya, D. K. Avasthi and Rajendra Prasad.
The 14th International Conference On Radiation Effects In Insulators in Caen, France, August 28 –September 1, 2007 (Accepted).

26. Free volume evolution in Si ion irradiated Polyethersulphone studied by positron annihilation lifetime spectroscopy
R. Kumar, S. Asad. Ali, H. S. Virk, S. K. Chaudhary, D. Das, D. K. Avasthi and R. Prasad.
The 14th International Conference On Radiation Effects In Insulators, Caen, France, August 28 –September 1, 2007 (Accepted).

27. Study of modifications in Lexan polycarbonate induced by swift $^{8}O^{6+}$ ion irradiation
S. Asad Ali , Rajesh Kumar, A. H. Naqvi, F. Singh, P. K. Kulriya, and Rajendra Prasad
24th Int. Conf. on Nucl. Tracks in Solids in Bologna, Italy, 2008(Accepted).

28. Dielectric response of 100 MeV Si^{8+} ion induced modification in polymers
Rajesh Kumar , S. Asad Ali, Rajendra Prasad
24th Int. Conf. on Nucl. Tracks in Solids in Bologna, Italy, 2008(Accepted).

29. Free volume evolution in 95 MeV O^{6+} ion irradiated LEXAN Polycarbonate studied by positron annihilation lifetime and Doppler broadening spectroscopy
Rajesh Kumar, S. Asad Ali, P.M.G. Nambissan, Rajendra Prasad
24th Int. Conf. on Nucl. Tracks in Solids Bologna, Italy, 2008(Accepted).

30. Positron lifetime studies of the 145 MeV Ne^{6+} ion induced modification of free volume in Polyvinylidene difluoride (PVDF) and Polyethersulphone (PES) polymers
Rajesh Kumar, S. Asad Ali, H.S. Virk, Udayan De and Rajendra Prasad
24th Int. Conf. on Nucl. Tracks in Solids in Bologna, Italy,2008(Accepted).

31. Study of Natural radinuclides and radon exhalation study in soil samples from some area of Jharkhand state, India
Rajesh Kumar, A. K. Mahur, S.Asad Ali, R.G. Sonkawade, V.N. Bhardwaj, B. S. Pandit, B. P. Singh and Rajendra Prasad
24th Int. Conf. on Nucl. Tracks in Solids in Bologna, Italy,2008(Accepted).

32. Study of Nano Scale Voids and free volume property of 145 MeV Ne^{6+} ion induced in PES polymer by positron annihilation lifetime studies
S. Asad Ali, Rajesh Kumar and Rajendra Prasad
Int. Conference in Nanotechnology, 2008 (ICN-08) Dubai (Accepted).
33. Study of swift $^{8}O^{6+}$ ion irradiation modifications in Lexan Polycarbonate
S. Asad Ali , Rajesh Kumar, A. H. Naqvi, F. Singh, P. K. Kulriya, and Rajendra Prasad
Int. Conference in Nanotechnology, 2008 (ICN-08) Dubai (Accepted)
34. Li ion induced modification in PANI-graphite composite studied through positron annihilation lifetime and coincidence gated Doppler broadening
S. Asad Ali, Rajesh Kumar, M. K. Ansari, P.M.G. Nambissan, Rajendra Prasad
XV^{th} Int. Conf. on Positron Annihilation (ICPA-09) to be held at SINP, Kolkata ,INDIA during Jan 18-23, 2009 (Accepted).
35. Li^{3+} ion irradiation effect s on polyamide nylon 6,6 studied by positron annihilation lifetime and Doppler broadening spectroscopy.
S. Asad Ali[1], Rajesh Kumar, P.M.G. Nambissan, Fouran Singh and Rajendra Prasad
***XV^{th} Int. Conf. on Positron Annihilation(ICPA-09) to be held at SINP,* Kolkata, INDIA during Jan 18-23, 2009(Accepted).**
36. o-Ps Lifetime, Free volume and Doppler broadening spectroscopy (DBS) Studies of 50 MeV Li^{3+} Ion Irradiated Polystyrene
S. Asad Ali, Rajesh Kumar, P.M.G. Nambissan, Fouran Singh and Rajendra Prasad
XV^{th} Int. Conf. on Positron Annihilation(ICPA-09) to be held at SINP, Kolkata ,India during Jan 18-23, 2009(Accepted).
37. Evolution of free volume in 95 MeV O^{6+} ion irradiated LEXAN Polycarbonate studied through positron annihilation lifetime and Doppler broadening spectroscopy
S. Asad Ali, Rajesh Kumar, P.M.G. Nambissan, Rajendra Prasad
XV^{th} Int. Conf. on Positron Annihilation (ICPA-09) to be held at SINP, Kolkata ,INDIA during Jan 18-23, 2009(Accepted).

Papers presented/Accepted in National Conferences/Workshop

38. Ion beam modification in Polyamide Nylon-6 Polymer by Positron Annihilation
Rajesh Kumar, S. Asad Ali, H. S. Virk and Rajendra Prasad
National Conference cum Workshop on Solid State Nuclear Track Detectors and Applications, November 1-3, 2004 at D. A. V., College Amritsar (Pb.) (Presented).
39. Modification In Makrofol-KG Polycarbonate By Heavy Ion Irradiation
Rajesh Kumar, S.Asad Ali S. A. Khan, D. K. Avasthi and Rajendra Prasad Third
National Conference on Thermo Physical Properties, Goa University, Jan. 19-20, 2005. (Accepted).
40. Study of Radon and its Daughters in Dwellings of Bhatinda near Thermal Power Plant
Rajesh Kumar, A.K. Mahur, S.Asad Ali, Ashvani Kumar and Rajendra Prasad
Nuclear and Radiochemistry Symposium at Guru Nanak Dev University, Amritsar, March 15-18, 2005 (Presented).
41. Modification in Makrofol-N Polycarbonate by SHI
Rajesh Kumar, S. Asad. Ali, D. K. Awasthi and Rajendra Prasad
14^{th} National Symposium on Solid State Nuclear Track Detectors (SSNTD's) Aligarh Muslim University, Aligarh, Nov.10-12, 2005. (Presented).
42. Si ion induced modification in Makrofol-KG Polycarbonate.

Rajesh Kumar, S. Asad. Ali, A. K. Mahur, S. A. Khan, D. K. Avasthi and R Prasad
50th DAE Golden Jubilee Solid State Physics Symposium, at Bhabha Atomic Research Centre (BARC), Mumbai, December 5-9, 2005.(Presented)

43. Characterization of optical modification in PES due to irradiation with Si^{8+} and Ne^{6+} ion
Rajesh Kumar[1], S. Asad. Ali, U. De[2], and Rajendra Prasad
National Conference on Laser, Smart Materials and Radiation Physics, at Longowal Institute of Engineering and Technology, Sangrur, Punjab, March 17-18, 2006. (Presented).

44. Ne^{6+} ion induced modification in free volume in PES polymer by positron annihilation lifetime studies
Rajesh Kumar, S. Asad Ali and Rajendra Prasad
Recent Advances in Material Science(Kurukshetra Univ.), Sept. 27-29, 2006. (Presented).

45. o-Ps Lifetime and Free Volume Studies of 100 MeV Si^{8+} Ion Irradiated Polystyrene
Rajesh Kumar, S. Asad Ali, S. K. Chaudhary, D. Das and Rajendra Prasad
51st| DAE Solid State Physics Symposium, Barkatullah University, Bhopal (M.P.), December 26-30, 2006.(Presented)

46 HI Ion Irradiation Effects on Makrofol-KG Polycarbonate Studied by Positron Annihilation
Rajesh Kumar, S. Asad Ali, A. K. Mahur, S. K. Chaudhary, D. Das, S. A. Khan, U. De and R. Prasad,
52nd DAE , Solid State Physics Symposium, 27-31 Dec. 2007, Univ. of Mysore Manasgangotri, Mysore-570 006 (Presented).

47. Study of optical band gap and carbon cluster sizes formed in 100 MeV Si^{8+} and 145 MeV Ne^{6+} ion irradiated Polypropylene Polymer
Rajesh Kumar, S. Asad Ali, A.H. Naqvi, H.S. Virk, U. De, D. K. Avasthi and Rajendra Prasad.
15th National Symposium on Solid State Nuclear Track Detectors (SSNTD's) at H.N.B. Garhwal Univ., Uttrakhand, June 21-23, 2007 (Presented).

48. Dielectric response of Makrofol-KG Polycarbonate irradiated with 145 MeV Ne^{6+} and 100 MeV Si^{8+} ions
Rajesh Kumar, S. Asad Ali, Udayan De, D. K. Avasthi and Rajendra Prasad
15th National Symposium on Solid State Nuclear Track Detectors (SSNTD's) at H.N.B. Garhwal Univ., Uttrakhand, June 21-23, 2007 (Presented).

49. Nano Scale Free Volume Study of 70 MeV Carbon C^{5+} Ion Induced Modification in PES Polymer by Positron Annihilation
Rajesh Kumar, S. Asad Ali, Avinash C. Sharma, Udyan De, S. K. Chaudhari, D. Das and Rajendra Prasad
53rd DAE Solid State Phys. Symp., to be held at BARC, Mumbai, Dec. 16-20, 2008 (accepted)

50. Dielectric response of Makrofol-N Polycarbonate irradiated with 100 MeV Si^{8+} ions
S. Asad Ali, Rajesh Kumar, R.G. Sonakawade, and Rajendra Prasad
53rd DAE Solid State Phys. Symp., to be held at BARC, Mumbai, Dec. 16-20, 2008 (Accepted).

(SYYED ASAD ALI)

macroscopic properties [8]. The concept of free volume has significant importance for the gas permeation properties of polymeric membranes and for other related subjects of polymer science.

In recent years, positron annihilation spectroscopy (PAS) has been developed as a useful tool in probing the nanoscopic and local properties of polymeric materials one of the great successes in this line of research is the determination of defect properties, such as free volumes and holes, at an atomic scale (0.2–2 nm) in polymers [9]. It has been demonstrated that positron annihilation lifetime spectroscopy (PALS) is capable of determining size distribution and fraction of free volumes and holes (often referred as free volume holes) in polymers [10,11]. The high sensitivity of PAS in probing defect properties arises from the fact that the positronium atom (Ps, an atom consisting of a positron and electron) is preferentially trapped (localized) in atomic scale free volumes holes.

In PALS the positron is used as a nuclear probe which is repelled by the ion cores and preferentially localized in the atomic size free volume holes of a polymeric material. Therefore, the positron and positronium (Ps) annihilation signals are found to be contributed mainly from the free volume holes in the polymer. Ps atom has two spin states: *para*-positronium (*p*-Ps) having spin zero (lifetime in vacuum, 125 ps) and *ortho*-positronium (*o*-Ps) having spin one (lifetime in vacuum 142 ns). *o*-Ps lifetime is reduced due to interaction of *o*-Ps with electrons from surrounding matter (pick off annihilation) and decays into two gamma rays. In polymers three positron lifetimes (τ_1, τ_2, τ_3) are often found which range from 100 ps to 5 ns. These lifetimes from shortest to longest are believed to be due to the self annihilation of *p*-Ps, the annihilation of free positron and the pick off annihilation of *o*-Ps respectively. The measured *o*-Ps lifetime is found to be proportional to the hole size and intensity provides a measure of the number of holes.

The purpose of the work is to estimate the change in free volume hole size due to irradiation of CR-39 (DOP) polycarbonate and polyamide Nylon-6 (PN-6) with 70 MeV C^{5+} ions to different fluences. CR-39 polycarbonate is a homopolymer and high grade optical plastic and has been widely used as ion track detector due to its intrinsic property of ion track detection [12]. It consists of polyallyl chains cross-linked by diethylene glycol carbonate linkages. Its chemical formula is

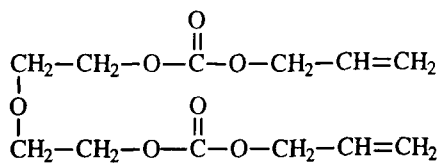

The optical and etching properties of CR-39 can be improved by incorporating additives such as dioctyl phthalate (DOP) in the polymer [12]. Another polymer investigated, is polyamide Nylon-6 whose structure is

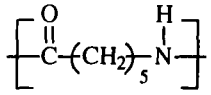

Polyamides are used extensively as high performance plastic materials because of their unique combination of superior mechanical, electrical, chemical and thermal properties.

Calculation using SRIM 2003 program shows that for C^{5+} ion irradiation of CR-39 (DOP) polycarbonate $(dE/dX)_{electronic}$ is about 100–2000 time of $(dE/dX)_{nuclear}$ for 1–70 MeV ion energy.

2. Experimental method

2 1. Irradiation

Self supporting 250 μm thick sheets (1.5×1.5 cm^2) of polyamide Nylon-6 (Good Fellow, Cambridge Ltd., UK) and CR-39 (DOP) (Pershore Moulding Ltd., UK) were used for irradiation. Polymer samples were mounted on a vacuum shielded vertical sliding ladder and were exposed to 70 MeV C^{5+} ion beam in the general purpose scattering chamber (GPSC) under high vacuum ($\sim 4 \times 10^{-6}$ Torr) using the 15 UD Pelletron accelerator at Nuclear Science Centre, New Delhi, India [13] to different fluences. In order to expose the whole target area uniformly, the beam was scanned in the X–Y plane (over 1.5×1.5 cm^2).

2.2. PAL measurement

PAL measurements were carried out at Inter University Consortium for DAE facilities, Kolkata Centre, Kolkata,

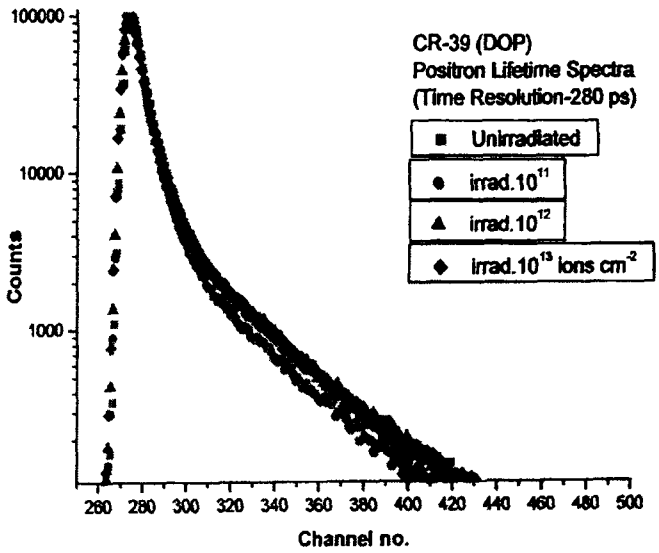

Fig 1 Positron lifetime spectra of CR-39 (DOP) polycarbonate

Available online at www.sciencedirect.com
SCIENCE DIRECT
ELSEVIER
Nuclear Instruments and Methods in Physics Research B 244 (2006) 257–260
NIM B
Beam Interactions with Materials & Atoms
www elsevier com/locate/nimb

Free volume study of 70 MeV carbon induced modification in polymers through positron annihilation

Rajesh Kumar [a,*], S.A. Ali [a], A.K. Mahur [a], D. Das [b], A.H. Naqvi [a], H.S. Virk [c], Rajendra Prasad [a]

[a] *Department of Applied Physics, Z H College of Engineering and Technology, Aligarh Muslim University Aligarh 202 002, India*
[b] *UGC-DAE Consortium for Scientific Research, Kolkata 700 098, India*
[c] *360/71, Mohali, SAS Nagar, Chandigarh 160 071, India*

Available online 10 January 2006

Abstract

Free volume properties of polymers have strong correlation with macroscopic properties and can be modified by radiations and ions Positron annihilation lifetime spectroscopy (PALS) provide direct information about the dimension, content and size distribution of free volume holes in polymers CR-39 (DOP), a polycarbonate widely used as ion track detector and polyamide Nylon-6, a high performance plastic having a unique combination of superior mechanical, electrical, chemical and thermal properties were irradiated with 70 MeV C^{5+} ion beam to different fluences ranging from 10^{11} to $3\,7 \times 10^{13}$ ions/cm^2 The results of characterization by PALS are reported here *o*-Ps lifetime and the average free volume for both the polymers are found to decrease with fluence, indicating the facilitation of cross-linking The results are interpreted in terms of change in the free volume Maximum change of 9 7% in average free volume was observed in PN-6 irradiated to 3.7×10^{13} ions/cm^2.

Keywords CR-39(DOP) polycarbonate, PN-6 polymer, C^{5+} ion irradiation, Positron lifetime, Ion beam modification; Free volume hole

1. Introduction

Ion irradiation has now a days become an established tool for the modification of structural, physical and chemical properties of polymers. The availability of heavy ion beams from the accelerators has brought new impetus to the field of ion beam modification as dramatic modifications in the properties of polymeric materials have been observed as a result of irradiation of polymers with swift heavy ions (SHI) [1,2] This causes bond cleavages; the formed free radicals are expected to come to rest and may react in a molecular site of a different type from their original site [3]. Transfer of high value of energy due to heavy ion irradiation causes an unusual density of electron hole pairs close to the ion path. Some of the modifications by incident ions have been attributed to the scission of the polymer chains, breaking of covalent bonds, promoting the cross-linkages, carbon cluster formation, release of gaseous molecular species (the most prominent emission is hydrogen) and even the formation of new chemical bonds in some cases [4–6]. The effectiveness of these modifications produced in the polymer depends on the structure and the ion beam parameters (energy, fluence, mass, charge) and the nature of the target material itself. It was well established that cross-linking or scission efficiency depends not only upon polymer structure but also upon the characteristics of the radiation sources, namely ion energy and ion species [7]. The existence of free volume holes in polymers has been postulated for more than four decades. A key problem in this regard is to relate the macroscopic properties of polymer to atomic scale (a few Å) free volume holes The damage produced in the form of latent tracks by heavy ions results into the change of free volume properties of the polymeric material which have strong correlation with its

* Corresponding author Tel +91 571 2742837/2742932
E-mail addresses rajendraprasad1@rediffmail com, drrajesh04@rediffmail com (R Kumar)

0168-583X/$ - see front matter © 2005 Elsevier B V All rights reserved
doi 10 1016/j nimb 2005 11 135

India. A ^{22}Na source (5 μ Ci) deposited on a rhodium foil was sandwiched between the stacks of two layers of polymer films. The PAL spectra were obtained using conventional fast–fast coincidence system. The thickness of the samples is adequate to absorb more than 99% of positron emitted. The BaF_2 scintillators coupled to Phillips XP2020 photomultipliers were used. ORTEC constant fraction differential discriminators were used for selecting energy and providing timing signal to time to amplitude converter. The time resolution (FWHM) of Co-60 prompt spectrum was 280 ps. Positron lifetime spectra for unirradiated and irradiated samples were recorded. Fig. 1 shows the lifetime spectra for pristine and irradiated CR-39 (DOP) polycarbonate samples.

3. Results and discussion

The lifetime spectra were analyzed as three lifetime components (τ_1, τ_2 and τ_3 with subsequent intensities I_1, I_2 and I_3) with the help of computer program PATFIT-88 [14] after applying proper source and background corrections. The short lived component τ_1 and intermediate lived component τ_2 are attributed to *para*-positronium (*p*-Ps) and positron annihilation, respectively. The long-lived component τ_3 which is very sensitive to structural changes in the polymer is attributed to *o*-Ps pick-off annihilation in free volume. In PALS, it is the *o*-Ps lifetime which is directly correlated to the free volume hole size. The intensity of this component contains information about free volume hole concentration [15].

A spherical hole model [16] gives the mean free volume hole radius by following equation:

$$\tau_3 = \frac{1}{\lambda_3} = \frac{1}{2}\left[1 - \frac{R}{R_0} + \frac{1}{2\pi}\sin\left(\frac{2\pi R}{R_0}\right)\right]^{-1}$$

where $R_0 = R + \Delta R$ and $\Delta R = 1.66$ Å, ΔR is an empirical parameter, related to the penetration of Ps wave function in to the bulk and has been determined by the fitting the experimental values of τ_3 obtained from the materials with known hole size [17]. When hole dimensions are distributed with a width ΔV around the average volume V, a corresponding distribution of *o*-Ps lifetime is expected. From this relation, the free volume radius R is calculated and the average volume of the free volume hole V_f is given as $V_f = 4/3\pi R^3$. The fractional free volume F_v can be estimated as $F_v = CV_fI_3$ where C is a structural constant evaluated from an independent isochronal experiment and is determined empirically to be ~0.0018 [18].

Table 1
Lifetime and intensities of virgin and irradiated CR-39 (DOP) polycarbonate

Fluence (ions/cm^2)	τ_1 (ns)	I_1 (%)	τ_2 (ns)	I_2 (%)	τ_3 (ns)	I_3 (%)
Unirradiated	0 184	37 6	0 420	43 3	1 987	19 1
10^{11}	0 151	38 5	0 377	45 7	1 862	15 8
10^{12}	0 168	34 5	0 403	46 2	1 929	19 3
10^{13}	0 173	32 8	0 406	48 9	1 970	18 4

Table 2
Lifetime and intensities of virgin and irradiated polyamide Nylon-6 polymer

Fluence (ions/cm^2)	τ_1 (ns)	I_1 (%)	τ_2 (ns)	I_2 (%)	τ_3 (ns)	I_3 (%)
Unirradiated	0 201	35.9	0 393	46 3	1 710	18 6
$9\,3\times10^{11}$	0 170	31 2	0 377	51 8	1 693	18 3
$3\,7\times10^{12}$	0 168	32 7	0 372	50 2	1 684	17 9
$1\,8\times10^{13}$	0 169	32 5	0 374	50 5	1 672	17 6
$3\,7\times10^{13}$	0 160	29 3	0 355	50 2	1 629	17 2

Table 3
The lifetime parameters of *o*-Ps and radius of free volume hole (R) and fractional free volume (F_v) in CR-39 (DOP) polycarbonate

Fluence (ions/cm^2)	τ_3 (ns)	I_3 (%)	R (Å)	V_f (Å^3)	F_v
Unirradiated	1 987 ± 0 011	19 1 ± 0 3	2 84	96 23	3 31
10^{11}	1 862 ± 0 012	15 8 ± 0 3	2 72	84 61	2 41
10^{12}	1 929 ± 0 011	19 3 ± 0 3	2 79	90 91	3 26
10^{13}	1 970 ± 0 011	18 3 ± 0 3	2 83	94 68	3 12

Table 4
The lifetime parameters of *o*-Ps and radius of free volume hole (R) and fractional free volume (F_v) in polyamide Nylon-6 polymer

Fluence (ions/cm^2)	τ_3 (ns)	I_3 (%)	R (Å)	V_f (Å^3)	F_v
Unirradiated	1 710 ± 0 01	18 6 ± 0 3	2 57	71 32	2 38
$9\,3\times10^{11}$	1 693 ± 0 01	18 3 ± 0 2	2 55	69 91	2 30
$3\,7\times10^{12}$	1 684 ± 0 01	17 9 ± 0 2	2 54	69 66	2 24
$1\,8\times10^{13}$	1 672 ± 0 01	17 6 ± 0 2	2 53	69 17	2 20
$3\,7\times10^{13}$	1 629 ± 0 01	17 2 ± 0 2	2 48	64 40	1 99

The lifetime values and intensities for CR-39(DOP) are tabulated in Table 1 and for PN-6 in Table 2. Tables 3 and 4 present the results obtained for *o*-Ps lifetime (τ_3), free volume hole radius (R), micro-void volume (V_f) and fractional free volume F_v for virgin and irradiated samples at different fluences. From the positron lifetime results of virgin and C ion irradiated samples, a decrease in τ_3 for C ion irradiated polymer samples is observed as compared to virgin samples. The effect of irradiation on the free volume of the sample is small. The free volume is decreased only by a few percent even if the sample was irradiated with the maximum dose of 3.7×10^3 ions/cm^2. Kobayashi et al [19] have observed small decrease in PEEK due to electron irradiation at high fluences and has attributed it to intermolecular cross-linking. The results of Lee et al [7] for PMMA on irradiation indicate that high LET produces a high concentration of free radicals over many neighboring molecular chains, facilitating track overlap and enhancing cross-linking over scission, while low LET affects only a simple molecular chain, leading to chain scission

The most important parameter for cross-linking is found to be the energy deposited per unit ion path length or linear energy transfer (LET). LET is a measure of energy deposited per unit ion path length, often expressed in SI units of eV/nm/ion or simply eV/nm. In our earlier studies [20–22] on CR-39 polycarbonates irradiated with ^{40}Ar and ^{197}Au

ions to low fluence of 10^5 ions/cm^2 and Makrofol-*N* polycarbonate irradiated with C^{5+} to 10^6 ions/cm^2 free volume has been found to increase with fluences and has been attributed to the chain scission along the tracks. During ion irradiation the energy transfer by the ion leads to radical formation, bond scission and cross-linking of polymer chains. The dominance of scission or cross-linking depends essentially on the polymer and energy loss per unit path length or linear energy transfer (LET). For low LET, spurs develop far apart and independently; the deposited energy tends to be confined in one chain (not in neighboring chain) often leading to scission [7,20,23]. In case of high LET, the tracks have large effective radius and spurs overlap more compactly, the probability of two radical pairs to be in neighboring chains is increased and cross-linking is facilitated. The scission causes increase in the free volume whereas the cross-linking causes decrease in available free volume [24]. *o*-Ps lifetime and, therefore, the average free volume are found to be decreased due to irradiation at the fluences used in the present experiment. At high fluences the track area where cross-linking is predominant becomes comparable to the sample area. This explains the observed decrease in the *o*-Ps lifetime, free volume hole radius (R), micro-void volume (V_f) and fractional free volume (F_v). Ion irradiation reduces the available free volume indicating the facilitation of cross-linking at high LET

4. Conclusion

Free volume study of 70 MeV C ion induced modifications in CR-39 (DOP) polycarbonate and polyamide Nylon-6 at various fluences was undertaken through positron annihilation lifetime measurements. Small decrease in *o*-Ps lifetime with the ion fluence was observed. Ion irradiation reduces the available free volume indicating the facilitation of cross-linking at high fluences. Opposite trend was observed at low fluences in our previous measurements of CR-39 polycarbonate irradiated with ^{40}Ar and C^{5+} [20–22] favoring scission. At high fluences scissioned segments cross-link randomly, resulting in the decrease of average free volume due to overlapping of tracks.

Acknowledgements

The authors wish to thank Dr. A.K. Sinha, Director, UGC-DAE Consortium for Scientific Research, Kolkata for providing PAL facilities. Thanks are also due to Dr D.K. Avasthi and the staff of the Nuclear Science Centre, New Delhi for their help during irradiation. One of the author, Prof. Rajendra Prasad is thankful to All India Council of Technical Education, Govt. of India for providing Emeritus Fellowship to carry out this work. Dr. Rajesh Kumar wishes to thank Council of Scientific and Industrial Research (CSIR), New Delhi for providing him the Research Associateship (No. 9/112 (369) 2K5 EMR-I) for the research work.

References

[1] E H Lee, Polyimides Fundamentals and Applications, Marcel Dekker Inc, New York, 1996
[2] L S Wielunski, R A Clissold, E Yap, D G McCulloch, D R McKenzie, M V Swain, Nucl Instr and Meth B 127–128 (1997) 698
[3] T Venkatesan, Nucl Instr and Meth B 7–8 (1985) 461
[4] C Liu, Z Zhu, Y Jin, Y Sun, M Hou, Z Wang, X Chen, C Zhang, J Liu, B Li, Y Wang, Nucl Instr and Meth B 166–167 (2000) 641
[5] H S Virk, Nucl Instr and Meth B 191 (2002) 739
[6] M E Abdel, O Amir, R Kalish, L C Feldman, J Appl Phys 66 (1999) 3248
[7] E H Lee, G R Rao, L K Mansur, Radiat Phys Chem 55 (1999) 293
[8] J D Ferry, Viscoelastic Properties of Polymers, third ed, John Wiley & Sons Inc, New York, 1980
[9] R A Pethrick, Prog Polym Sci 22 (1997) 1
[10] Y C Jean, in A Dupasquier, A P MillsJr (Eds), Positron Spectroscopy of Solids, IOS Pub, Amsterdam, 1995, p 563
[11] A H Baugher, W J Kosslar, K G Petzinger, Macromolecules 29 (1996) 7280
[12] A Kumar, R Prasad, Nucl Instr and Meth B 93 (1994) 277
[13] D Kanjilal, S Chopra, M M Narayanan, I S Iyer, V Jha, R Joshi S K Datta, Nucl Instr and Meth A 238 (1993) 97
[14] P Kirkegaard, N J Pedersen, M Eldrup, PATFIT-88 a data processing system for positron annihilation spectra for mainframe and personal computers, Riso National Laboratory, Roskilde, Denmark, 1989
[15] Y C Jean, Free volume hole properties of polymers probed by positron annihilation spectroscopy, 3rd International Workshop on Positron and Positronium Chemistry, Milwaukee, USA, July 16–18, 1990
[16] M Eldrup, D Lightbody, J N. Sherwood, Chem. Phys 63 (1981) 51
[17] H Nakanishi, S J Wang, Y C Jean, in S C Sharma (Ed), Positron Annihilation Studies of Fluids, World Sci. Pub, Singapore, 1988, p 292
[18] Y Y Wang, H Nakanishi, Y.C Jean, J Polym Sci B Polym Phys 28 (1990) 1431
[19] Y Kobayashi, K Haraya, S Hattori, T Sasuga, Nucl Instr and Meth B 91 (1994) 447
[20] R Kumar, S Rajguru, D Das, R Prasad, Radiat Meas 36 (2003) 151
[21] R Kumar, B K Nath, D Das, R Prasad, Indian J Phys 78A (2) (2004) 221
[22] R Kumar, A K Mahur, D Das, K K Dwivedi, R Prasad, Indian J Phys 78A (2) (2004) 225
[23] E H Lee, Nucl Instr and Meth B 151 (1999) 29.
[24] D Fink, M Muller, S Ghosh, K K Dwivedi, J Vacik, V Hnatowicz, J Cervena, Y Kobayashi, K Hirata, Nucl Instr and Meth B 156 (1999) 170

Available online at www.sciencedirect.com
ScienceDirect
Radiation Measurements 43 (2008) S578–S582
Radiation Measurements
www.elsevier.com/locate/radmeas

Studies of the *o*-Ps lifetime and free volume in ion irradiated Makrofol-KG polycarbonate by positron annihilation

Rajesh Kumar[a,*], S.A. Ali[a], Udayan De[b], A.H. Naqvi[a], S.K. Chaudhary[c], D. Das[c], Rajendra Prasad[a]

[a]*Department of Applied Physics, Z. H. College of Engineering and Technology, Aligarh Muslim University, Aligarh 202002, India*
[b]*Variable Energy Cyclotron Centre, 1/AF, Bidhan Nagar, Kolkata 700064, India*
[c]*UGC-DAE Consortium for Scientific Research, Kolkata 700098, India*

Abstract

Passage of energetic heavy ions produces damage in a polymeric material resulting into the creation of latent tracks due to dissociation of bonds, cross-linking, formation of free radicals, etc. This results in the change of free volume properties which have strong correlation with the macroscopic properties of the materials. Positron annihilation lifetime spectroscopy (PALS) has been developed into a powerful characterization tool for the study of free volume size and free volume fraction in polymeric materials. By measuring the lifetimes of the positron, it may be possible to get fairly accurate estimates of the free volume of Angstrom (0.2–1 nm) range. Makrofol-KG polycarbonate films widely used for ion track registration were irradiated by 145 MeV Ne^{6+} ion beam at Variable Energy Cyclotron Centre (VECC), Kolkata, India to the fluences of 10^{10}, 10^{11}, 10^{12} and 10^{13} ions/cm^2. From *o*-Ps lifetime parameters average free volume were obtained. *o*-Ps lifetimes were found to decrease with the ion fluence. Microvoid volume decreased by 10.52% at 10^{13} ions/cm^2.

Keywords: Ion beam modification; Makrofol-KG polycarbonate; Positron annihilation lifetime; Free volume

1. Introduction

Solid state nuclear track detectors (SSNTDs), being threshold-type detectors are applied for ionographic registration and are well studied for heavy ion research. Amorphous bisphenol A polycarbonate is widely used today to prepare track-etched membrane. Latest process development allow the production of PC particle track-etched membranes (nano-PTM) with pore shape and size very well controlled within diameters from 10 to 100 nm (Ferain and Legras, 2001a, b). These membranes are used as template for nanotubes and nanowires manufacturing (Piraux et al., 1997, 1999; Jérôme et al., 2000). As polycarbonate (PC) track detectors such as Makrofol are intensive to light charged particles, X- and γ-rays, they offer a very convenient way of detecting heavy ions in the study of cosmic rays, heavy ion nuclear reactions, exploration of super heavy elements, etc. (Fleischer et al., 1975; Durrani and Bull, 1987).

Swift heavy ion (SHI) irradiation provides a unique way of material modification by including such a high degree of localized electronic excitation which otherwise is not possible by any other means. Its effect on the materials depends mainly on the electronic energy loss of the ion in material and ion fluence. The ions lose their energy as they pass through the material. The energy lost is either spent in displacing atoms (of the sample) by elastic collisions or it is spent in exciting or ionizing the atoms via inelastic collisions. The former is the dominant process at low energies. The inelastic collisions are dominant at higher energies (MeV). The information about these processes is stored in the resulting damage, such as size, shape and structure of defects. The degree of disorder can range from point defects to a continuous amorphized zone along the ion path, commonly called latent track.

* Corresponding author. Tel.: +91 571 2742837; fax: +91 9410643341.
E-mail address: drrajesh04@rediffmail.com (R. Kumar).

1350-4487/$ - see front matter © 2008 Elsevier Ltd. All rights reserved.
doi:10.1016/j.radmeas.2008.04.059

Ion irradiation has now a days become an established tool for the modification of structural, physical and chemical properties of polymers. Desired physical and chemical properties can be obtained for some specific application by exposing the polymers to radiation. Although radiations such as UV, γ-rays and electron beam can produce very small modification in the physical properties of the polymers, energetic heavy ion irradiation modification induces dramatic physical and chemical modifications (Percolla et al., 1994). Some of the modifications by incident ions have been attributed to the scissoring of the polymer chains, breaking of covalent bonds, promoting the cross-linkages, carbon cluster formation, liberation of volatile species and even the formation of new chemical bonds in some cases (Lee, 1996; Wielunski et al., 1997). The effectiveness of these modifications produced in the polymer depends on the structure of polymer and the ion beam parameters (energy, fluence, mass and charge).

Existence of free volume in polymers has been known since decades and it is an important parameter that characterizes polymer properties. The local free volume "holes" in structurally disordered polymers play a crucial role in determining its physical properties. Latent tracks formed due to the damage produced by energetic ions result into the change of free volume properties of the polymeric material which have strong correlation with its macroscopic properties (Venkatesan, 1985).

During the past two decades, positronium (Ps), the bound state of a positron (e^+) with an electron (e^-) has been used as a probe of molecular solids, especially of polymers (Schrader and Jean, 1988). Thus many applications of the positron annihilation techniques have been developed as Ps presents a rather unique probe for the quantitative study (viz. size and concentration) of the free spaces present in these solids: intrinsic or extrinsic defects, as well as free volumes. In recent years Positron annihilation spectroscopy has provided a unique probe to study the size and number distribution of the subnanometer cavities (Tao, 1972; Nakahishi and Jean, 1988; Schrader and Jean, 1988; Jean, 1995a,b; Mogensen, 1995).

Positron annihilation lifetime spectroscopy (PALS) has emerged as one of the most popular techniques which enables one to measure the lifetimes and relative abundances or intensities of various positron states. Both these parameters are sensitive to the physico-chemical environment of the sites of annihilation, Ps triplet state (*o*-Ps) intensity is correlated with the number of free space, while its lifetime can be quantitatively correlated with the size of these spaces (Schrader and Jean, 1988; Jean, 1990, 1995a,b).

Characterization of physico-chemical properties of Makrofol-KG polycarbonate modified by SHIs have been carried out using various characterization techniques, but we present the characterization by PALS a non-destractive sensitive probe for nanosize free volume holes for the first time. In this paper, we will describe our recent measurements, focusing our attention on Makrofol-KG polycarbonate polymer bulk properties such as changes in the free volume size with ion fluences by SHI irradiation.

2. Experimental method

2.1. Sample preparation

Makrofol-KG polycarbonates manufactured by a casting process into the form of thin sheets by Bayer AG of Leverkussen, Germany have same composition ($C_{16}H_{14}O_3$) as Lexan (G.E.C., USA). However, they have different type of behavior than Lexan polycarbonate. Thin Makrofol-KG polycarbonate sheets (40 μm) were procured from Bayer AG of Leverkussen, Germany. The structure of Makrofol-KG polycarbonate is given as

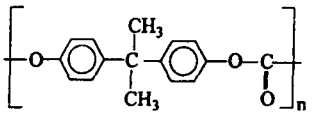

2.2. Irradiation

Parts of each sample were irradiated by 145 MeV Ne^{6+} ion beam at Variable Energy Cyclotron Centre (VECC), Kolkata, India using a low beam current (~ 15 nA) and a specially designed aluminum sample holder of sufficiently large thermal mass to avoid beam heating. The beam current was measured by integrating the target or sample current by a Dynfisik current integrator which has the provision of pre-set count. Significant secondary electron emission from the target due to the bombardment by the high energy positive ion beam usually adds a large current to the true ion current. A metal cup in our target holder was designed to eliminate this secondary electron contribution. Ion fluences of 10^{10}, 10^{11}, 10^{12} and 10^{13} ions/cm^2 were used. SRIM 2003 calculation showed the range of 145 MeV Ne^{6+} ions to be larger than the sample thickness, ensuring no ion implantation in the sample.

2.3. PAL measurements

Positron annihilation lifetime (PAC) measurements were made at UGC-DAE Consortium for Scientific Research, Kolkata Centre, India. A specially designed 1.85 × 10^5 Bq ^{22}Na source deposited on a rhodium foil was sandwiched between the stacks of eight layers of PC polymer film. The thickness of the samples is adequate enough to absorb more than 99% of positrons emitted. Fast–fast coincidence spectrometer, which entails monitoring the signal (1.28 MeV) gamma ray from positron decay of the source as start time and 0.511 MeV gamma ray from the positron annihilation in the material sample under study as the end time, was used for recording the PAL spectra. Fast BaF_2 scintillators coupled to Phillips XP2020 photomultipliers were used. ORTEC constant fraction differential discriminators (CFDD) were used for selecting energy and providing time signals to time to amplitude converter (TAC). Spectra were obtained as a function of acquiring time. The time resolution (FWHM) of prompt spectra was 291 ps. Fig. 1. shows the lifetime spectra for virgin and irradiated Makrofol-KG polycarbonate samples.

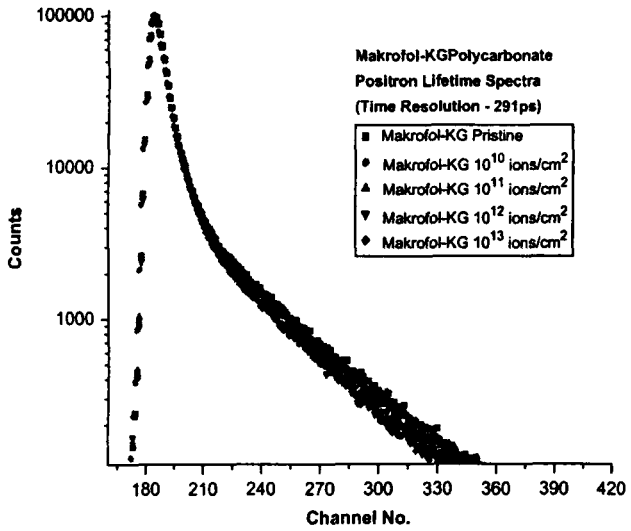

Fig. 1. Positron lifetime spectra of Makrofol-KG polycarbonate.

2.4. Data analysis of PAL spectra

A significant fraction of positron injected into a polymer migrate to the free volume holes where they preferentially form and annihilate from a bound-state Ps. Ps exists in either a para-positronium (*p*-Ps: anti-parallel electron–positron spin) or ortho-positronium (*o*-Ps: parallel spins) state with a relative formation rate of 1:3 (Mogensen, 1995). In vacuum *p*-Ps has a lifetime of 125 ps and annihilates via two photons while *o*-Ps annihilates via three photons with lifetime 142 ns. During its lifetime in a hole the *o*-Ps undergoes numerous collisions with the molecules of the surrounding medium, resulting in a finite probability of the positron annihilating with an electron other than its bound-state partner (and of opposite sign). This pickoff process leads to a drastically reduced *o*-Ps lifetime (few ns) compared with vacuum and annihilation into two photons instead of three. All obtained PAL spectra were analyzed by finite term lifetime analysis employing the PATFIT program (Kirkegaard et al., 1989). It decomposes a PAL spectrum into 2–5 terms of negative exponentials. In polymers three lifetime results give the best fit $\chi^2 < 1.1$ and most reasonable standard deviation (Jean and Dai, 1993). Thus LT spectra may be described as a sum of three discrete negative exponentials $s(t) = \Sigma(1/\tau_i)I_i \exp(-t/\tau_i)$, $(i = 1 \ldots 3)$ which originates from *p*-Ps, free positron annihilation and from *o*-Ps annihilation in crystalline and amorphous regions of polymer. It is generally accepted that $\tau_{o\text{-Ps}}$ can serve as a measure of the free volume hole size seen by Ps. In a simple quantum mechanical model Ps is assumed to be confined in a spherical potential well of radius R and infinite depth. The Ps overlaps with molecules in a thin layer δR at the potential well. This model leads to correlation between $\tau_{o\text{-Ps}}$ and radius of the hole R (Eldrup et al., 1981)

$$\tau_{o\text{-Ps}} = 0.5\left[1 - \frac{R}{R+\delta R} + \frac{1}{2\pi}\sin\left(\frac{2\pi R}{R+\delta R}\right)\right]^{-1} \quad (1)$$

where $\delta R = 0.166$ nm is an empirical parameter and $\tau_{o\text{-Ps}}$ is given in ns. Despite the simplicity of the model assumption, Eq. (1) seems to hold surprisingly well in region of R up to 1 nm and constitutes a base for numerous PAS applications to the studies of free volume and its changes in polymers (Jean, 1995a,b). This equation can also be used for cylindrical free volume (pore) with the value of δR set at 0.196 nm (Ciesielski et al., 1998). In this case, for the same lifetime value, one gets a higher value for the radius as compared with the spherical case.

The fractional free volume is $f_v = CV_f I_3 = C(\frac{4}{3}\pi R^3)I_3$, where C is a structural constant empirically determined to be ~ 0.0018 from an independent isochronal experiment (Wang et al., 1990) and I_3 is the intensity (in %) of *o*-Ps.

3. Results and discussion

PAL spectra for virgin and irradiated samples were analyzed in terms of three lifetime components, each lifetime corresponding to the average annihilation rate of a positron in a different state. The shortest lifetime component ($\tau_1 = 0.165$–0.178 ns and $I_1 = 40.92$–46.61%) belongs to the annihilation of *p*-Ps atoms, while the intermediate one ($\tau_2 = 0.384$–0.414 ns and $I_2 = 31.63$–38.38%) arises from the free annihilation of positrons in the polymer matrix. The longest lived component ($\tau_3 = 2.090$–2.218 ns and $I_3 = 16.11$–22.54%) is attributed to the *o*-Ps atoms in free volumes of amorphous regions of polymer via the pick-off annihilation. Values of lifetime and intensity are presented in Table 1 and radius, free volume, fractional free volume and radius calculated for cylindrical free volume are presented in Table 2. *o*-Ps lifetime is directly correlated to the free volume whereas the intensity of this component contains information about free volume hole concentration. The decrease in τ_3 is related to the change in the free volume as a result of the formation of new bonds or cross-linking. This decrease in τ_3 implies some shrinking of inner and inner-chain of free volume holes (i.e. impact structure was attained). Fig. 2 shows the variation of average free volume (V_f) with ion fluence. V_f is found to decrease from 118.59 to 106.11 Å^3 with a decrease in 10.52% at 10^{13} ions/cm^2. Kobayashi et al. (1994) have attributed the small decrease in free volume in PEEK due to electron irradiation, to intermolecular cross-linking. The results of Lee (1999) and Lee et al. (1999) for PMMA on ion irradiation indicate that high LET produce a high concentration of free radicals over many neighboring molecular chains, facilitating track overlap and enhancing cross-linking over scission while low LET affects only a simple molecular chain, leading to chain scission. In our earlier PAL measurements (Kumar and Prasad, 2004, 2005; Kumar et al., 2003, 2004a,b, 2006) on polymers (i) irradiated with different SHIs to low fluences (10^5–10^6 ions/cm^2), average free volume has been found to increase with fluence and has been attributed to the chain scission along the tracks and (ii) irradiation to high fluences leads to the decrease in free volume, indicating cross-linking of scissioned segments.

In the present case I_3 is found to decrease with ion fluence and, more generally speaking, cross-linking resulting in a loss in the number of those free spaces where Ps can form in either the crystalline or amorphous phases can be responsible for this.

Table 1
Lifetime and intensity of unirradiated and irradiated Makrofol-KG polycarbonate

Fluence (ions/cm^2)	τ_1 (ns)	I_1 (%)	τ_2 (ns)	I_2 (%)	τ_3 (ns)	I_3 (%)
Unirradiated	0.176 ± 0.010	46.613 ± 2.22	0.409 ± 0.010	34.469 ± 2.11	2.218 ± 0.010	18.418 ± 0.17
10^{10}	0.174 ± 0.010	45.124 ± 2.18	0.405 ± 0.010	34.045 ± 2.01	2.214 ± 0.010	20.831 ± 0.16
10^{11}	0.178 ± 0.010	45.817 ± 2.21	0.414 ± 0.010	31.637 ± 2.11	2.210 ± 0.010	22.546 ± 0.17
10^{12}	0.165 ± 0.010	40.922 ± 2.27	0.388 ± 0.010	36.207 ± 2.16	2.196 ± 0.010	21.872 ± 0.16
10^{13}	0.166 ± 0.010	42.702 ± 2.35	0.384 ± 0.010	38.380 ± 2.25	2.090 ± 0.010	16.118 ± 0.16

Table 2
Lifetime parameters of *o*-Ps and radius of free volume hole in Makrofol-KG Polycarbonate

Fluence (ions/cm^2)	τ_3 (ns)	I_3 (%)	R spherical × 10^{-2} (nm)	V_f × 10^{-3} (nm)	F_v	R cylindrical × 10^{-2} (nm)
Unirradiated	2.218 ± 0.010	18.418 ± 0.17	30.48	118.590	4.038	35.98
10^{10}	2.214 ± 0.010	20.831 ± 0.16	30.44	118.143	4.429	35.94
10^{11}	2.210 ± 0.010	22.546 ± 0.17	30.41	117.795	4.780	35.90
10^{12}	2.196 ± 0.010	21.872 ± 0.16	30.29	116.410	4.583	35.76
10^{13}	2.090 ± 0.010	16.118 ± 0.16	29.37	106.118	3.613	34.67

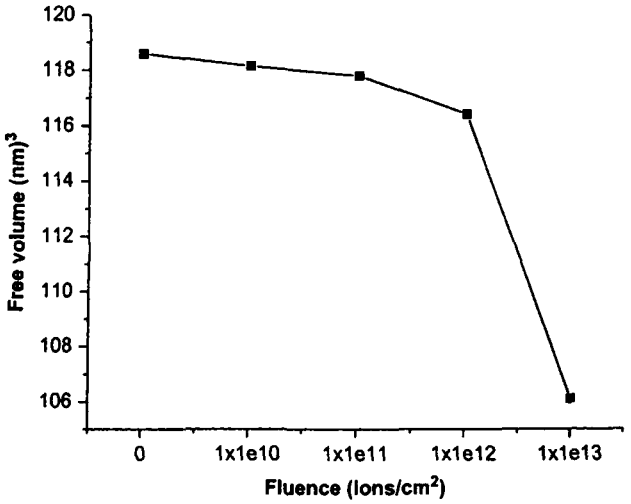

Fig. 2. Variation of average free volume (nm)^3 with the fluence (ions/cm^2).

Note that, on the basis of the spur model, one may further hypothesize that cross-linking would result in decrease in the diffusive properties of either e^+ or e^-, resulting in a lesser probability for Ps formation.

The cross-linking as an essential phenomenon, is known to be the most effective process in polystyrene, PN-6 and CR-39 polymers as bombarded with high energy particles (Klaumünzer et al., 1996; Kumar and Prasad, 2005, 2007; Kumar et al., 2006) due to the free radical recombination and various degradations, possibly resulting in the changes in amorphousity. For low LET, tracks develop far apart and independently; the deposited energy tends to be confined in one chain (not in neighboring chain) leading to scission (Lee et al., 1999; Fink et al., 1999). In case of high electronic LET, tracks overlap, the probability of two radical pairs to be in neighboring chains is increased and cross-linking is facilitated. The scission causes increase in the free volume whereas the cross-linking causes decrease in the free volume (Fink et al., 1999; Kumart et al., 2003, 2004a, b; Kumar and Prasad, 2004, 2005). At high fluences the track area where cross-linking is predominant becomes comparable to the sample area. This may explain the observed decrease in the *o*-Ps lifetime as observed in the present case.

4. Conclusion

Free volume study of 145 Mev Ne ion induced modifications in Makrofol-KG polycarbonate at various fluences was undertaken through positron annihilation lifetime measurements. Small decrease in *o*-Ps lifetime with the ion fluence was observed. Ion irradiation reduces the available free volume indicating the facilitation of cross-linking at high fluences. In the present case I_3 is found to decrease with ion fluence and, more generally speaking, cross-linking resulting in a loss in the number of those free spaces where Ps can form in either the crystalline or amorphous phases can be responsible for this. At high fluence scissioned segments cross-link randomly, resulting into the decrease in average free volume due to overlapping of the tracks. To our knowledge, there have not been reports of such studies of such heavy ion irradiation in Makrofol-KG polycarbonate.

Acknowledgments

The authors thank Dr. A.K. Sinha, Director, UGC-DAE Consortium for Scientific Research, Kolkata, for providing PAL facilities and constant encouragement. Thanks are also due to Dr. D. K. Srivastava, Variable Energy Cyclotron Centre, Kolkata, and staff of the cyclotron operation group for their help during irradiations. One of the authors, Prof. Rajendra Prasad, is thankful to All India Council of Technical Education, Government of India for providing Emeritus Fellowship to carry out this

work. Financial assistance provided by Department of Science and Technology (D.S.T.), Government of India to Dr. Rajesh Kumar as Young Scientist (Award No. SR/FTP/PS-31/2004) is gratefully acknowledged.

References

Ciesielski, K., Dawidowicz, A.L., Goworek, T., Jasinska, B., Wawryszczuk, J., 1998. Positronium lifetimes in porous vycor glass. Chem. Phys. Lett. 289, 5–41.

Durrani, S.A., Bull, R.K., 1987. Solid State Nuclear Track Detection. Pergamon Press, New York.

Eldrup, M., Lightbody, D., Sherwood, J.N., 1981. The temperature dependence of positron lifetimes in solid pivalic acid. J. Chem. Phys. 63, 51–58.

Fink, D., Muller, M., Ghosh, S., Dwivedi, K.K., Vacik, J., Hnatowicz, V., Cervena, J., Kobayashi, Y., Hirata, K., 1999. New ways of polymeric ion track characterization. Nucl. Instrum. Methods B 156, 170–176.

Ferain, E., Legras, R., 2001a. Pore shape control in nanoporous particle track etched membrane. Nucl. Instrum. Methods B 174, 116–122.

Ferain, E., Legras, R., 2001b. Efficient production of nanoporous particle track etched membranes with controlled properties. Radiat. Meas. 34, 585–588.

Fleischer, R.L., Price, P.B., Walker, R.M., 1975. Nuclear Tracks in Solids, Principles and Applications. University of California Press, Berkeley.

Jean, Y.C., 1990. Positron annihilation spectroscopy for chemical analysis: a novel probe for microstructural analysis of polymers. Microchem. J. 42 (1), 72–102.

Jean, Y.C., 1995a. Positron annihilation in polymers. Mater. Sci. Forum 59, 175–178.

Jean, Y.C., 1995b. In: Dupasquier, A., Mills Jr.,A.P. (Eds.), Positron Spectroscopy of Solids. IOS Publisher, Amsterdam, pp. 503–569.

Jean, Y.C., Dai, G.H., 1993. Free volume hole distribution of polymers probed by positron annihilation spectroscopy. Experiences of using the CONTIN program. Nucl. Instrum. Methods B 79, 362–365.

Jérôme, C., Demoustier-Champagne, S., Legras, R., Jérôme, R., 2000. Electrochemical synthesis of conjugated polymer wires and nanotubules. Chem. Eur. J. 6 (17), 3089–3093.

Kirkegaard, P., Pedersen, N.J., Eldrup, M., 1989. PATFIT-88, a Data Processing System for Positron Annihilation Spectra for Mainframe and Personal Computers. Riso National Laboratory, Rosklide, Denmark.

Klaumünzer, S., Zhu, Q.Q., Schnabel, W., Schumacher, G., 1996. Ion beam induced cross-linking of polystyrene still an unsolved puzzle. Nucl. Instrum. Methods B 116, 154–158.

Kobayashi, Y., Haraya, K., Hattori, S., Sasuga, T., 1994. Effect of electron irradiation on the free volume of PEEK studied by positron annihilation. Nucl. Instrum. Methods B 91, 447–449.

Kumar, R., Prasad, R. 2004. Study of positron annihilation lifetime of swift heavy ion irradiated polyamide nylon-6 polymer. In: Proceedings of the International Seminar on Advances in Polymer Technology, APT '04, Kochin, India, pp. 698–703.

Kumar, R., Prasad, R., 2005. 70 MeV carbon C^{5+} ion induced modification in polystyrene by positron annihilation. Radiat. Meas. 40, 750–753.

Kumar, R., Prasad, R., 2007. Ion induced modification in free volume in PN-6 and PES polymers by positron annihilation lifetime studies. Nucl. Instrum. Methods B 256, 238–242.

Kumar, R., Rajguru, S., Das, D., Prasad, R., 2003. SHI induced modification in CR-39 polycarbonate by positron annihilation lifetime studies. Radiat. Meas. 36, 51–154.

Kumar, R., Nath, B.K., Das, D., Prasad, R., 2004a. Positron annihilation lifetime measurements for C^{5+} ion irradiated Makrofol-N polycarbonate Ind. J. Phys. 78A 2, 221–223.

Kumar, R., Mahur, A.K., Dwivedi, K.K., Das, D., Prasad, R., 2004b. ^{197}Au ion irradiated modification in CR-39 by positron annihilation. Ind. J. Phys. 78A 2, 225–227.

Kumar, R., Ali, S.A., Mahur, A.K., Das, D., Naqvi, A.H., Virk, H.S., Prasad, R., 2006. Free volume study of 70 MeV carbon induced modification in polymers through positron annihilation. Nucl. Instrum. Methods B 244, 257–260.

Lee, E.H., 1996. Polyimides: Fundamentals and Applications, Vol. 54. Marcel Dekker Inc., New York.

Lee, E.H., 1999. Ion-beam modification of polymeric materials fundamental principles and application. Nucl. Instrum. Methods B 151, 29–41.

Lee, E.H., Rao, G.R., Mansur, L.K., 1999. LET effect on cross-linking and scission mechanisms of PMMA during irradiation. Radiat. Phys. Chem. 55, 293–305.

Mogensen, O.E., 1995. Positron Annihilation in Chemistry. Springer, Berlin.

Nakahishi, N., Jean, Y.C., 1988. In: Schrader, D.M., Jean, Y.C. (Eds.), Positron and Positronium Chemistry, Studies in Physical and Theoretical Chemistry, Vol. 57. p. 159.

Percolla, R., Calcagno, L., Foti, G., Ciavola, G., 1994. Ordering induced by swift ions in semi crystalline polyvinylidene fluoride. Appl. Phys. Lett. 65 (23), 2966–2968.

Piraux, L., Dubois, S., Demoustier-Champagne, S., 1997. Template synthesis of nanoscale materials using the membrane porosity. Nucl. Instrum. Methods B131, 357–363.

Piraux, L., Dubois, S., Duvail, J.L., Radulescu, A., Demoustier-Champagne, S., Ferain, E., Legras, R., 1999. Fabrication and properties of organic and metal nanocylinders in nanoporous membranes. J. Mater. Res. 14 (7), 3042–3050.

1988. In: Schrader, D.M., Jean, Y.C. (Eds.), Positron and Positronium Chemistry, Studies in Physical and Theoretical Chemistry, vol. 57. Elsevier, Amsterdam.

Tao, S.J., 1972. Positronium annihilation in molecular substances. J. Chem. Phys. 56 (11), 5499–5510.

Venkatesan, T., 1985. High energy ion beam modification of polymer films. Nucl. Instrum. Methods B 7/8, 461–467.

Wang, Y.Y., Nakanishi, H., Jean, Y.C., Sandreczki, T.C., 1990. Positron annihilation inamine-cured epoxy polymers-pressure dependence. J. Polym. Sci. B: Polym. Phys. 28, 1431–1441.

Wielunski, L.S., Clissold, R.A., Yap, E., McCulloch, D.G., McKenzie, D.R., Swain, M.V., 1997. Mechanical and structural modification of CR-39 polymer surface by 50-keV hydrogen and argon ion implantation. Nucl. Instrum. Methods B 127/128, 698–701.

Available online at www sciencedirect com
ScienceDirect
Nuclear Instruments and Methods in Physics Research B 266 (2008) 1783–1787
NIM B
Beam Interactions with Materials & Atoms
www elsevier com/locate/nimb

Positron lifetime studies of the dose dependence of nanohole free volumes in ion-irradiated conducting poly-(ethylene-oxide)–salt polymers

Rajesh Kumar [a], Udayan De [b], P.M.G. Nambissan [c], M. Maitra [d], S. Asad Ali [a], T.R. Middya [d], S. Tarafdar [d], F. Singh [e], D.K. Avasthi [e], Rajendra Prasad [a,*]

[a] Department of Applied Physics Z H College of Engineering and Technology Aligarh Muslim University Aligarh 202 002 India
[b] Variable Energy Cyclotron Centre IIAF Bidhan Nagar Kolkata 700 064 India
[c] Saha Institute of Nuclear Physics IIAF Bidhan Nagar Kolkata 700 064 India
[d] CMPR Centre Department of Physics Jadavpur University Kolkata 700 032 India
[e] Inter-University Accelerator Centre Aruna Asaf Ali Marg New Delhi 110 067 India

Received 25 September 2007, received in revised form 23 November 2007
Available online 29 January 2008

Abstract

Polymer based ion conducting materials have potential applications as an electrolyte and separator in the field of lithium batteries Solid polymer electrolytes for lithium batteries are one of the best applications The irradiation of polymeric materials with swift heavy ions results into the change of their free volume properties which have strong correlation with their macroscopic properties Poly-ethylene-oxide (PEO)–salt polymers were prepared using solution-cast method Irradiation of the films with 95 MeV oxygen (O^{6+}) ions from the pelletron accelerator at IUAC, New Delhi, India, to different fluences up to 10^{13} ions/cm^2 was carried out under high vacuum of the order of 4×10^{-6} Torr Nanosized free volume parameters in PEO-salt polymer complex have been studied by positron annihilation lifetime spectroscopy (PALS) and Doppler broadening spectroscopy (DBS) From orthopositronium (o-Ps) lifetime, free volume hole radius, free volume of micro voids and fractional free volume are computed Free volume changes with the fluence are studied The variation of o-Ps lifetime, mean free volume and fractional free volume with the ion fluence is studied o-Ps lifetime, free volume radius, mean free volume and fractional free volume decrease for the fluence 10^{10} and 10^{11} ions/cm^2 and then increase with fluences of 10^{12} and 10^{13} ions/cm^2 The S parameter showed a continuous decrease with increasing fluence of irradiation The intermediate lifetime τ_2 also showed a similar decrease These results indicate the occurrence of scission in the polymer chains and the fragmentation of larger free volumes into smaller ones

PACS 42 88 +h 78 70 Bj 71 20 Rv

Keywords PEO-salt polymer O^{6+} ion irradiation Positron lifetime Free volume S parameter

1. Introduction

Since the discovery of ionic conductivity in polymer-alkali salt systems in the mid-seventies, research and development into ion conductive polymers have become increasingly interesting from applied and theoretical aspects

Remarkable interest has been generated in polymers based ion conducting materials in the field of lithium batteries due to their potential application as an electrolyte and separator [1–3] Solid polymer electrolytes are one of the best applications for lithium batteries A polymer–salt electrolyte like one involving poly-(ethylene-oxide) or PEO is composed of a low lattice energy salt, (NH_4CLO_4 in the present work), dissolved in polymers with electronegative atoms in the polymer chains But the relatively free cations

* Corresponding author Tel +91 571 2742837 +91 9411654869
E-mail address rajendraprasad1@rediffmail com (R Prasad)

0168-583X/$ - see front matter © 2007 Elsevier B V All rights reserved
doi 10 1016/j nimb 2007 11 059

of the salt need suitably sized holes or free volumes in the polymer to carry electricity. The irradiation of polymeric materials with swift heavy ions (SHI) results into the change of their free volume properties which have strong correlation with their macroscopic properties. Radiation damage in metals and alloys can be understood fairly well from theory, however, radiation damage in complex systems like polymers cannot yet be predicted even roughly from theory [4,5]. Ion conducting polymers can be prepared by dissolving low lattice energy salts in to polar polymer material such as poly-(ethylene-oxide) (PEO).

A key issue is the understanding of the nature of the ionic transport mechanism of these electrolytes. Free volume or holes in solid polymer electrolytes (SPEs) or polymer solid electrolytes (PSEs) are required for ion movement and hence the electrical conduction. Since the work of Cohen and Turnbull [6], the transport processes in polymers are frequently described in terms of redistribution of the local free volume that appears due to the structural disorder in amorphous materials [7]. However, a limited amount of experimental data has been reported on free volume and radiation induced modification due to lack of suitable probes for open volumes of molecular dimensions.

Irradiation of polymers with swift heavy ion beams results into the change of free volume properties of polymeric material. Energetic ion beams can cause scission as well as cross-linking of the polymer chains leading to opposite effects and scission or cross-linking efficiency depends not only upon the polymer structure but also upon the characteristic of the radiation sources, namely ion energy fluence and ion species. All these factors make the study of irradiation effects of free volume very important and essential.

Positron annihilation lifetime spectroscopy or PALS has recently emerged as an excellent non-destructive and non-interfering nano-probe, capable of measuring the free volume hole size (of nm order radius) in polymers with high detection efficiency [8–10]. Previous study demonstrates that the local free volume decreases with increasing salt content [10,11]. It is known that the conductivity of SPEs can be varied to some extent by changing the compositions, thus making it an interesting field of study [12–14]. It has been found that electrical conductivity in PEO complexes is induced by the addition of NH_4CLO_4 [13,15] and it increases for low percentage as the added ionic salt provides salt ions as charge carriers. But salt addition in excess of 19% leads to a fall in conductivity. Thus the present work has been carried out on PEO-salt complex with 17% salt. Free volume study by PALS for pristine sample and the samples irradiated with ions to different fluences has been undertaken to investigate the SHI induced modification in free volume properties.

2. Experimental method

Solution-cast films each of total mass 3 g of PEO (BDH, England) and of average molecular weight 600 kg/mol complexed with NH_4ClO_4 (Fluka AG, 99.5% purity) were prepared in salt concentration of 17%. PEO salt polymer that form the sample was around 170 μm in thickness. Pure PEO is non-conducting while its complexes $PEO_{(1-x)}(NH_4ClO_4)_x$ with weight fraction $x = 17\%$ is an ion conducting polymer. Polymer samples were mounted in a vaccum shielded vertical sliding ladder and were exposed in the general purpose scattering chamber (GPSC) under high vacuum ($\sim 4 \times 10^6$ Torr) to 95 MeV oxygen ion beam at the 15 UD Pelletron accelerator at Inter-University Accelerator Centre, New Delhi, India to different fluences. To expose the whole target area uniformly, the beam was scanned in the x–y plane.

Positron annihilation lifetime (PAL) and Doppler broadening (DBA) measurements were carried out at the Saha Institute of Nuclear Physics (SINP), Kolkata, India, using a ^{22}Na source of approximately strength 400 kBq and a standard γ–γ coincidence setup. The source was in the form of residual deposit on a thin (~ 2 mg cm^{-2}) nickel foil and covered by an identical foil. The source was sandwiched between the stacks of the polymer complex sample. The thickness of the stacks was ensured sufficient enough to make the annihilation of all positrons within the sample.

The coincidence spectrometer had a resolution of 240 ps (full width at half maximum) for the γ-rays from ^{60}Co source. The spectra were analyzed using computer programs RESOLUTION and POSITRONFIT [16]. Measurement of broadening of the spectrum of Doppler energy shifted annihilation γ-rays was also carried out and line shape parameters S and W were estimated. S and W are representative of the central and wing regions, corresponding to the annihilation of positrons with valence and core electrons [17]. DBS spectra were recorded using a high resolution (1.28 keV FWHM at 511 keV) high purity Ge detector.

3. Results and discussion

The three lifetime components decomposed from the positron lifetime spectra arise from the annihilation of para positronium (p-Ps, $\tau_1 \sim 155$–175 ps), free positron annihilation ($\tau_2 \sim 300$–400 ps) and ortho positronium pick off process (o-Ps, $\tau_3 \sim 1.5$–3.5 ns) [9,18]. In polymers, o-Ps is formed in small free volume (holes) that appears due to their (static or dynamic) structural disorder. Due to pick off annihilation of o-Ps with an electron other than its bound one and with opposite spin during a collision with a molecule in hole wall, the o-Ps lifetime is reduced from its value 142 ns (in a vacuum) to the low ns range [19]. Based on a semi empirical model [8,9], the o-Ps pick off annihilation lifetime τ_{po} is related to the hole (assumed spherical) radius r_h via

$$\tau_{po} = 0.5\ \text{ns}\left[1 - \frac{r_h}{r_h + \delta_r} + \frac{1}{2\pi}\sin\left(\frac{2\pi r_h}{r_h + \delta_r}\right)\right]^{-1} \quad (1)$$

where $\delta r = 1.66$ Å, a length parameter, called the electron layer thickness that accounts for the overlap of the positron

and the electron wave functions. When spin conversion and chemical quenching of Ps are negligible, the experimental *o*-Ps lifetime is described by equation $\tau_3 = \tau_{po}$. δr has been determined by fitting the experimental values of τ_3 obtained for the material with known hole size [19]. This long-lived component, τ_3, attributed to *o*-Ps pick off annihilation in free volume, is very sensitive to the structural changes in the polymer.

When the hole dimensions are distributed with a width δV around the average volume V, a corresponding distribution of *o*-Ps lifetime is expected. From this relation, the free volume radius r_h is calculated and the mean value of the free volume hole V_h is given as

$$V_h = \frac{4\pi r_h^3}{3}$$

The fractional free volume F_v can be estimated as $F_v = CV_hI_3$, where C is a structural constant evaluated from an independent isochronal experiment and is determined empirically to be ~0.0018 [20].

The intensity of *o*-Ps (I_3) that is proportional to the probability of positronium (Ps) formation, in the past has been related to the concentration of free volume holes in the polymer [21]. However, it was found that I_3 is also affected by a number of other non-structural variables [22–27].

The positron lifetimes and intensities for PEO complex are presented in Table 1. Table 2 shows the results obtained from *o*-Ps lifetime τ_3 for the values of the free volume hole radius r_h and volume of free holes V_h for the pristine samples and irradiated with 95 MeV O^{6+} ion beam to different fluences. The variation of V_h and F_v as a function of ion fluence are shown in Figs. 1 and 2.

From the above tables, it is seen that the *o*-Ps lifetime τ_3 decreases for the fluences 10^{10} and 10^{11} ions/cm^2 and then increases for 10^{12} and 10^{13} ions/cm^2. This is contrary to our earlier measurements [28,29] on CR-39 polycarbonate irradiated with ^{40}Ar and ^{197}Au ions to low fluences of 10^5 ions/cm^2 and Makrofol-N polycarbonate irradiated with C ions to 10^6 ions/cm^2 where free volume was found to increase with fluences and has been attributed to the chain scission along the track. The results on CR-39 polycarbonate, polystyrene and polyamide nylon-6 [20,30] irradiated with C ions to higher fluences indicated the facilitation of cross-linking [28]. The modification (scission or cross-linking) due to ion irradiation depends essentially on the polymer and energy loss per unit path length or linear energy transfer (LET). Thus the dominance of scission and cross-linking will depend on polymer and LET. For low LET spurs develop far apart and independently, the deposited energy tends to the confined in one chain (not in the neighboring chain) leading to scission [31,32]. In the case of High LET, tracks have large effective radius and spurs overlap more compactly, the probability of two radical pairs to be in neighboring chains is increased and cross-linking is facilitated. The scission causes increase in the free volume whereas cross-linking causes decrease in available free volume [32]. The intensity of the *o*-Ps lifetime component I_3 shows almost no change up to 10^{12} ions/cm^2 and then a slight decrease at 10^{13} ions/cm^2. Values of S parameter are given in Table 2. Generally the production of more and more vacancy-type defects during increased dose of irradiation should have caused an increase of the S parameter. On the contrary, the S parameter continuously decreased due to the irradiation. The initial decrease of the longer lifetime τ_3 indicated a decreasing free volume and could support the initial fall of S as well. This should have happened if free volume defects of sizes relatively smaller than the initially present ones are freshly created during the irradiation. However, the nearly constant intensity I_3 does not support such a possibility. The intermediate lifetime τ_2 continuously decreases and levels off to a constant at the largest dose of irradiation while its intensity I_2 shows the opposite trend, indicating that vacancy cluster-type defects less than the sizes of free volume defects are created during

Table 1
Positron lifetime and intensities of unirradiated and irradiated poly-(ethylene-oxide) salt polymer

Fluence (ions/cm^2)	τ_1 (ns)	I_1 (%)	τ_2 (ns)	I_2 (%)	τ_3 (ns)	I_3 (%)
Unirradiated	0.147 ± 0.003	39.50 ± 1.2	0.392 ± 0.006	45.3 ± 1.1	1.702 ± 0.012	15.2 ± 0.19
10^{10}	0.145 ± 0.003	39.3 ± 1.2	0.391 ± 0.006	45.7 ± 1.1	1.685 ± 0.012	15.0 ± 0.19
10^{11}	0.147 ± 0.004	38.4 ± 1.4	0.382 ± 0.007	45.9 ± 1.3	1.623 ± 0.012	15.6 ± 0.21
10^{12}	0.145 ± 0.003	37.2 ± 1.2	0.371 ± 0.005	48.8 ± 1.1	1.820 ± 0.011	14.0 ± 0.13
10^{13}	0.141 ± 0.003	36.3 ± 1.2	0.369 ± 0.005	48.6 ± 1.1	1.876 ± 0.011	15.0 ± 0.14

Table 2
The lifetime parameters of *o*-Ps, radius of free volume hole, mean free volume, fractional free volume and S parameter in poly-(ethylene-oxide) salt polymer

Fluence (ions/cm^2)	τ_3 (ns)	I_3 (%)	r_h (Å)	V_h (Å^3)	F_v	S Parameter
Unirradiated	1.702 ± 0.012	15.2 ± 0.19	2.565 ± 0.012	70.68 ± 0.57	1.93 ± 0.03	0.4059 ± .0010
10^{10}	1.685 ± 0.012	15.0 ± 0.19	2.544 ± 0.012	68.95 ± 0.56	1.86 ± 0.03	0.4035 ± .0010
10^{11}	1.623 ± 0.012	15.6 ± 0.21	2.481 ± 0.013	63.96 ± 0.58	1.80 ± 0.03	0.4040 ± .0010
10^{12}	1.820 ± 0.011	14.0 ± 0.13	2.684 ± 0.011	80.98 ± 0.58	2.04 ± 0.03	0.4026 ± .0010
10^{13}	1.876 ± 0.011	15.0 ± 0.14	2.739 ± 0.010	86.06 ± 0.55	2.32 ± 0.03	0.4018 ± .0010

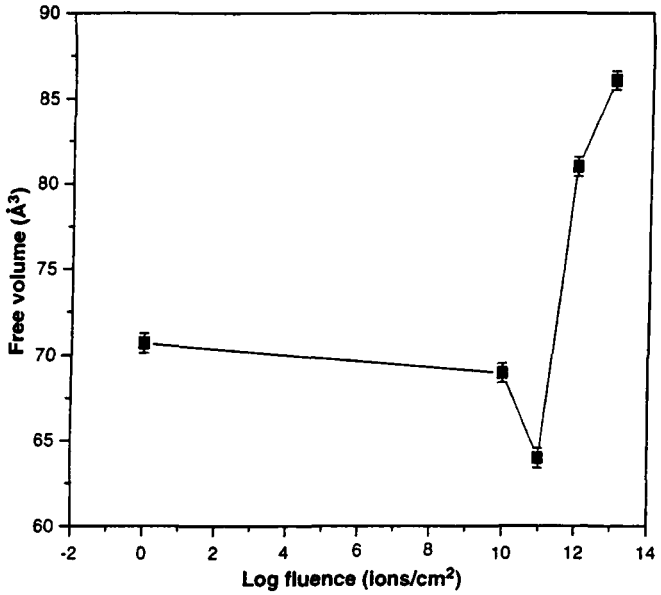

Fig 1 Variation of mean free volume (V_h) with the fluence (ions/cm^2)

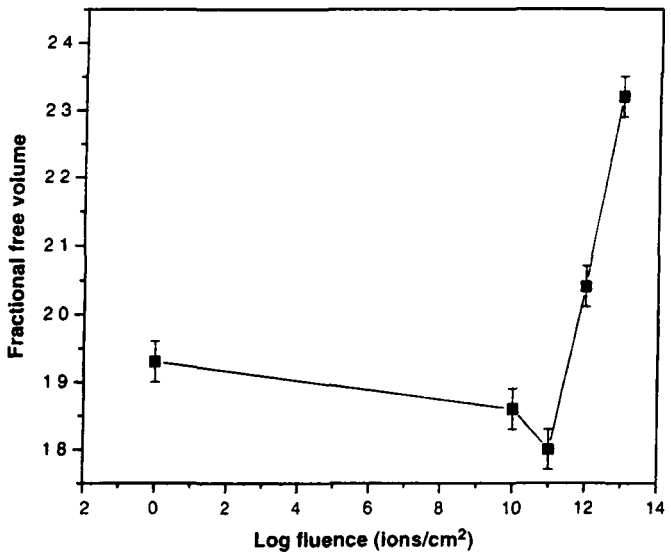

Fig 2 Variation of fractional free volume (F_v) with the fluence (ions/cm^2)

the irradiation Since such defects, owing to their smaller sizes, do not favor the formation of positronium (the origin of τ_3), the peak of the Doppler broadened line shape no more become sharper and the S parameter decreases accordingly

4. Conclusion

Solution cast films of PEO-salt polymer were irradiated to different fluences with O ion beam of 95 MeV energy. o-Ps lifetime τ_3 obtained from PAL studies, free volume radius r_h and mean free volume decrease for the fluences 10^{10} and 10^{11} ions/cm^2 and then increase with 10^{12} and 10^{13} ions/cm^2 The results are contrary to our earlier study of SHI induced modifications in pure polymer carried out through PAL measurements The intensity of the o-Ps lifetime component I_3 shows only minor variation at highest fluence The S parameter showed a continuous decrease with increasing fluence of irradiation The intermediate lifetime τ_2 also showed a similar decrease These results indicate the occurrence of scission in the polymer chains and the fragmentation of larger free volumes into smaller ones

Acknowledgments

The authors wish to thank, Chairman, Department of Applied Physics, Aligarh Muslim University, Aligarh for providing the facilities for this work Prof Rajendra Prasad wishes to thank, All India Council of Technical Education, Government of India for providing Emeritus Fellowship to carry out this work. Financial assistance provided by Department of Science and Technology (DST), Government of India to Dr Rajesh Kumar as Young Scientist under Fast Track Scheme (Award No SR/FTP/PS-31/2004) is gratefully acknowledged

References

[1] J R MacCallum, C A Vincent (Eds), Polymer Electrolyte Reviews I and II, Elsevier, London, 1987 and 1989
[2] P V Wright, Electrochim Acta 43 (1998) 1137
[3] F M Gray, Polymer Electrolyte, RSC Materials Monographs, The Royal Society of Chemistry, Information Services, Letchworth, UK, 1997
[4] J Davenas, I Stevenson, N Celette, S Cambon, J L Gardette, A Rivaton, L Vignoud, Nucl Instr and Meth B 191 (2002) 653
[5] Rajesh Kumar, Rajendra Prasad, Y K Vijay, N K Acharya, K C Verma, U De, Nucl Instr and Meth B 212 (2003) 221
[6] M H Cohen, D Turnbull, J Chem Phys 31 (1959) 1164, D Turnbull, M H Cohen, J Chem Phys 52 (1970) 3038
[7] J Prez, Physics and Mechanics of Amorphous Polymers, A A Balkema, Rotterdamm, Brookfield, 1998
[8] S J Tao, J Chem Phys 56 (1972) 5499
[9] Y C Jean, Microchem J 42 (1990) 72 in Y-J He B-S Cao Y C Jean (Eds) Positron Annihilation Proceedings of the 10th International Conference on Positron Annihilation, Mater Sci Forum, Vols 175–178 (1995) 59
[10] M Forsyth, P Meakin, D R MacFarlane, A J Hill, J Phys Condens Matter 7 (1995) 7601
[11] C A Furtado, G Goulart Silva, J C Machado, M A Pimenta, T A Silva, J Phys Chem B 103 (1999) 7102
[12] A Nitzan, M A Ratner, J Phys Chem 98 (1994) 1765
[13] S Tarafdar, T R Middya, A Banerjee D Sanyal, D Banerjee K C Verma U De Solid State Ion 152–153 (2002) 235
[14] Minakshi Maitra K C Verma, Mrinal Sinha, Rajesh Kumar, T R Middya, S Tarafdar, P Sen, S K Bandyopadhyay, Udayan De, Nucl Instr and Meth B 244 (2006) 239
[15] Minkashi Maitra, T R Middya, U De, S Tarafdar, Ionics 10 (2004) 68
[16] P Kirkegaard, M Eldrup, O E Mogensen, N J Pedersen, Comput Phys Commun 23 (1981) 307
[17] P Ashoka-Kumar, K G Lynn, D O Welch, J Appl Phys 76 (1994) 4935
[18] O E Mogensen, Positron Annihilation in Chemistry, Springer-Verlag, Berlin, Heidelberg, New York, 1995
[19] H Nakanishi, S J Wang, Y C Jean, in S C Sharma (Ed), Positron Annihilation Studies of Fluids World Scientific Publishing Co Ltd Singapore, 1988, p 292
[20] Rajesh Kumar, S A Ali, A K Mahur, D Das, A H Naqvi, H S Virk, Rajendra Prasad, Nucl Instr and Meth B 244 (2006) 257
[21] V P Shantarovich, J Radioanal Nucl Chem 210 (1996) 357
[22] C Wastlund, F H J Maurer, Polymer 39 (1998) 2897
[23] M Welander, F H J Maurer, Mater Sci Forum 105–110 (1992) 1811
[24] D Cangialosi, H Schut, M Wbbenhorst, J van Turnhout, A van Veen, Radiat Phys Chem 68 (2003) 507
[25] C L Wang, K Hirata, J Kawahara, Y Kobayashi, Phys Rev B 58 (1998) 14864
[26] A Alba Garcia, L D A Siebbeles, H Schut, A van Veen, Radiat Phys Chem 68 (2003) 515
[27] J Zrubcova, J Kristiak, W B Pedersen, N J Pedersen, M Eldrup, Mater Sci Forum 363 (2001) 359
[28] Rajesh Kumar, S Rajguru, D Das, Rajendra Prasad, Radiat Meas 36 (2003) 151
[29] Rajesh Kumar A K Mahur D Das K K Dwivedi Rajendra Prasad Indian J Phys 78 A (2) (2004) 225
[30] Rajesh Kumar Rajendra Prasad Radiat Meas 40 (2005) 750
[31] E H Lee, Nucl Instr and Meth B 151 (1999) 29
[32] D Fink M Muller, S Ghosh, K K Dwivedi, J Vacik, V Hnatowicz, J Cervena, Y Kobayashi K Hirata, Nucl Instr and Meth B 156 (1999) 170

Available online at www.sciencedirect.com
ScienceDirect
Nuclear Instruments and Methods in Physics Research B 266 (2008) 1788–1792
NIM B
Beam Interactions with Materials & Atoms
www.elsevier.com/locate/nimb

Study of optical band gap and carbonaceous clusters in swift heavy ion irradiated polymers with UV–Vis spectroscopy

Rajesh Kumar [a], S. Asad Ali [a], A.K. Mahur [a], H.S. Virk [b], F. Singh [c], S.A. Khan [c], D.K. Avasthi [c], Rajendra Prasad [a,*]

[a] Department of Applied Physics, Z.H. College of Engineering and Technology, Aligarh Muslim University, Aligarh 202 002, India
[b] 360 Sector-71, SAS Nagar (Mohali), Chanigarh 160 071, India
[c] Inter University Accelerator Centre, Aruna Asaf Ali Marg, New Delhi 110 067, India

Received 24 September 2007; received in revised form 4 December 2007
Available online 15 January 2008

Abstract

The formation of carbonaceous clusters in swift heavy ion irradiated polymer films has been investigated extensively. The information about these clusters may be obtained from Ultraviolet–Visible (UV–Vis) spectroscopic studies. The optical band gap (E_g), calculated from the absorption edge of the UV spectra of these polymers can be correlated to the number of carbon atoms (N) in a cluster with the Tauc equation. Films of 50 μm, 80 μm, 125 μm, 250 μm thicknesses of PET, PTFE, PMMA and PES polymers, respectively, were irradiated with Si^{8+} ions of energy 100 MeV to different fluences from 10^{10} to 10^{13} ions/cm^2 at Pelletron accelerator, Inter University Accelerator Centre, New Delhi, India. UV–Vis absorption studies show that optical energy gap decreases with transferred energy density of the ion beams. The energy band gap (E_g) values were computed from the absorption edge in the 200–800 nm region with the Tauc relation. The values vary from 3.86 to 1.61 eV for the pristine and various irradiated polymer samples. Maximum change of 40% is observed in PES irradiated to 10^{13} ions/cm^2. The cluster size shows a variation in the range of 79–454 carbon atoms per cluster for the polymers studied here.

PACS: 61.80.Jh; 78.4.Me; 79.20.Rf

Keywords: SHI irradiation; Ion beam modification; UV–Vis spectra; Carbon clusters

1. Introduction

Interest in ion beam irradiation of polymers has increased in recent years, prompted by the ion induced improvements of the mechanical, optical and electrical properties of various polymer substrates [1–5]. A wide variety of material modification in polymers has been studied by using ion irradiation technique [6–9]. Extensive research has focused onto swift heavy ions (MeV's energy) probably because of good controllability and the large penetration length in polymers. High energy ion irradiation tends to damage polymers significantly by electronic excitation and ionization. The nature of defects and the relative radiative sensitivity of different polymers depend on the properties such as their composition and molecular weight, on the charge, mass and energy of the impinging ion and also on the environmental conditions during irradiation. The use of ion beam irradiation is getting high impetus as chemical composition and the related physical properties of the polymers can be modified in a controlled way by easy to control parameters like the ion fluence. The effect of ionizing radiation on polymers is generally classified in to main chain scission (degradation) and cross-linking. These may initiate modifications such as formation of chemical bonds between different molecules, intermolecular cross linking, irreversible cleavage of bonds (scission) in the main chain, fragmentation of molecules and the formation of saturated and unsaturated groups with stimulated evolution of gases

* Corresponding author. Tel.: +91 571 2742837; mobile: +91 941 1654869.
E-mail address: rajendraprasad1@rediffmail.com (R. Prasad).

0168-583X/$ - see front matter © 2008 Elsevier B.V. All rights reserved.
doi:10.1016/j.nimb.2008.01.010

[9] At very high ion fluences carbonization may also take place [10]

In the present study modification in optical properties of four polymers induced by Si ion beam irradiation has been investigated by UV–Vis spectroscopy The aim is to investigate the modification in optical properties by swift heavy ion, Si in different group of polymers such as PET, PTFE, PMMA, PES films, having wide applications and their dependence on ion fluence

Polyethylene terephthalate (PET) is polyester having a high melting point due to the presence of aromatic ring and has a very good mechanical strength It is semi crystalline in nature and is resistant to heat and moisture and virtually unattacked by many chemicals It has extensive use in textile fibres Mishra et al [11] studied the changes in its thermal and chemical properties by exposing it to electrons and protons Steckenreiter et al [12] did an in depth study of chemical modification of PET exposed to Mo and Kr ions Recently Liu et al [13] and Zhu et al [14] have extended its study by exposing it to heavy ions of Ar, Kr, Xe and U having energy in the range of 1 4–2 7 GeV Singh et al [15] too have also recently reported a study on the electrical and structural properties of PET films modified by 50 MeV Li ions The Molecular structure of PET is

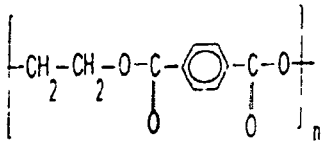

Aromatic polymers such as polyethersulphone (PES) are finding extensive use in electronics For particular sensor applications the physical properties of these films may be tailored It has been shown that ion irradiation improves the sensor properties of PES films [16,17] In our earlier studies [18,19] investigation of change in free volume properties and physical and chemical response of PES films modified by 70 MeV carbon ions were carried out Its molecular structure is

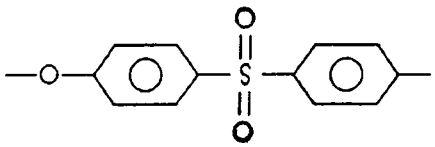

Polymethyl methacrylate (PMMA) is an excellent material which is easy to structure and has the desired optical properties [20] PMMA, known as a positive photo-resist for its degradation upon irradiation, has been the subject of more investigations in radiolysis than many other polymers This was partly due to a growing interest in the application of PMMA in ion beam lithography and in the semiconductor industry [21] We have chosen PMMA polymer for our present investigation because of its wide range of utilization such as it is finding extensive use in expending optical networks in the field of telecommunication The Molecular structure of PMMA is

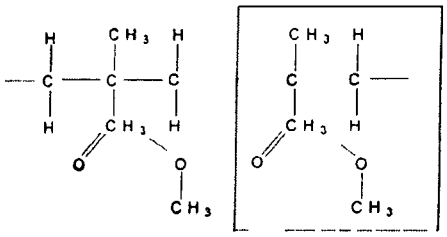

Poly(tetrafluoroethylene) PTFE has been classified for many years as a polymer that undergoes main chain scission by irradiation [22] In some recent papers [23–26] it was described that PTFE is cross linked by ionizing radiation in an oxygen-free atmosphere at a temperature above its melting point Therefore, the effect of irradiation on high crystalline PTFE (at room temperature) has to be smaller than on amorphous PTFE (in the melt) Additionally further qualitative changes are expected by irradiation of molten PTFE Lappan et al [27] have also studied the behavior of PTFE in such special irradiation conditions. Its structure is

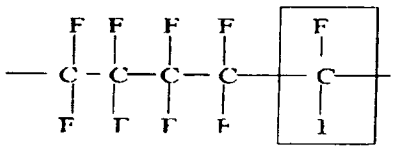

2. Experimental

Films of 50 μm, 80 μm, 125 μm and 250 μm thickness of PET, PTFE, PMMA and PES polymers were procured from Goodfellow, Cambridge Ltd England (UK) Without any further treatment, the specimens of the size (1 5 × 1 5 cm^2) were prepared for irradiation Polymer samples, mounted on a vacuum shielded vertical ladder were irradiated in the General Purpose Scattering Chamber(GPSC) under high vacuum of the order of 4×10^{-6} Torr by using 100 MeV Si^{8+} ion beam with a beam current of four particle nano ampere (pnA) available from the 15 UD Pelletron accelerator at Inter University Accelerator Centre (IUAC), New Delhi [28,29] In order to expose the whole target area, the beam was scanned in the X–Y plane Thus thermal damage effects were avoided by using low current and X–Y scanner The ion beam fluence was measured by integrating the ion charge on the sample ladder, which was insulated from the chamber The fluence was varied in the range of 10^{10}–10^{13} ions/cm^2 The nature of the ion induced optical changes has been analysed by using the HITACHI U3300 UV–Visible spectrometer in the wavelength range 200–1100 nm

3. Results and discussion

In the present study, significant changes of different amounts have been observed in optical response of the

polymers after irradiation with Si ions. UV–Vis spectroscopy gives an idea about the value of optical band gap energy (E_g) and thus provides an important tool for investigation. The absorption of light energy by polymeric materials in the ultraviolet and visible regions involves promotion of electrons in σ, π and n-orbitals from the ground state to higher energy states which are described by molecular orbital [30]. The electronic transitions (→) that are involved in the ultraviolet and visible regions are of the following type $\sigma \rightarrow \sigma^*$, $n \rightarrow \pi^*$, and $\pi \rightarrow \pi^*$. Many of the optical transitions which result from the presence of impurities have energies in the visible part of the spectrum; consequently the defects are referred to as colour centers [31]. Ion beam interaction with polymers generates damage which leads to the formation of new defects and new charge states.

The absorption spectra with UV–Vis spectrophotometer carried out on virgin and irradiated polymer samples are presented in Figs. 1–4. Optical absorption spectra of the virgin sample (Figs. 1–4(a)) show a sharp decrease with increasing wavelength up to a certain value, followed by a plateau region, except in the case of PTFE spectra, Figs. 1–4((b)–(e)) show the optical spectra for different polymer samples irradiated to various fluences. It is observed that optical absorption increases with increasing fluence and this absorption shifts from UV–Vis towards the visible region for all irradiated polymer samples as the fluence increases. The increase in absorption with irradiation may be attributed to the formation of a conjugated system of bonds due to bond cleavage and reconstruction [32].

The optical absorption method can be used for the investigation of the optically induced transitions and can provide information about the bond structure and energy gap in crystalline and non-crystalline materials [11]. The optical band gap E_g is determined using Tauc's expression [33].

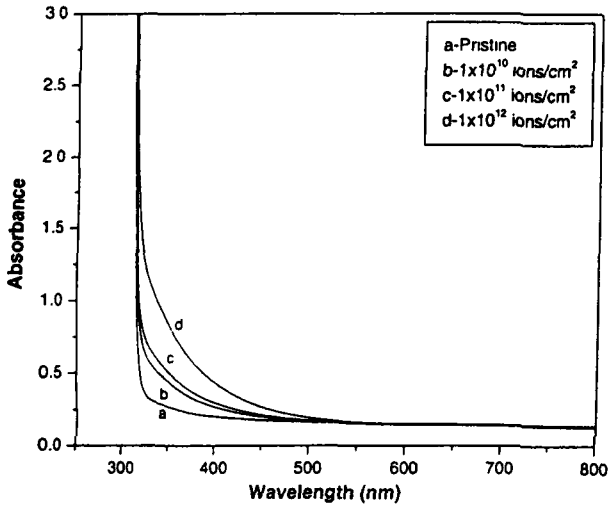

Fig. 1. Optical absorption spectra of PET polymer samples: pristine and irradiated with 100 MeV Si^{8+} ion beam

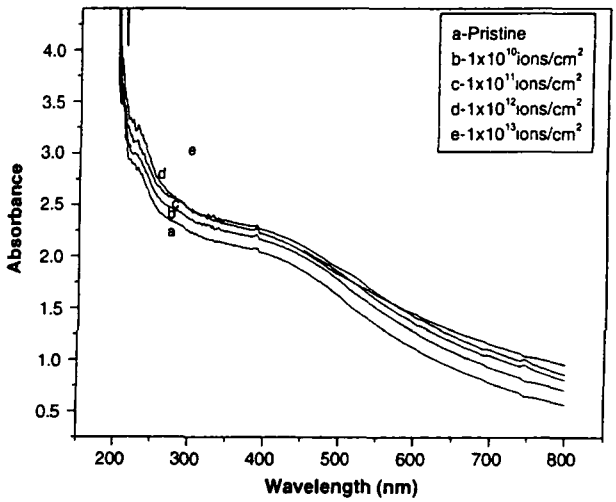

Fig. 2. Optical absorption spectra of PTFE polymer samples: pristine and irradiated with 100 MeV Si^{8+} ion beam.

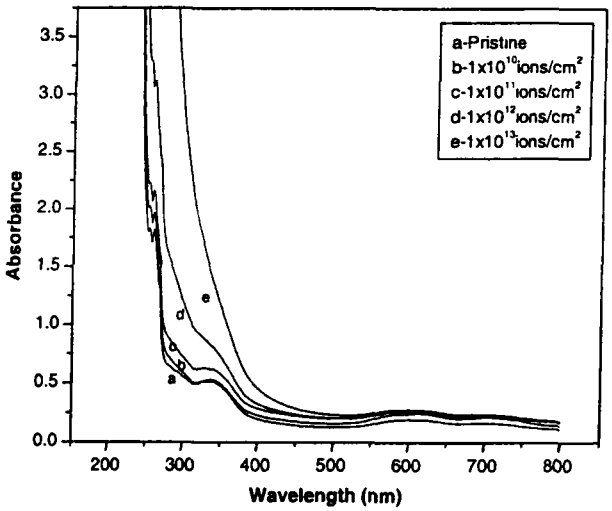

Fig. 3. Optical absorption spectra of PMMA polymer samples: pristine and irradiated with 100 MeV Si^{8+} ion beam.

$$\omega^2 \varepsilon(\lambda) = (h\omega - E_g)^2, \tag{1}$$

where $\varepsilon_2(\lambda)$ is the optical absorbance, λ the wavelength and $\omega = 2\pi\upsilon$ the angular frequency of the incident radiation. Solving Eq. (1) one gets

$$\sqrt{\varepsilon_2}/\lambda = h/2\pi\lambda - E_g/2\pi c.$$

Therefore, the plot of $\sqrt{\varepsilon_2}/\lambda$ versus $1/\lambda$ must be a straight line with an intercept of $-E_g/2\pi c$. If θ is the inclination of the straight line with X-axis, the slope of the straight line should be $\tan\theta$ and we have

$$\frac{h}{2\pi} = \frac{E_g/2\pi c}{1/\lambda_g},$$

where $1/\lambda_g$ (λ_g, being the gap wavelength) represents the abscissa of the point of intersection of the straight line with the X-axis and $E_g = hc/2\pi$.The number of carbon hexagon

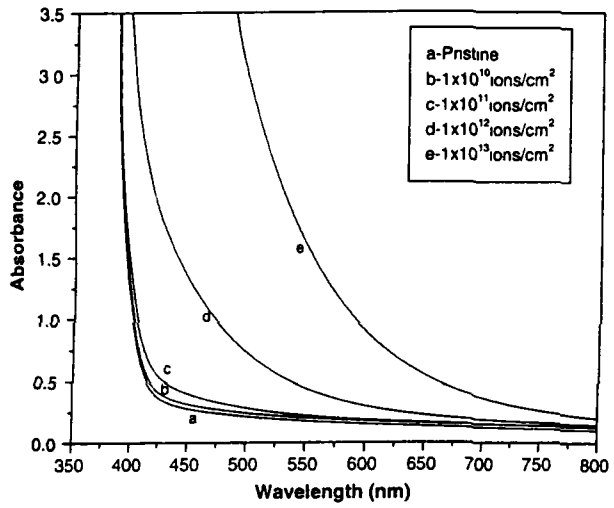

Fig. 4. Optical absorption spectra of PES polymer samples: pristine and irradiated with 100 MeV Si^{8+} ion beam.

rings in the cluster, N can be found from the Robertson relation [34].

$$E_g = \frac{2\beta}{\sqrt{N}}\ \text{eV}.$$

Here, 2β is the band structure energy of a pair of adjacent π sites and its value is taken as -2.9 eV for a six numbered carbon ring. Fink et al. [35] have pointed out that the Robertson equation underestimates the cluster size in irradiated polymers. Thus the structure of the cluster was assumed to be like a buckminsterfullerene a C_{60} ring instead of C_6) and the relation emerges:

$$E_g = \frac{34.3}{\sqrt{N}}\ \text{eV}.$$

where N is the number of carbon atoms per cluster in the irradiated polymer. Above relation has been used to calculate the number of carbon atoms per cluster in the irradiated samples.

The values of λ_g and the corresponding results of energy gap (E_g) and the number of carbon atoms per conjugation length (N) for virgin as well as irradiated samples are reported in Table 1. It can be observed that energy gap decreases with the increase in ion fluence in all the four polymers. But the percentage decrease is different in different polymers. At the highest fluence of $\sim 10^{13}$ ions/cm^2 maximum decrease in energy gap of almost 40% is found in PES polymer samples and a minimum decrease of about 2.1% in PET. The cluster size showed a range of 79–454 carbon atoms per cluster for the polymers studied here. Carbon enriched domains created in polymers during irradiation may be responsible for the decrease in band gap as indicated by earlier studies [18,35–39]. The optical absorption method can be used for investigation of the optically induced transitions and can provide information about the bond structure and energy gap in crystalline and non-crystalline materials [11].

Table 1
Variation of absorption edge (λ_g), energy gap (E_g) and number of carbon atoms per conjugation length (N) in pristine and 100 MeV Si^{8+} ion irradiated polymer samples of PET, PTFE, PMMA and PES at different fluences

Polymers sample	Fluence (ions/cm^2)	Absorption edge (λ_g) (nm)	Band gap energy (eV)	Number of carbon atoms (N)
PET	0	321.44	3.86	79
	10^{10}	323.58	3.84	80
	10^{11}	326.24	3.81	81
	10^{12}	328.12	3.78	82
PTFE	0	556.01	2.23	236
	10^{10}	565.97	2.19	245
	10^{11}	582.21	2.13	259
	10^{12}	585.81	2.12	261
	10^{13}	594.38	2.09	269
PMMA	0	399.24	3.11	122
	10^{10}	404.06	3.07	124
	10^{11}	414.84	2.99	131
	10^{12}	422.22	2.94	136
	10^{13}	426.41	2.91	138
PES	0	463.22	2.68	164
	10^{10}	497.21	2.50	188
	10^{11}	498.30	2.49	190
	10^{12}	681.05	1.82	355
	10^{13}	772.00	1.61	454

4. Conclusion

In the present study modification in optical properties of four polymers induced by 100 MeV Si ion irradiation is investigated by UV–Vis spectroscopy. Significant changes of different amounts are observed in optical response of the polymers after irradiation. Optical absorption spectra of the virgin sample show a sharp decrease with increasing wavelength up to a certain value, followed by a plateau region except in the case of PTFE spectra. It is observed that optical absorption increases with increasing fluence and this absorption shifts from UV–Vis towards the visible region for all the irradiated polymer samples as the fluence increases. Energy gap decreases with the increase in ion fluence in all the four polymers. But the percentage decrease is different in different polymers. At the highest fluence of $\sim 10^{13}$ ions/cm^2 maximum decrease in energy gap of almost 40% is found in PES polymer samples and a minimum decrease of about 2.1% in PET. The cluster size showed a range of 79–454 carbon atoms per cluster for the polymers studied here.

Acknowledgements

One of the authors, Prof. Rajendra Prasad, is thankful to All India Council of Technical Education, Government of India for providing Emeritus Fellowship to carry out this work. Financial assistance provided by Department

of Science and Technology (D.S.T.), Government of India to Dr. Rajesh Kumar as Young Scientist (Award No. SR/FTP/PS-31/2004) is gratefully acknowledged.

References

[1] E.H. Lee, Polyimides: Fundamentals and Applications, Marcel Dekker, New York, 1996.
[2] L.S. Wielunski, R.A. Clissold, E. Yap, D.G. McCulloch, D.R. Mckenzie, M.V. Swain, Nucl. Instr. and Meth. B 127–128 (1997) 698.
[3] R. Kumar, R. Prasad, Y.K. Vijay, N.K. Acharya, K.C. Verma, U. De, Nucl. Instr. and Meth. B 212 (2003) 221.
[4] H.S. Virk, S. Amrita Kaur, G.S. Randhawa, J. Phys. D: Appl. Phys. 31 (1998) 3139.
[5] J.N. Randall, D.C. Flanders, N.P. Economou, J.P. Donnelly, E.I. Bromley, Appl. Phys. Lett. 42 (1983) 457.
[6] E. Balanzat, S. Bouffard, A. Le Moel, N. Betz, Nucl. Instr. and Meth. B 91 (1994) 140.
[7] E.H. Lee, Nucl. Instr. and Meth. B 151 (1999) 29.
[8] S. Bauffard, B. Gervais, C. Leray, Nucl. Instr. and Meth. B 105 (1995) 1.
[9] D.M. Ruck, Nucl. Instr. and Meth. B 166–167 (2000) 602.
[10] J.P. Durand, A.L. Moel, Nucl. Instr. and Meth. B 105 (1995) 71.
[11] R. Mishra, S.P. Tripathy, D. Sinha, K.K. Dwivedi, S. Ghosh, D.T. Khating, M. Muller, D. Fink, W.H. Chung, Nucl. Instr. and Meth. B 168 (2000) 59.
[12] T. Steckenreiter, E. Balanzat, H. Ruse, C. Trautmann, Nucl. Instr. and Meth. B 131 (1997) 159.
[13] C. Liu, Z. Zhu, Y. Jin, Y. Sun, M. Hou, Z. Wang, C. Zhang, X. Chen, J. Liu, L. Baoquan, Nucl. Instr. and Meth. B 169 (2000) 78.
[14] Z. Zhu, Y. Sun, C. Liu, J. Liu, Y. Jin, Nucl. Instr. and Meth. B 193 (2002) 271.
[15] N.L. Singh, A. Sharma, D.K. Avasthi, Nucl. Instr. and Meth. B 206 (2003) 1120.
[16] G. Gerlach, K. Baumann, R. Buchhold, A. Nakladal, German Patent D E 198 53 732 (1998).
[17] M. Guenther, K. Sahre, G. Suchaneck, G. Gerelach, K.J. Eichhorn, Surf. Coat. Technol. 142–144 (2001) 482.
[18] R. Kumar, U. De, R. Prasad, Nucl. Instr. and Meth. B 248 (2006) 79.
[19] R. Kumar, R. Prasad, Nucl. Instr. and Meth. B 256 (2007) 238.
[20] J.R. Kulish, H. Franke, A. Singh, R.A. Lessard, J. Knystautas, J. Appl. Phys. 63 (1988) 2517.
[21] M. Dole (Ed.), The Radiation Chemistry of Macromolecules, Vol. 2, Academic Press, New York, 1973.
[22] J. Sun, Y. Zhang, X. Zhong, X. Zhu, Radiat. Phys. Chem. 44 (1994) 655.
[23] A. Oshima, Y. Tabata, H. Kudoh, T. Seguchi, Radiat. Phys. Chem. 45 (1994) 269.
[24] A. Oshima, S. Ikeda, T. Seguchi, Y. Tabata, Radiat. Phys. Chem. 49 (1997) 581.
[25] E. Katoh, H. Sugisawa, A. Oshima, Y. Tabata, T. Seguchi, T. Yamazaki, Radiat. Phys. Chem. 54 (1999) 165.
[26] U. Lappan, U. Geißler, K. Lunkwitz, J. Appl. Polym. Sci. 74 (1999) 1571.
[27] U. Lappan, U. Geißler, K. Lunkwitz, Radiat. Phys. Chem. 59 (2000) 317.
[28] G.K. Mehta, A.P. Patro, Nucl. Instr. and Meth. A 268 (1988) 334.
[29] D. Kanjilal, S. Chopra, M.M. Narayanan, I.S. Iyer, V. Jha, R. Joshi, S.K. Datta, Nucl. Instr. and Meth. A 238 (1993) 97.
[30] R. Dyer John, Applications of Absorption Spectroscopy of Organic Compounds, Prentice-Hall Inc., NJ, 1994.
[31] A.K. Srivastava, H.S. Virk, J. Polym. Mater. 17 (2000) 325.
[32] L.S. Farenza, R.M. Papaleo, A. Hallen, M.A. Araujo, R.P. Livi, B.U.R. Sundqvist, Nucl. Instr. and Meth. B 105 (1995) 134.
[33] J. Tauc, R. Grigorovici, A. Vaneu, Phys. Status Solidi 15 (1996) 627.
[34] J. Robertson, E.P. O'Reilly, Phys. Rev. B 35 (1987) 2946.
[35] D. Fink, R. Klett, L.T. Chadderton, J. Cardoso, R. Montiel, M.H. Vazquez, A. Karanovich, Nucl. Instr. and Meth. B. 111 (1996) 303.
[36] D. Fink, W.H. Chung, R. Klett, A. Schmoldt, J. Cardoso, R. Montiel, M.H. Vazquez, L. Wang, F. Hosoi, H. Omichi, P. Goppelt-Langer, Radiat. Eff. Defect Solids 133 (1995) 193.
[37] A. Saha, V. Chakraborty, S.N. Chintalpudi, Nucl. Instr. and Meth. B 168 (2000) 245.
[38] .H.S. Virk, P.S. Chandi, A.K. Srivastava, Nucl. Instr. and Meth. B 183 (2001) 329.
[39] T. Phukan, D. Kanjilal, T.D. Goswami, H.L. Das, Radiat. Meas. 36 (2003) 611.